

DESALINATION BRINE DISCHARGE MODEL FINAL REPORT

Ben R. Hodges, Ph.D.
Principal Investigator

Paula S. Kulis, M.S. Cédric H. David, M.S.
Research Assistants

Center for Research in Water Resources
University of Texas at Austin

August 30, 2006

Submitted to Texas Water Development Board
Interagency Cooperation Contract 2005-001-059

EXECUTIVE SUMMARY

To improve modeling of desalination brine discharges, this project investigated an existing high-salinity outflow from a small embayment (Oso Bay) into a larger embayment (Corpus Christi Bay). The premise of this investigation was that the existing high salinity outflow from the narrow Oso Bay channel is similar to what might be postulated from a large-scale desalination plant. The project demonstrated that: 1) a thin-layer, high-salinity plume may exist in a shallow embayment and can be linked to hypoxia; and 2) the grid resolution necessary for the EFDC sigma-coordinate model to adequately capture such a thin-layer plume is prohibitively expensive. A new approach to vertical mixing is developed that addresses the creation and destruction of thin-layer plumes using an approach that is suitable for coarser (more practical) model grid resolution.

This page intentionally left blank.

TABLE OF CONTENTS

EXECUTIVE SUMMARY	1
TABLE OF CONTENTS	3
LIST OF FIGURES	5
LIST OF TABLES	8
BACKGROUND	9
FIELD STUDIES	10
GRAVITY CURRENT MODELING	10
A NEW VERTICAL MIXING MODEL FOR THIN-LAYER STRATIFICATION.....	13
PROJECT GOALS AND ACHIEVMENTS	15
CONCLUSIONS FROM THE RESEARCH	16
FUTURE WORK.....	17
APPENDIX A FIELD STUDIES OF CORPUS CHRISTI BAY, 2005	19
A.1 INTRODUCTION.....	19
A.2 RESEARCH OBJECTIVES.....	20
A.3 BACKGROUND.....	20
A.4 EXPERIMENTAL METHODS.....	21
A.5 DESCRIPTION OF THE DATA COLLECTION MISSIONS	38
A.6 DATA PROCESSING	51
A.7 APPLICATION OF THE DATA ANALYSIS METHODS	59
A.8 AVAILABILITY OF THE DATA	64
A.9 EFFICIENCY OF THE SOFTWARE	64
A.10 SUMMARY	64
A.11 SUGGESTED FUTURE WORK	64
A.12 INFORMATION ON FIELD DEPLOYMENT	65
A.13 MATLAB FUNCTIONS.....	76
APPENDIX B IDEALIZED 2D MODELING OF A GRAVITY UNDERFLOW	99
B.1 GRAVITY CURRENT THEORY.....	99

B.2	BASIN CHARACTERISTICS AND COMPUTATIONAL SPACE	102
B.3	TEST CASES.....	103
B.4	RESULTS AND DISCUSSION.....	104
B.5	CONCLUSION.....	107

APPENDIX C 3D MODELING OF THE OSO BAY OUTFLOW..... 109

C.1	INTRODUCTION.....	109
C.2	BASIN CHARACTERISTICS AND COMPUTATIONAL SPACE.....	109
C.3	RESULTS AND DISCUSSION.....	112
C.4	COMPUTATIONAL EXPENSE.....	116
C.5	CONCLUSION.....	116
C.6	MATLAB FUNCTIONS.....	117

APPENDIX D THEORY FOR A NEW VERTICAL MIXING MODEL..... 121

D.1	INTRODUCTION.....	121
D.2	OUTLINE FOR MODEL IMPLEMENTATION.....	122
D.3	NOTES ON NOTATION	123
D.4	GOAL OF TIME STEP AND GRID SIZE INDEPENDENCE.....	123
D.5	DEFINING SUB-TIME STEPS	123
D.6	REPRESENTATIVE AND MEAN CONCENTRATIONS	123
D.7	MIXING ENERGY FROM WIND	126
D.8	INTEGRATING THERMODYNAMICS, CONVECTIVE MIXING AND THE SURFACE MIXED LAYER .	126
D.9	SURFACE AND BOTTOM MIXING LAYERS	127
D.10	MIXING BY KELVIN-HELMHOLTZ BILLOWS	130

APPENDIX E FIELD REPORT ON A HYPOXIC EVENT IN SE CORPUS CHRISTI BAY... 137

E.1	SUMMARY.....	137
E.2	GOALS AND SCOPE	137
E.3	INSTRUMENTS AND METHODS	138
E.4	LESSONS LEARNED	141
E.5	DATA TYPES COLLECTED	142
E.6	DATA FILES ON CD-ROM.....	144
E.7	TABLES	146
E.8	CHRONOLOGY FROM LOGBOOK	155
E.9	DATA FROM ALL MANTA PROFILES	162

APPENDIX F REVIEW COMMENTS FROM TWDB ON DRAFT REPORT..... 193

F.1	COMMENTS BY JORDAN FURNANS, PH.D., P.E., 7/10/06	193
F.2	COMMENTS BY DHARHAS POTHINA	197
F.3	COMMENTS BY RUBEN S. SOLIS, PH.D. 7/20/2006	198

REFERENCES..... 203

LIST OF FIGURES

- Figure 1. Conceptual development of thin-layer gravity currents and hypoxia in a shallow estuary. Development or avoidance of hypoxia depends on wind-induced mixing.
- Figure 2. Field study site for 2005 identifying the typical profiling locations at the nexus of Oso bay and Corpus Christi Bay.
- Figure 3. Typical evolution of temperature, salinity and dissolved oxygen from the Oso Bay nexus with Corpus Christi Bay. Contours are developed from Manta profiles collected at the 10 stations in Figure 2. Day profiles were collected on 8/22/2005 from 1515 hours to 1652 hours. Night profiles were collected on 8/23/2005 from 0323 to 0617 hours..
- Figure 4. EFDC model results for a) stretched grid of 48 layers with thinnest at bottom; b) uniform grid of 20 layers, and c) sparse grid of 3 layers. Obtaining model results with 44 psu salinity requires the stretched grid, which has 2 cm grid spacing near the bottom boundary.
- Figure 5. Proposed relationship between the representative scalar concentration (ϕ_R) with top (h_T) and bottom (h_B) gradient regions in each grid cell for a new mixing model.
- Figure A.1 Location of Corpus Christi Bay in the State of Texas
- Figure A.2 Corpus Christi Bay and surrounding counties
- Figure A.3. Documented hypoxia in Corpus Christi Bay. Solid lines are areas with documented hypoxia, $DO < 2.0$ mg/L; dashed lines are areas that are argued to be effectively hypoxic with $DO < 3.0$ mg/L.. From Ritter and Montagna (1999) their Figure 6.
- Figure A.4 Principal features around Corpus Christi Bay
- Figure A.5 Map of all the sampled locations
- Figure A.6 SCAMP (from <http://pme.com/scamp.htm>)
- Figure A.7 Example of SCAMP plot obtained with the software provided by PME. July 27 2005.
- Figure A.8 Positions of sensors on SCAMP
- Figure A.9 Deployment of SCAMP (not to scale)
- Figure A.10 Manta (from <http://www.eurekaenvironmental.com>)
- Figure A.11 Deployment of Manta
- Figure A.12 Sample graph of the data produced by the Manta (plot created by Jordan Furnans)
- Figure A.13 Magellan Meridian Marine (from <http://www.magellangps.com/>)
- Figure A.14 Trimble GPS (from <http://www.trimble.com/>)
- Figure A.15 Kestrel 4100 (from <http://www.nkhome.com/>)
- Figure A.16. CES weather station at location Weather1
- Figure A.17. CES weather station at location Weather2
- Figure A.18 The three locations of the two land-based weather stations
- Figure A.19 Locations of boat ramp and weather stations
- Figure A.20 CES wind data for Mission 1 (Location Weather1), with boat operation times
- Figure A.21 Locations for mission 1
- Figure A.22. Accurate temperature profiles - location A039 - 1047 hours on July 6th
- Figure A.23. Accurate temperature profiles - location A104 - 0720 hours on July 7th

Figure A.24. Accurate temperature profiles - location A042 - 0910 hours on July 7th

Figure A.25. Salinity profiles - location A039 - 1047 hours on July 6th

Figure A.26. Salinity profiles - location A104 - 0720 hours on July 7th

Figure A.27. Salinity profiles - location A042 - 0910 hours on July 7th

Figure A.28. Wind data and boat operation for mission 1

Figure A.29. Crew changes for mission 2

Figure A.30. CES and Kestrel wind data for Mission 2 (Location Weather2), with boat operation times

Figure A.31. Transects studied during mission 2

Figure A.32 Route connecting sampled locations for Mission 2

Figure A.33 Wind data and boat operation for mission 2

Figure A.34. Area investigated during Missions 3 and 4

Figure A.35. Organization of SCAMP data processing

Figure A.36. Organization of the Matlab files

Figure A.37. Binning and averaging

Figure A.38. Summary of data processing

Figure A.39. One location and one parameter figure

Figure A.40. Spatial transect: Transect 2, on July 28th between 0925 and 1110 hours

Figure A.41. Temporal evolution at one location, Location A037 on July 07th between 0754 and 1420 hours

Figure A.42. Anomaly in one of the deployments

Figure A.43. Interesting changes in temperature 1

Figure A.44. Interesting change in temperature 2

Figure A.45 Sudden change in the salinity profile 1

Figure A.46. Sudden change in the salinity profile 2

Figure A.47. Transect 1; July 7th 2005, between 0720 and 0910 hours

Figure A.48. Transect 1; July 7th 2005, between 0945 and 1120 hours

Figure A.49. Transect 1; July 7th 2005, between 1155 and 1325 hours

Figure A.50. Transect 3; July 28th 2005, between 0309 and 0606 hours

Figure B.1. x-z plane view of the basin simulated in these tests. The shallow left boundary is a source boundary, while the right dashed boundary is an open boundary. The diagram is not drawn to scale.

Figure B.2. Profiles of salinity and velocity (at 2475 meters from the source) for select MY tests. Velocity and salinity values are non-dimensionalized by v_{max} , and s_{max} , where v_{max} and s_{max} are the maximum velocity and salinity in the water column, respectively. The symbol δ refers to z at the maximum density gradient. The values of Δz^* in these tests are (a) 0.001, (b) 0.005, and (c) 0.02.

Figure B.3 Profiles of salinity and velocity (at 2475 meters from the source) for select NT tests. Velocity and salinity values are non-dimensionalized by v_{max} , and s_{max} , where v_{max} and s_{max} are the maximum velocity and salinity in the water column, respectively. The symbol δ refers to z at the maximum density gradient. The values of Δz^* in these tests are (a) 0.001, (b) 0.005, and (c) 0.02..

Figure B.4. Square of the Densimetric Froude Number, varying in resolution and in distance along slope..

Figure B.5. Mean Froude Number (squared) plotted against grid resolution.

Figure B.6. Log-log plot of mean Entrainment Rate plotted against grid resolution.

Figure C.1 Bathymetry of Computational Domain. The vertical black lines represent the physical location of model results.

Figure C.2 Temperature forcing in Oso Bay, plotted with real temperature data taken from a pressure transducer placed in Oso Bay by the Texas Water Development Board. Data is shown for 8/21/05 at 12:35 p.m. through 8/23/05 at 12:34 a.m.

Figure C.3 A sample column of cells in each of the three test cases.

Figure C.4 Evolution of temperature from the Oso Bay nexus with Corpus Christi Bay.

Figure C.5 Contours of the temperature signature from the stretched test case in EFDC. The “Day” plot is a transect taken from what is effectively 4 p.m. on the temperature sinusoid in Oso Bay, and the “Night” plot is a transect taken from 4 a.m.

Figure C.6 EFDC model results for a) stretched grid of 48 layers with thinnest at bottom; b) uniform grid of 20 layers, and c) sparse grid of 3 layers. Obtaining model results with 44 psu salinity requires the stretched grid, which has 2 cm grid spacing near the bottom boundary.

Figure C.7 Change in Sigma-t value between bottom and surface waters at a given sample location in Oso Bay based on field and model results.

Figure C.8 Energy flow showing the relationship between the wind and the potential energy of the water column.

Figure C.9 Potential Energy Deficit in the test cases in EFDC and the field data from the summer of 2005, all calculated from profiles at the same location in the bay.

Figure D.1 Scalar concentration profile over two grid cells with the representative scalar concentration (ϕ_R) and mixing layer heights (h) identified

Figure D.2. Case where thin layer KH mixing from the $k-1/2$ and $k+1/2$ boundaries causes mixing of representative scalar values. The dashed line represents the scalar profile prior to thin layer mixing, the solid line represents the unacceptable profile that would result from thin-layer mixing in violation of eq. (D.1).

Figure E.1. Data from profile M19a

Figure E.2. TCOON data for wind at Ingleside station 006 during mid-July 2006. The field experiment was conducted during the times indicated by the arrow. Data were available hourly through 7/12/06 and at 6 minute intervals thereafter.

LIST OF TABLES

- Table A.1 Sampling time and time between samples for the CES weather station
- Table A.2 Change in water density with salinity and temperature according to the UNESCO equation
- Table A.3 Sampling locations
- Table B.1 Summary of vertical grid resolution for simulations run.
- Table C.1 CPU time required to run a 36 hour simulation. Values for All of Corpus Christi Bay are determined by linear extrapolation.
- Table E.1. Manta calibration
- Table E.2. Waypoint and profile coordinates (part 1)
- Table E.3. Waypoint and profile coordinates (Part 2)
- Table E.4. Waypoint and profile coordinates (Part 3)
- Table E.5. Time correction from Amphibian time to Central Daylight Time
- Table E.6. Time correction for Manta files of third boat deployment
- Table E.7. Time correction for Manta files of fourth boat deployment
- Table E.8. Time correction for Manta files of fifth boat deployment
- Table E.9. Time correction for Manta files of sixth boat deployment
- Table E.10. Time correction for Manta files of seventh boat deployment
- Table E.11. Time correction for Manta files of eighth boat deployment
- Table E.12. Headers and interpretation of sonar *.csv file
- Table E.13. Sonar file start time

BACKGROUND

Desalination plants are an option for providing drought-proof water supplies for the coastal United States. Beyond the technical and financial issues of plant construction, a key potential environmental impact is the disposal of high salinity water (brine) that is the principal desalination plant effluent. As longer disposal outfalls are more expensive, the shortest outfall that is environmentally feasible is generally preferred. Along Texas coastline (and other areas of the U.S.) many potential desalination plant sites are close to shallow embayments, which become the least expensive option for brine disposal. Where winds are regular and strong, embayments with depths of 3 to 5 meters (such as Corpus Christi Bay) are generally considered “well-mixed” for most natural processes. Under well-mixed conditions, development of hypoxia (low oxygen) is generally attributable to excessive nutrient loading. However, desalination brine salinity concentrations (50 to 70 psu) are significantly higher than are seen in many natural systems, so there is an open question as to whether shallow embayments would remain well-mixed in the presence of a desalination plant brine discharge.

Figure 1 provides a schematic of the processes that may occur when high-salinity water is introduced into a shallow embayment. The key questions to be answered are:

1. Is such a thin-layer gravitational flow possible in a shallow embayment?
2. Is it practical to resolve the thin-layer flow with a standard hydrodynamic model?
3. How can we model the mixing that replenishes dissolved oxygen?

This project demonstrated that: such flows can exist; standard hydrodynamic models are computationally expensive when applied at the small grid scales required to resolve the flow; and a new approach to vertical mixing may provide a means modeling dissolved oxygen replenishment.

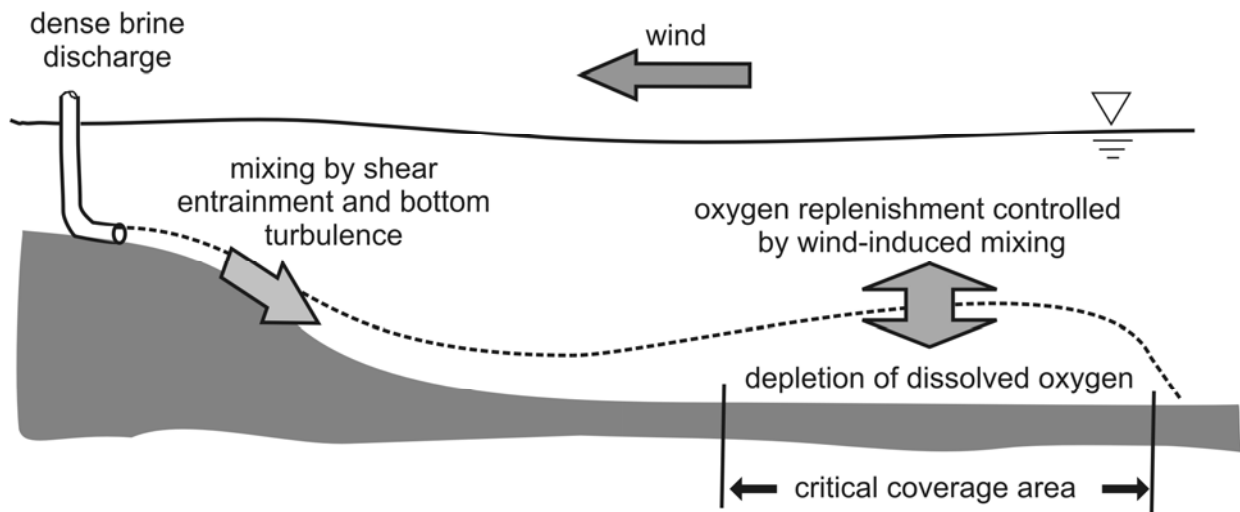


Figure 1. Conceptual development of thin-layer gravity currents and hypoxia in a shallow estuary. Development or avoidance of hypoxia depends on wind-induced mixing.

FIELD STUDIES

To answer the first of the above key questions, several field studies were conducted in Corpus Christi Bay over the summer of 2005 (Appendix A) and 2006 (Appendix E). During the first study, the gravity current outflow from Oso Bay (Figure 2) was examined. The principal findings of the first study are illustrated with some of the field data shown in Figure 3. High salinity water from Oso Bay forms a thin (30 to 50 cm) underflow into Corpus Christi Bay. During the initial gravitational flow down the slope, turbulent entrainment of Corpus Christi Bay water into the underflow decreases the bottom salinity from 50 to 40 psu, but cannot fully mix the underflow. When the underflow reaches 3 m depth, the bay bottom begins to flatten out, therefore reducing the underflow velocity and entrainment rate. It follows that where such an underflow penetrates into the main flat basin of Corpus Christi Bay, stratification will occur unless destroyed by current-driven shear or wind-driven turbulence. The stratification isolates bottom sediments from the ambient water, reducing the oxygen replenishment rate near the benthos.

Due to the shallow depths (< 0.5 m), water that is warmed in Oso Bay during the day has a higher temperature than the ambient water in Corpus Christi Bay. Conversely, water that is cooled in Oso Bay during the night is colder than ambient Corpus Christi Bay water. Because the water density is dominated by the salinity, the temperature field in Figure 3 can be used to infer when the water in the underflow was released from Oso Bay. It can be seen that low dissolved oxygen levels (located approximately 1500 to 2000 m from Oso Bay) are formed in high-salinity underflowing water, whether the water is warm or cold. Similarly, low oxygen levels occur during both day and night, so the effect is not simply due to diel cycling of production/respiration (which is not to say the diel cycle is irrelevant; the night DO levels are lower than the daytime levels, a clear indication of a respiration/production cycle) From these data, we argue the development of hypoxia in this case is related to the length of time the sediments are isolated from the ambient water by the thin saline layer. It follows that the field studies of this project give support to the concept of hypoxia development illustrated in Figure 1. From the field studies we conclude that thin-layer stratification can occur in a shallow embayment, and does influence hypoxia.

During the second field study, the development of stratification in southeastern Corpus Christi Bay during a strong wind event was examined. The data from this experiment has been collated (see Appendix E), but significant analysis has not been undertaken. Further analysis of this data will be undertaken by the PI Hodges in the next year to prepare a journal paper on stratification in Corpus Christi Bay.

GRAVITY CURRENT MODELING

For gravity currents such as a brine underflow or the Oso Bay outflow, a sigma-coordinate hydrodynamic model (also known as a boundary-fitted model) is generally preferred to a z-coordinate model. The former represents the bottom boundary as a smooth line of grid cells, whereas the latter requires a stair-step bottom with abrupt transitions that tends to increase numerical diffusion. The US EPA has encouraged consulting engineers to use the EFDC sigma-

coordinate model for estuarine simulations, so we evaluated the suitability of EFDC for modeling thin-layer gravity currents. We determined that the principal factor controlling the model's ability to correctly represent a gravity current is the model vertical grid resolution. For preliminary tests (Appendix B) on an idealized 2D domain using EFDC with the standard Mellor-Yamada 2.5 level turbulence closure, we found that 20 grid cells were required *within the gravity current* to reach a converged solution (i.e. a solution where further grid refinement did not change the results). In the Oso Bay salinity plume, this would imply a vertical grid spacing of approximately 2 cm for a fully converged solution. To further test these results, we developed a 3D model of the region surrounding Oso Bay and tested this model with several grid resolutions (Appendix C). Results confirmed the preliminary analysis that a very fine grid is required to obtain a reasonable representation of the gravity plume thickness.

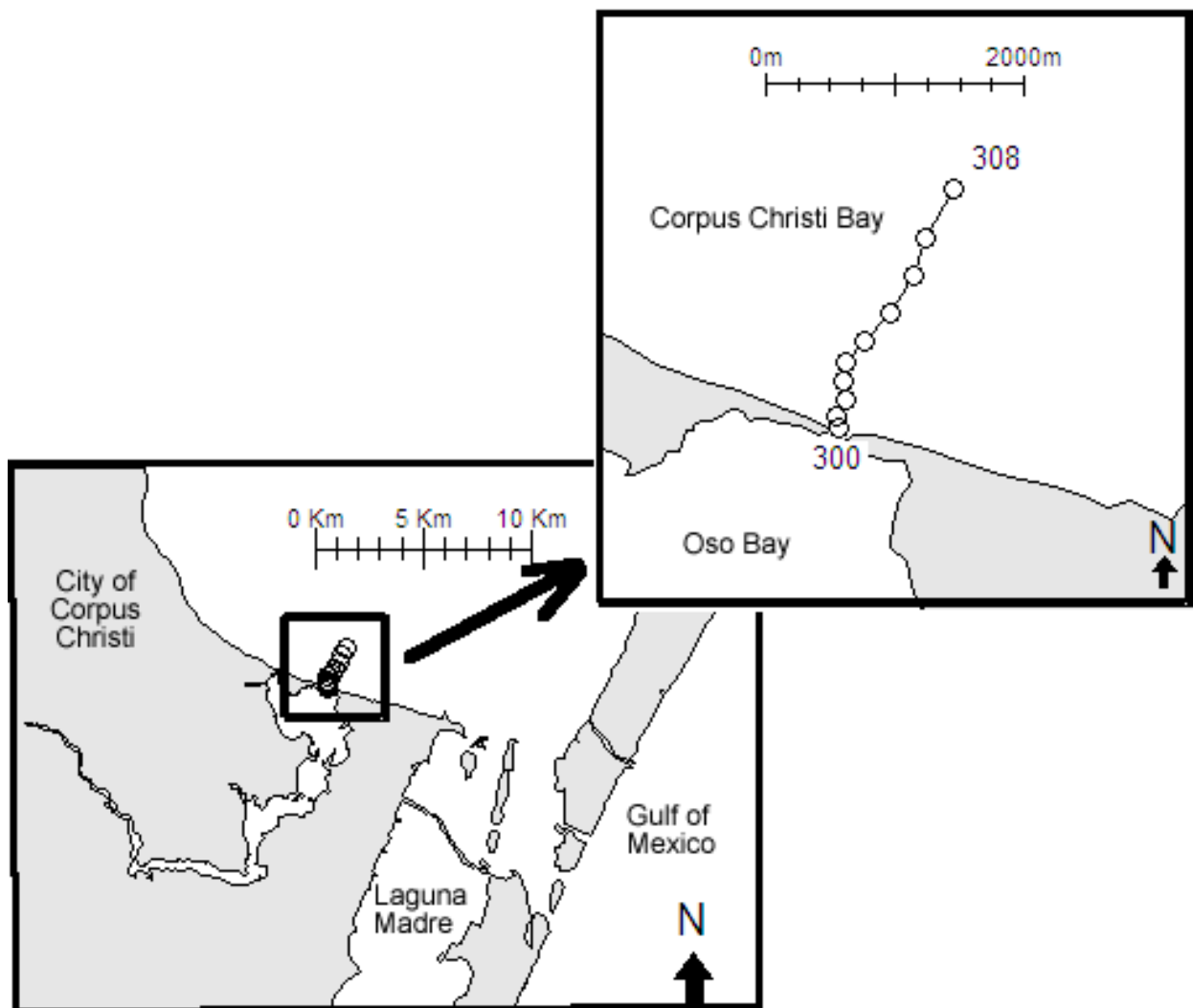


Figure 2. Field study site for 2005 identifying the typical profiling locations at the nexus of Oso bay and Corpus Christi Bay (Graphics provided by J. Furnans, TWDB).

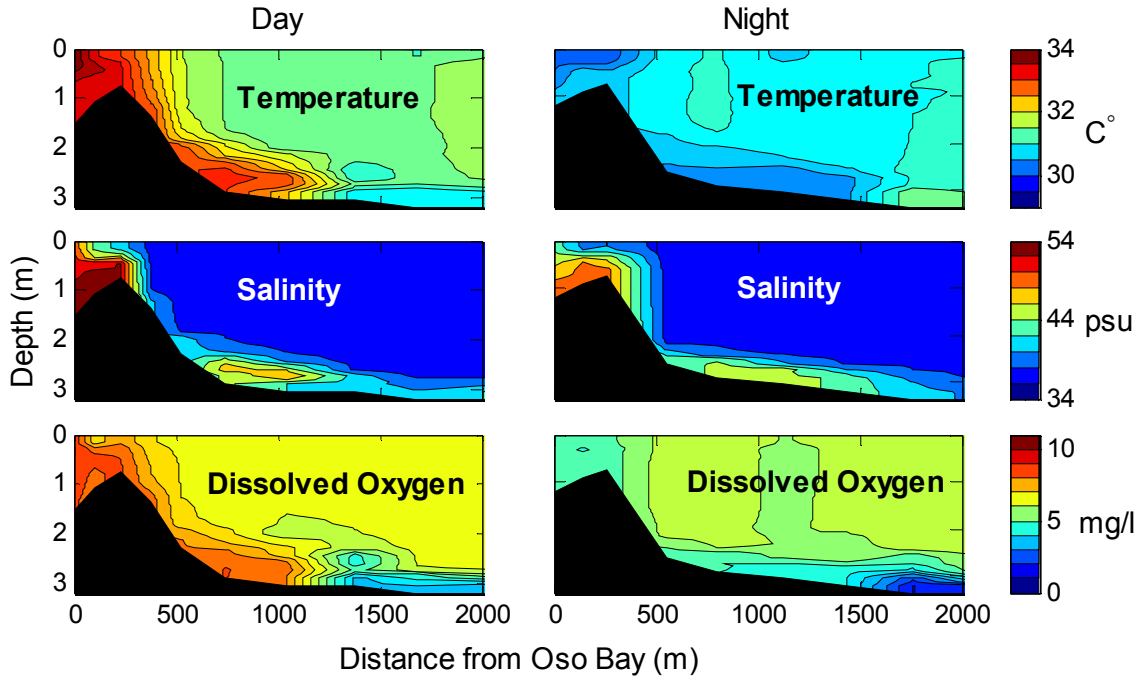


Figure 3. Typical evolution of temperature, salinity and dissolved oxygen from the Oso Bay nexus with Corpus Christi Bay. Contours are developed from Manta profiles (without any averaging) collected at the 10 stations in Figure 2. Day profiles were collected on 8/22/2005 from 1515 hours to 1652 hours. Night profiles were collected on 8/23/2005 from 0323 to 0617 hours.

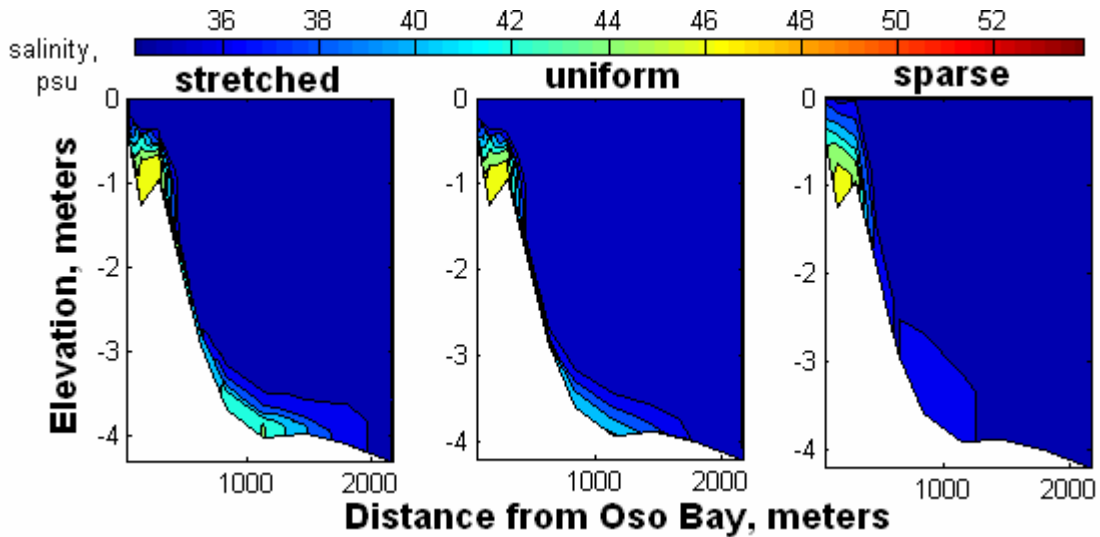


Figure 4. EFDC model results for a) stretched grid of 48 layers with thinnest at bottom; b) uniform grid of 20 layers, and c) sparse grid of 3 layers. Obtaining model results with 44 psu salinity requires the stretched grid, which has 2 cm grid spacing near the bottom boundary.

Results from the EFDC analysis indicate that the using a sufficiently fine vertical mesh over all of Corpus Christi Bay would be too computationally intensive for present desktop computers. The EFDC model with a fine grid resolution representing only the vicinity around the mouth of Oso Bay ran at less than real time on a Pentium IV processor (i.e. 1 second of real time took more than 1 second of computational time). From this portion of the research we conclude that practical models of thin-layer brine underflows will need to incorporate some form of benthic boundary layer model that couples 3D hydrodynamics to a 2D gravity current solution (e.g. Dallimore et al. 2003, 2004). A benthic boundary gravity current model was developed as part of another project (Kulis, 2005) and is planned for later inclusion in a 3D Corpus Christi Bay model under an NSF-sponsored project that was recently funded.

By using a coupled benthic boundary layer model to represent the underflow, we expect that a 3D model vertical grid resolution can be coarsened to the level required to resolve structure in large-scale currents. This expectation is supported by the prior work of Dallimore et al. (2003). Recently the Texas A&M Shoreline Environmental Research Facility has been documenting the Corpus Christi Bay velocity structure with an Acoustic Doppler Current Profiler (ADCP). From their preliminary data (J. Bonner, pers. comm.), we believe the large-scale vertical structure is likely resolvable with 10 to 15 grid cells over the entire water depth (i.e. a vertical grid size on the order of 20 to 30 cm), which will be more practical than the 2 cm vertical spacing required to have EFDC resolve the gravity underflow.

A NEW VERTICAL MIXING MODEL FOR THIN-LAYER STRATIFICATION

While modeling a gravity current using a benthic boundary layer approach has been established as a viable technique (e.g. Dallimore et al. 2003, 2004), there remains an open question as how to model the vertical mixing dynamics that control the oxygen replenishment rate (see Figure 1 above) in a shallow embayment. The principal difficulty of representing mixing in standard hydrodynamic models (such as EFDC) is that vertical grid resolution constrains the solution of partial differential equations (PDE) for turbulence. Existing hydrodynamic models represent the fluid in a grid cell by a single value for any scalar, effectively creating a stair-step structure to the salinity and temperature fields that is controlled by the grid. Because of the stair-step structure, any vertical mixing (i.e. vertical turbulent diffusion) across the boundary between two grid cells must occur over the entire thickness of each cell. That is, when grid cell 'k' is mixed with cell 'k-1' below it, the mean scalar concentration in both 'k' and 'k-1' are changed. The mixing occurs over a length scale of $2\Delta z$ (where Δz is the grid cell thickness), even if the physical mixing should be across a much smaller scale. It follows that mixing approaches using mean concentrations will always weaken stratification over length scales that are proportional to the model grid scale, which is only acceptable if the grid scale is small compared to the scale of the mixing events.

To take the above thought problem to another level, we may imagine what happens if, during the next model time step, the grid cell 'k-1' is mixed with layer 'k-2' below it. In such a case, scalar that was in grid cell 'k' and mixed into 'k-1' in the prior time step will now be mixed into layer 'k-2'. Thus, where mixing uses mean concentrations there is an underlying celerity for vertical scalar transport that is simply $\Delta z / \Delta t$, where Δt is the model time step. Clearly this

transport rate is simply a numerical artifact. However, as long as the physical mixing rate provides a net vertical transport celerity larger than $\Delta z / \Delta t$, the model results may be reasonable. Unfortunately, in the presence of strong stratification the physical vertical transport rate due to mixing and diffusion may be close to zero, making a model that resolves the process an impractical goal.

If the real-world physical mixing is limited to length scales smaller than the Δz of the model (i.e. ‘thin-layer’ mixing), then scalar propagation at the rate of $\Delta z / \Delta t$ is entirely a numerical artifact that can be classified as numerical diffusion. Such numerical diffusion of salinity and temperature may violate the energy constraints of a stratified flow. To elaborate, we note that vertical mixing in a stratified flow requires a portion of turbulent kinetic energy (TKE) must be expended to raise the heavy fluid in the water column (i.e. increasing the background potential energy). At coarse grid resolutions, the conventional PDE approach using mean concentrations may allow more mixing than is physically possible for the available TKE. As a result, such a mixing model applied to the dissolved oxygen ventilation of a thin-layer gravity underflow is likely to significantly overpredict the DO replenishment.

The above mixing energy issues were partially addressed for surface mixed layers in lakes by Hodges et al. (2000) and Laval et al. (2003). Their approach replaced the conventional PDE turbulence model for vertical diffusion with a “mixed-layer” model, similar to techniques previously used for 1D lake and ocean modeling of near-surface stratification. The mixed-layer approach computes vertical mixing in a stratified region on a layer-by-layer basis that is decoupled from advection, horizontal diffusion and non-conservative scalar reaction equations. Energy arguments are used to constrain the mixing such that the increase in background potential energy is always less than the available TKE and dissipation. By removing the vertical diffusion term in the hydrodynamics and transport PDE’s, the mixed-layer approach applied on a coarse model grid retains a sharper stratification than generally possible for the pure PDE approach. The key insight supporting mixed-layer modeling is that our hydrodynamic models are generally solving PDE’s in the horizontal direction that are well-resolved (i.e. many horizontal grid cells over the scales of interest), whereas the vertical grid resolution is often fairly limited and is quite poor compared to the length scales associated with sharp thermoclines or haloclines.

However, the mixed-layer approach has not been examined in the context of benthic boundary layers for shallow bays. Furthermore, the mixed-layer approach retains the fundamental problem that mixing always occurs over an entire grid cell (similar to the PDE approach discussed above). To address these issues, Appendix D provides the theoretical foundations for a new method of representing the scalar structure that separately models gradient regions between grid cells (Figure 5). This new approach creates a mixing region between each grid layer that allows only partial mixing of a grid cell, which should allow a coarse-grid model to retain a sharper stratification than would be allowed with a conventional approach. The new approach is applicable to both conservative and non-conservative scalars (i.e. those with source/sink terms). The non-conservative source/sink reactions can generally be decoupled from the mixing algorithm in a mixed-layer model and computed either sequentially or in conjunction with the advection equation.

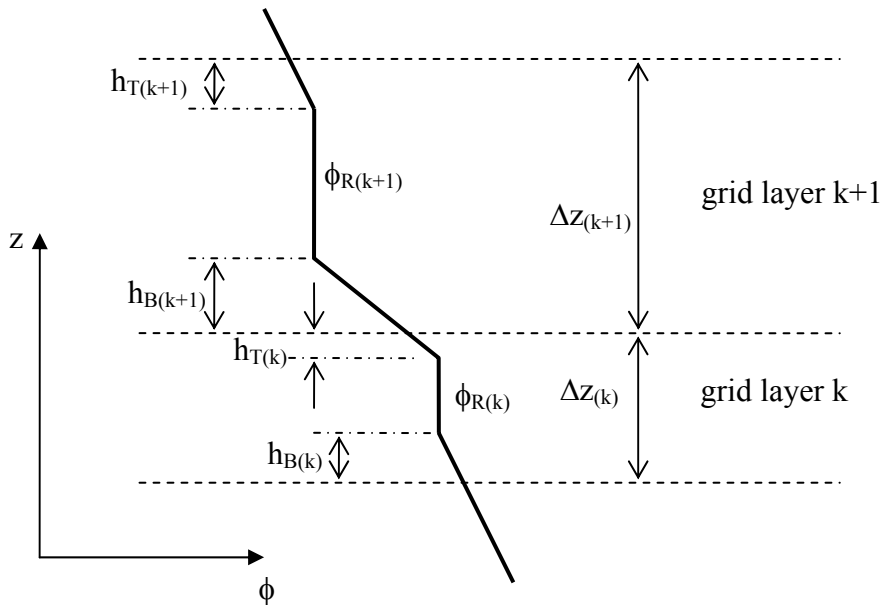


Figure 5. Proposed relationship between the representative scalar concentration (ϕ_R) with top (h_T) and bottom (h_B) gradient regions in each grid cell for a new mixing model.

PROJECT GOALS AND ACHIEVEMENTS

The principal aim of this project was to develop improved tools for modeling the fate of brine discharges from desalination plants into shallow embayments. Towards this end, there were three principal issues that required analysis:

- What stratification effects are likely to occur from a brine discharge into a shallow bay?
- What are practical approaches to modeling the stratification?
- What are the physical processes that control stratification, mixing and DO replenishment in a brine plume?

Towards these ends, the tasks in the statement of work (SOW) to CRWR were:

- Task 1. Develop an improved mixing model.
- Task 2. Validate the mixing model.
- Task 3. Couple the mixing model with a hydrodynamics model.
- Task 4. Conduct field experiments for model validation data.

The above tasks were partially completed for the reasons discussed below.

An improved mixing model (Task 1) was developed (Appendix D) and validation field data was collected (Task 4). However the mixing model proved much more complex than originally envisioned. The SOW was predicated on the idea that the principal problem for a vertical mixing model in a shallow embayment would be the coupling between the 2D underflow model and the 3D hydrodynamic model, a relatively straightforward problem similar to previous work (Dallimore et al. 2004) that would allow Tasks 2 and 3 to be accomplished. Unfortunately, the field data showed a much more complex stratification structure than was originally thought

possible in only three meters of water. During the mixing model development, it became clear that the principal model problem is maintaining a multi-layered stratification with a vertical grid resolution that is coarse relative to the layer thicknesses. The new mixing model theory is a novel way of using gradients to maintain stratification in such a coarsely-resolved system; unfortunately, development of a consistent theoretical framework for this mixing model was more time-consuming than development of the mixing model for the 2D/3D coupling that was originally envisioned. Continued development of the vertical mixing model is planned under different projects (see Future Work, below).

A further issue that affected the project achievements was the concurrent development of a coupled 2D underflow/3D hydrodynamics model for the brine discharge. This model development is part of the ongoing Ph.D. work of Ms. Paula Kulis under an NSF graduate fellowship (preliminary model development information is documented in Kulis, 2005; Kulis and Hodges, 2005). The original plan was to couple the Kulis underflow model to the existing ELCOM hydrodynamic model. However, TWDB was unable to obtain a license for use of ELCOM. Furthermore, ongoing discussions with TWDB led to the conclusion that an unstructured grid model (e.g. ELCIRC) or curvilinear grid model (e.g. EFDC) was preferred instead of the Cartesian ELCOM grid. Coupled model development was stalled in a preliminary stage so that we could definitively answer the question as to whether EFDC, a curvilinear sigma-coordinate model, could effectively and efficiently capture a thin-layer underflow without a coupled underflow model. If the sigma-coordinate model proved effective, the Texas Water Development Board could consider adopting EFDC for its Bays and Estuaries Program. However, our work under the NSF project showed that the EFDC model required vertical grid resolution on the order of centimeters to correctly model a thin-layer underflow. Such a fine level of grid resolution would be impractical for modeling the entire bay. Thus, we have demonstrated the necessity of using a coupled 2D/3D model. Once a coupled model is required to represent the benthic boundary layer, the advantages of a sigma-coordinate system (e.g. EFDC) are significantly reduced. Thus, the focus of our ongoing NSF-sponsored work is being shifted to developing the 2D underflow model for the 3D unstructured-grid, z-coordinate ELCIRC code.

CONCLUSIONS FROM THE RESEARCH

This project demonstrated that thin-layer gravity currents may be a concern in shallow embayments such as Corpus Christi Bay. Effective modeling of such currents cannot be accomplished with simple application of the sigma-coordinate EFDC hydrodynamic model as the required grid resolution is computationally prohibitive. Based on our experience, the only computationally-effective approach to modeling such thin-layer gravity currents is through the use of a 2D benthic boundary layer model coupled to a 3D hydrodynamic model (e.g. Dallimore et al. 2003, 2004). Creating a benthic boundary layer sub-model for an unstructured grid model (e.g. ELCIRC) remains an open issue. Beyond resolving the downslope propagation and entrainment of the underflow, effective modeling must capture the destruction of the underflow by wind and current-driven turbulence. The destruction of thin-layer stratification must be modeled at relatively coarse grid resolutions (i.e. 10 to 15 grid cells in the water column). The

new vertical mixing model theory provides a framework for to representing the mixing energetics when the grid resolution is too coarse to represent sharp density discontinuities.

FUTURE WORK

Issues of hypoxia in Corpus Christi Bay have led to an NSF project entitled “An Environmental Information System for Hypoxia in Corpus Christi Bay” on which Hodges is a co-PI with B. Minsker (U. Illinois), D. Maidment (Univ. of Texas), J. Bonner (Texas A&M), and P. Montagna (Univ. of Texas). This NSF project (funded Aug 2006 - Aug 2008), will include continued development of 3D hydrodynamic modeling of Corpus Christi Bay. We will be using the unstructured grid model ELCIRC (Zhang et al. 2004) as modified by TWDB (TXELCIRC). The Kulis (2005) underflow model will be coupled with ELCIRC during this project. The vertical mixing model will be further developed, implemented and tested in ELCIRC under a TWDB contract with Hodges in FY07, thereby completing Tasks 2 and 3 of the original SOW. We are also pursuing a NOAA Coastal Hypoxia Research Program grant for field work to further quantify the physics of vertical mixing in Corpus Christi Bay.

This page intentionally left blank.

APPENDIX A Field studies of Corpus Christi Bay, 2005¹

A.1 Introduction

Corpus Christi Bay is located on the Texas coast, adjacent to the city of Corpus Christi (Figure A.1 and, A.2). This water body has an area of 434 km² (Ward 1997), and an average depth of 3.2 meters (Orlando et al. 1991). The bay is microtidal (typical tidal amplitudes varying from 150 to 600 mm in the summer) and subject to strong meteorological forcing (Ward 1980) by winds, which may routinely peak at 7-10 m/s in summer (according to measurements herein).

The National Estuary Program (NEP, part of US Environmental Protection Agency) was established by Congress in 1987 to improve the quality of estuaries of national importance. Corpus Christi Bay was designated as a National Estuary in 1992, and the Coastal Bend Bays National Estuaries Program (CCBNPEP, the NEP including Corpus Christi Bay) was created. The State of Texas has continued to support the Coastal Bend Bays Estuary Program (CBBEP), a non profit organization whose goal is to protect the health of the bays while supporting their economic growth.

The construction of a water desalination plant is being considered near Corpus Christi Bay, as a demonstration initiative funded by the State of Texas to determine whether desalination is a practical approach to obtaining a drought-proof water supply. Unfortunately, desalination plants discharge brine (i.e. hypersaline water) in the process of creating fresh water. Existing hypersaline water inflows to Corpus Christi Bay from adjacent waters are suspected to enhance density stratification in the water column (Applebaum et al. 2005). Stratification is often correlated with hypoxia (in Mobile Bay, Alabama (Turner et al. 1987), in Pamlico River Estuary, North Carolina (Stanley and Nixon 1992), in Corpus Christi Bay (Applebaum et al. 2005; Ritter and Montagna 1999; Ritter and Montagna 2001). Therefore the desalination brine could possibly affect the development of hypoxia. Episodic hypoxia was first documented in Corpus Christi Bay in 1988 (Montagna and Kalke 1992) and was reported most years since then (Ritter and Montagna 1999). Thus, there remains an open question as to whether disposal of desalination brine into Corpus Christi Bay would have negative ecological effects.

Corpus Christi Bay hypoxia has been documented, but its physical causes have not been clearly identified. Hypoxia in Corpus Christi Bay is usually an overnight or early morning phenomenon, and its duration is generally on the order of an hour (for more than 50% of the hypoxic events measured in 1999 and 2000, (Ritter and Montagna 2001). In Mobile Bay, Alabama (also shallow: 1-6 m depth), Turner found the order of magnitude for period of stratification and mixing to be as small as a day, if not hours (Turner et al. 1987). As a consequence, short-term study of hypoxic events can lead to an improved understanding of their development and disappearance.

¹ Appendix A is substantially the M.S. thesis of Cedric David and the associated online technical report: David, C.H. and B.R. Hodges, *Deployment of a microstructure profiler in Corpus Christi Bay*, CRWR online technical report 06-07, August 9, 2006. Available online at <http://www.crwr.utexas.edu/online.shtml>

There is a need to understand the physical conditions leading to temporary stratification and hypoxia in a bay which is generally vertically mixed and has no long-duration dissolved oxygen (DO) problems. The episodic hypoxia is associated with a stable layer of high-salinity water and is arguably controlled by hydrodynamics. While the stratification phenomenon studied herein has only been demonstrated within a specific area of Corpus Christi Bay, the results are likely applicable to understanding the fate of brine reject water from desalination plants sited on other Texas estuaries and embayments.

To investigate stratification on short time scales, measurements were taken at two different areas in Corpus Christi Bay (near Oso Bay and Laguna Madre) using a variety of instruments (microprofiler, weather stations, water quality profiler, etc.) during four field trips that were conducted during the summer of 2005.

A.2 Research Objectives

The present study investigates the short-time scale physics of density currents entering Corpus Christi Bay from the adjacent upper Laguna Madre and Oso Bay. There are two principal objectives to this work: 1) document the temporal and spatial behavior of salinity and temperature near the outlet of Laguna Madre where hypoxia has previously been recorded; and 2) develop new data processing, display and analysis methods for the SCAMP microstructure profiler. Note that this research project is not intended to provide a conclusive demonstration that high-salinity density currents are directly linked to hypoxia, but is instead building the foundations for future analysis of this problem.

A.3 Background

In the open waters of a shallow bay (e.g. Mobile Bay, Alabama: average depth of 3 m), vertical mixing due to wind, tidal shear and river inflows usually occurs frequently enough to control the spatial and temporal extent of low oxygen events (Turner et al. 1987). Since Texas bays are usually shallow, windy and well mixed, hypoxia should not be expected based on the Turner et al. 1987 definition; however, it has been reported in isolated locales as far back as 1942 in Galveston Bay (Gunter 1942), and has more recently been extensively documented in Corpus Christi Bay by Montagna and coworkers at the University of Texas Marine Science Institute (UTMSI) (Applebaum et al. 2005; Montagna and Kalke 1992; Morehead and Montagna 2003; Morehead and Montagna 2004; Ritter and Montagna 1999; Ritter and Montagna 2001).

Hypoxia creates physiological stress that is poorly tolerated by most animals (Ritter and Montagna 1999). Estuarine hypoxia is commonly defined as dissolved oxygen (DO) concentrations below 2 mgL^{-1} (Dauer et al. 1992); however, Ritter and Montagna (1999) have shown that the appropriate definition of hypoxia for Corpus Christi Bay is $\text{DO} < 3 \text{ mgL}^{-1}$, which is the threshold for measurable negative ecological effects in this bay. Hypoxia occurs in summer, predominantly in the southeast region of Corpus Christi Bay (the area surrounded by a solid line in Figure A.3, taken from Ritter and Montagna 2001) and typically only in the bottom waters, i.e. 1 to 2 m above the bottom (Ritter and Montagna 2001). Hypoxic events are predominantly intermittent, locally developing and persisting on the order of hours (Ritter and Montagna 2001) rather than days or weeks.

Stratification, defined as a persistent vertical density gradient, has been linked to hypoxia in Corpus Christi Bay (Applebaum et al. 2005; Ritter and Montagna 1999; Ritter and Montagna 2001). Stratification inhibits vertical mixing, which prevents DO introduced at the water surface from penetrating through the water column. Thus, stratification effectively isolates the sediments and the lower part of the water column, so that biogeochemical oxygen demand may deplete available DO. Stratification can be a particular problem during the summer because of high respiration (Stanley and Nixon 1992). It has been postulated that water column stratification impedes mixing processes and is a key factor in the onset of hypoxia in Corpus Christi Bay (Applebaum et al. 2005; Ritter and Montagna 1999; Ritter and Montagna 2001). Several related hypotheses about the physical processes have been raised to explain stratification in Corpus Christi Bay. First, there is minimal circulation of the water in the southeast region of the bay (Ritter and Montagna 1999) which limits the exchange of water. Second, episodic low wind speeds are considered a factor, as high speed winds help mix stratification and replenish oxygen, while low speed winds tend to allow persistent stratification (Morehead et al. 2002). Third, it is known that stratification can be enhanced by high evaporation rates (Turner 1973), but whose relationship to Corpus Christi Bay hypoxia has not been studied. Finally, gravity currents of denser waters (presumably from hypersaline Laguna Madre) are suspected to play a role (Ritter and Montagna 1999).

A.4 Experimental Methods

A.4.a Introduction

Prior physical/hypoxia studies of Corpus Christi Bay have principally concentrated on the longer time-scale physics associated with hypoxia (Applebaum et al. 2005; Montagna and Kalke 1992; Ritter and Montagna 1999; Ritter and Montagna 2001). However, the development and destruction of stratification may be attributable to shorter time-scale phenomena, e.g. daily cycles of tides, evaporation and wind mixing. To address the gap in our knowledge, a program of field measurements was designed and conducted during the summer of 2005. In the following section of this appendix, geographical location, methods, equipment and data collection missions are described.

A.4.b Geographical information

Corpus Christi Bay is located in the south part of the Texas Coastal Bend (see Figure A.1). Corpus Christi Bay is surrounded by the counties of Nueces and San Patricio (see Figure A.2).

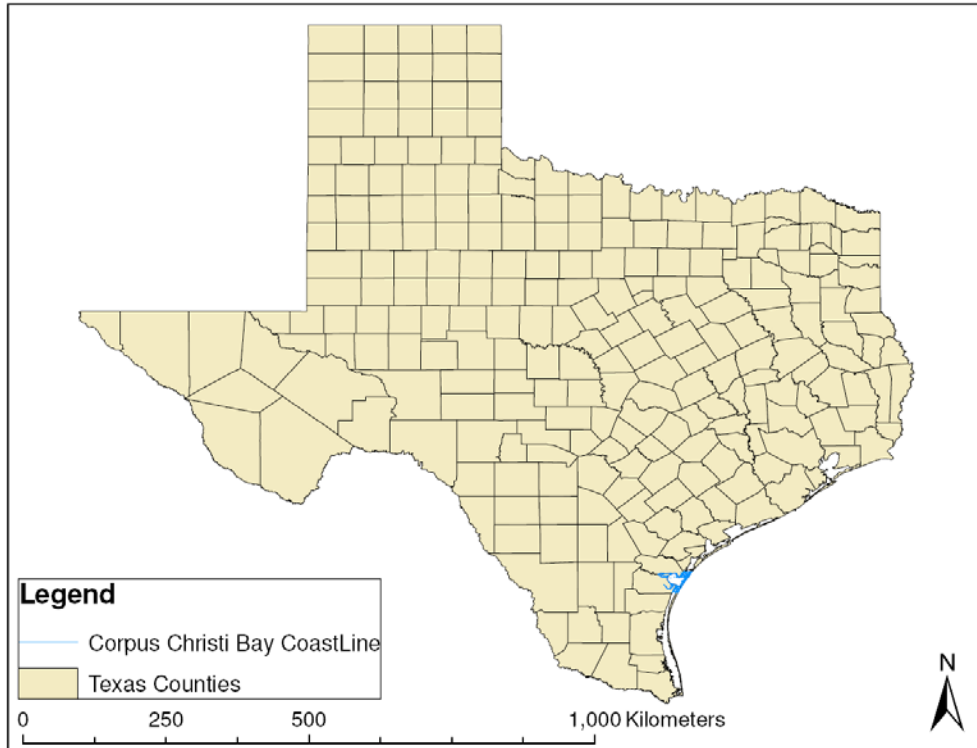


Figure A.1 Location of Corpus Christi Bay in the State of Texas

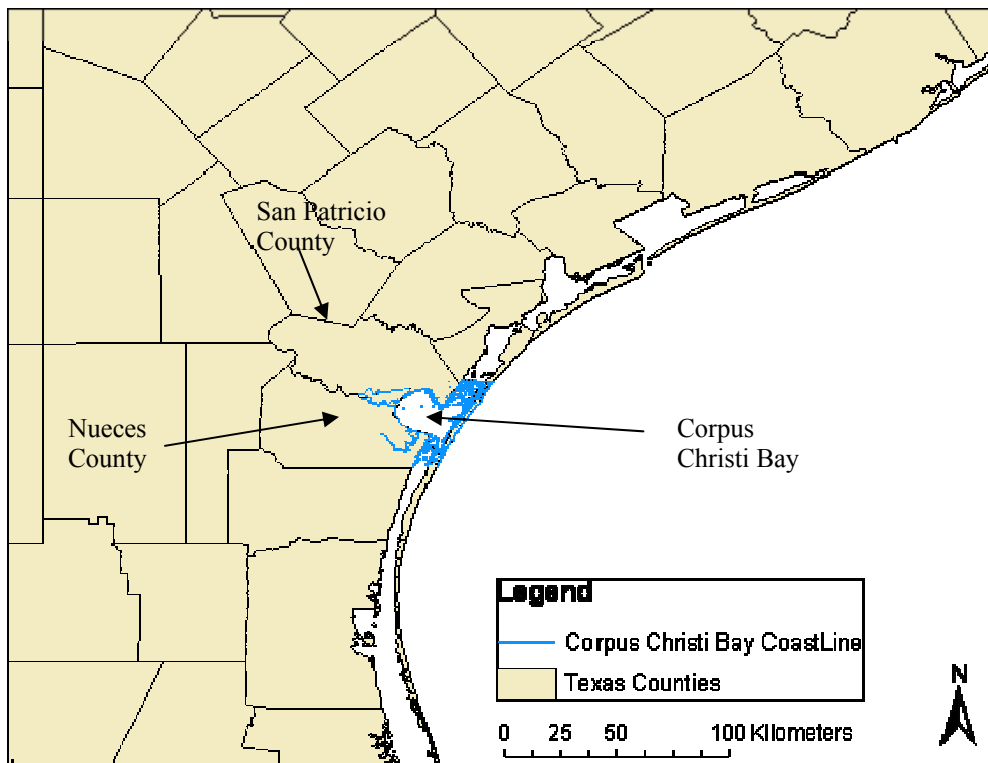


Figure A.2 Corpus Christi Bay and surrounding counties

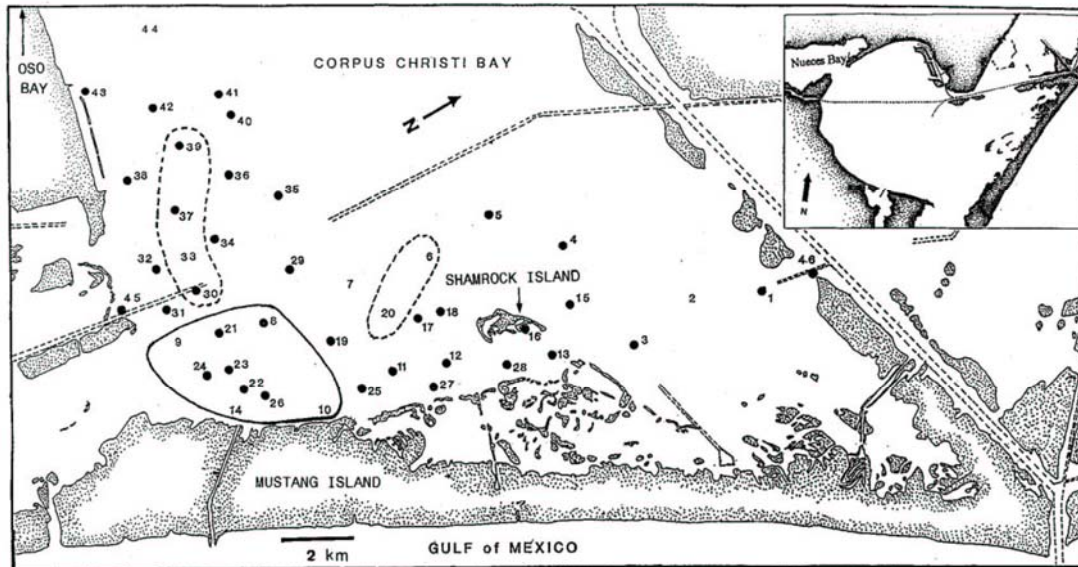


Figure A.3. Documented hypoxia in Corpus Christi Bay. Solid lines are areas with documented hypoxia, $DO < 2.0$ mg/L; dashed lines are areas that are argued to be effectively hypoxic with $DO < 3.0$ mg/L. From Ritter and Montagna (1999) their Figure 6.

Freshwater inflows, ocean inlets and channels are the main water exchange sources for Corpus Christi Bay. The principal sources of freshwater inflow are the Nueces River and Oso Creek; the latter draining into Oso Bay along the southern boundary of the bay (Figure A.4). According to USEPA (1999), Corpus Christi Bay has a 49700 km² drainage area, an average daily freshwater inflow of 34 m³/s and an average salinity of 22 ppt. Although the bay is considered shallow — average depth of 3.2 meters (Orlando et al. 1991) — relative to estuaries along the eastern and western coasts of the USA, it is one of the deepest bays on the Texas coast (Ward 1997). At its northern end, Corpus Christi Bay is connected to Aransas Bay via the Gulf Intracoastal Waterway (GIWW), which continues through the bay and into the Upper Laguna Madre at the southern end of Corpus Christi Bay. The bay is separated from the Gulf of Mexico by Mustang and North Padre Islands, which are low barrier islands typical to the North American Gulf coast. Aransas Pass (northeast end of the bay) is the main water inlet connecting Corpus Christi Bay and the Gulf of Mexico. Other inlets have been temporarily opened (Corpus Christi Pass, Corpus Christi fish pass, etc.) but are now closed by sand. Corpus Christi Bay is also connected to Aransas Bay (through Aransas Channel and Lydia Ann Channel) and Baffin Bay (through Laguna Madre). The re-opening of Packery Channel, a tidal inlet into the Upper Laguna Madre (project directed by US Army Corps of Engineers, started in Oct. 2004, still in progress), is providing another source of water exchange with the Gulf of Mexico.

The demonstration water desalination plant that is being considered by the State of Texas would be co-located with the Barney Davis power plant for efficiency and economy. The power plant is located between Upper Laguna Madre and Oso Bay (Figure A.4). The Barney Davis power plant was built in 1975 (G. Ward, pers. comm.). The inlet water for the proposed desalination plant would be pumped from Laguna Madre using the existing power plant inlet piping and the brine would be discharged into Oso Bay through the existing power plant discharge piping.

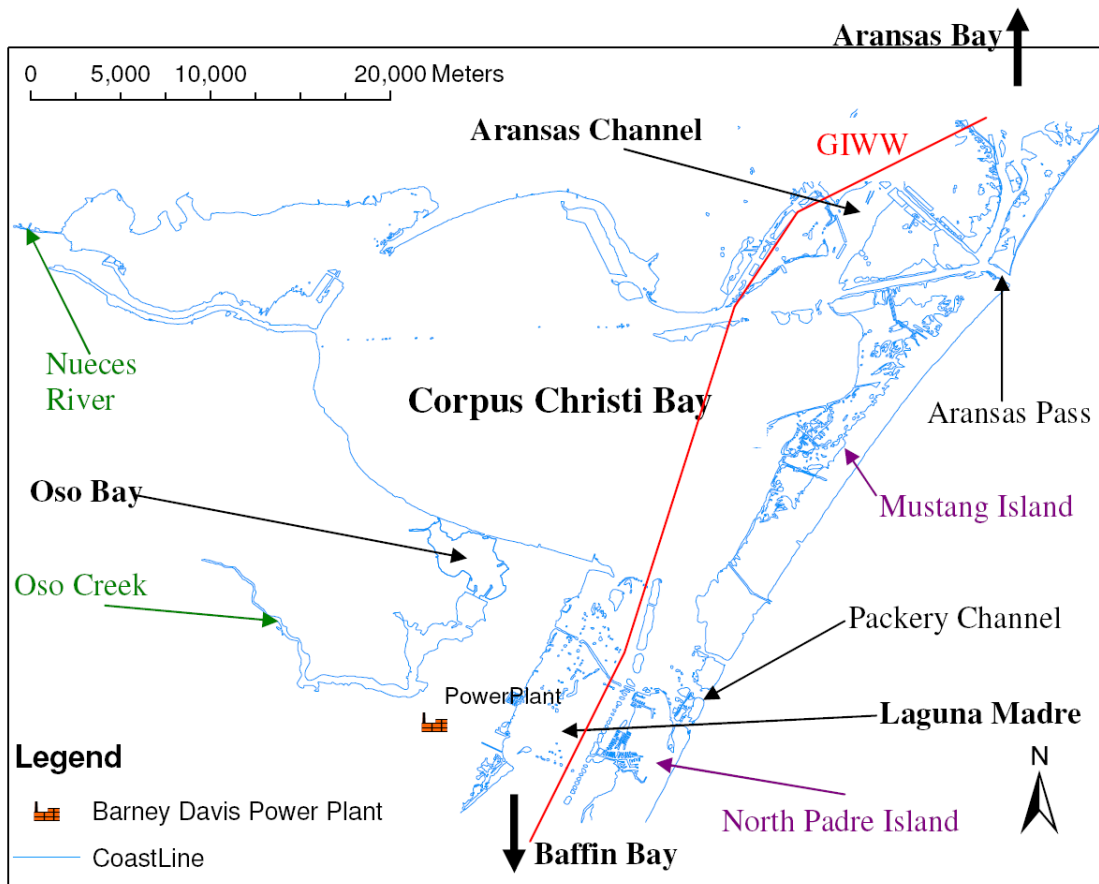


Figure A.4 Principal features around Corpus Christi Bay

A.4.c Overview of the experimental methods

Field experiments were conducted over short time scales (intensive sampling for one or two days) and limited spatial scales (< 5 km) to capture the development of dense gravity currents created through the daily salinity and heating/cooling cycles. The experiments were focused on two zones in Corpus Christi Bay near the connections to Upper Laguna Madre (Site A as shown in Figure A.5) and Oso Bay (Site B as shown in Figure A.5). The selection of the area near the Upper Laguna Madre was based upon the previous documentation of hypoxia in this region (Ritter and Montagna 1999). The selection of the area near Oso Bay was to determine if the outflow from this bay could create stratification that allows hypoxia development.

Four missions (each of two to three days) were conducted in the summer of 2005, with the help of 10 people. In order to gain a good understanding of physical behaviors in both sites A and B, detailed vertical and horizontal resolution was obtained over small distances (less than 5 km), with short time scales (few hours to a day).

Vertical profiling was conducted at selected locations (between 5 and 10 locations per day) that were repeated several times during the day (3 to 6 times depending on the weather conditions, the duration of the mission and the number of locations). This profiling method enabled the documentation and analysis of both spatial and temporal changes in the water column at selected sites.

The principal measured variables were temperature, salinity and dissolved oxygen as a function of depth. Secondary variables (wind speed, tidal elevation) were also measured and/or obtained from other sources. Temperature and salinity were used to compute water density to examine the water column stratification that affects mixing and hypoxia. DO concentration measurements allow determination of the oxygen conditions (anoxic = no oxygen; hypoxic = low oxygen concentration). Winds and tides were documented as they generally play a role as driving forces in the mixing process.

Sampling locations at Site A included positions previously sampled by UTMSI (33, 34, 37, 39 and 42 in Ritter and Montagna 1999, named here A033, A034, A037, A039 and A042) and new positions (A101, A102, A103, A104, A105) to provide finer spatial resolution (700 m to 1 km between neighbor locations). Sampling locations at Site B (with distance between neighbor locations ranging between 100 m and 500 m) were newly identified for the purpose of this study. At each sampling location, sampling time was typically 10 minutes. A single SCAMP profile typically required 50 seconds whereas Manta profiles typically required 5 to 10 minutes (depending on depth). An interval of approximately 20 minutes was required between sampling sites (including travel time and boat positioning). The vertical profile resolution was approximately 1 mm for the microstructure profiler (SCAMP) and 30 cm for the water quality profiler (Manta). Both instruments are described below.

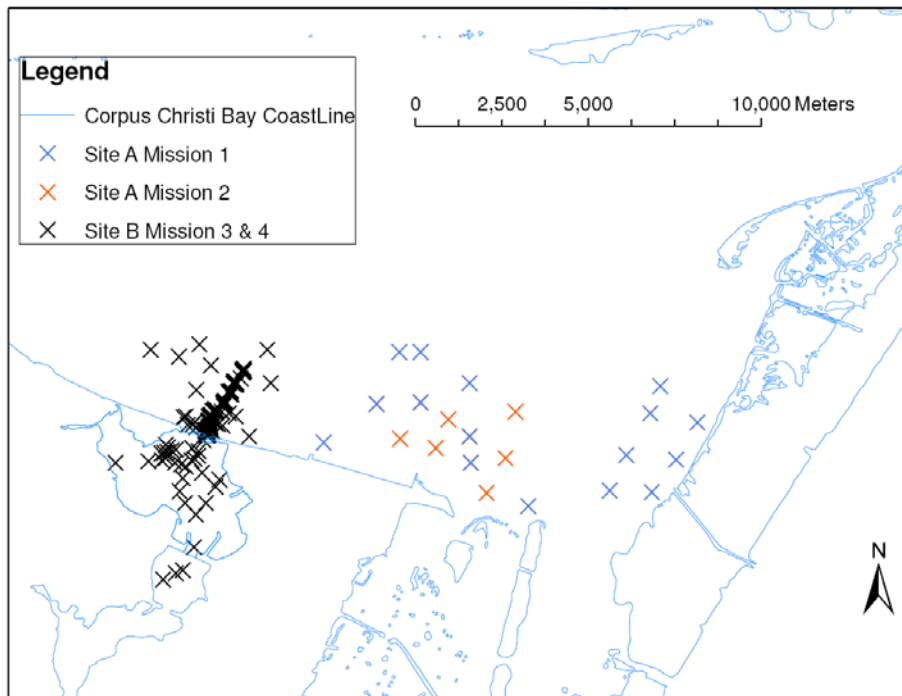


Figure A.5 Map of all the sampled locations

A.4.d Equipment

For the purpose of our project, various pieces of equipment were used: two boats, two water profiling instruments (one water quality profiler and one microstructure profiler), two GPS receivers and two weather stations. The equipment is described in the following sections of this appendix.

A.4.e SCAMP

Microstructure profiling was conducted using the Self Contained Autonomous MicroProfiler (SCAMP), which is manufactured by Precision Measurement Engineering Inc. (PME, based in California) in cooperation with the Centre for Water Research (CWR, part of the University of Western Australia).



Figure A.6 SCAMP (from <http://pme.com/scamp.htm>)

The SCAMP is a portable, lightweight microstructure profiler designed to measure extremely small scale (order 1 mm) fluctuations of temperature and salinity. The fine-scale changes of temperature with depth (i.e. the temperature gradient), provide information on active mixing. The fine-scale measurements provided by the SCAMP allow computation of temperature and salinity gradients that indicate turbulent overturns in the water column. The SCAMP was used to measure temperature (with two fast and one accurate sensors), electrical conductivity (with one fast and one accurate sensor), photo active radiation (one PAR sensor), fluorescence (one fluorometer) and turbidity (one turbidity sensor). The fast sensors are used with the SCAMP to provide gradients of temperature and salinity at the millimeter scale. These sensors have a fast response but do not have the absolute accuracy of the accurate sensors. The accurate sensors are used to provide higher quality measurements of temperature and salinity. The Matlab based software supplied with the SCAMP allows the user to upload, record, view, and analyze measurements (see Figure A.7).

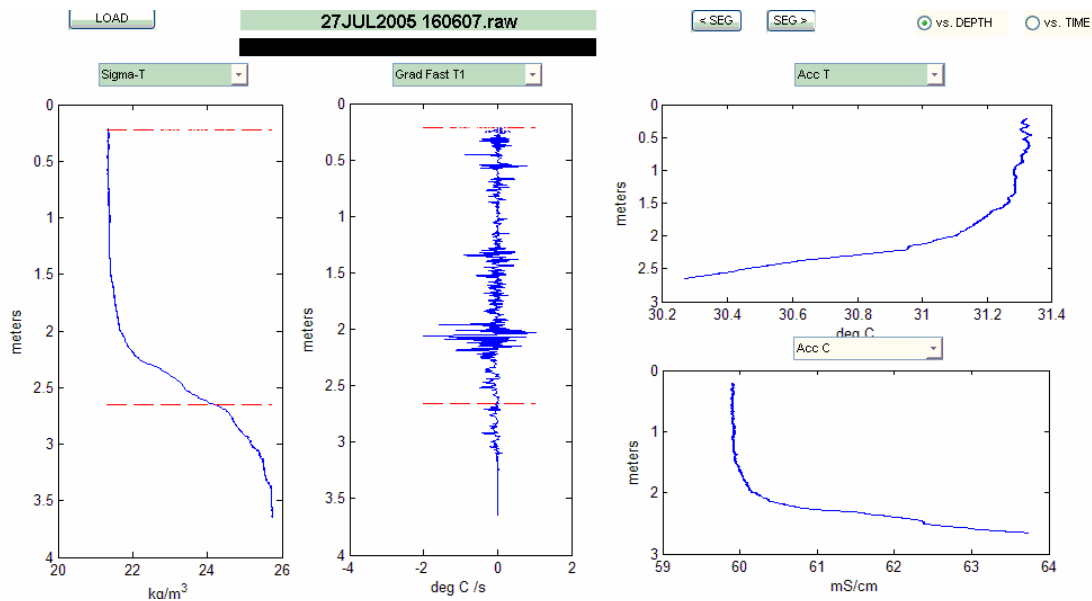


Figure A.7 Example of SCAMP plot obtained with the software provided by PME. July 27 2005.

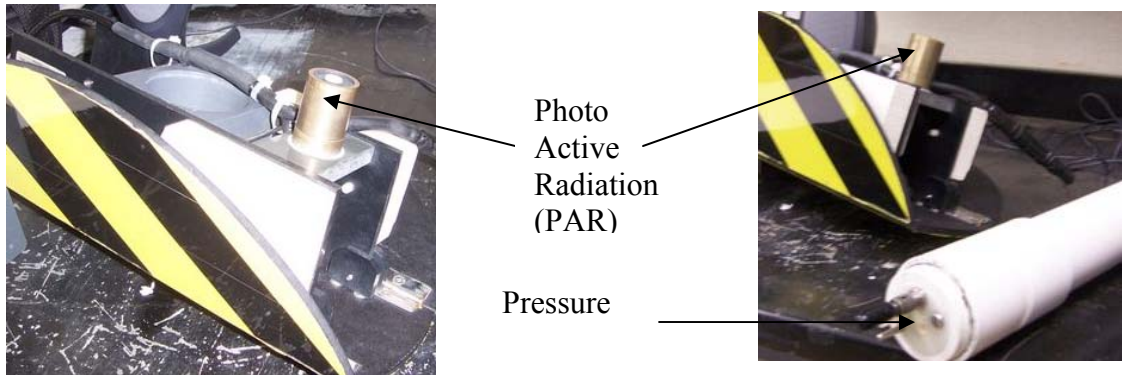
The SCAMP is free falling; the depth is continuously recorded and is computed based upon pressure sensor measurement. The instrument is quite tall (around 1 m) and cannot be practically deployed in depths shallower than 2.5 m. The SCAMP was deployed only at Site A because some areas in Site B were deemed generally too shallow to obtain effective measurements. The SCAMP is tethered by a string for retrieval after deployment, but is otherwise autonomous; it is battery-operated and executes a pre-programmed measurement sequence. Pre-programming sets the number of datapoints recorded in the water column, start time and/or start depth and end time and/or end depth.

While the SCAMP can be deployed in either a downwards mode (sinking down with weights) or an upwards mode (floating up with buoyancy rings), the present work used only the downwards mode as the focus is on the turbulence near the bottom that affects stratification. The ideal travel rate for the SCAMP is near 10 cm/s. This rate has to be checked every measurement

day, and adjusted by adding floats or weights to the instrument body. Because the instrument takes several tenths of a second to reach a consistent falling speed after deployment, the initial second (corresponding to the first 10 cm at the 10 cm/s fall rate) of the SCAMP data deployment may be unreliable. In the present work, it was observed that the data recorded in the initial second of the deployment appeared to have some of the greatest differences between profiles. Therefore it is preferable not to use the data obtained at the surface (from 0 to 10 cm deep) in downwards mode and the data from the bottom (from the deepest measurement point to 10 cm above) of the water column in upwards mode. Thus, the initial 10 cm of data was filtered out in the present data analysis. This research is focused on the stratification near the sediment, therefore the data measured near the bottom needed to be reliable and the downwards mode was used. It should be noted that the SCAMP temperature and conductivity sensors are approximately 75 cm below the pressure sensor, so the good instrument data typically begin 85 cm below the water surface. Because the SCAMP drifts horizontally with the currents during deployment, the actual location of the SCAMP during data collection is not precisely at the boat location. Based on visual estimates of line deployed and visible surface drift, the SCAMP typically remained within about 10 to 20 m of the boat location.

The SCAMP supports multiple sensors. In this research, the focus is on temperature, conductivity and pressure measurements (see Section A.6.b). Temperature sensors have a characteristic temporal response. The thermal time constants corresponding to the fast temperature sensors and the accurate temperature sensor on the SCAMP are respectively 0.007 s and 0.2 s. Usually, the shorter the thermal time is, the faster the sensor responds, but the less accurate it is. Conductivity sensors have a characteristic spatial response. The space constants are 2.5 mm and 15 mm for the fast and accurate conductivity sensors, respectively. Conductivity sensors with smaller space constants are faster but less accurate. The SCAMP takes a measurement every 10 ms (corresponding to 1 mm at the 10 cm/s fall rate). The pressure sensor used for depth computation gives an accuracy smaller than 1 mm. Fast sensors are designed to react quickly, so their output is suitable for computing small-scale gradients of a measured variable. Accurate sensors are used to obtain the profile of a measured variable, but cannot be used to compute small-scale gradients.

Figure A.8 shows the location of each mounted sensor on the SCAMP and Figure A.9 shows how the instrument is deployed.



Laser Turbidity

Chlorophyll Fluorometer

Fast Temperature 2

Accurate Conductivity and Temperature (AccC and AccT)

Fast Conductivity

Fast Temperature 1

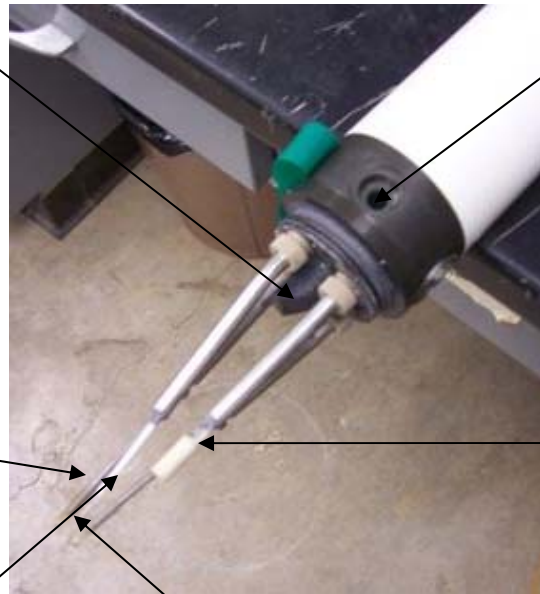


Figure A.8 Positions of sensors on SCAMP

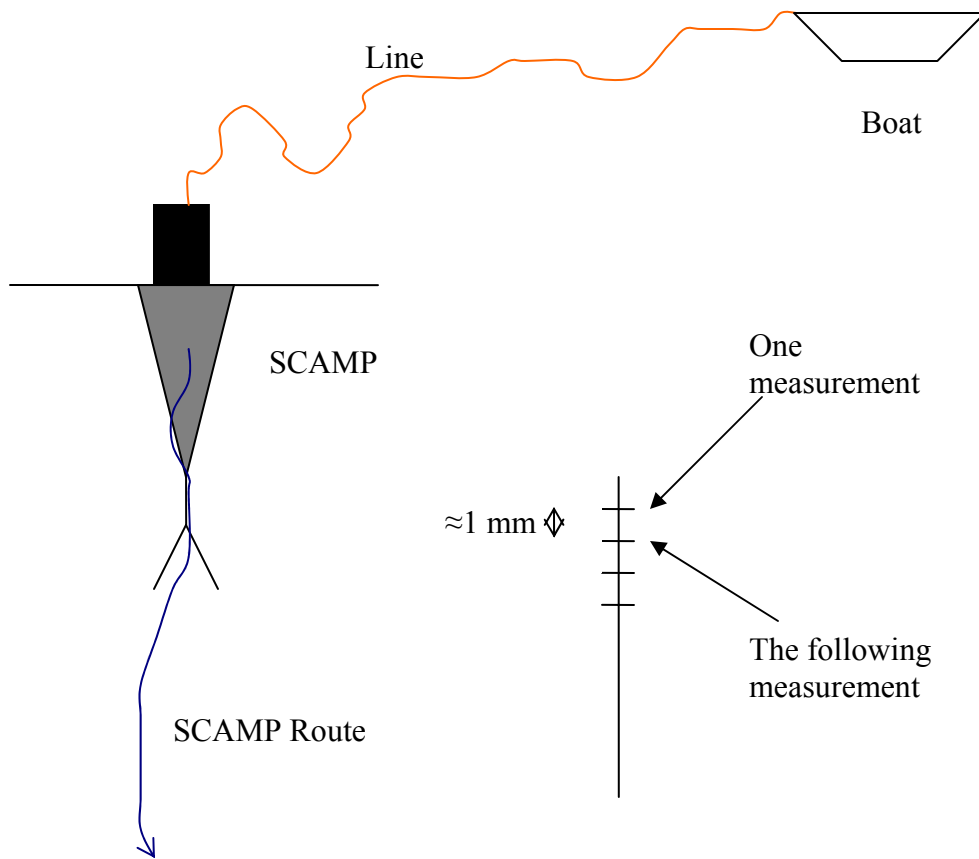


Figure A.9 Deployment of SCAMP (not to scale)

A.4.f Manta

Manta instruments are designed and manufactured by Eureka Environmental Engineering, and are used to measure parameters typically important in water quality investigations. In this investigation, two similar Manta instruments were used. One instrument was provided by the Texas Water Development Board (TWDB) and was deployed with the supervision of their personnel. A second instrument was provided on loan from Eureka for part of the experiments.



Figure A.10 Manta (from <http://www.eurekaenvironmental.com>)

The Mantas that were used have five sensors, measuring temperature, conductivity, pH, pressure and Dissolved Oxygen (DO) concentration. A cable connects the Manta to a handheld computer that records the data. The same cable may be used to lower the instrument to the desired sampling depth, or (as in the case of the TWDB instrument) an additional line may be added to limit forces on the cable connections. The Manta (whose length is 50 cm) is smaller than the SCAMP and is deployed by hand. Unlike the SCAMP, only the bottom part (10 cm) of the Manta needs to be immersed in water to take measurements. Hence the Manta can take measurements in 10 cm of water. The size of the Manta and its deployment technique enable Manta profiling in shallow waters. The Manta was preferred for part of the experiment because it measures DO concentration (the SCAMP does not) and can be used in shallow waters. However, unlike the SCAMP, the Manta cannot be used to measure small-scale gradients and as a consequence cannot be used to infer turbulence characteristics. For effective use of manpower (not enough human resources were available to deploy both the SCAMP and the Manta during the 48 hour experiment) only the Manta was deployed at Site B because it can be used in shallow waters and can measure DO.

The Manta data collection is conducted by lowering the instrument to a desired depth, waiting for the instrument readings to stabilize (~10 s, sometimes longer), recording; then lowering to another depth. The stabilization time is necessary because the DO sensor does not respond quickly (which is why SCAMP DO sensors are still in the research stage). Thus, the Manta collects data at depths selected by the user. Measurements were taken at approximately 15 cm (6 in) intervals over most of the water column, with additional measurements at the bottom and approximately 5 cm off the bottom (Figure A.11 shows how the instrument is deployed). The vertical resolution of the profiles obtained with the Manta is approximately 15 cm. Because the Manta depth is being controlled by a person in a boat, the instrument may move up and down slightly with the boat. In the presence of waves, it is difficult to hold the Manta at a

steady depth. Vertical excursions of the instrument during deployment are estimated as between 2 cm (calm conditions) to about 10 cm (rougher conditions). Due to malfunction of the pressure sensor on the TWDB Manta during most of the deployments, the depth was estimated using marks on the deployment line. The formal depth measurement accuracy for the Manta pressure sensor is 1 mm; however, for the depth measurements based on the deployment line, an accuracy of ± 5 cm is a more reasonable estimate. The accuracies of the other main Manta sensors are 0.08°C for temperature, 0.2 mg/L for DO, and 1 mS/cm for conductivity.

A single Manta deployment was performed at each location of Site B (Figure A.5). Figure A.12 shows an example plot created from data collected with the Manta along the transect shown in Figure 2. Nine Manta profiles at nine locations (B300 to B308) were used to draw this spatial contour plot of the dissolved oxygen concentration. All deployments were done on August 22nd 2005 between 1703 and 1806 hours.

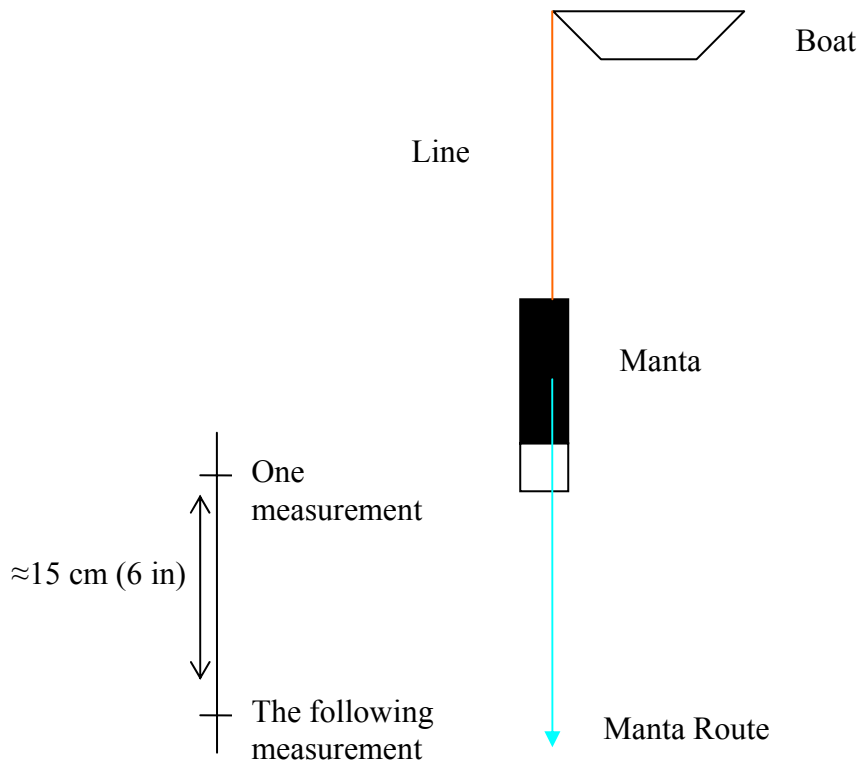


Figure A.11 Deployment of Manta

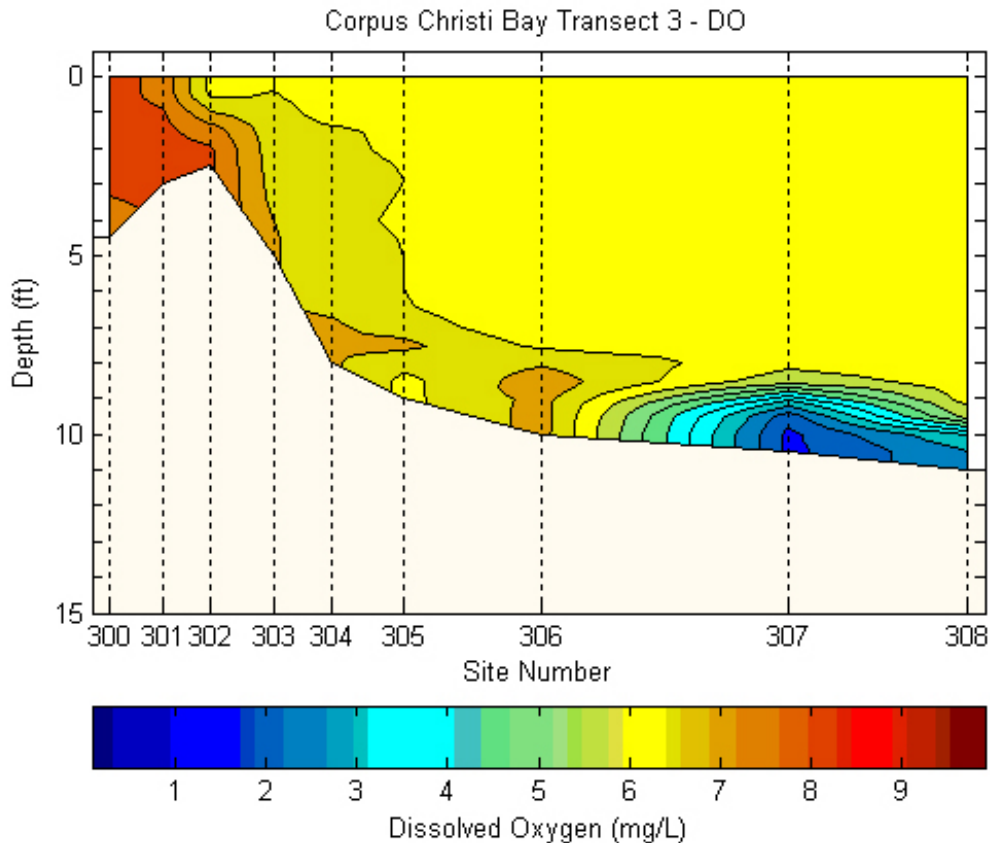


Figure A.12 Sample graph of the data produced by the Manta (plot created by Jordan Furnans)

A.4.g GPS receivers

Two different GPS receivers were used during the missions. A Magellan Meridian Marine GPS unit was used for most of the SCAMP deployments. This unit has the standard GPS accuracy of within 3 meters or better (assisted by the U.S. Wide Area Augmentation System WAAS).



Figure A.13 Magellan Meridian Marine (from <http://www.magellangps.com/>)

A more accurate GPS receiver was available on the TWDB boat used during some SCAMP deployments and the majority of the Manta deployments. The GPS Pathfinder Pro XRS receiver is designed for GIS data collection and data maintenance. This receiver has accuracy better than 1 m.



Figure A.14 Trimble GPS (from <http://www.trimble.com/>)

The GPS receivers were used to position the boat near the deployment site and record the actual position of the boat during the deployment. Because the boat position is affected by wind, current, anchor location and length of the anchor rope, the deployment position was typically within about 10 to 40 m of the target site. The average distance between the first deployment position and the target site was computed to be 43 m. Only four first deployment positions were more than 100 m away from the target site (on July 27th: A101 at 1720 hours; on July 28th A101 at 0424 hours, A042 at 1420 hours and A104 at 1520 hours). Another difficulty was caused by dragging anchor (due to current, wind and waves), but only a few times did this occur. Dragging anchor was reported on the log book for locations A042, A102, A103 and A104 on July 28th between 1420 and 1520 hours. Inglefield anchors were used in both boats.

A.4.h Weather Stations

A hand-held weather station (Kestrel 4100) and a land-based weather station (CES weather station) were both used in this study. The Kestrel 4100 measures air speed, temperature and humidity, and stores these measurements in flash memory. Additional measurements of dew point, wind chill and heat stress index can be taken, but were not considered relevant to the present work. The Kestrel does not provide wind direction. Data points were recorded manually at each deployment location. To use the instrument, the operator stood at the front of the boat, facing the wind and stored four consecutive measurements (approximate time of 10 s between each). The distance between the measurement point and the water surface water was visually estimated as on the order of 2.5 m. The instrument was oriented towards the strongest wind, requiring personal interpretation for alignment. Figure A.15 shows a picture of the Kestrel 4100.



Figure A.15 Kestrel 4100 (from <http://www.nkhome.com/>)

The land-based weather station was manufactured by Coastal Environmental Systems (CES) and uses their Zeno 3200 logger. For safety and security, the weather station was first deployed within sight of the ranger's office at Mustang Island State Park (see Figure A.16). After analysis of Mission 1 (see discussion below), the weather station was moved to an isolated location along the bay side of Mustang island (see Figure A.17). Locations Weather1 and Weather2 can be seen on Figure A.18.



Figure A.16. CES weather station at location Weather1



Figure A.17. CES weather station at location Weather2

The land-based weather station measures wind speed, wind direction, wind gusts (the highest wind speed over the sampling time), standard deviation of wind speeds, air temperature, relative humidity, solar radiation, barometric pressure, and rainfall. The recordings are based on an average of the measurements taken during the sampling time (10 s). The time between the samples was programmed differently during missions and between missions to optimize the data storage between downloads. The elevation of the sensors placed on the land based weather station is approximately 2.5 m above the ground surface.

Table A.1 shows the sampling times and the times between samples for the CES weather station.

Table A.1 Sampling time and time between samples for the CES weather station

	Location	Sampling Time	Time between samples
Mission 1	Weather1	10 s	0.5 min
Between Missions 1 and 2	Weather1	10 s	10 min
Mission 2	Weather2	10 s	1 min
Between Missions 2 and 3	Weather2	10 s	15 min
Mission 3	Weather2	10 s	1 min
Between Missions 3 and 4	Weather2	10 s	10 min
Mission 4	Weather2	10 s	2 min

The wind field over and near Corpus Christi Bay is subject to local effects as well as larger-scale weather patterns. As a consequence, the wind speeds measured with the land-based station did not always correlate with those measured on the boat. Qualitative comparison of data from the handheld and fixed weather stations is provided in Section A.5.b; further quantitative evaluation remains a subject for future investigation.

The weather data collected in these experiments was supplemented by data available from the TCOON (Texas Coastal Ocean Observation Network) observatory. The data used were downloaded from <http://lighthouse.tamucc.edu/pq>. In Corpus Christi Bay, the data from four TCOON stations are available at Texas State Aquarium, Ingleside, Port Aransas and Packery Channel. The station closest to the sampling locations with both wind and water elevation measurements is Ingleside. Therefore, Ingleside was chosen as the TCOON station to be used in this study. It is located at 27°49.3' N, 97°12.2' W (Figure A.18). The vertical station datum for water elevation measurements is located 0.717 m above the North American Vertical Datum 1988 (NAVD88). Figure A.18 shows the three locations of the two land based weather stations.

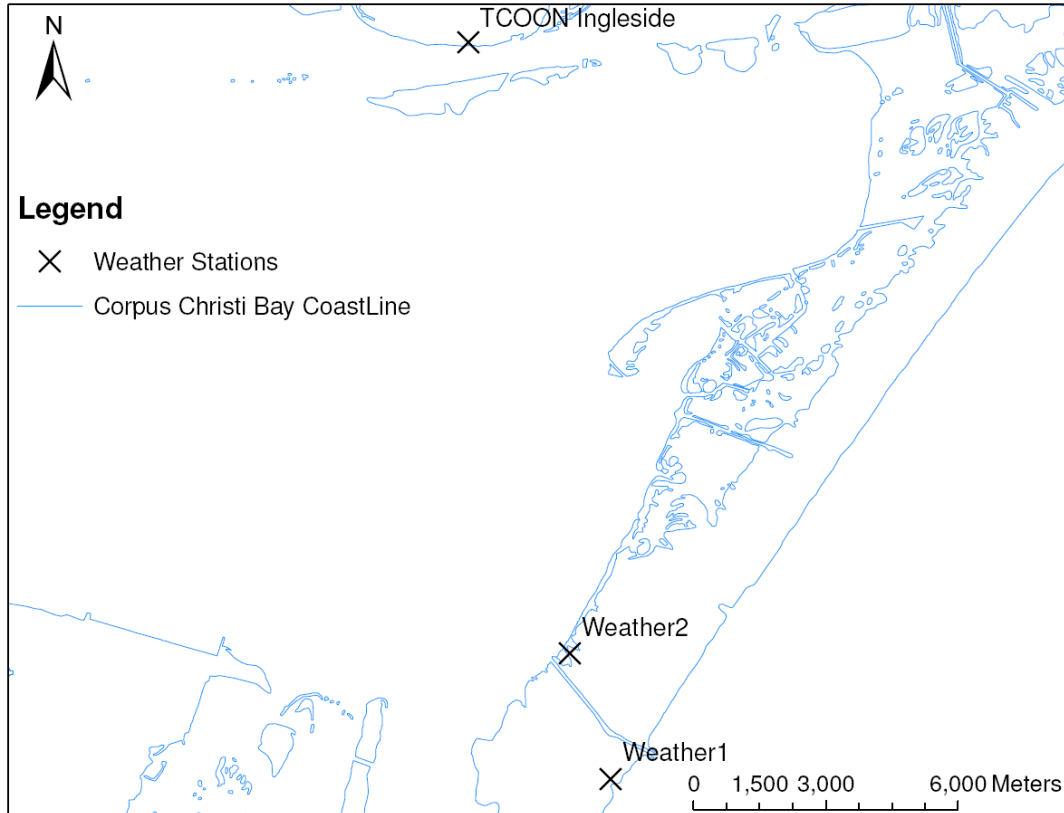


Figure A.18 The three locations of the two land-based weather stations

A.5 Description of the data collection missions

A total of four missions were conducted during the summer 2005. The two first missions were located at Site A. The purpose of the last two missions was to investigate Site B. In this section we will describe all missions.

A.5.a Mission 1: 07/05/2005 – 07/07/2005

DESCRIPTION AND GOALS

The goals of this mission were: 1) familiarization with the equipment in general and with SCAMP deployments in particular, 2) replacing the CES weather station, and 3) collection of SCAMP data at sites where UTMSI had previously sampled to provide guidance in developing future field experiments.

The people that participated in this field trip were Cédric David (UT), Jordan Furnans (TWDB) and Ben Hodges (UT). During this mission only the SCAMP was deployed. Both GPS receivers were used at different times during the experiment. The boat was deployed from the public boat ramp on the Laguna Madre side of Mustang Island at GIWW. The CES weather station was deployed on July 5th 2005 at 1300 hours at Mustang Island state park near the park office, location Weather1. Figure A.19 shows the locations of the boat ramp and the weather stations.

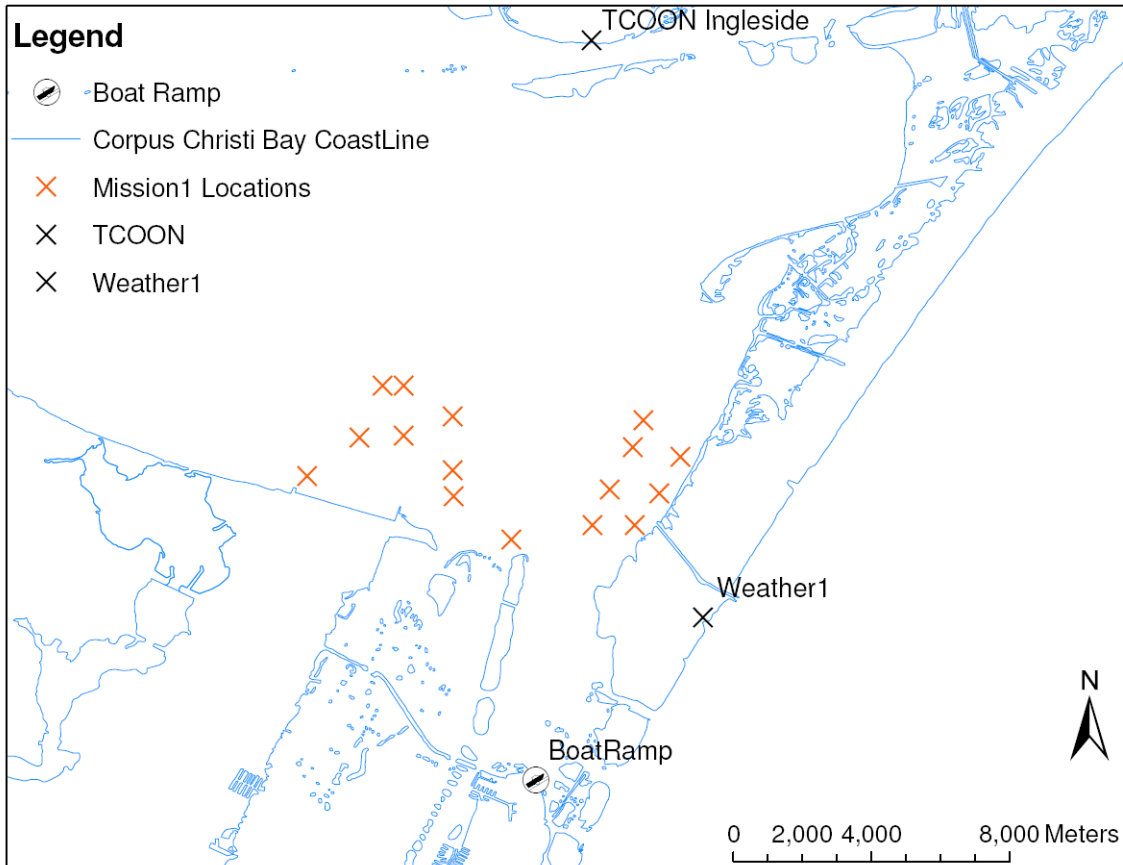


Figure A.19 Locations of boat ramp and weather stations

The boat was deployed between 1600 and 1900 hours on the 5th, between 0800 and 1400 hours on the 6th and between 0700 and 1500 hours on the 7th. One crew (with the three members cited above) was deployed on the 5th and the 6th. On the 7th, another crew was deployed (Cédric David and Ben Hodges). The weather was mostly sunny, and the water calm, without wind on the 5th and the 6th. On the morning of the 7th the wind speeds ranged between 6 and 10 m/s (recorded by the CES weather station at location Weather1) and the water became choppy with whitecaps. By early afternoon the wind waves began to build. By 1500 hours, further boat operations were deemed dangerous, so the experiment was discontinued. The CES weather station was checked after sampling on July 6th. The frequency of measurements was changed from every 30 s to every 10 min to allow enough memory for recording the next month of weather data. Figure A.20 shows the wind data recorded by the CES weather station at location Weather1 during Mission 1.

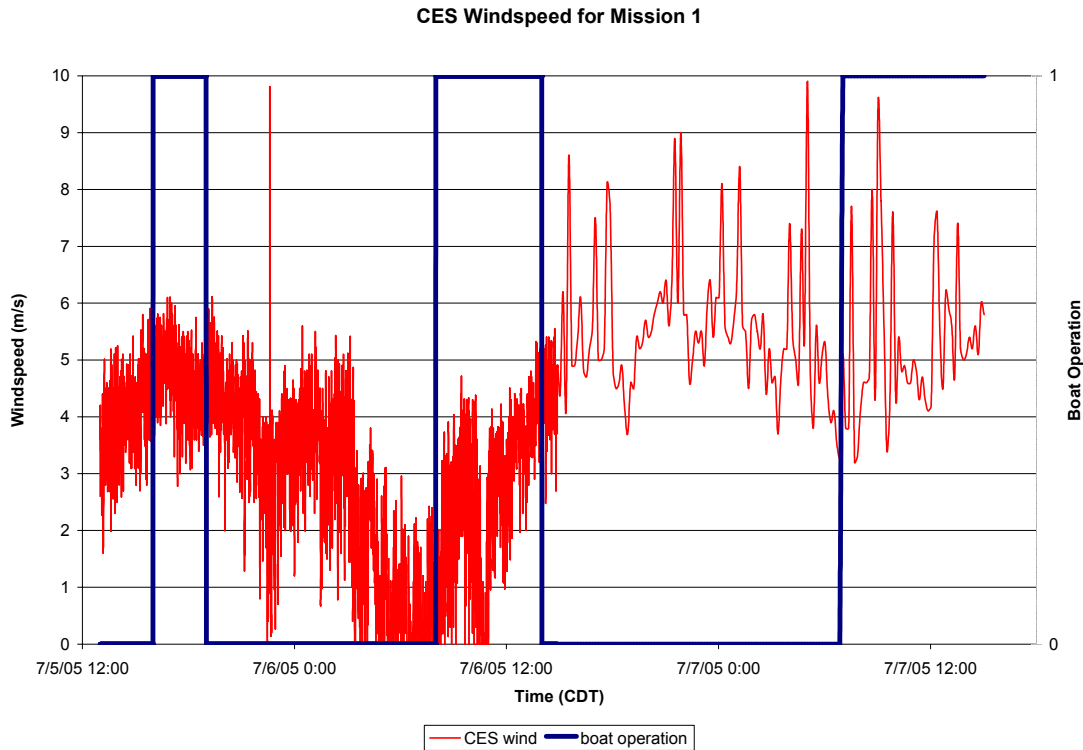


Figure A.20 CES wind data for Mission 1 (Location Weather1), with boat operation times. The data recorded by the CES are 10 second averages. Up until 7/6/05, the data were recorded at 30 second intervals, and then switched to 10 minute intervals to allow more data storage on the instrument.

LOCATIONS

Site A was investigated during this mission. Figure A.21 shows the locations where samplings were conducted. Location A104 was created as a result of one of UTMSI locations being uploaded incorrectly in the GPS receiver. Figure A.21 also shows Transect1 that was investigated for data analysis.

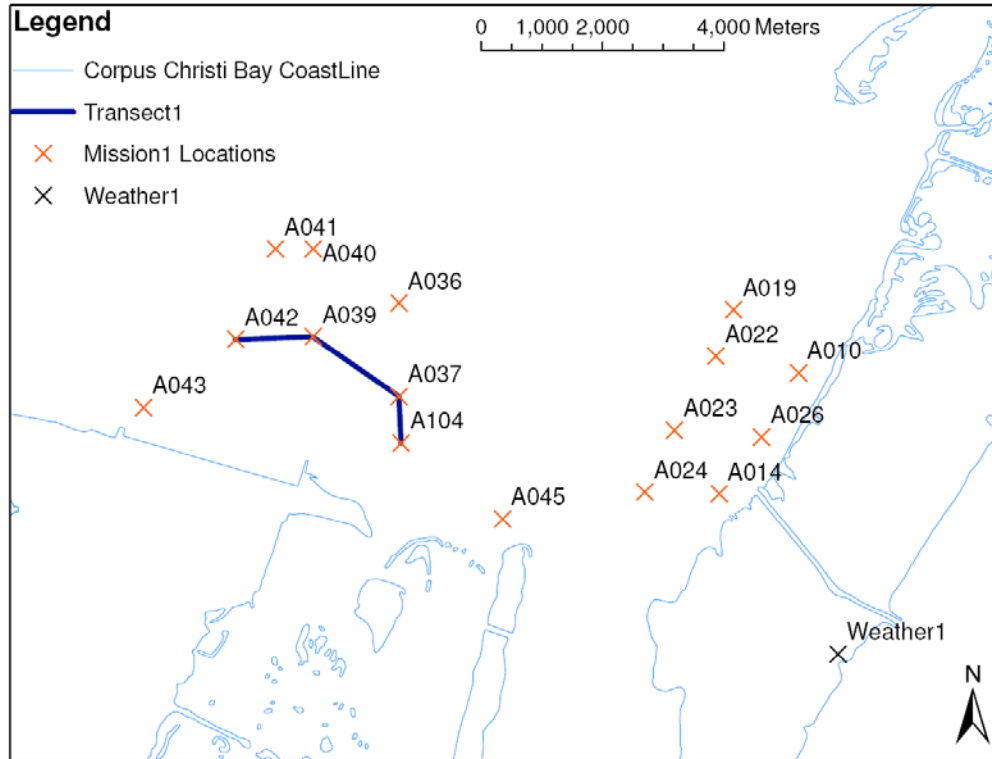


Figure A.21 Locations for mission 1

KEY FINDINGS FROM MISSION 1

Figures A.22 to A.27 show typical temperature (A.22. - A.24) and salinity (A.25 - A.27) measurements taken during Mission 1 at locations A039 (July 6th, 1047 hours), A042 (July 7th, 0720 hours) and A104 (July 7th, 0910 hours). Four SCAMP deployments were executed at each location and time during Mission 1. The first four profiles of each plot correspond to four consecutive profiles taken at a given location. The fifth profile is a binned average of the four previous profiles. Analysis of the temperature and salinity profiles on consecutive profiles show that they are in good visual agreement. The scales of measured variables are therefore very similar over multiple deployments conducted within about 10 minutes (approximate time required for four deployments) over a 20 m space scale (horizontal drift of the SCAMP). As a consequence of this visual analysis, the water at Site A has spatial and temporal similarity over at least a 10 min time scale and a 20 m space scale, so three deployments were judged sufficient to provide description of the water column at a given time and location for future missions. Additional deployments were conducted when one (or more) of the three planned deployments was (were) aborted. Each SCAMP deployment recorded 50 s of measurements, suitable for a depth of approximately 5 meters at a fall rate of 10 cm/s. As this depth is greater than any of the study locations, the bottom was always reached by the SCAMP prior to the end of the sampling time.

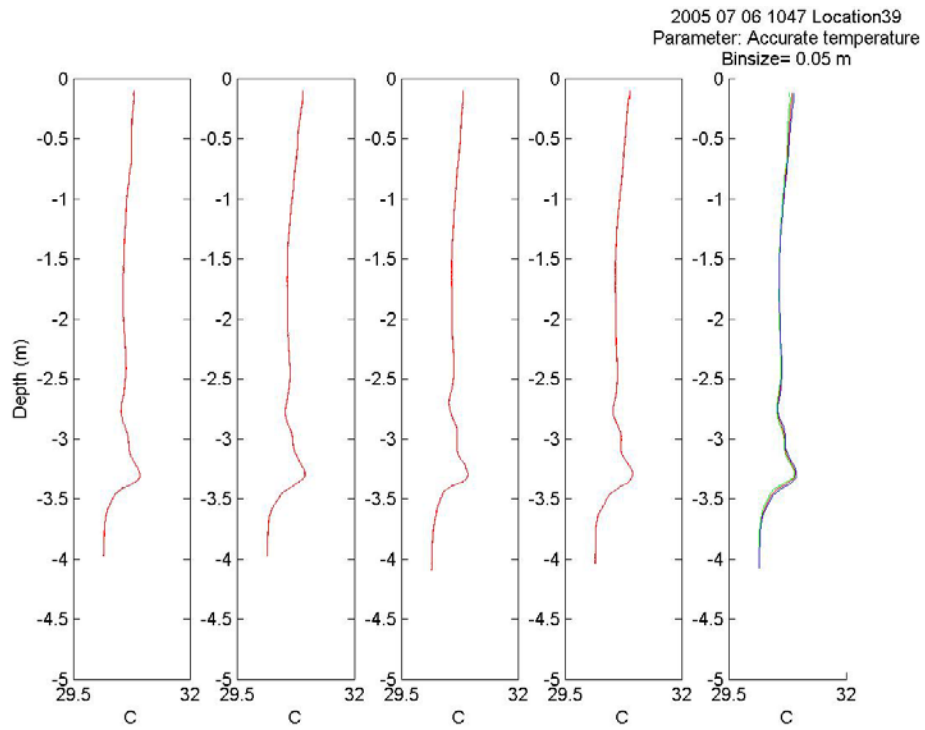


Figure A.22. Accurate temperature profiles - location A039 - 1047 hours on July 6th

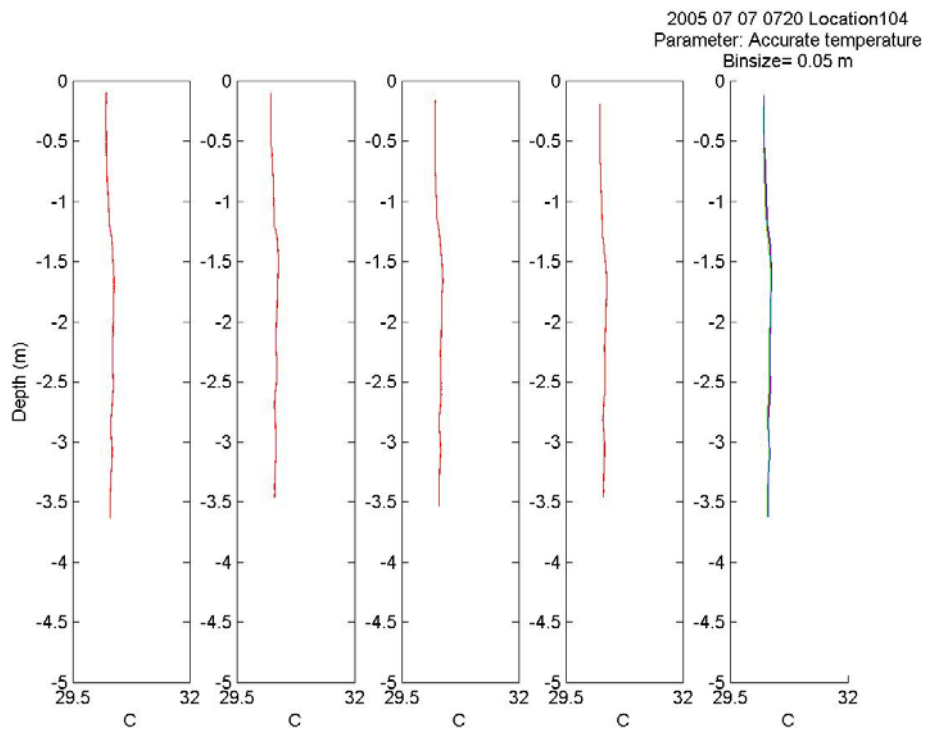


Figure A.23. Accurate temperature profiles - location A104 - 0720 hours on July 7th

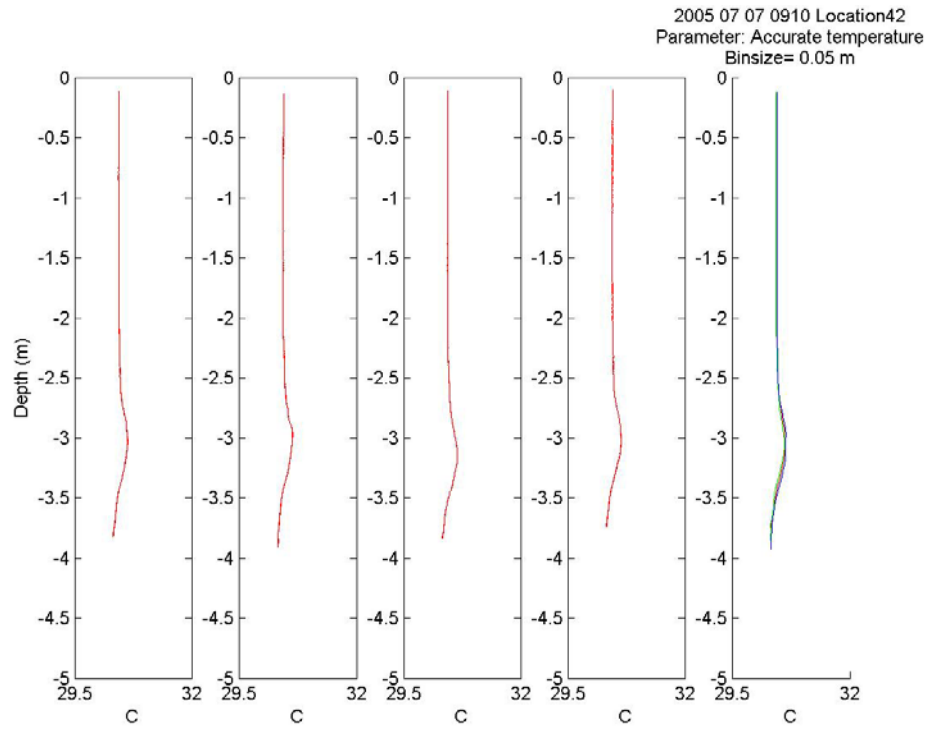


Figure A.24. Accurate temperature profiles - location A042 - 0910 hours on July 7th

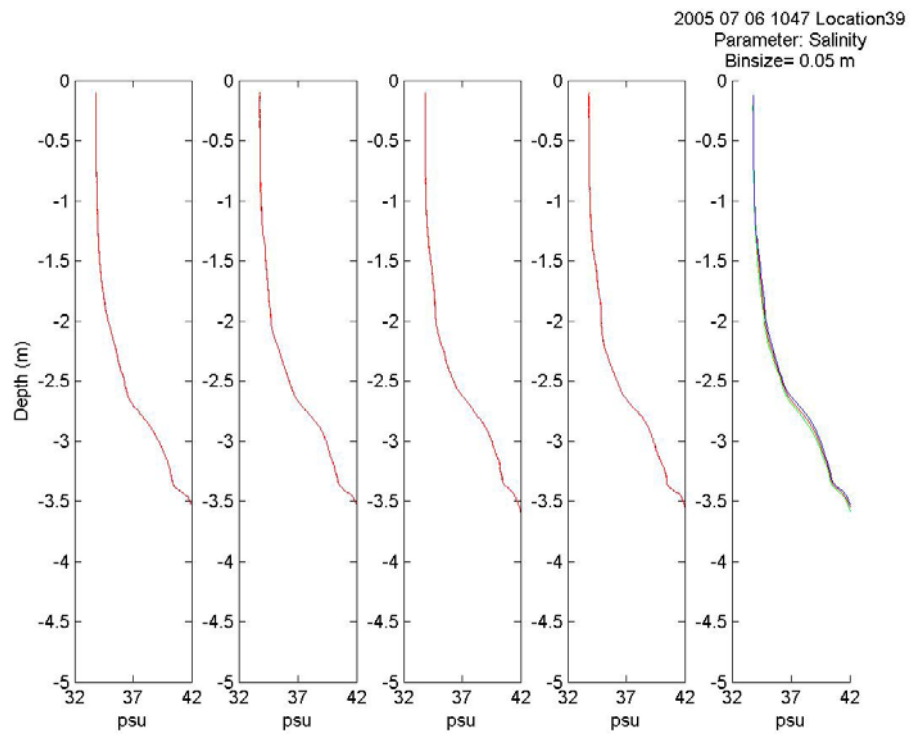


Figure A.25. Salinity profiles - location A039 - 1047 hours on July 6th

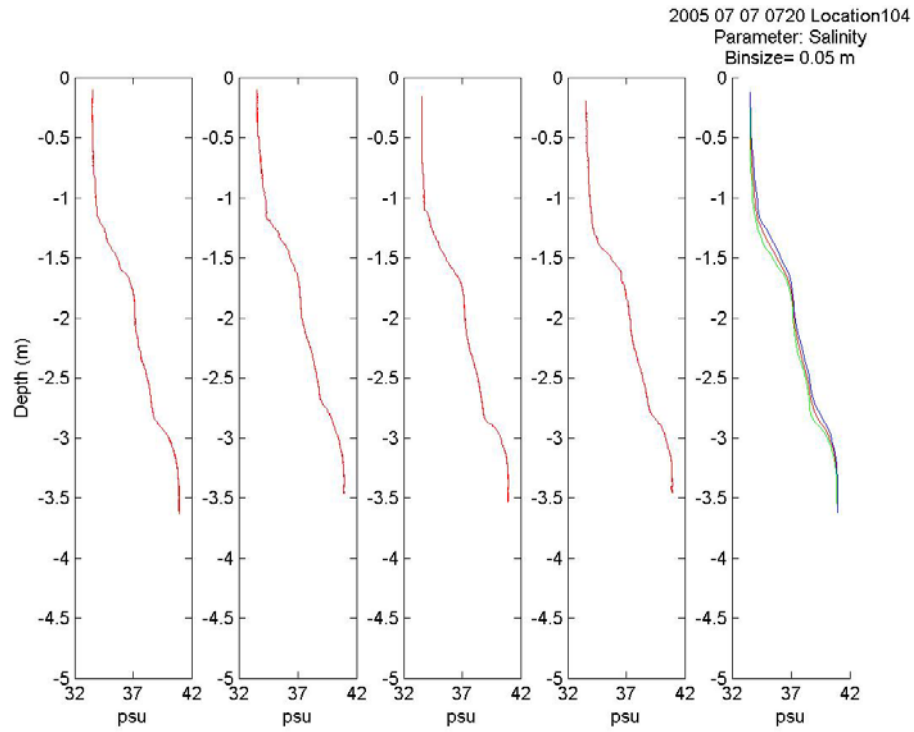


Figure A.26. Salinity profiles - location A104 - 0720 hours on July 7th

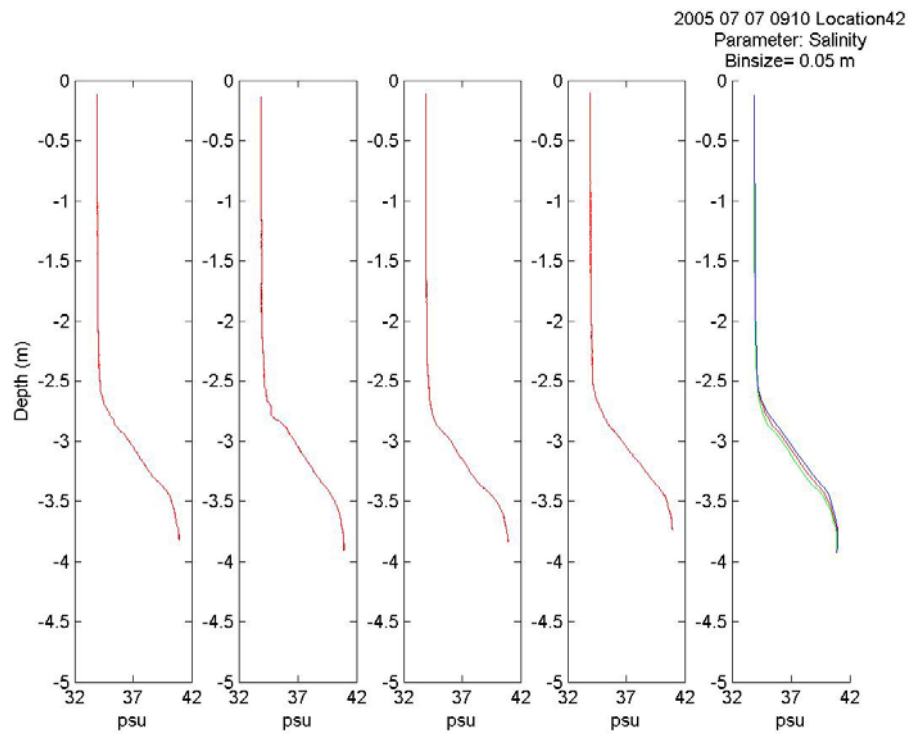


Figure A.27. Salinity profiles - location A042 - 0910 hours on July 7th

Comparison of the CES weather station data to weather notations in the log book (kept on the boat) indicated substantial disagreement during the first mission. Typical wind speeds during boat operations on July 5th and 6th were in the range of 2 to 4 m/s (from CES weather station, see Figure A.28), whereas the log book included notations such as “no wind, no white caps, not choppy” as general comments for July 5th and 6th. Thus, it appears that even the low dunes of Mustang Island were sufficient to cause significant spatial gradients in the wind. As a result of these findings it was decided to move the CES weather station to location Weather2 during the following mission. To obtain a more quantitative understanding of the difference between the land-based measurements and the wind at the sampling locations, the Kestrel 4100 hand-held weather station was acquired for future missions. Figure A.28 shows wind data from both the CES weather station at location Weather1 and the TCOON weather station at Ingleside. Visual inspection of this figure shows that the winds measured by the two stations are quite different.

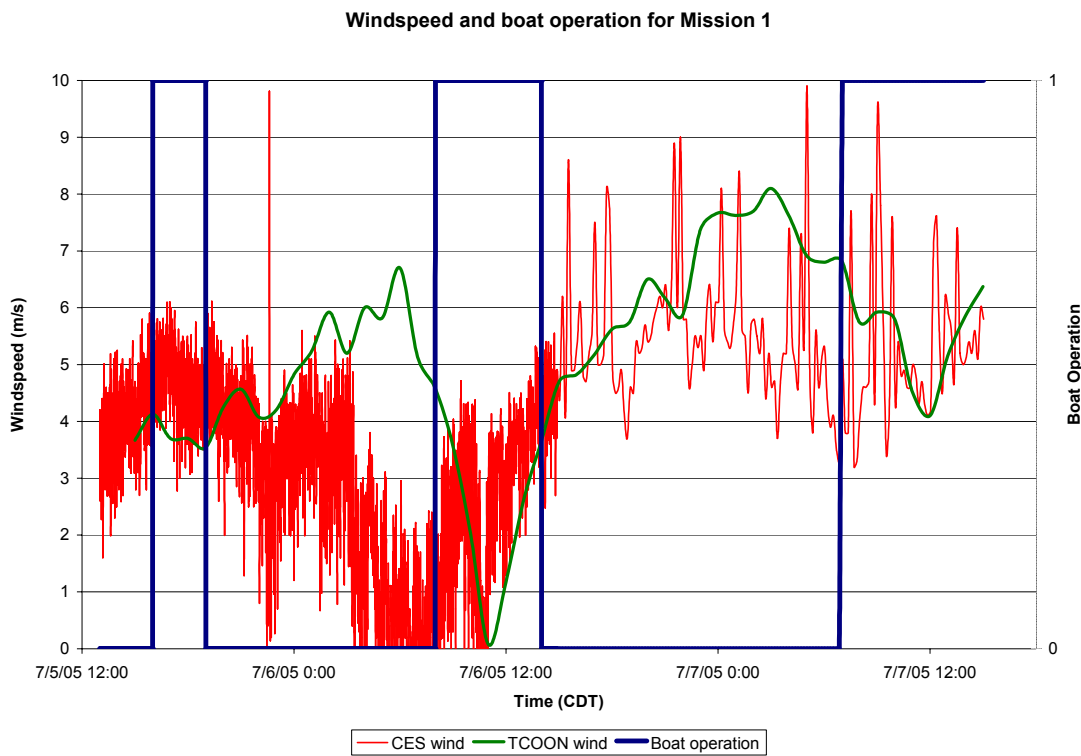


Figure A.28. Wind data and boat operation for mission 1

A.5.b Mission 2: 07/27/2005 – 07/28/2005

DESCRIPTION AND GOALS

The goals of this mission were: 1) moving the CES weather station to location Weather2 on the bay side (see Figure 18) conducting further investigation at Site A, including overnight sampling, with four new sampling locations.

The people that participated in this field trip were Cédric David (UT), Shipeng Fu (UT), Jordan Furnans (TWDB), Carla Guthrie (TWDB), Ben Hodges (UT), and Paula Kulis (UT). During this second mission both the SCAMP and the Manta were deployed, from a single boat. Both GPS receivers were used. Both the CES and the Kestrel handheld weather stations were used. The west side of Mustang Island, on the beach, was chosen as the new location for the CES weather station (location name: Weather2). Recordings at the new location started at 1230 hours on July 27th, and were taken every minute until 1830 hours on July 28th.

The boats were deployed between 1420 27th and 1520 hours on the 28th (overnight sampling was done in the night between the 27th and the 28th). Measurements were stopped between 1630 and 2030 hours on the 27th because of strong winds. Figure A.29 summarizes the crew changes.

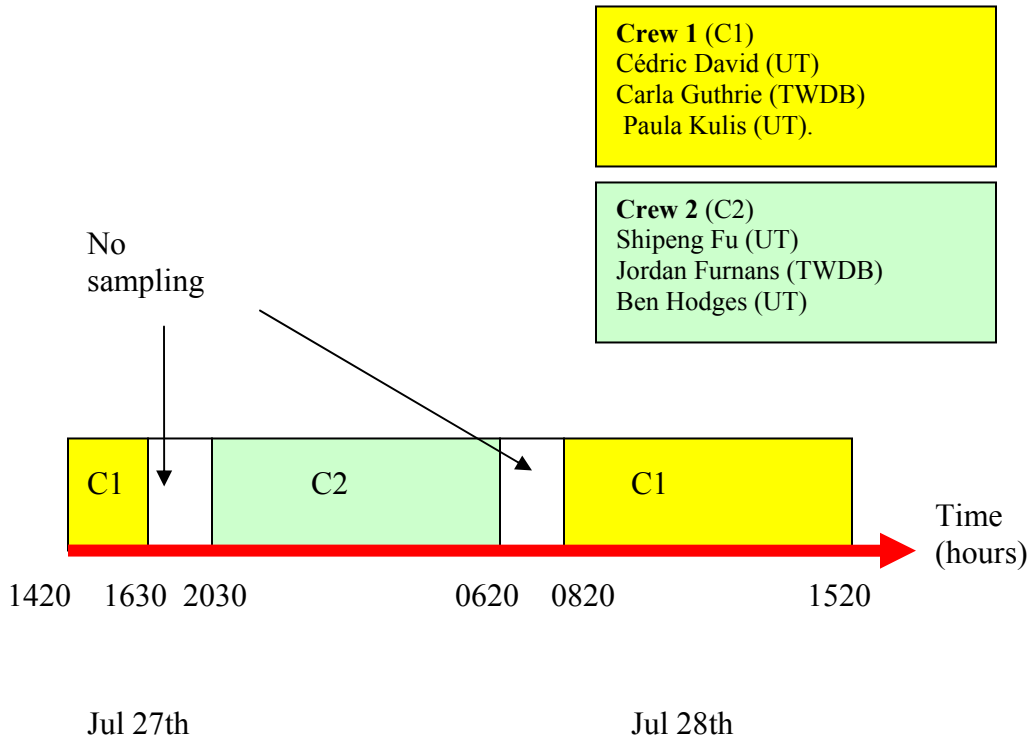


Figure A.29. Crew changes for mission 2

The weather was mostly sunny with winds varying from 1 to 8 m/s. The bay was weakly agitated (height of waves around 20 cm, from visual observations) for the first 30 hours. In high wind conditions (6 m/s) on the 28th, the boat dragged anchor during deployments at locations A042 at 1420 hours and A104 at 1520 hours. Based on the GPS locations at the start and end of the sampling runs, the boat dragged up to 320 m during these deployments. As the waves built up (around 1 m high, estimated from visual observations), instrument deployment was discontinued.

Figure A.30 shows winds recorded by the CES (land-based) and the Kestrel (handheld) weather stations.

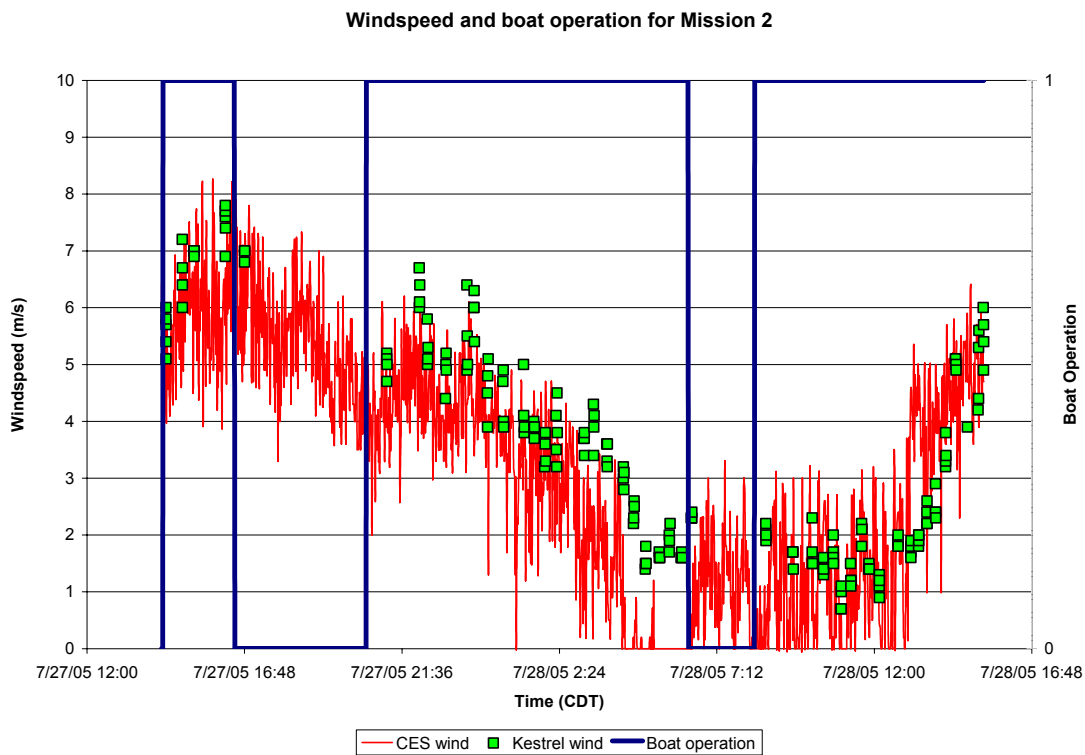


Figure A.30. CES and Kestrel wind data for Mission 2 (Location Weather2), with boat operation times

LOCATIONS

The documentation of a dense underflow during Mission 1 motivated the creation of transects shown on Figure A.31. The route that was followed for Mission 2 is plotted on Figure A.32. The new sampling locations (A101, A102, A103 and A105) and the route were chosen in order to be able to study two transects perpendicular and one parallel to Laguna Madre.

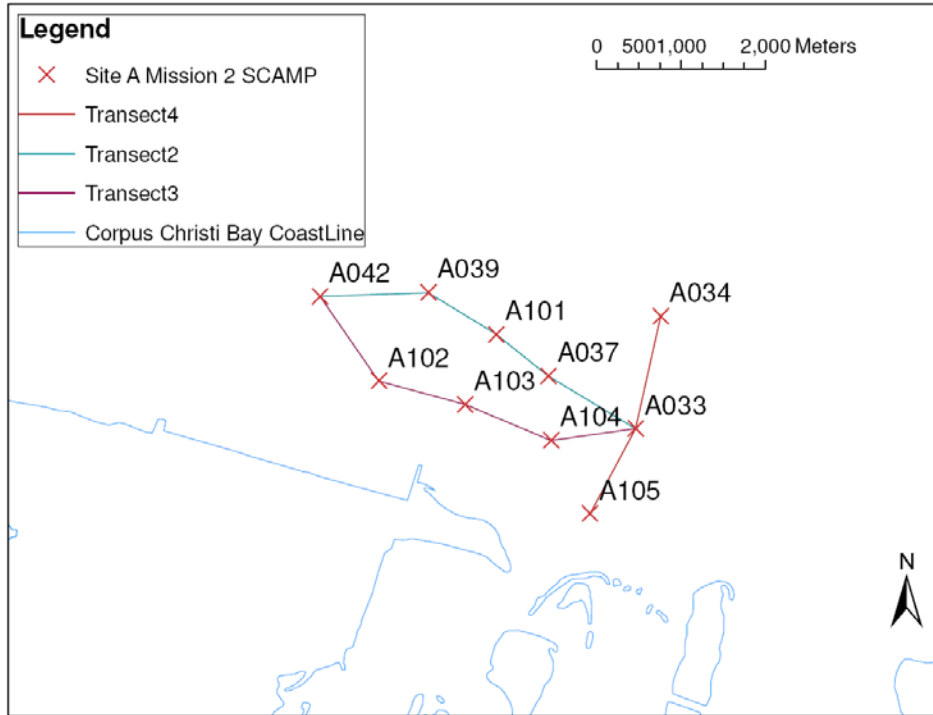


Figure A.31. Transects studied during mission 2

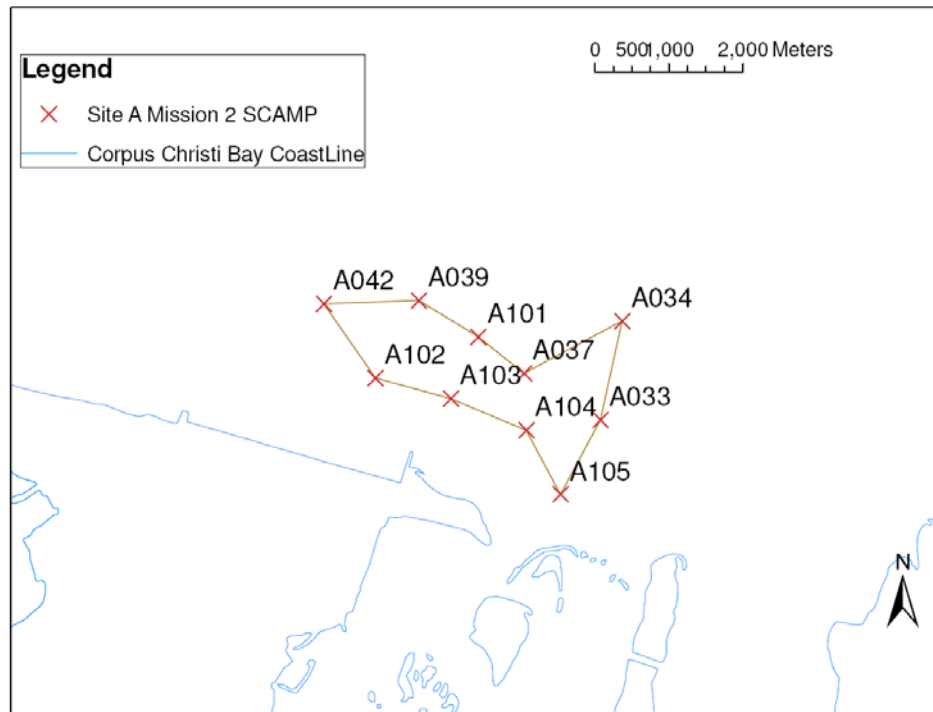


Figure A.32 Route connecting sampled locations for Mission 2

KEY FINDINGS FROM MISSION 2

The decreased distance between sampling locations, associated with a decreased number of deployments at each location and time (3 deployments planned instead of 4) and with increased experience in the use of the equipment led to increased efficiency. Thirty-seven sites were sampled in 3 days during mission 1; forty-seven sites were sampled in two days during mission 2.

Figure A.33 shows the wind data that was recorded by the three weather stations (CES, Kestrel and TCOON) during Mission 2. Visual analysis of the curves shows that the data are in good agreement. As a consequence it was decided to use TCOON data for analysis, as it is the only set of data that was consistently recorded during all missions.

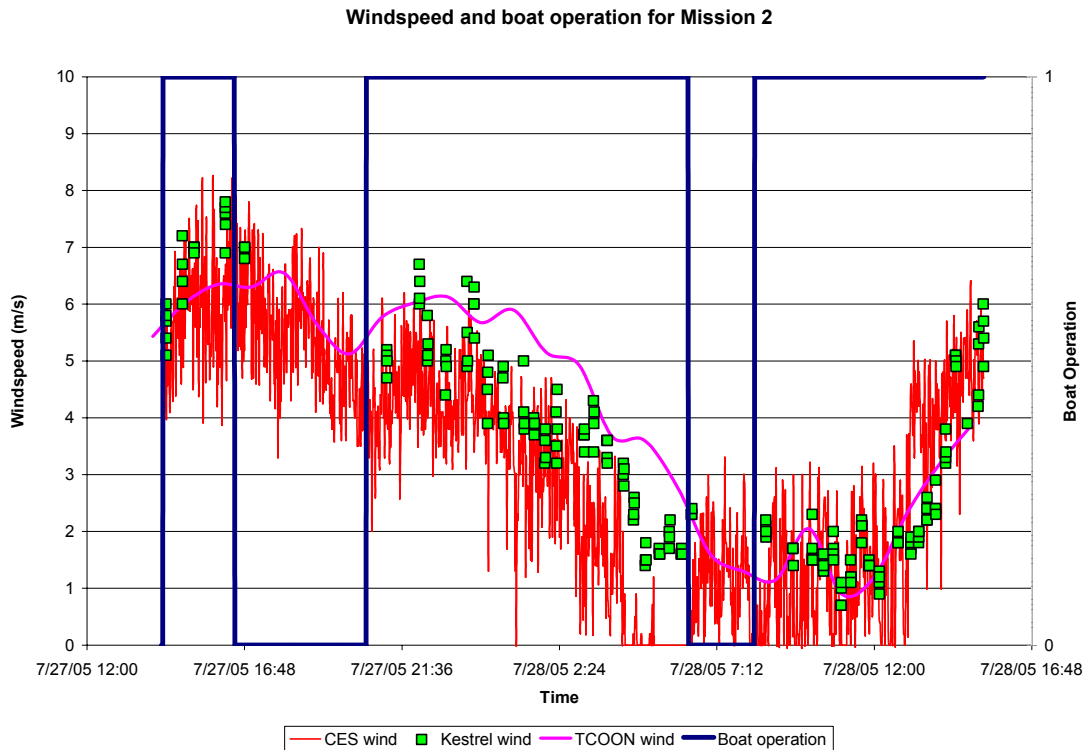


Figure A.33 Wind data and boat operation for mission 2

The maximum wind speed that we found comfortable for launching the SCAMP in Corpus Christi Bay was approximately 7 m/s, based upon data recorded by the weather stations at on July 27th at 1600 hours. It was decided to use TCOON wind data in the SCAMP data processing because the visual agreement with two other wind datasets during Mission 2 and TCOON data is available for both first and second mission.

A.5.c Mission 3: 08/08/2005 – 08/10/2005 and Mission 4: 08/22/2005 – 08/24/2005

Only the Manta was deployed during mission 3 and 4. This appendix is focused on SCAMP work and will only provide a basic description of the last two missions. The persons that participated in Mission 3 are Cédric David (UT), Jordan Furnans (TWDB), Ben Hodges (UT) and Keith Hodges (guest). During Mission 4, Shipeng Fu (UT), Jordan Furnans (TWDB), Ben Hodges (UT), Paula Kulis (UT), John Middleton (UT), Jessica Watts (UT), Holly Weynant (TWDB) and Terry Palmer (UTMSI) participated. The Manta, both GPS receivers and both weather stations were used. Figure A.34 shows the area investigated during Missions 3 and 4.

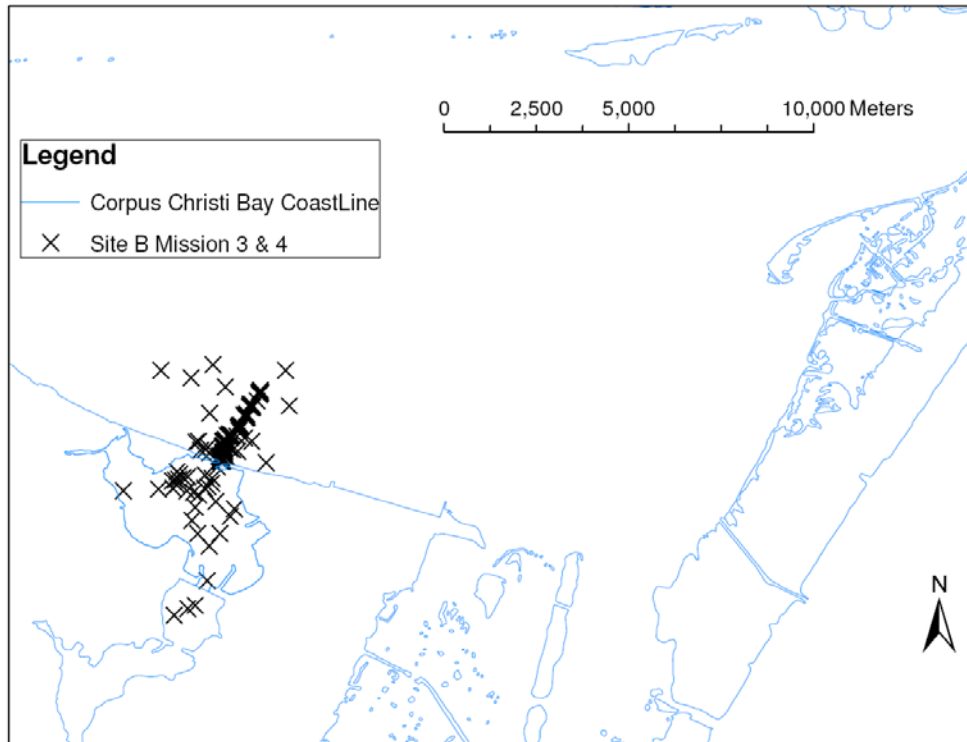


Figure A.34. Area investigated during Missions 3 and 4

A.5.d Summary

This section describes how and where measurements were taken in Corpus Christi Bay. The measurements provide with the basic material to reach research objectives: 1) document the temporal and spatial behavior of salinity and temperature near the outlet of Laguna Madre where hypoxia has previously been recorded, and 2) document the temporal and spatial behavior of salinity, temperature and oxygen near the outlet of Oso Bay. Oso Bay is where the proposed desalination plant outfall would be located.

A.6 Data processing

A.6.a Introduction

The goal of this section is to portray the methods used for processing the data collected during the experiments. The emphasis is on how the experimental data was organized, scrubbed, filtered and plotted for analysis and interpretation. The data processing for data recorded with the Manta was created by Jordan Furnans at TWDB and will not be discussed in this appendix.

A.6.b Parameters recorded or computed

DEPTH

“Depth” is used generically to denote the distance from the water surface to a measurement point that was sampled. “Water depth” is the distance from the water surface to the seafloor. All depths are expressed in meters (m).

CONDUCTIVITY

Electrical conduction is an electrical phenomenon where a material (here water) contains movable particles with electric charge, which can carry electricity. When a difference of electrical potential is placed across a conductor an electric current is induced. Conductivity is defined as the ratio of the current density to the electric field strength. It is the reciprocal of electrical resistivity. Electrical conductivity is a measure of how well a material allows the movement of electric charges. The SI derived unit is the Siemens (named after Werner von Siemens) per meter, Sm^{-1} (or $\text{A}^2\text{s}^3\text{m}^{-3}\text{kg}^{-1}$, where A is the SI base unit of electric current: ampere). According to measurements herein, a typical electrical conductivity for sea water in Corpus Christi Bay at the time of the study is 50 mS/cm (5 S/m).

SALINITY

Salinity is the dissolved salt concentration of water (g salt/ kg water). In oceanography, it has been traditional to express salinity as concentration (mass of salt per unit mass of water) not as percent, but in parts per thousand (ppt or ‰), which is roughly equivalent to grams of salt per liter of water.

Salinity is now usually given in PSU or Practical Salinity Units. The Practical Salinity scale allows salinity to be measured by conductivity, and defines salinity in terms of the conductivity ratio of a sample to that of a solution of 32.4356 g of KCl at 15°C in a 1 kg solution. A sample of seawater at 15°C with conductivity equal to this KCl solution has a salinity of exactly 35 practical salinity units (PSU). SCAMP and Manta salinity measurements are given in PSU, whereas SCAMP measurements are in ppt.

TEMPERATURE

Temperature is a measure of the average kinetic energy of the particles in a sample of matter, in this study: water. In other words, temperature is a measure of activity and the frequency of collisions of molecules. Temperatures will be expressed here in Celsius °C.

DENSITY

Density is a measure of mass per unit of volume. The SI unit of density is the kilogram per cubic meter (kg/m^3). In sea water, density is related to both salinity and temperature. Density increases with decreased temperature and/or increased salinity. Density differences due to higher salinities or lower temperatures are associated with gravity-driven underflows. During the course of this study the range of water temperatures recorded was 29.5 to 32 C and the range of salinity recorded was 32 to 42 PSU. Table A.2 shows results of applying the UNESCO equation for density at constant pressure (UNESCO 1981) to the extremes of the parameter ranges. In the encountered climatic conditions, the influence of the salinity range on density (7.5 kg/m^3) is much higher than the effect of temperature on density (0.9 kg/m^3).

Table A.2 Change in water density with salinity and temperature according to the UNESCO equation

Temperature ($^{\circ}\text{C}$)	Salinity (PSU)	Density (kg/m^3)	Δ (kg/m^3)
29.5	37	1023.4	0.9
32	37	1022.5	
30.75	32	1019.2	7.5
30.75	42	1026.7	

TEMPERATURE AND CONDUCTIVITY GRADIENTS

Turbulent stirring increases the surface area between fluids with two different properties, which increases the mixing rate (i.e. diffusion depends on the gradient of the property and the area over which diffusion acts). Thus, the ability to measure the fine-scale gradients with fast-response sensors provides the ability to see the turbulent overturns that are stirring the fluid faster than it can diffuse. In this study, density stratification of the water column is due to temperature and conductivity (upon which salinity is computed) gradients. As a consequence, turbulent stirring can lead to small scale gradients of temperature and conductivity. At the microscale (order of 1 mm) high temperature and/or conductivity gradients are a sign for presence of active mixing in the stratified flow. However, all mixing occurs at the molecular level which occurs at very low diffusivities. T being the temperature, C the conductivity and z the depth, the mathematical definitions of the temperature gradients ($^{\circ}\text{C/m}$) and conductivity gradients (S/m^2) are:

$$\text{grad}T = \frac{\partial T}{\partial z} \quad (\text{A.1})$$

$$\text{grad}C = \frac{\partial C}{\partial z} \quad (\text{A.2})$$

DISSOLVED OXYGEN CONCENTRATION

The dissolved oxygen (DO) concentration is the mass of gaseous oxygen dissolved in the water. DO is commonly expressed in mgL^{-1} . Oxygen gets into the water from mixing with the atmosphere and as a waste product of photosynthesis. Oxygen is also used by animals and plants. The combination of loading and use of oxygen influences its concentration. Hypoxia is defined based on DO concentrations. Ritter and Montagna (1999) have shown that the appropriate definition of hypoxia for Corpus Christi Bay is $\text{DO} < 3 \text{ mgL}^{-1}$.

WIND AND TIDAL ELEVATION

Wind speed is the speed of movement of air relative to a fixed point on the Earth; it will be given in m/s in this study. Tidal elevation is the result of the regular rising and falling of water surface caused by changes in gravitational forces external to the Earth (mainly the Moon, but also the Sun and other celestial bodies). Tidal elevation will be given in meters (m) above the TCOON Ingleside station datum.

Both tidal elevation and wind are important physical forcing mechanisms in Corpus Christi Bay (Ward 1980). Wind speed was measured by two weather stations (Kestrel 4100, CES weather station). Wind speed and tidal elevation were downloaded from TCOON.

A.6.c SCAMP Data

A total of 314 SCAMP deployments were made during the two first field trips. With an average deployment to 3 m depth, an instrument resolution of 1 mm, and 21 data fields, this provides approximately 20 million data points. To ensure consistency of the data and facilitate their sharing, metadata (i.e. information on the data themselves) have been created. During the missions, log books were kept on the boats in order to record additional information on the measurements.

Various types of files associated with SCAMP data were used for this research. The “raw” data files (.raw filename extension) are the direct experimental data recorded by the instrument. The converted Matlab-format data files (.mat filename extension) are a copy of a reduced set of the original measurement files stored in a binary format that is easily loaded into Matlab. The converted files contain only the parameters that are the focus of this appendix (temperature, salinity, density, depth and temperature gradient). Picture files (.jpg filename extension) using the standard JPEG format are used for plots that have been created for data interpretation. Matlab scripts, functions and tools (.m filename extension) have been built to create the converted files and the figures.

All the file names are as self-explanatory as possible. Comments and summary of the programs are included in each file, and can be found in section A.13. The organization of the data processing can be sketched as shown in Figure A.35.

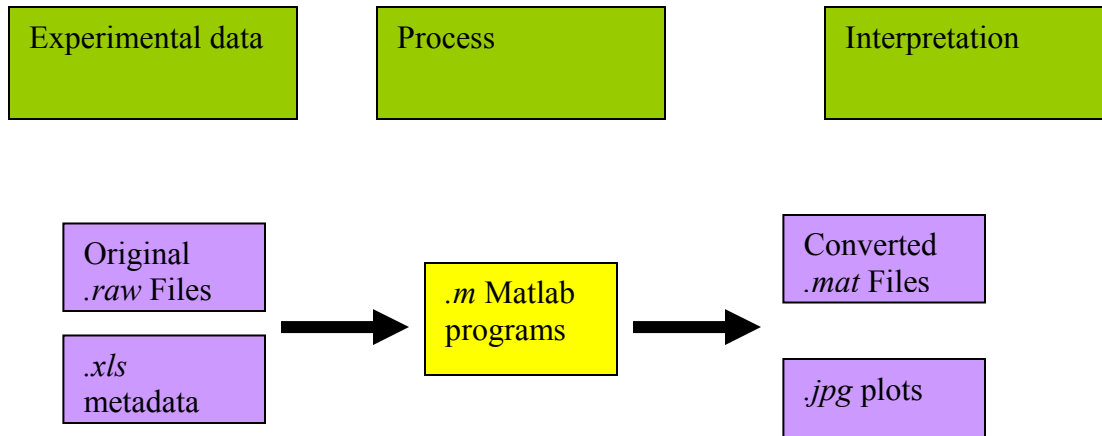


Figure A.35. Organization of SCAMP data processing

The SCAMP provides 21 data fields. Nine fields are actual measurements and 12 are computed from the measurements. The nine measured fields are:

- Two fields for the fast temperature measurements,
- Two fields for the accurate temperature and conductivity,
- One field for the fast conductivity,
- One field for the photoactive radiation,
- One field for the fluorescence,
- One field for turbidity,
- One field for pressure.

For this research, PAR, fluorescence and turbidity measurements were not analyzed. The following focuses on measurements of temperature (two fast and one accurate temperature sensors) and conductivity (one fast and one accurate conductivity sensor). The purpose of the following is to shed light on how the other parameters (depth, density and salinity) were computed.

The water depth above the sensors is computed based upon the measurements of the pressure sensor itself (internal computation by the SCAMP). The instrument manufacturer calibrates the depth computation by using air pressure to press SCAMP's depth sensor. The calibration is based on depth for fresh water of constant density and is valid for up to 70 m. The relationship that is used is linear (i.e. the density is assumed to be constant), and given in the SCAMP manual.

$$D = k P \quad (\text{A.3})$$

where D is the depth, P is the measured pressure and k is a coefficient. The SCAMP uses a combination of English and SI units, with pressure as psi and depth as m. For fresh water, $k = k_{\text{fresh}} = 0.7030696 \text{ m/psi}$ is the default SCAMP calibration. When depth is desired for different density, the coefficient k can be updated in the SCAMP through the user interface. For the present work the density correction was not made prior to taking measurements. A correction for the recorded freshwater depth to an equivalent saltwater can be computed as follows. The gage pressure at any depth is:

$$P = \int_D \rho g dz \quad (\text{A.4})$$

where g is the gravitational constant. For a constant density, this is simply

$$P = \rho g D \quad (\text{A.5})$$

It follows that a consistently-dimensioned K can be defined as

$$K \equiv \frac{D}{P} = \frac{D}{\rho g D} = \frac{1}{\rho g} \quad (\text{A.6})$$

where K has the units m^2/Pa . The SCAMP coefficient ‘ k ’ is then

$$k = \frac{6894.757 \text{ Pa}}{\text{psi}} K \quad (\text{A.7})$$

Approximating the density of Corpus Christi Bay salt water as a constant value of 1023 kg/m^3 (which is correct within $\pm 4 \text{ kg/m}^3$), the value for k_{salt} is:

$$k_{\text{salt}} = 0.68729 \text{ m/psi} \quad (\text{A.8})$$

The linear constant k_{salt} that is found is different from the constant k_{fresh} used in default SCAMP computation. It is possible to correct the depth measurements in the SCAMP processing. However, this was not done in the present work as the difference between k_{salt} and k_{fresh} generates the following error in the depth measurement:

$$\epsilon_{\%} = 100 \times \left(1 - \frac{k_{\text{salt}}}{k_{\text{fresh}}}\right) = 2.30\% \quad (\text{A.9})$$

This error is equivalent to 6.9 cm at 3 m depth. The 2.30% error translates into approximately 2.30 % error in the gradients computation.

Matlab Executable (MEX) modules were coded by PME. In the MEX files, salinity (ppt) and density are computed from temperature and conductivity (by `S_SAL.m` and `S_SIGT.m` functions respectively). The computations of both salinity and density use the equations for sea water neglecting pressure effects (UNESCO 1981).

The data format (.raw), data processing and display software provided with the SCAMP are not suitable for concurrent analysis of multiple profiles. As part of the present research, a method of saving the data in a custom Matlab file (.mat) and new display software were developed. The Matlab file uses a vector format. Each element of the vector is a Matlab structure containing the sampling data from one SCAMP deployment (depth, temperature,

temperature gradient, salinity, density: each is a separate vector). There are usually three to five elements (structures) in the main vector, corresponding to sequential deployments made at one location around the same time. All data files were converted to Matlab format.

Figure A.36 shows the organization inside a typical Matlab file developed in this project. The name of the file (2005_07_28_0822_Location105.mat) is created with the date (here, July 28th 2005 at 0822 hours) when sampling started at the sampling location (here, location A105). Each of the .mat files contains a vector generically named Rawdata. Rawdata(1) to Rawdata(n) are the elements of the vector Rawdata, each corresponding to a SCAMP deployment (n is the number of profiles that were taken at location A105). Components of the Rawdata structure provide the raw data produced by the SCAMP. For example, Rawdata(1).FastT0 gives one of the two fast temperature profiles taken during the first deployment. A.12.a gives the meaning of all abbreviations.

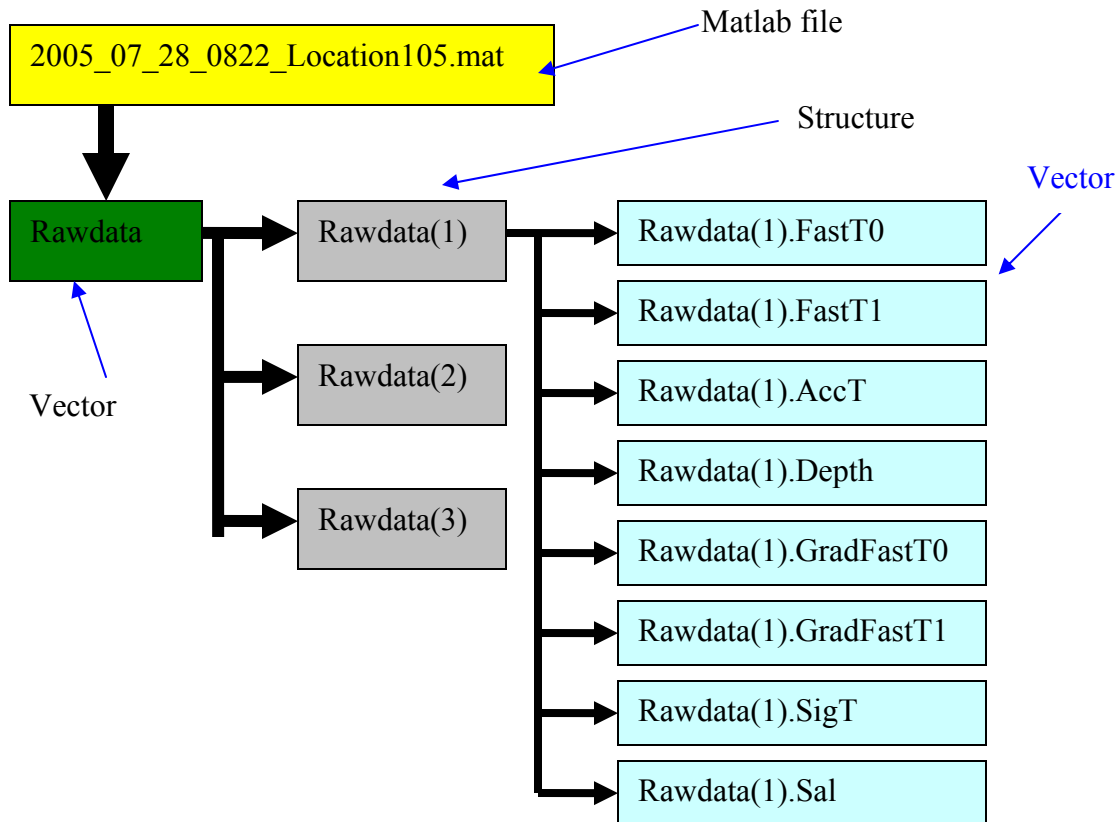


Figure A.36. Organization of the Matlab files

Visual identification of anomalies at the start of a profile is possible. However the size of the data set makes it impractical to visually examine every profile and identify the appropriate starting point for a good profile. As a consequence an automated approach to filtering the data was created. Two options were examined for automated identification and removal of questionable data created in the initial deployment of the SCAMP. The first option was filtering the entire profile to remove data points outside of some multiple (two to three) of the standard deviation for temperature and conductivity in the bin. This approach proved unsuccessful as some profiles with active turbulence had large standard deviations of temperature and/or conductivity. Thus, the first approach removed some data that was deemed reliable. The second option was simply removing all measurements recorded above 10 cm depth. This data visually appeared to have some of the strongest differences between profiles and therefore was considered the most unreliable due to the instrument deployment method (see Section A.4.d).

Several consecutive vertical profiles were taken at the same location. Averaging was done to provide confidence in the data, limit the number of vertical profiles and facilitate the analysis. At each location and time, the average profile based on all available profiles was computed. The data were averaged in 5 cm bins starting at the water surface and proceeding down through the water column. The depth of the binned data is given at the center of the bin. For clarity, only two to three measurements per 5 cm bin are drawn in Figure A.37, there are actually about 500 measurements per bin.

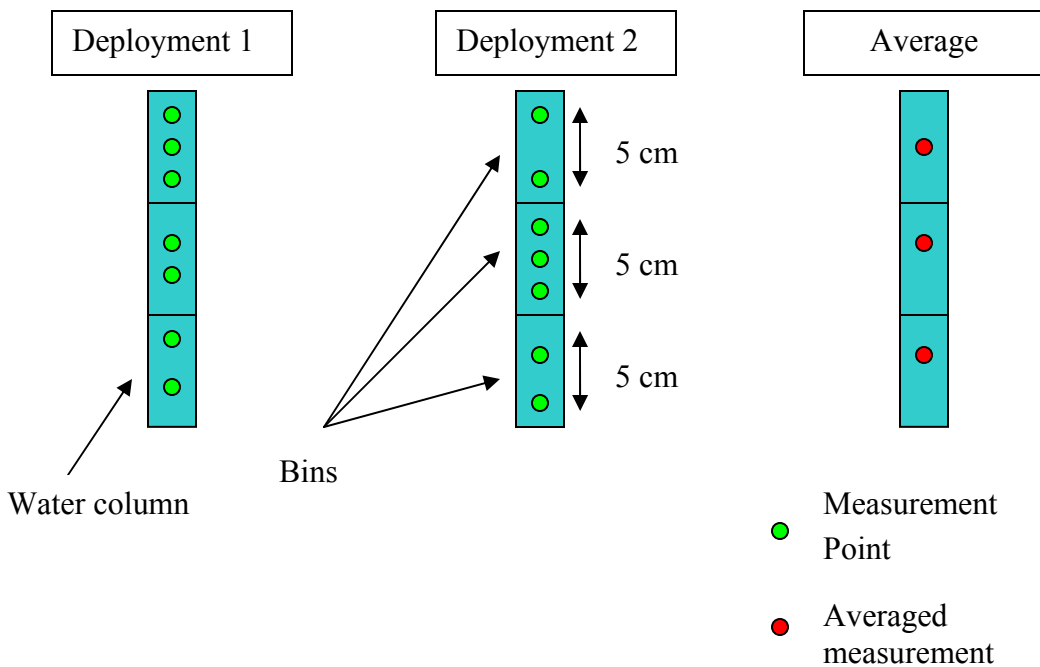


Figure A.37. Binning and averaging

Figure A.38 summarizes the data processing procedure. Detailed explanations on the use of Matlab functions are given in section A.13. Matlab functions are used to translate the SCAMP original files to figures suitable for analysis.

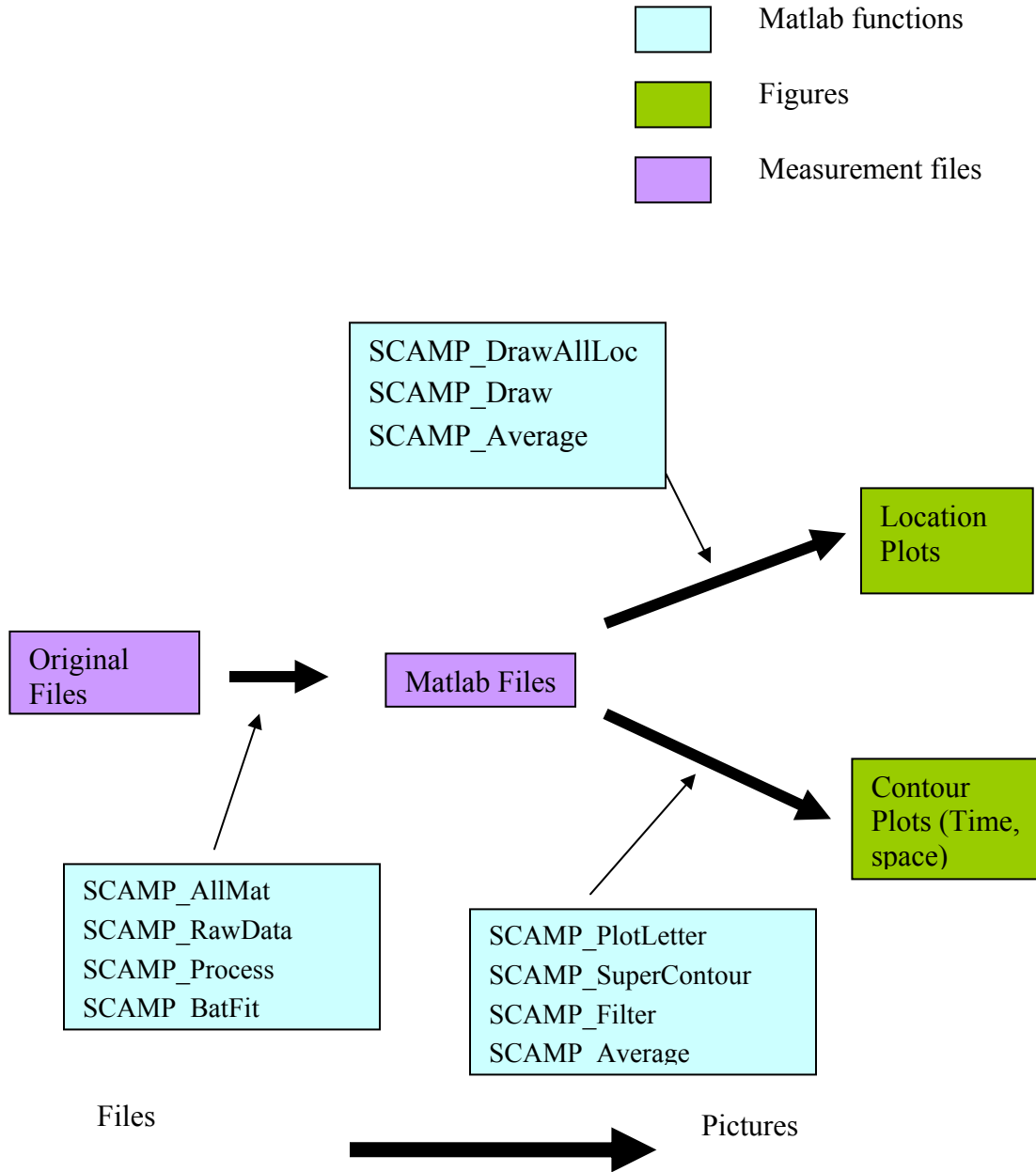


Figure A.38. Summary of data processing

A.6.d TCOON data

In 1989, the Conrad Blucher Institute for Surveying and Science (CBI) at Texas A&M University-Corpus Christi commenced the installation of a water-level measurement system in Corpus Christi Bay. The first systems installed provided real-time water level and meteorological data. This initial work motivated other state agencies (Texas General Land Office and the Texas Water Development Board) in contracting CBI to provide similar information for other areas along the Texas coast. Following a Texas Legislative mandate in 1991, this network of water level gauges became the Texas Coastal Ocean Observation Network (TCOON). As a result, TCOON expanded from an initial three stations in Corpus Christi in 1989 to over forty stations along the entire Texas coast by 1992. Matlab scripts were used in this thesis work to plot TCOON data with spatial transects and temporal evolutions created with SCAMP data.

A.7 Application of the data analysis methods

A.7.a Introduction

The purpose of this part is to provide and explain example figures that were created based upon the data analysis methods. The principal features, commonalities and differences that can be observed will be explained and associated with possible physical meanings.

A.7.b Explanation of the figures

FIGURES AT ONE LOCATION, WITH ONE PARAMETER

Figure A.39 shows data from four deployments executed between 2222 and 2231 hours on July 27th 2005 at location A034. The parameter plotted is accurate temperature (AccT). The size of the bins is 0.05 m.

The first profile is shorter than the others at this location, indicating the deployment was aborted prior to completion. Deployments were typically aborted when the drag plate retaining pin on the instrument was inadvertently pulled, the instrument's path was crossing under the boat, or the instrument recording was instigated prior to placement in the water. The filtering process has been by-passed in this figure, for explanation purposes. The low temperatures above 10 cm depth in the first profile are an indication of the instrument recording the air temperature when out of the water. It can be seen in the binned profile that the inclusion of these anomalous temperatures in the averages provides unreliable data. The sudden decrease of the temperature around 3 m deep is a sign of stratified water column.

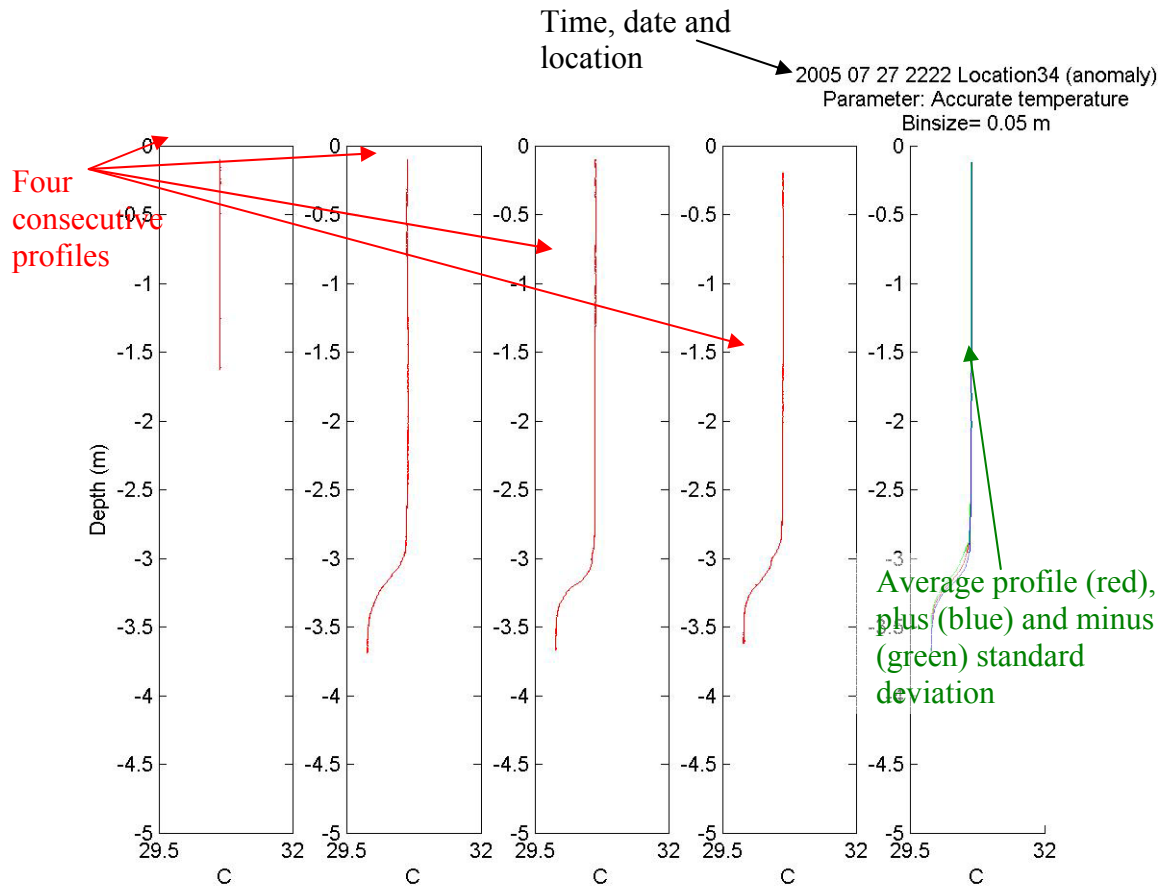


Figure A.39. One location and one parameter figure

TRANSECTS

Averaged profiles at nearby locations that were taken within several hours of each other can be combined to provide a transect that allows visualization of quasi-synoptic horizontal distributions of a property. As an example, Figure A.40 shows data for the fifteen deployments starting at 0925 and ending at 1105 hours on July 28th 2005 at locations A033, A037, A101, A039 and A042 (transect 2). The deployments moving from left to right are increasing in time, so the warming of the near-surface water may be due to time as well as space. The salinity field appears to show an intrusion that is stronger to the left and weaker to the right. The temperature inversion at the bottom indicates that the high salinity water probably originated in a location and time where warm salty water is created by evaporation.

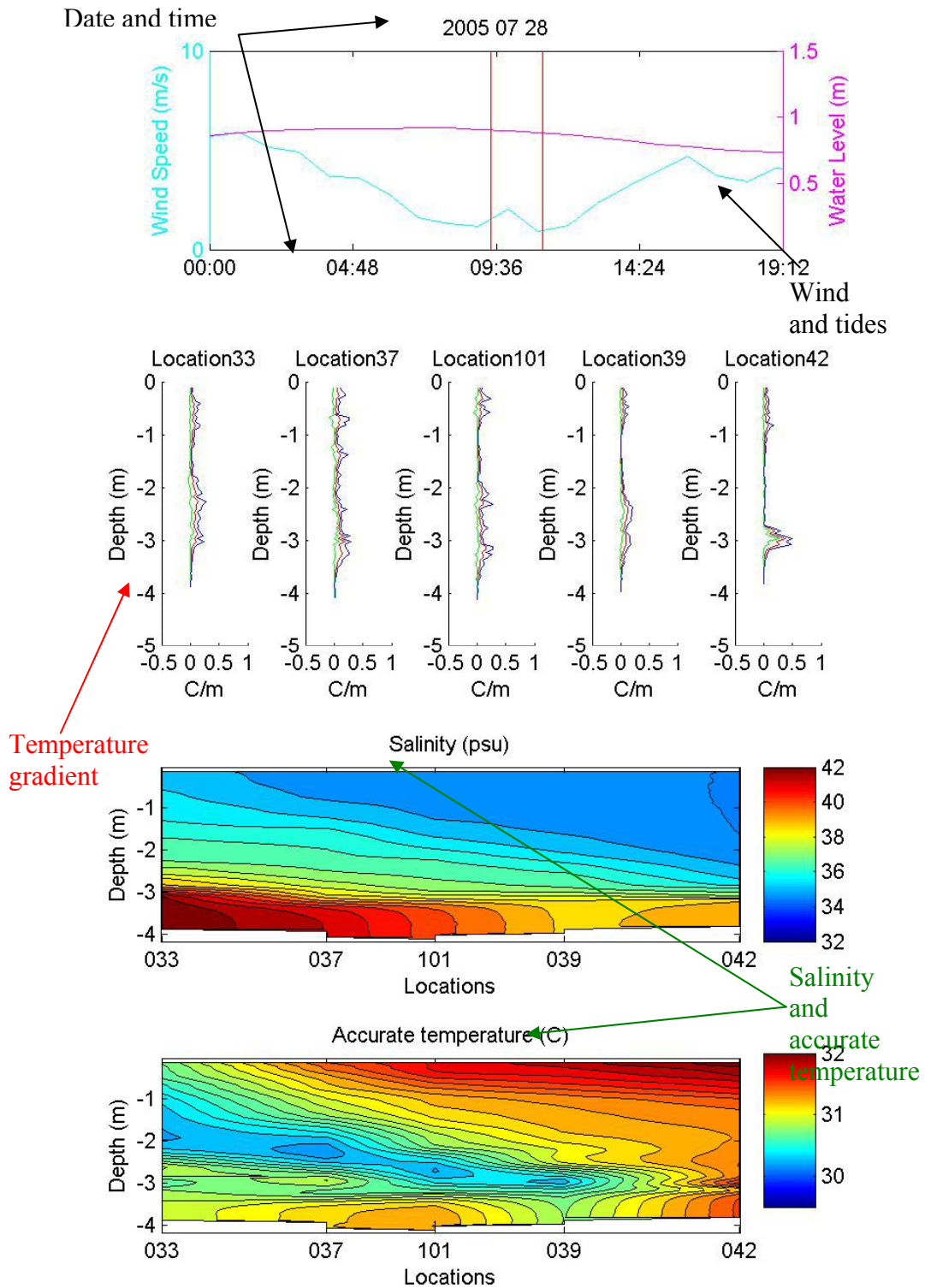


Figure A.40. Spatial transect: Transect 2, on July 28th between 0925 and 1110 hours. Temperature gradient profiles use red lines for the average profile, blue lines for the average plus standard deviation and green for average minus standard deviation.

A set of formats for displaying the data was developed to allow analysis, comparison and graph for transects of SCAMP data. The driving forces (wind and tides) are placed at the top of the figure. The wind speed and tidal elevation data are TCOON data. The vertical bars on the wind speed and tides figure indicate the start and end time of the experiments. The binned average of the absolute value of temperature gradient profile, and its standard deviation for each location are plotted in the middle. Finally, contours of averaged accurate temperature and average salinity are plotted along the cross section. On the contours, the distance between each location is proportional to the actual distance in situ. The averaging is done over all deployments at each location.

TEMPORAL EVOLUTION AT ONE LOCATION

Averaged profiles at one location that were taken within several hours of each other can be combined to provide a contour of temporal evolution of a property over a short period of time (several hours to a day). As an example, Figure A.41 shows data for the sixteen deployments taken at location A037 on July 7th 2005; at 0754, 1005, 1220 and 1420 hours. The deployments moving from left to right are increasing in time, the warming of surface water between morning (left hand side) and early afternoon (right hand) is clearly noticeable. The salinity field appears to be quite steady. The binned average of the absolute value of the temperature gradient shows peaks at the depth (approximately 2.5 m) where temperature stratification appears (at 1220 and 1420 hours). The same set of format for displaying the data was used for temporal evolution and spatial transects. The statistics of the absolute value of the temperature gradient in these graphs is useful for examining the consistency of the turbulence measurements of the multiple SCAMP deployments at each location.

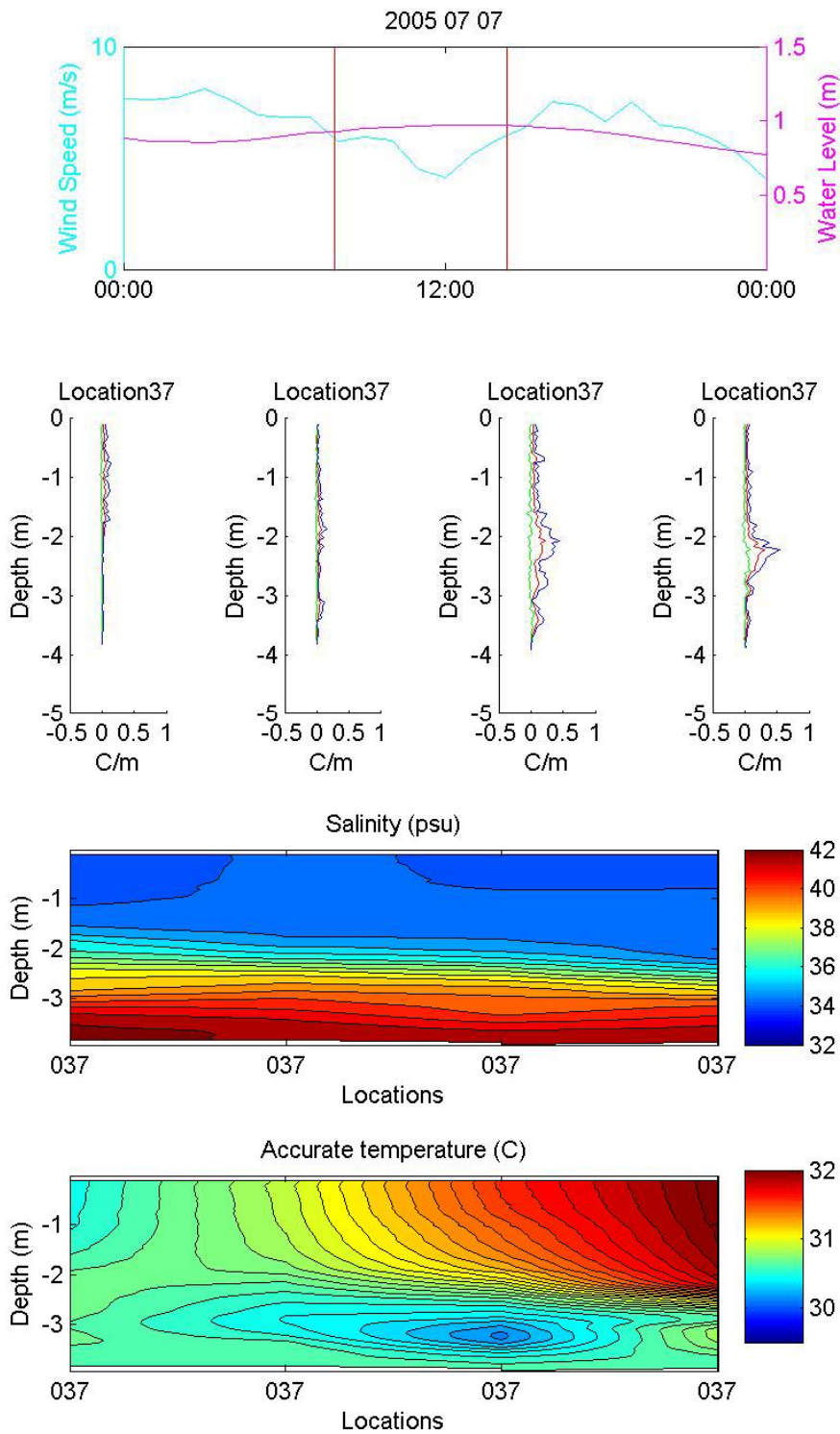


Figure A.41. Temporal evolution at one location, Location A037 on July 07th between 0754 and 1420 hours. Temperature gradient profiles use red lines for the average profile, blue lines for the average plus standard deviation and green for average minus standard deviation.

A.8 Availability of the data

The experimental data, the programs created for the purpose of this thesis as well as the three types of figures (location figures, space transects and temporal evolution) are saved on a CD and kept by Ben Hodges (hodges@mail.utexas.edu).

A.9 Efficiency of the software

The computer used for this thesis work is a Motion Computing M1200 with a Mobile Intel Pentium III 933 MHz processor and 1 GB of RAM. On this machine, plotting one single deployment profile using the PME software takes approximately 23 s. Using the software that were developed for this thesis work, it takes 52 s to plot multiple profiles for a transect with 17 deployments, averaged and filtered, with wind and tides plots. The data processing developed for this thesis is more suitable for concurrent analysis of multiple profiles, and around 7.5 times less time consuming.

A.10 Summary

The first research objective for the field work was to document the temporal and spatial behavior of salinity and temperature near the outlet of Laguna Madre (Site A) where hypoxia has previously been recorded. Sampling was conducted during missions 1 and 2, with special emphasis on two transects parallel to the shoreline. Site A included positions previously sampled by UTMSI and newly identified positions. Short time scale data (few hours to a day) over small horizontal distances (less than 5 km) were gathered to enable the study of both spatial and temporal changes. Four spatial transects were studied with relatively close instrument deployments (700 m to 1 km between neighbor locations). Display methods for temperature, salinity, wind and tidal elevation data were developed to help future analysis of the physical processes. Metadata were created to ensure consistency and facilitate the sharing of the data.

The second research objective was to develop new data processing, and display methods for the SCAMP microstructure profiler. The data format (.raw), processing and display software provided with the SCAMP are not suitable for concurrent analysis of large numbers of multiple profiles. A methodology was developed for analyzing, comparing and graphing the datasets for transects of SCAMP data. SCAMP experimental data was converted and recorded in a Matlab file. Matlab programs were developed in order to average, filter and graph multiple SCAMP profiles and contours. The new software is about 7.5 times less time-consuming than the original software for displaying data.

A.11 Suggested future work

The research related to this report is ongoing at the Center for Research in Water Resources. The work described in this section could help improve the understanding of the phenomena studied.

Visual analysis of the profiles at a given location and time led to the conclusion that three profiles were sufficient to provide description of the water column. An actual statistical analysis on binned profiles could help support this hypothesis. Further studies on the meaning of binned average temperature gradient could provide with a way to statistically quantify and relate stratification to mixing. Comparison of the DO data provided by the Manta and the SCAMP data from mission 2 could help connect hypoxia to stratification and/or dense underflows.

A.12 Information on field deployment

A.12.a Abbreviations

AccC Accurate Conductivity

AccT Accurate Temperature

DO Dissolved Oxygen

FastC Fast Conductivity

FastT Fast Temperature

GradFastT Temperature gradient based upon the fast temperature sensors

GradFastC Conductivity gradient based upon the fast conductivity sensor

GIWW Gulf Intracoastal Waterway

Sal Salinity

SigT σ_T Density

TWDB Texas Water Development Board

UT University of Texas at Austin

UTMSI University of Texas Marine Science Institute

A.12.b Table of GPS locations

Following are the GPS locations that were used for this study:

Table A.3 Sampling locations

NAME	LAT	LONG
A001	27.813880	-97.140830
A002	27.797220	-97.150830
A003	27.783050	-97.146120
A004	27.781670	-97.176950
A005	27.767780	-97.194170
A006	27.750280	-97.195830
A007	27.732500	-97.200830
A008	27.715830	-97.203620
A009	27.693050	-97.211120
A010	27.713250	-97.180120
A011	27.728730	-97.173730
A012	27.743620	-97.166950
A013	27.764170	-97.157500
A014	27.695280	-97.191950
A015	27.773100	-97.165520
A016	27.762050	-97.180700
A017	27.742850	-97.184820
A018	27.747500	-97.181150
A019	27.722670	-97.189780
A020	27.734730	-97.186450
A021	27.737130	-97.207450
A022	27.715720	-97.192450
A023	27.704750	-97.198570
A024	27.695520	-97.202980
A025	27.722950	-97.177020
A026	27.703700	-97.185630
A027	27.738150	-97.170180
A028	27.754250	-97.161770

NAME	LAT	LONG
A029	27.723620	-97.212780
A030	27.705280	-97.220830
A031	27.698230	-97.220800
A032	27.693620	-97.229720
A033	27.704080	-97.230170
A034	27.716120	-97.227500
A035	27.731670	-97.226950
A036	27.723620	-97.239450
A037	27.709720	-97.239450
A038	27.702780	-97.252220
A039	27.718620	-97.252220
A040	27.731670	-97.252220
A041	27.731670	-97.257770
A042	27.718200	-97.263750
A043	27.708130	-97.277420
A044	27.722870	-97.277630
A045	27.691530	-97.224130
A046	27.824230	-97.139010
A101	27.714170	-97.245000
A102	27.709170	-97.257500
A103	27.706670	-97.248330
A104	27.702830	-97.239170
A105	27.695000	-97.235000
Weather1	27.671420	-97.174250
Weather2	27.697040	-97.182630
T'COON Ingleside	27.821667	-97.203333
PowerPlant	27.616667	-97.333333
BoatRamp	27.629320	-97.217980

A.12.c Boats

Two boats were used for the field trips. The Texas Water Development Board owns a 17 feet long boat that has a 120 horse power engine.



The Center for Research in Water Resources (CRWR) owns a 14 feet long boat that has a 15 horse power engine.



A.12.d Notes on SCAMP

The SCAMP is a very high definition measuring instrument. Learning how to use it has to be done through both reading of the very well written user's manual and trying it in actual experimental settings on a boat. The following few comments on its use associated to the user's manual might be valuable:

CLEANING OF THE SENSORS.

It has to be done after each day of measurements. De-ionized water should be used. Extra attention should be paid to the pressure sensor, which has to be rinsed softly (very fragile sensor) for at least 15 seconds.

WHITE PLASTIC CLOSURE SCREW RING.

The closure ring can easily be wedged and impossible to unscrew without damaging it. Therefore, it should be greased with O-Ring grease whenever put back on. Also unscrew a quarter of a revolution when it has reached the maximum.

CONDITIONS OF USE.

Due to the size of the instrument (approximately one meter), the SCAMP gives better results in at least 2 meters deep water.

PENS AN TRIGGER MAGNETS.

These items are to be used very frequently during measurements; they are also the easiest to lose. The magnet is used on the SCAMP to trigger the start of a measuring sequence. Pens are used with the log book. It can be very convenient to have them attached with a piece of string to the toolbox or the SCAMP stand.

A.12.e Metadata

During the missions, log books were kept on the boats, providing additional information on the measurements, such as:

- The actual GPS location at the sampling point,
- The start and end time of the measurement,
- The operator,
- The weather conditions on the water,
- Comments on the actual deployment of the instrument.

This information has been typewritten in an Excel file, in table format, with the following fields:

- Name of the SCAMP file,
- Location,
- Start and end time at this particular location,
- Time of the actual measurement,
- Desired latitude and longitude,

- GPS device,
- Actual GPS location,
- Operator,
- Whether or not the profile was aborted,
- Comments

The file SCAMP_Journal.xls containing all the metadata is provided with the measurement files. A ReadMe.txt file was also created to give explanation on the different files that are provided.

A.12.f MEX files

The computations for salinity and density in the SCAMP software were coded (by PME) in C programming language, as routines or subroutines. MEX-files are a way to call custom C or FORTRAN routines directly from MATLAB as if they were MATLAB built-in functions. MEX-Files were used here in the computations because they have the ability to call large existing C or FORTRAN routines directly from MATLAB without having to rewrite them as M-files. MEX stands for MATLAB Executable. MEX-files are dynamically linked subroutines produced from C or Fortran source code that, when compiled, can be run from within MATLAB in the same way as MATLAB M-files or built-in functions.

A.12.g SCAMP accurate temperature Graphs

In Figure A.42, the temperature profile on the first deployment show features at the surface that don't match with the two other deployments. No particular comment has been made on the log book for this deployment.

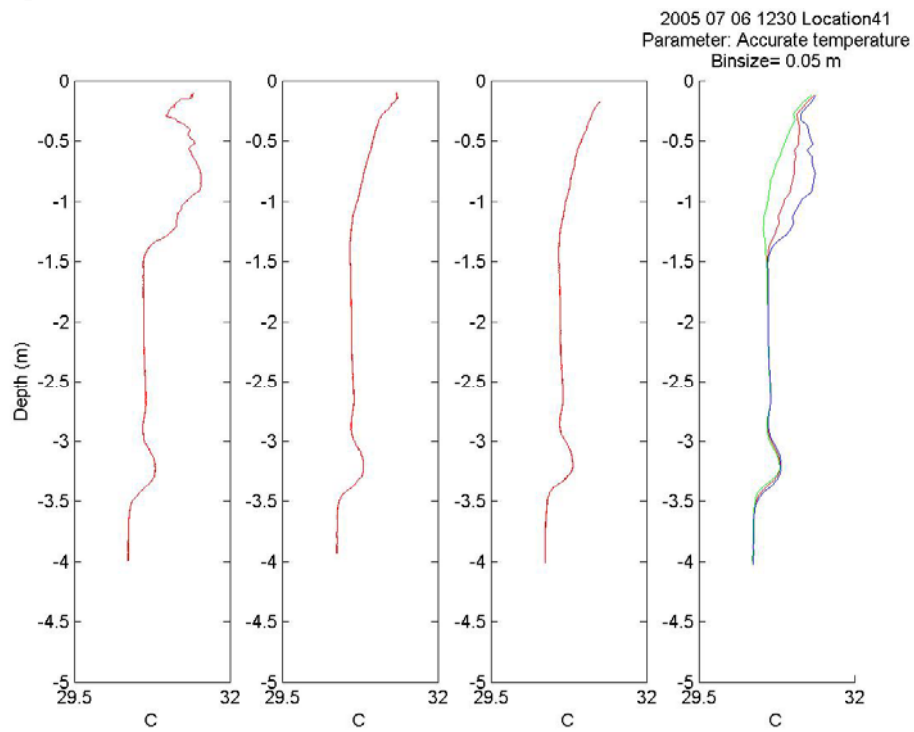


Figure A.42. Anomaly in one of the deployments

Figure A.43 and Figure A.44 show interesting features in temperature variations in the water column. At the approximate depths of 3.2 and 3.5 meters respectively, colder water can be found above warmer water.

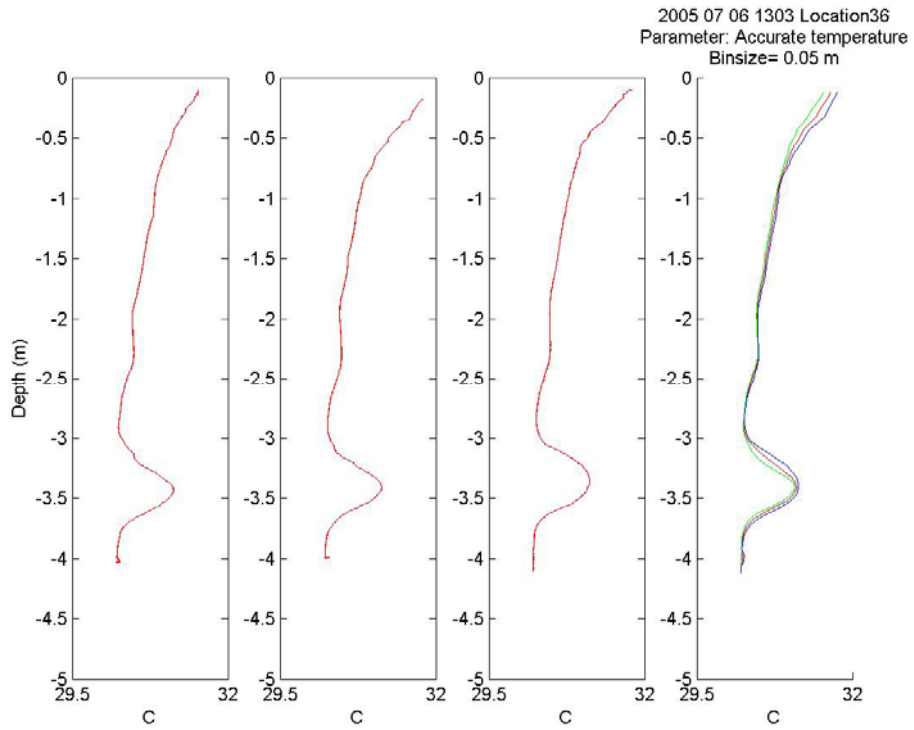


Figure A.43. Interesting changes in temperature 1

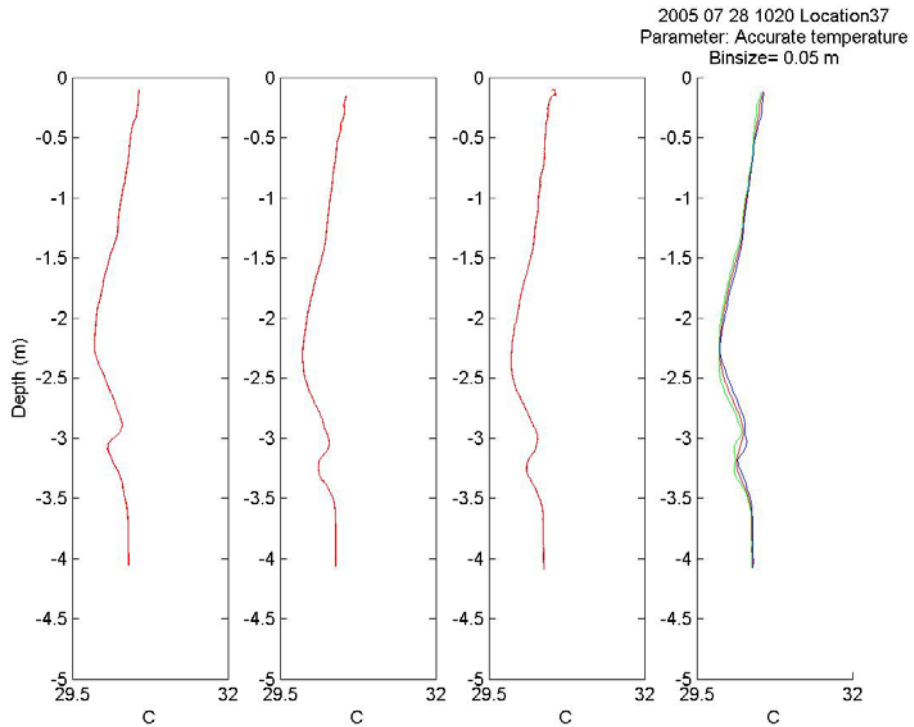


Figure A.44. Interesting change in temperature 2

A.12.h SCAMP salinity graphs

Figure A.45 and Figure A.46 show sudden changes in the salinity profiles, evidences of highly stratified water column.

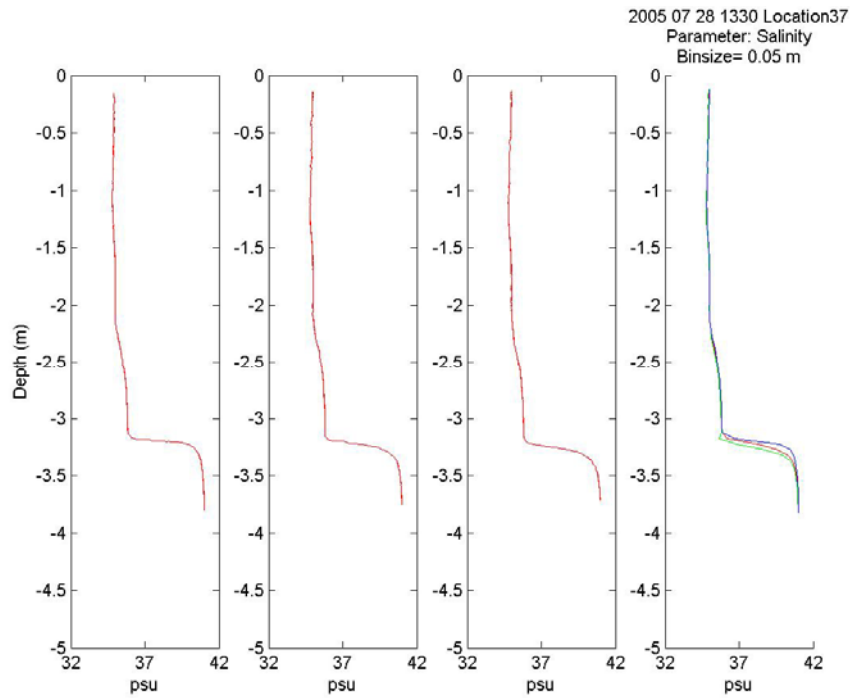


Figure A.45 Sudden change in the salinity profile 1

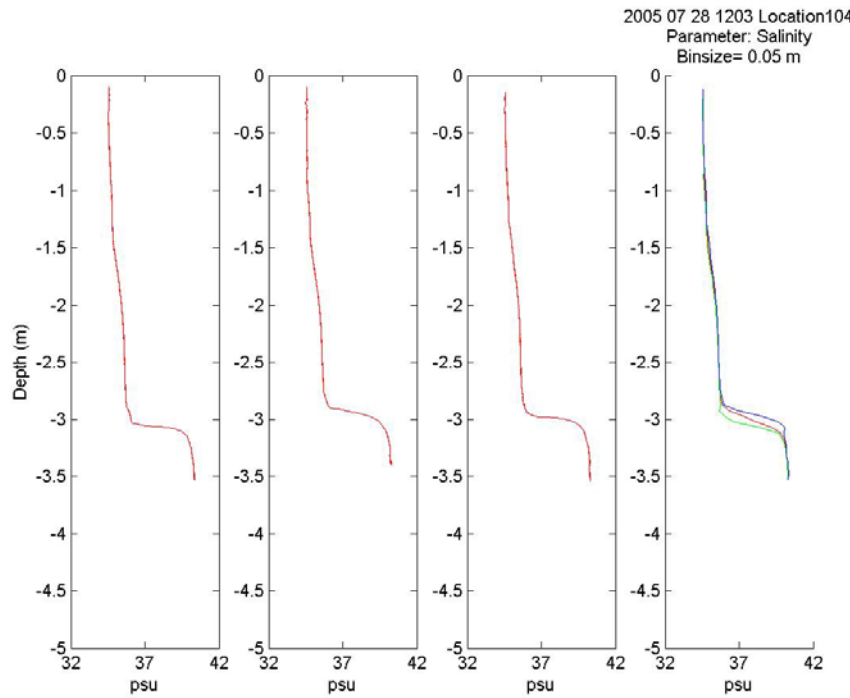


Figure A.46. Sudden change in the salinity profile 2

A.12.i SCAMP spatial transects

Figure A.47, Figure A.48 and Figure A.49 show the temporal evolution of Transect 1 between 0720 and 1325 hours on July 7th 2005. An intrusion of cold salty water appears at 0945 and is bigger at 1145 hours. Figure A.50 shows Transect 3 on July 28th between 0309 and 0606 hours. On this spatial transect, warmer water can be found underneath colder water.

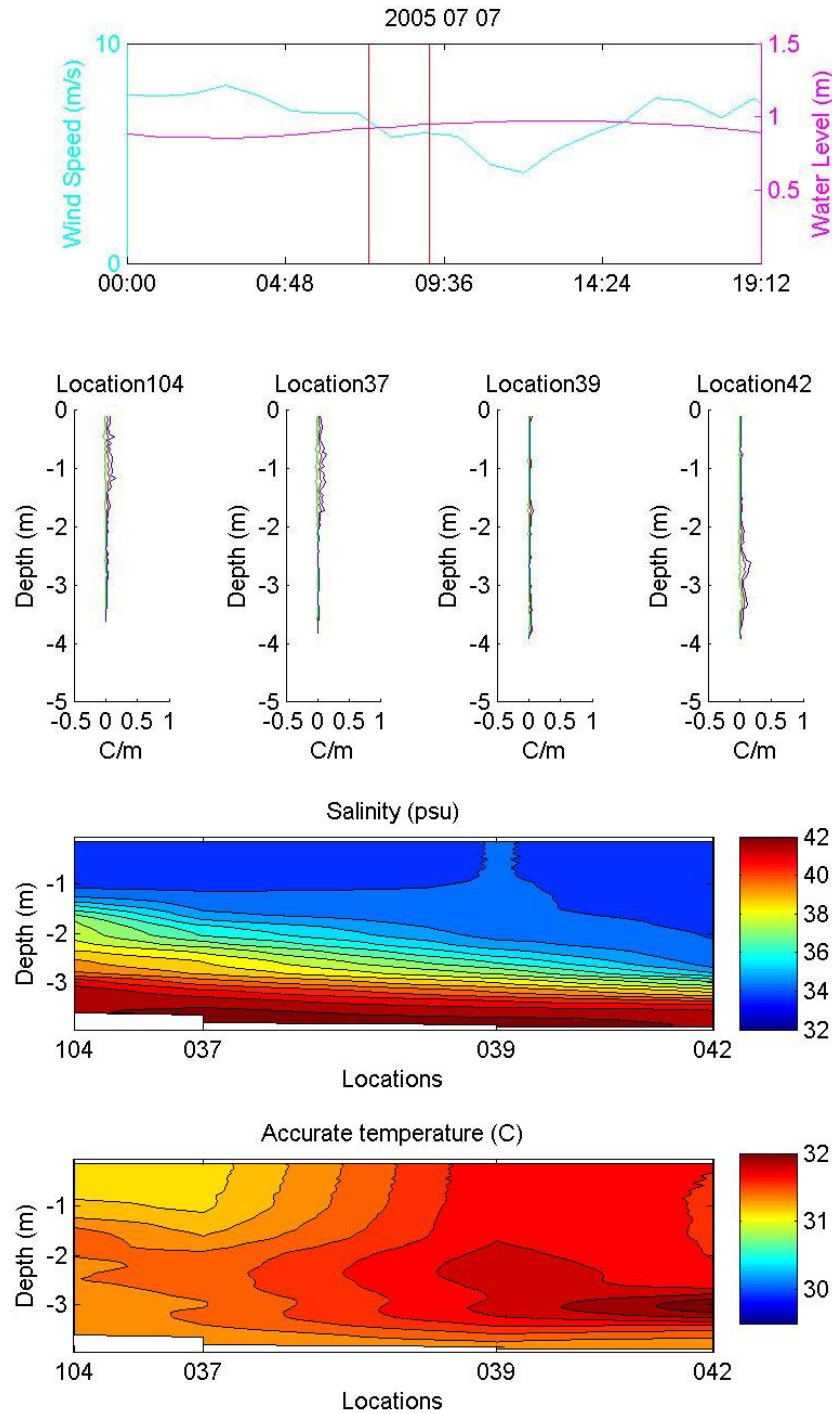


Figure A.47. Transect 1; July 7th 2005, between 0720 and 0910 hours

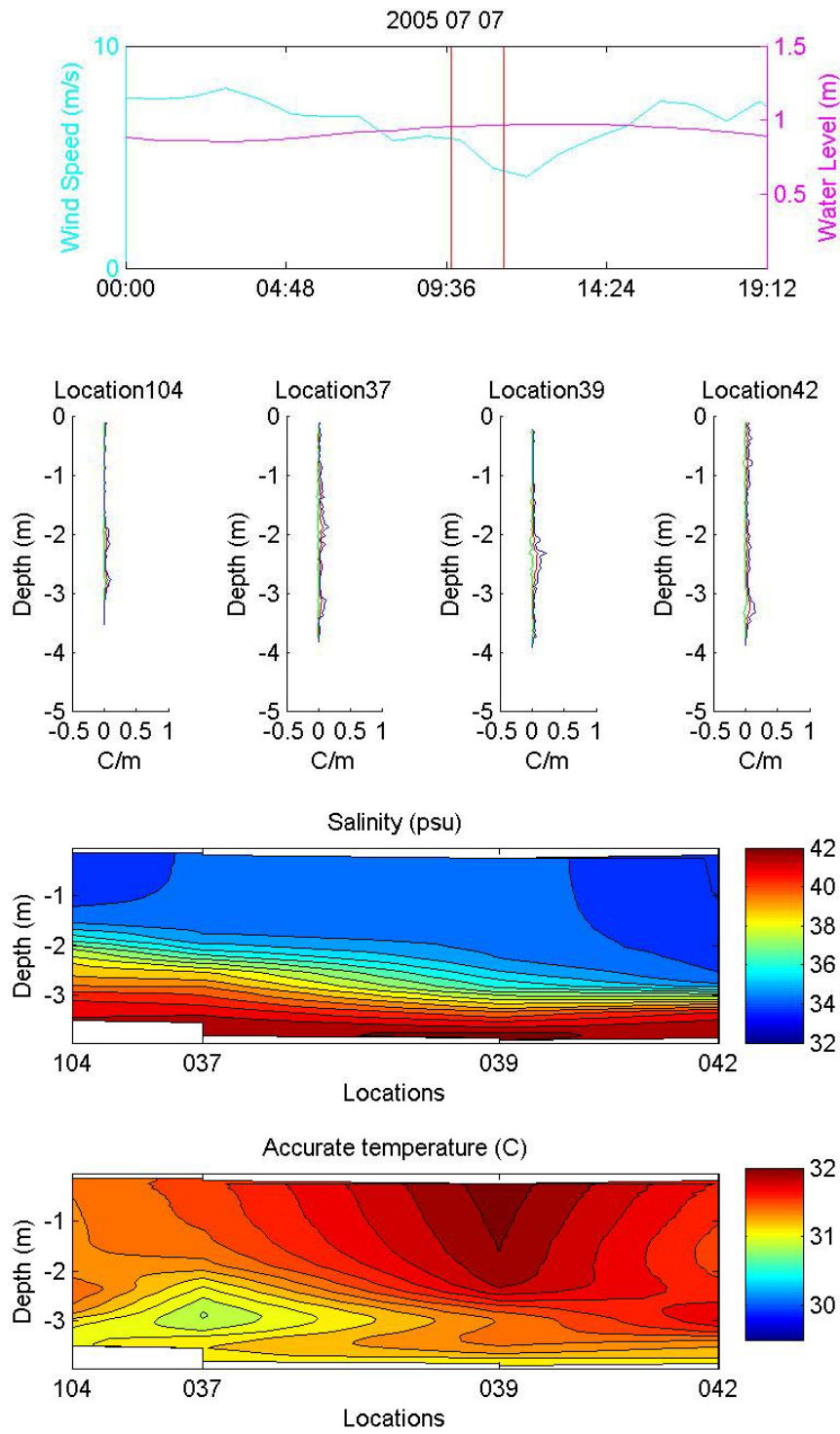


Figure A.48. Transect 1; July 7th 2005, between 0945 and 1120 hours

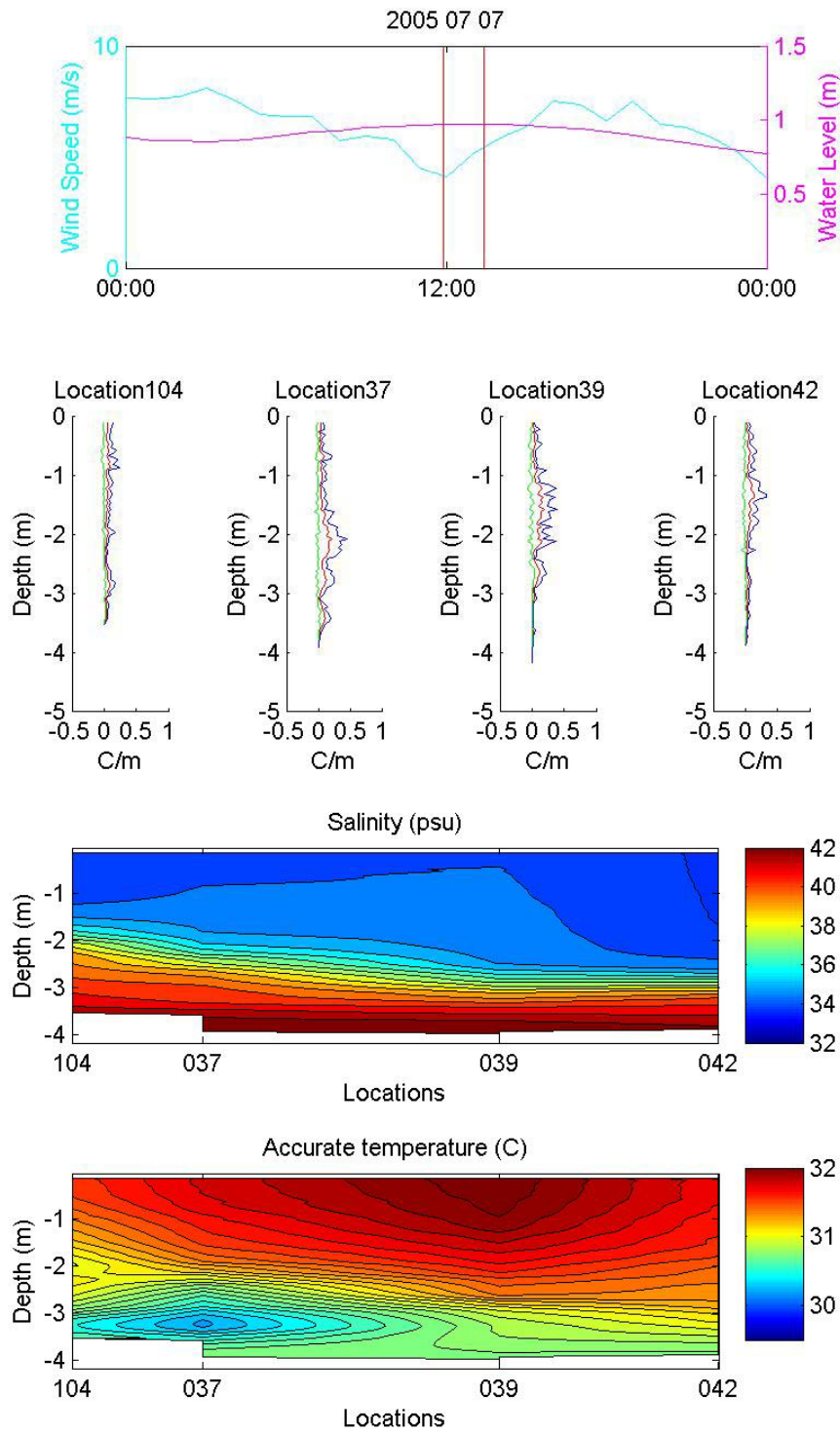


Figure A.49. Transect 1; July 7th 2005, between 1155 and 1325 hours

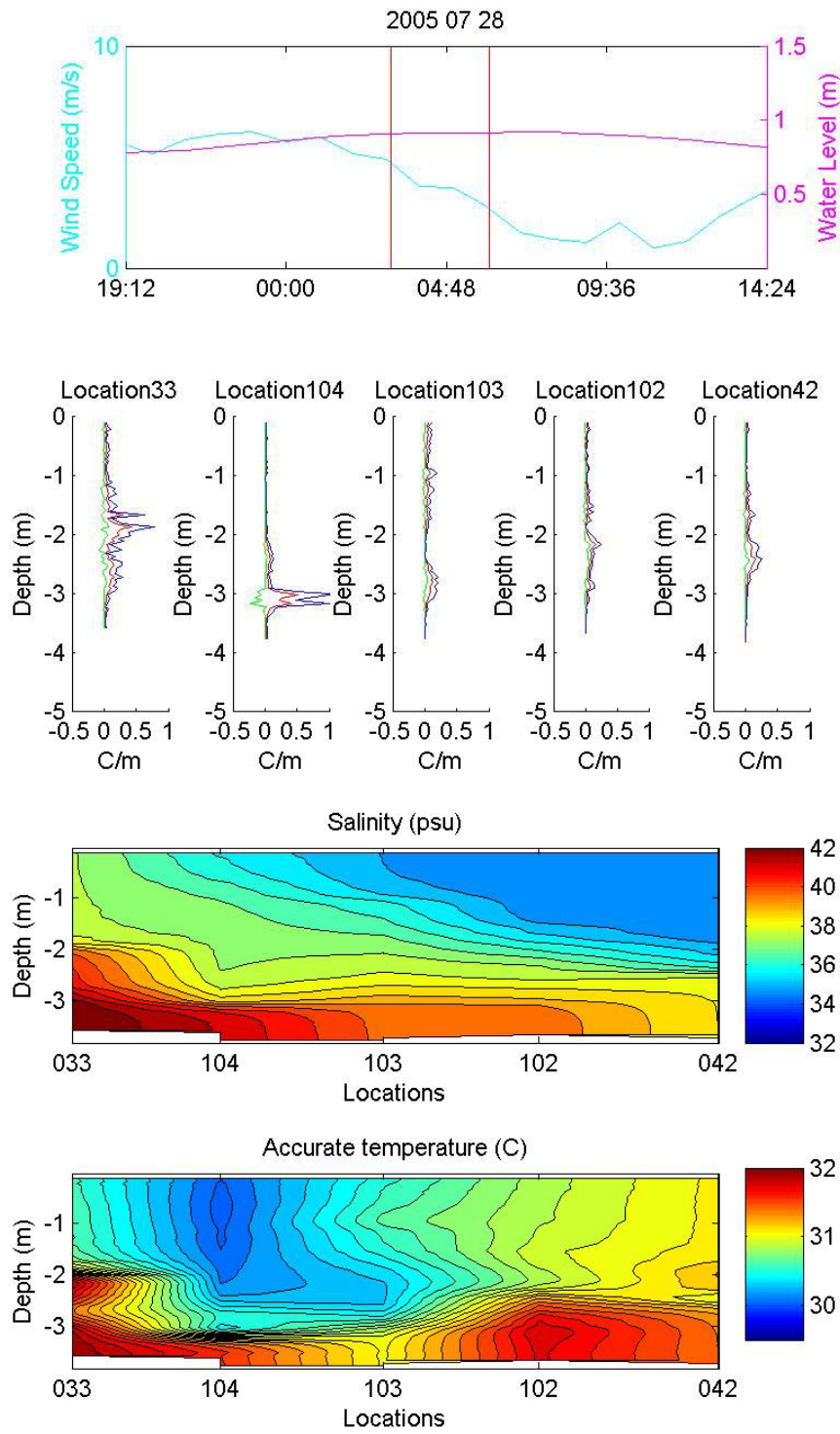


Figure A.50. Transect 3; July 28th 2005, between 0309 and 0606 hours

A.13 Matlab Functions

Following are the Matlab functions and scripts that were used in order to process the data. The first lines of each program describe its use.

SCAMP_RAWDATA

```
function rawdata = SCAMP_RawData(TextFile)
    %%% SCAMP_RawData = SCAMP_RawData(TextFile)
    %%% rawdata is a vector which elements are structures.
    %%% Each structure corresponds to one deployment of the SCAMP.
    %%% Example:
    %%% rawdata(1) = - Depth    --> Vector
    %%%             - FastT0    --> Vector
    %%%             - FastT1    --> Vector
    %%% rawdata(2) = etc.
    %%%
    %%% This function prompts for a text file (textfile.txt) containing the name
    %%% of the .raw files that are to be added to the vector rawdata.
    %%% It returns the vector rawdata and saves it in a .mat file
    %%% (textfile.mat)
    %%%
    %%% Designed for use with SCAMP output data
    %%% calling SCAMP_Process
    %%% called by: SCAMP_AllMat
    %%% Cedric David
    %%% University of Texas
    %%% March 8, 2006

    %If used as a function-----
    FileName=importdata(TextFile);
    iimax=length(FileName);
    %-----
    %Choice of the text file summarizing the .raw files-----
    % TextFile=uigetfile('* .txt','Select Text File');
    % FileName=importdata(TextFile);
    % iimax=length(FileName);
    %-----
    %OR Choice of the .raw files separately-----
    % FileName=uigetfile('* .raw','Select SCAMP Profiles','MultiSelect','on');
    % iimax=length(FileName);
    %-----
    %Creation of ChanEU_i and ChanName_i for each file-----
    for ii = 1:iimax
        myfile = char(FileName{ii});
        SCAMP_Process;
```

```

thischan = ['ChanEU_',num2str(ii)];
eval([thischan,' = ChanEU;']);
%ChanEU_1 = ChanEU;
thisname = ['ChanName_',num2str(ii)];
eval([thisname,' = ChanName;']);
%ChanName_1 = ChanName;
end
%-----
%Creation of the rawdata structure-----
for ii=1:iimax
    thisprofile = eval(['ChanEU_',num2str(ii)]);
    rawdata(ii).FastT0=thisprofile{1};
    rawdata(ii).FastT1=thisprofile{2};
    rawdata(ii).FastC=thisprofile{3};
    rawdata(ii).AccT=thisprofile{6};
    rawdata(ii).Depth=thisprofile{15};
    rawdata(ii).GradFastT0=thisprofile{17};
    rawdata(ii).GradFastT1=thisprofile{18};
    rawdata(ii).SigT=thisprofile{35};
    rawdata(ii).Sal=thisprofile{36};
end
%-----
%Saving the rawdata structure in a .mat file-----
Name=strep(TextFile, '.txt', "");
save(char(['D:\+Research\Research Data#\mat Files\',Name, '.mat']), 'rawdata');
%-----

```

SCAMP_ALLMAT

```
function out=SCAMP_AllMat(TextTextFile)
%% SCAMP_AllMat = SCAMP_AllMat(TextTextFile)
%%
%% This function prompts for a text file (texttextfile.txt) containing the
%% name of the text files corresponding to the deployments at each
%% location. It then calls the function SCAMP_RawData at every location
%% and creates the corresponding .mat file in a specified folder.
%%
%% Designed for use with SCAMP output data
%% calling SCAMP_RawData
%% called by: N/A
%% Cedric David
%% University of Texas
%% March 8, 2006

%Reads the text file containing the textfiles names-----
TextFile=importdata(TextTextFile);
%-----
%Number of locations-----
jjmax=length(TextFile);
%jj is the index number for locations
%-----
%Creation of all the .mat files (for each location)-----
for jj=1:jjmax
    SCAMP_RawData(TextFile{jj});
end
%-----
```

SCAMP_AVERAGE

```
function [outmean,outstd,outdepth]=SCAMP_Average(rawdata,datafield,binsize)
    %%% [outmean,outstd,outdepth] = SCAMP_Average(rawdata,'datafield',binsize)
    %%% rawdata is a vector of structures which one field (datafield) is to be
    %%% averaged.
    %%% rawdata(1) = - Depth    --> Vector
    %%%          - FastT0     --> Vector
    %%%          - FastT1     --> Vector
    %%% rawdata(2) = etc.
    %%%
    %%% binsize is the size, in meters of each bin
    %%% outmean is the computed average
    %%% outstd is the standard deviation
    %%% outdepth is a vector with depth points (1/2 interval), in meters
    %%%
    %%% designed for use with SCAMP output data
    %%% calling: N/A
    %%% called by: SCAMP_DrawAverage, SCAMP_SuperContour
    %%% Cedric David
    %%% University of Texas
    %%% July 14, 2005

    %ii variable for profiles to be average
    %jj variable for bins
    %Taking the absolute value of the parameter-----
    absolute=1 %Turn the absolute value on
    % absolute=0 %Turn the absolute value off
    %-----
    %Number of profiles-----
    nnp=length(rawdata);
    %-----
    %Number of bins, as the maximum number of bins over all the profiles-----
    for ii=1:nnp
        nbin(ii) = round(max(rawdata(ii).Depth)/binsize)+1;
    end
    nnbin=max(nbin);
    %-----
    %Building the intervals-----
    for jj=1:nnbin+1
        border(jj)=(jj-1)*binsize;
    end
    for jj=1:nnbin
        outdepth(jj) = 0.5*(border(jj) + border(jj+1));
```

```

end
%-----
%Selecting the datapoints position in the interval-----
for jj=1:nnbin
    concat=[];
    for ii=1:nnp
        sel{ii}=find((rawdata(ii).Depth>=border(jj))&(rawdata(ii).Depth<border(jj+1)));
        concat=[concat;rawdata(ii).(datafield)(sel{ii})];
    end
    conc{jj}=concat;
end
%-----
%Averaging-----
for jj=1:nnbin
    if absolute
        outmean(jj) = mean_with_NaN(abs(conc{jj}));
        outstd(jj) = std_with_NaN(abs(conc{jj}));
    else
        outmean(jj) = mean_with_NaN(conc{jj});
        outstd(jj) = std_with_NaN(conc{jj});
    end
end
%-----

```


SCAMP_FILTER

```
function rawdataf = SCAMP_Filter(rawdata,top,bot)
    %%% SCAMP_Filter(rawdata,top,bot)
    %%%
    %%% This function removes the top and the bottom part of the measurements
    %%% according to the user's needs. It can also remove the points that have
    %%% big standard deviation although this part is not activated here.
    %%%
    %%% Designed for use with SCAMP output data
    %%% calling N/A
    %%% called by: SCAMP_SuperContour, SCAMP_Draw, SCAMP_DrawAverage
    %%% Cedric David
    %%% University of Texas
    %%% March 8, 2006

    %Finding fieldnames and number of fields-----
    Names=fieldnames(rawdata);
    kkmax=length(Names);
    %-----
    %FNumber of profiles-----
    jjmax=length(rawdata);
    %-----
    %Bottom and top cutoff-----
    for jj=1:jjmax
        posb=find(rawdata(jj).Depth>bot);
        post=find(rawdata(jj).Depth<top);
        for kk=1:kkmax
            vec=rawdata(jj).(char(Names(kk)));
            vec(posb)=NaN;
            vec(post)=NaN;
            rawdata(jj).(char(Names(kk)))=vec;
        end
    end
    %Eliminating the points with big std-----
    % for jj=1:jjmax
    %     for kk=1:kkmax
    %         vec=rawdata(jj).(char(Names(kk)));
    %         pos=find(abs((vec-mean_with_NaN(vec)))>2*std_with_NaN(vec));
    %         vec(pos)=NaN;
    %         rawdata(jj).(char(Names(kk)))=vec;
    %     end
    % end
    rawdataf=rawdata;
```

SCAMP_DRAW

```
function SCAMP_Draw(MatFile,datafield,binsize)
    %%% SCAMP_Draw(MatFile,datafield,binsize)
    %%%
    %%% This function plots all the profiles corresponding to the datafield and
    %%% adds the average profile with standard deviation for the same datafield
    %%% at the end.
    %%% This function also saves the plot as a .jpg file in an appropriate
    %%% folder.
    %%%
    %%% Designed for use with SCAMP output data
    %%% calling SCAMP_Average, SCAMP_Filter
    %%% called by: SCAMP_DrawAllLoc
    %%% Cedric David
    %%% University of Texas
    %%% March 8, 2006

    %Loading of the data corresponding to the location-----
    load(MatFile);
    %-----
    %Taking the absolute value of the parameter-----
    absolute=1 %Turn the absolute value on
    % absolute=0 %Turn the absolute value off
    %-----
    %Cleans the name for proper appearance on plot-----
    Name=strrep(MatFile,'_',' ');
    Name=strrep(Name,'.mat',' ');
    %-----
    %Number of profiles in rawdata-----
    iimax=length(rawdata);
    %-----
    %Filter and average-----
    rawdataf=SCAMP_Filter(rawdata,0.1,10);
    [outmean,outstd,outdepth]=SCAMP_Average(rawdataf,datafield,binsize);
    %-----
    %Changing scale for each datafield-----
    if (strcmp(datafield,'Sal'))
        inter=[32 42];
        dist=[32 37 42];
    elseif strcmp(datafield,'AccT')
        inter=[29.5 32];
        dist=[29.5 32];
    elseif strcmp(datafield,'GradFastT1')
```

```

inter=[-0.5 0.5];
dist=[-0.5 0 0.5];
else
inter=[0 100];
end
%-----
%Plotting procedure-----
for ii=1:iimax
subplot(1,iimax+1,ii)
plot (rawdataf(ii).(datafield),-rawdataf(ii).Depth);
ylim([-5 0]);
xlim(inter);
set(gca,'XTick',dist)
end
if absolute
inter=[-0.5 1];
dist=[-0.5 0 0.5 1];
end
subplot(1,iimax+1,iimax+1)
hold on
plot(outmean,-outdepth,'r')
plot(outmean-outstd,-outdepth,'g')
plot(outmean+outstd,-outdepth,'b')
ylim([-5 0]);
xlim(inter);
set(gca,'XTick',dist)
title({Name;['Parameter: ',datafield];['Binsize= ',num2str(binsize)]});
hold off
%-----
%Saving the .jpg file-----
Name2=strrep(MatFile,'.mat','');
saveas(gcf,char(['D:\+Research\Research Data#\ .jpg Files\' ,num2str(datafield),'_',Name2,'.jpg'])); %gcf
is the number of the current figure
%-----

```

SCAMP_DRAW_ALLLOC

```
function SCAMP_DrawAllLoc(TextMatFile,datafield,binsize)
%% SCAMP_DrawAllLoc(TextMatFile,datafield,binsize)
%%
%% This function plots (using SCAMP_Plot) all the profiles corresponding
%% to the datafield and adds the average profile with standard deviation
%% for the same datafield at the end.
%% It also saves the plot as a .jpg file in an appropriate folder.
%% This is done for all the Locations using the list in a text file
%%
%% Designed for use with SCAMP output data
%% calling SCAMP_Draw
%% called by: N/A
%% Cedric David
%% University of Texas
%% March 8, 2006

% Cleans the name to appear correctly in the plotting window-----
Name=strep(TextMatFile, '_ ');
Name=strep(Name, '.txt,');
%-----
% Reads the text file containing the textfiles names-----
MatFile=importdata(TextMatFile);
%-----
% Number of locations-----
jjmax=length(MatFile);
%-----
%-----
% jj is the index number for locations (=nbr of average profiles)
%-----
% Plotting and Saving Procedure-----
for jj=1:jjmax
    close all;
    SCAMP_Draw(MatFile{jj},datafield,binsize);
end
%-----
```

SCAMP_DRAWAVERAGE

```
function outstd=SCAMP_DrawAverage(MatFile,datafield,binsize)
    %%% SCAMP_DrawAverage(MatFile,datafield,binsize)
    %%%
    %%% This function plots the average only
    %%% adds the average profile with standard deviation for the same datafield
    %%% at the end.
    %%% This function also saves the plot as a .jpg file in an appropriate
    %%% folder.
    %%%
    %%% Designed for use with SCAMP output data
    %%% calling SCAMP_Average, SCAMP_Filter
    %%% called by: SCAMP_PlotLetter
    %%% Cedric David
    %%% University of Texas
    %%% March 8, 2006

    %To test as script-----
    % MatFile='2005_07_06_1047_Location39.mat';
    % datafield='GradFastT1';
    % binsize=0.05;
    %-----
    %Loading of the data corresponding to the location-----
    load(MatFile);
    %-----
    %Taking the absolute value of the parameter-----
    absolute=1 %Turn the absolute value on
    % absolute=0 %Turn the absolute value off
    %-----
    %Cleans the name for proper appearance on plot-----
    Name1=strrep(MatFile,'_',' ');
    Name1=strrep(Name1,'.mat',' ');
    Name2=Name1(17:size(Name1,2));
    %-----
    %Number of profiles in rawdata-----
    iimax=length(rawdata);
    %-----
    rawdataf=SCAMP_Filter(rawdata,0.1,10);
    [outmean,outstd,outdepth]=SCAMP_Average(rawdataf,datafield,binsize);
    %Changing scale for each datafield-----
    if (strcmp(datafield,'Sal'))
        inter=[32 42];
        dist=[32 37 42];
```

```

elseif strcmp(datafield,'AccT')
    inter=[29.5 32];
    dist=[30 31 32];
elseif strcmp(datafield,'GradFastT1')
    if absolute
        inter=[-0.5 1];
        dist=[-0.5 1];
    else
        inter=[-0.5 0.5];
        dist=[-0.5 0 0.5];
    end
else
    inter=[0 100];
end
%-----
%Plotting procedure-----
hold on
plot(outmean,-outdepth,'r')
plot(outmean-outstd,-outdepth,'g')
plot(outmean+outstd,-outdepth,'b')
ylim([-5 0]);
xlim(inter);
set(gca,'XTick',dist)
xlabel(datafield)
ylabel('Depth (m)')
title(Name2)
hold off
%title({Name;['Parameter: ',datafield];['Binsize= ',num2str(binsize)]});
%-----

```

SCAMP_SUPERCONTOURS

```
function Cont=SCAMP_SuperContourS(TextMatFile,datafield,binsize)
    %%% SCAMP_SuperContourS(TextMatFile,datafield,binsize)
    %%%
    %%% This function plots a contour filled figure of the files
    %%% It also saves the plot as a .jpg file in an appropriate folder.
    %%%
    %%%
    %%% Designed for use with SCAMP output data
    %%% calling SCAMP_Filter and SCAMP_Average
    %%% called by: SCAMP_PlotLetterS
    %%% Cedric David
    %%% University of Texas
    %%% March 8, 2006

    %To be tested as a script-----
    % TextMatFile='2005_07_28_0309_0606_033_104_103_102_042.txt';
    % datafield='AccT';
    % binsize=0.05;
    %-----
    %Creation of the vector giving the contour values-----
    if (strcmp(datafield,'Sal'))
        col=32:.5:42;
    elseif strcmp(datafield,'AccT')
        col=29.5:.05:32;
    else
        col=0:.5:100;
    end
    %-----
    %Cleans the name to appear correctly in the plotting window-----
    Name=strrep(TextMatFile,'_',' ');
    Name=strrep(Name,'.txt','');
    %-----
    %Reads the text file containing the textfiles names-----
    MatFile=importdata(TextMatFile);
    %-----
    %Number of locations-----
    jjmax=length(MatFile);
    %-----
    %Creates a cell with the locations names to annotate the contour plots-----
    for jj=1:jjmax
        annot{jj}=TextMatFile(22+(jj-1)*4:24+(jj-1)*4);
    end
```

```

%-----
%computes the distance dist between the points-----
load('GPS_Loc.csv')
dist=0;
lat=0;
long=0;
anglat=0;
anglong=0;
for jj=1:jjmax
    for kk=1:51
        if isequal(str2double(annot(jj)),GPS_Loc(kk,1))
            lat(jj)=GPS_Loc(kk,2);
            long(jj)=GPS_Loc(kk,3);
        end
    end
end
leng(1)=0;
dist(1)=0;
for jj=2:jjmax
    leng(jj)=6380*sqrt((tan((long(jj)-long(jj-1))*pi/180))^2+(tan((lat(jj)-lat(jj-1))*pi/180))^2);
    dist(jj)=dist(jj-1)+leng(jj);
end
%-----
%jj is the index number for locations (=nbr of average profiles)
%ii is used as the scan number index
%kk is used as the GPS location index
%-----
%Computation of the average profiles-----
for jj=1:jjmax
    load(MatFile{jj});
    rawdataf=SCAMP_Filter(rawdata,0.1,10);
    [aa,bb,cc]=SCAMP_Average(rawdataf,datafield,binsize);
    meanstruct(jj).mean=aa;
    meanstruct(jj).std=bb;
    meanstruct(jj).depth=cc;
end
%-----
%Max number of scans-----
for jj=1:jjmax
    nscan(jj)=length(meanstruct(jj).depth);
end
nnscale=max(nscan)
%-----

```



```

%Finding the deeper depth-----
depth=[];
for jj=1:jjmax
    if length(meanstruct(jj).depth)==nnscan
        depth=meanstruct(jj).depth;
    end
end
%-----
%Normalization of the length of the average profiles-----
for jj=1:jjmax
    for ii=1:nnscan
        if ii>length(meanstruct(jj).mean)
            meanstruct(jj).mean(ii)=NaN;
        end
    end
    meanstruct(jj).depth=depth;
end
%-----
%Concatenating the profiles in a matrix-----
conc=zeros(nnscan,jjmax);
for jj=1:jjmax
    conc(:,jj)=meanstruct(jj).mean;
end
%-----
%Plotting-----
fig=contourf(dist,-depth,conc,col);
set(gca,'XTick',dist)
set(gca,'XTickLabel',annot)
% legend(datafield,'Location','NorthEast')
ylabel('Depth (m)')
colormap jet;
colorbar;
title(datafield)
% title(['Contour: ',Name];['Field: ',datafield];['Binsize (meters): ',num2str(binsize)]);
% saveas(gcf,char(['D:\SCAMP\Matlab#\SCAMP Files#\
Files\',num2str(datafield),'_',strrep(TextMatFile,'.txt',''),' .jpg'])); %gcf is the number of the current figure
%-----

```

SCAMP_SUPERCONTOURT

```
function Cont=SCAMP_SuperContourT(TextMatFile,datafield,binsize)
    %%% SCAMP_SuperContourT(TextMatFile,datafield,binsize)
    %%%
    %%% This function plots a contour filled figure of the files
    %%% It also saves the plot as a .jpg file in an appropriate folder.
    %%%
    %%%
    %%% Designed for use with SCAMP output data
    %%% calling SCAMP_Filter and SCAMP_Average
    %%% called by: SCAMP_PlotLetterT
    %%% Cedric David
    %%% University of Texas
    %%% October 6, 2005

    %To be tested as a script-----
    % TextMatFile='2005_07_27_2347_1404_039.txt';
    % datafield='AccT';
    % binsize=0.05;
    %-----
    %Creation of the vector giving the contour values-----
    if (strcmp(datafield,'Sal'))
        col=32:.5:42;
    elseif strcmp(datafield,'AccT')
        col=29.5:.05:32;
    else
        col=0:.5:100;
    end
    %-----
    %Cleans the name to appear correctly in the plotting window-----
    Name=strrep(TextMatFile,'_',' ');
    Name=strrep(Name,'.txt','');
    %-----
    %Reads the text file containing the textfiles names-----
    MatFile=importdata(TextMatFile);
    %-----
    %Number of profiles at the same location-----
    jjmax=length(MatFile);
    %-----
    %Creates a cell with the locations names to annotate the contour plots-----
    for jj=1:jjmax
        annot{jj}=TextMatFile(22:24);
    end
```

```

%-----
%distance constont between each section of the plot-----
dist=1:1:jjmax;
%-----
%-----
%jj is the index number for locations (=nbr of average profiles)
%ii is used as the scan number index
%-----
%Computation of the average profiles-----
for jj=1:jjmax
    load(MatFile{jj});
    rawdataf=SCAMP_Filter(rawdata,0.1,10);
    [aa,bb,cc]=SCAMP_Average(rawdataf,datafield,binsize);
    meanstruct(jj).mean=aa;
    meanstruct(jj).std=bb;
    meanstruct(jj).depth=cc;
end
%-----
%Max number of scans-----
for jj=1:jjmax
    nscan(jj)=length(meanstruct(jj).depth);
end
nnscale=max(nscan)
%-----
%Finding the deeper depth-----
depth=[];
for jj=1:jjmax
    if length(meanstruct(jj).depth)==nnscale
        depth=meanstruct(jj).depth;
    end
end
%-----
%Normalization of the length of the average profiles-----
for jj=1:jjmax
    for ii=1:nnscale
        if ii>length(meanstruct(jj).mean)
            meanstruct(jj).mean(ii)=NaN;
        end
    end
    meanstruct(jj).depth=depth;
end
%-----
%Concatenating the profiles in a matrix-----
conc=zeros(nnscale,jjmax);

```

```

for jj=1:jjmax
    conc(:,jj)=meanstruct(jj).mean;
end
%-----
%Plotting-----
fig=contourf(dist,-depth,conc,col);
set(gca,'XTick',dist)
set(gca,'XTickLabel',annot)
% legend(datafield,'Location','NorthEast')
ylabel('Depth (m)')
colormap jet;
colorbar;
title(datafield)
% title({'Contour: ',Name};['Field: ',datafield];['Binsize (meters): ',num2str(binsize)]);
% saveas(gcf,char(['D:\SCAMP\Matlab\#SCAMP Files\#.jpg
Files\',num2str(datafield),'_',strrep(TextMatFile,'.txt',''),' .jpg'])); %gcf is the number of the current figure
%-----

```

SCAMP_PLOTLETTERS

```
function SCAMP_PlotLetterS(TextMatFile,TextWSD,binsize)
    %%% SCAMP_PlotLetterS(TextMatFile,binsize)
    %%%
    %%% This function plots tides and wind (from TCOON data), Contour plots at
    %%% the locations given in the matfile (salinity and temperature), and
    %%% average of Temperature gradient.
    %%% It also saves the plot as a .jpg file in an appropriate folder.
    %%%
    %%%
    %%% Designed for use with SCAMP output data
    %%% calling SCAMP_SuperContourS, SCAMP_DrawAverage, and PlotWeather
    %%% called by: N/A
    %%% Cedric David
    %%% University of Texas
    %%% March 8, 2006

    %To be tested as Script-----
    % TextMatFile='2005_07_27_2157_0200_033_104_103_102_042.txt';
    % binsize=0.05;
    % TextWSD='WSD_CES.csv'
    %-----
    %Cleans the name to appear correctly in the plotting window-----
    Name=strrep(TextMatFile,'_',' ');
    Name=Name(1:10);
    %-----
    %Graphical Definitions-----
    set(gcf,'Position',[400 100 325 450]) %Position of the figure on the screen, pixels
        %[left bottom width height]
    set(gcf,'PaperPositionMode','manual')
    set(gcf,'PaperUnits','inches')
    set(gcf,'PaperSize',[8.5,11]) % [width, height] inches
    set(gcf,'PaperPosition',[1, 1, 6.5, 9]) %[left, bottom, width, height] inches
    bigaxes=axes;
    set(bigaxes,'Visible','off')
    %-----
    %Reads the text file containing the .mat files names, gets their number----
    MatFile=importdata(TextMatFile);
    jjmax=length(MatFile);
    %-----
    %Plotting-----
    clf reset
```

```

axes('Position',[0.2, 0.8, 0.6, 0.15])    %[left bottom width height] %
PlotWeather(TextMatFile,TextWSD)
title(Name)
for jj=1:jjmax
    axes('Position',[0.15+0.6*(jj-1)/(jjmax-1), 0.50, 0.09, 0.2]) %[left bottom width height] %
    SCAMP_DrawAverage(MatFile{jj},'GradFastT1',binsize);
end
axes('Position',[0.15, 0.25, 0.7, 0.15])    %[left bottom width height] %
SCAMP_SuperContourS(TextMatFile,'Sal',binsize)
axes('Position',[0.15, 0.05, 0.7, 0.15])    %[left bottom width height] %
SCAMP_SuperContourS(TextMatFile,'AccT',binsize)
%-----
%Saving the picture file-----
saveas(gcf,char(['D:\+Research\Research Data#\jpg
Files\Transect\','Letter_',strrep(TextMatFile,'.txt',''),'jpg'])); %gcf is the number of the current figure
%-----

```

SCAMP_PLOTLETTERT

```
function SCAMP_PlotLetterT(TextMatFile,TextWSD,binsize)
    %%% SCAMP_PlotLetterT(TextMatFile,binsize)
    %%%
    %%% This function plots tides and wind (from TCOON data), Contour plots at
    %%% the locations given in the matfile (salinity and temperature), and
    %%% average of Temperature gradient.
    %%% It also saves the plot as a .jpg file in an appropriate folder.
    %%%
    %%%
    %%% Designed for use with SCAMP output data
    %%% calling SCAMP_SuperContourT, SCAMP_DrawAverage, and PlotWeather
    %%% called by: N/A
    %%% Cedric David
    %%% University of Texas
    %%% March 8, 2006

    %To be tested as Script-----
    % TextMatFile='2005_07_28_0200_1520_104.txt';
    % binsize=0.05;
    % TextWSD='WSD_CES.csv'
    %-----
    %Cleans the name to appear correctly in the plotting window-----
    Name=strrep(TextMatFile,'_',' ');
    Name=Name(1:10);
    %-----
    %Graphical Definitions-----
    set(gcf,'Position',[400 100 325 450]) %Position of the figure on the screen, pixels
        %[left bottom width height]
    set(gcf,'PaperPositionMode','manual')
    set(gcf,'PaperUnits','inches')
    set(gcf,'PaperSize',[8.5,11])      %[width, height] inches
    set(gcf,'PaperPosition',[1, 1, 6.5, 9]) %[left, bottom, width, height] inches
    bigaxes=axes;
    set(bigaxes,'Visible','off')
    %-----
    %Reads the text file containing the .mat files names, gets their number----
    MatFile=importdata(TextMatFile);
    jjmax=length(MatFile);
    %-----
    %Plotting-----
    clf reset
```

```

axes('Position',[0.2, 0.8, 0.6, 0.15])    %[left bottom width height] %
PlotWeather(TextMatFile,TextWSD)
title(Name)
for jj=1:jjmax
    axes('Position',[0.15+0.6*(jj-1)/(jjmax-1), 0.50, 0.09, 0.2]) %[left bottom width height] %
    SCAMP_DrawAverage(MatFile{jj},'GradFastT1',binsize);
end
axes('Position',[0.15, 0.25, 0.7, 0.15])    %[left bottom width height] %
SCAMP_SuperContourT(TextMatFile,'Sal',binsize)
axes('Position',[0.15, 0.05, 0.7, 0.15])    %[left bottom width height] %
SCAMP_SuperContourT(TextMatFile,'AccT',binsize)
%-----
%Saving the picture file-----
saveas(gcf,char(['D:\+Research\Research Data#\jpg
Files\Transect\Time\','Letter_',strep(TextMatFile,'.txt',''),'jpg']));    %gcf is the number of the current figure
%-----

```


PLOTWEATHER

```
function PlotWeather(TextMatFile,TextWSD)
    %%% PlotWeather(TextMatFile,TextWSD)
    %%%
    %%% This function plots winds and tides from normalized files. It includes
    %%% a time window of the experiments inside a 24 hours period.
    %%%
    %%% Designed for use with SCAMP output data
    %%% calling N/A
    %%% called by: SCAMP_PlotLetterS, SCAMP_PlotLetterT
    %%% Cedric David
    %%% University of Texas
    %%% March 8, 2006

    %To be tested as a script-----
    % TextMatFile='2005_07_28_0309_0500_033_037_101_039_042.txt';
    % TextWSD='WSD_CES.csv';
    %-----
    %Primary water level data-----
    TextPWL='PWL_TCOON.csv';
    %-----
    %Loading the weather data in a matrix-----
    WSD=load(TextWSD);
    PWL=load(TextPWL);
    %-----
    %Get the time stamps from the name of the TextMatFile, manage if next day--
    Time1=[TextMatFile(1:4),TextMatFile(6:7),TextMatFile(9:10),'T',TextMatFile(12:15),'00'];
    if str2num(TextMatFile(17:20))>str2num(TextMatFile(12:15))
        Time2=[TextMatFile(1:4),TextMatFile(6:7),TextMatFile(9:10),'T',TextMatFile(17:20),'00'];
    else
        d=str2num(TextMatFile(9:10));
        if d<10
            Time2=[TextMatFile(1:4),TextMatFile(6:7),'0',
num2str(str2num(TextMatFile(9:10))+1)],'T',TextMatFile(17:20),'00'];
        else
            Time2=[TextMatFile(1:4),TextMatFile(6:7),'',
num2str(str2num(TextMatFile(9:10))+1)],'T',TextMatFile(17:20),'00'];
        end
    end
end
%-----
%Number of weather data points-----
iimax=size(WSD,1);
jjmax=size(PWL,1);
%-----
```

```

%Creation of the date numbers-----
julwsd=0;
julpwl=0;
for ii=1:iimax
    julwsd(ii)=datenum([WSD(ii,1) WSD(ii,2) WSD(ii,3) WSD(ii,4) WSD(ii,5) WSD(ii,6)]);
end
for jj=1:jjmax
    julpwl(jj)=datenum([PWL(jj,1) PWL(jj,2) PWL(jj,3) PWL(jj,4) PWL(jj,5) PWL(jj,6)]);
end
%-----
%Limits on the plot-----
T1=datenum(Time1,'yyyymmddTHHMMSS');
T2=datenum(Time2,'yyyymmddTHHMMSS');
L1=T1-0.5;
L2=T2+0.5;
for jj=1:jjmax
    B1(jj)=T1;
    B2(jj)=T2;
    V(jj)=jj/jjmax*10;
end
%-----
%Plotting Procedure-----
[AX,H1,H2]=plotyy(julwsd,WSD(:,8),julpwl,PWL(:,7));
axes(AX(1));
xlim([L1 L2]);
ylim([0 10]);
ylabel('Wind Speed (m/s)');
hold on
plot(B1,V,'r');
plot(B2,V,'r');
datetick(AX(1),'x',15,'keepticks')
axes(AX(2));
xlim([L1 L2]);
ylim([0 1.5]);
ylabel('Water Level (m)');
datetick(AX(2),'x',15,'keepticks')
hold off
%-----

```

APPENDIX B Idealized 2D modeling of a gravity underflow

This appendix examines the impact of insufficient grid resolution on gravity current representation in the Environmental Fluid Dynamics Computer Code (EFDC) of Hamrick (Hamrick, 1992). EFDC solves the free surface, hydrostatic, Reynolds averaged equations of motion for a variable density fluid using a Cartesian or curvilinear orthogonal horizontal grid and a sigma-coordinate vertical grid. To understand and document the capabilities of EFDC, we examine 2-dimensional gravity currents at various grid resolutions and assess numerically-induced changes in flow characteristics. Tests are run with and without turbulence closure, in order to differentiate between background numerical effects and modeled turbulent entrainment. We then discuss consequences on mixing and energetics calculations, and finally propose solutions.

B.1 Gravity Current Theory

B.1.a Characteristic Variables

Although the modeled gravity current is clearly a continuum of properties, it is reasonable to define a characteristic gravity current thickness, from which follows definitions of characteristic velocity, density anomaly and Froude number that describe the gravity current at a given location along the slope. While there are many ways to quantify these characteristic scales, we begin by following the approach of Ellison and Turner (1959), which has been well-established and frequently used in the literature (Ellison and Turner 1959; Dallimore et al, 2001; Garcia, 1993; Felix 2004, Buckee et al 2001, e.g.). Because these variables are obtained using integration over depth, we will also refer to these variables as “bulk” variables.

Ellison and Turner (1959) defined the gravity current bulk velocity and thickness together by integrating over the entire water depth:

$$v_E h_E = \int_0^{\infty} v dz \quad (B.1)$$

Here v_E and h_E are the characteristic bulk (depth-averaged) velocity and thickness of the current. Similar relationships also follow for density and momentum:

$$\Delta_E h_E = \int_0^{\infty} g' dz \quad (B.2)$$

$$v_E^2 h_E = \int_0^{\infty} v^2 dz \quad (B.3)$$

where Δ_E is the depth-integrated reduced gravity term, and g' is the vertically local reduced gravity term, defined as follows:

$$g' = \frac{\Delta\rho}{\rho_o} g \quad (\text{B.4})$$

where g is the acceleration due to gravity, $\Delta\rho$ is the vertically local density anomaly, and ρ_o is the ambient density. By this definition, h and v are both defined uniquely irrespective of the density:

$$v_E = \frac{v_E^2 h_E}{v_E h_E} = \frac{\int_0^\infty v^2 dz}{\int_0^\infty v dz} \quad (\text{B.5})$$

$$h_E = \frac{v_E h_E}{v_E} = \frac{\int_0^\infty v dz}{v_E} \quad (\text{B.6})$$

and the value of Δ_E is therefore determined by the momentum distribution in the current. A flow of depth h_E , vertically uniform velocity v_E and vertically uniform density anomaly Δ_E would have the same momentum as the gravity current defined by h_E , v_E and Δ_E . In this way, we are treating the gravity current as a “uniform slab”.

An alteration of the Ellison and Turner analysis involves defining the thickness of the current based on δ , the distance above the bed at which the maximum vertical density gradient is found:

$$h_\delta = 2.5\delta \quad (\text{B.7})$$

This analysis, used by Dallimore et al (2001), follows by defining a characteristic velocity and buoyancy term using equations (B.1) and (B.2) from the Ellison and Turner analysis:

$$v_\delta h_\delta = \int_0^\infty v dz \quad (\text{B.8})$$

$$\Delta_\delta h_\delta = \int_0^\infty g' dz \quad (\text{B.9})$$

In this definition, h_δ is predefined as proportional to δ , leaving equations (B.1) and (B.2) capable of uniquely defining v_δ and Δ_δ , without use of the integral momentum of equation (B.3). It is perhaps significant to note that the limits of integration are extended to infinity for this analysis, despite the limitation of the gravity current thickness to a finite value. By integrating to infinity, the characteristic variables become proportional to the Ellison and Turner variables discussed above:

$$v_\delta = \frac{v_E h_E}{h_\delta}, \quad \Delta_\delta = \frac{\Delta_E h_E}{h_\delta} \quad (\text{B.10})$$

B.1.b Derived Variables

We use the denismetric Froude number to classify the gravity current as super critical or sub critical. We define the gravity current Fr based on the integrated variables. Because we are interested in Fr as a classifier for the hydrodynamics, we use the Ellison and Turner variables rather than the δ variables:

$$Fr^2 = \frac{v^2}{\Delta_E h_E} \quad (B.11)$$

Ellison and Turner (1959) found experimentally that the gravity current should reach a steady state, after which the velocity is not changing along the slope. At this steady state, the Froude Number is also not a function of slope. Dallimore et al (2001) also confirmed this characteristic of gravity currents. In the present work, Fr is calculated using the Ellison and Turner variables (h_E , etc.), rather than the Dallimore variables (h_δ , etc.). Using the Ellison and Turner method, the thickness of the current is defined based on the velocity profile rather than the salinity. Because Fr is a parameter characterizing the flow of the current, it is appropriate to calculate it using variables that represent the flow, rather than the density distribution.

In this study, model simulations are run with and without turbulence closure. Because turbulence is a sink of kinetic energy, the Froude numbers of the turbulent and non-turbulent tests do not match. In order to compare different test cases, it is necessary that they have similar hydraulic characteristics. To ensure that this is the case, the molecular viscosity in the non turbulent test cases is altered to match Fr of the turbulent cases to within 20%.

A term that quantifies vertical mixing of the gravity current is the entrainment rate, E. This is another characteristic that remains constant once a steady state is reached for the gravity current (Ellison and Turner, 1959, Dallimore et al, 2001, Tanny et al, 1995). The entrainment rate is defined as the ratio of the vertical velocity into the current from the ambient fluid (the entrainment velocity) to the mean flow velocity:

$$E = \frac{W_e}{v} \quad (B.12)$$

Using the derivation of Ellison and Turner (1959), which is based on equations (B.1), (B.2), and (B.3), we have by continuity of the 2-D gravity current:

$$W_e = \frac{\partial(vh)}{\partial x} \quad (B.13)$$

where W_e is the entrainment velocity, v and h are the depth-integrated velocity and height of the gravity current, defined by either integration method discussed above. By combining equations (B.12) and (B.13), we have:

$$E = \frac{1}{v} \frac{\partial(vh)}{\partial x} \quad (B.14)$$

This definition of entrainment is robust and has been used extensively in the literature. However, because the flow field for the non-turbulent test cases has been altered to match

Froude Numbers with the turbulent tests, it is more informative to calculate E using the density profile. Using the method of Hebert et al (1979) and Dallimore et al (2001), we begin with conservation of mass:

$$\frac{\partial(\Delta v h)}{\partial x} = 0 \quad (\text{B.15})$$

and combine this with equation with (B.14) to get:

$$E = -\frac{h}{\Delta} \frac{\partial \Delta}{\partial x} \quad (\text{B.16})$$

which is used in Dallimore et al (2001) to form the equation:

$$E = \frac{-h}{S'_{\max}} \frac{\partial S_{\max}}{\partial x} \quad (\text{B.17})$$

where S_{\max} is the maximum salinity in the underflow, and S'_{\max} is the maximum salinity anomaly. Scaling arguments are used to justify these substitutions. Dallimore et al (2001) use equation (B.17) to evaluate the entrainment rate for field data. We use h_{δ} to calculate entrainment with the equation, because in this method entrainment is based on salinity measurements. This, along with the substitutions in equation (B.17), remove E from all dependence on the velocity profile; all variables in the equation are taken from the salinity profile.

B.2 Basin Characteristics and Computational Space

The basin used for our analysis in EFDC is depicted in Figure B.1. Our basin is uniform in the y-direction, so that we can treat the basin as 2-D. The depth at the shallow end in the figure (boundary A) is 10 m. Boundary A is also where the gravity current enters our computational space. The basin has a uniform slope of 0.5% (1/200) in the x-direction, as compared to the 0.6% slope of Corpus Christi Bay. After a distance of 3.5 km from the source boundary, the basin jumps to a depth of 50 m. The deep region of the basin stretches for a kilometer, followed by an open boundary at boundary B in the figure. This is done to avoid complications of boundary effects on the current.

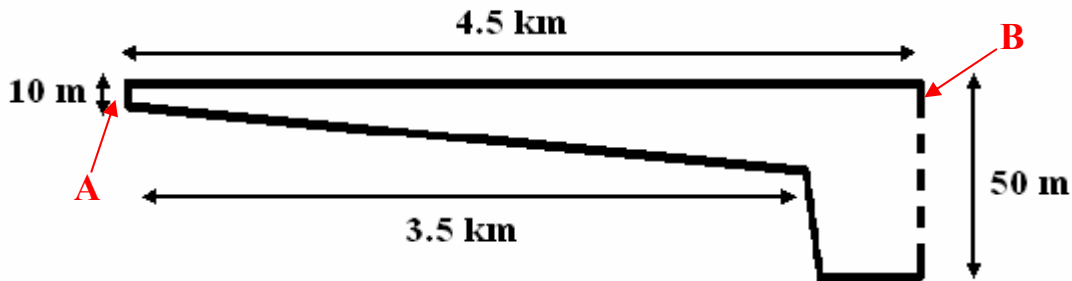


Figure B.1. *x-z* plane view of the basin simulated in these tests. The shallow left boundary is a source boundary, while the right dashed boundary is an open boundary. The diagram is not drawn to scale.

We have refined the horizontal grid in an effort to avoid any effects of poor horizontal resolution on our results. For all simulations, Δx is 50 m. The vertical thickness of each layer is stored in EFDC as a fraction of the total depth, so that the absolute thickness of each layer grows as we move down slope. The term Δz^* is related to the dimensional Δz by:

$$\Delta z^* = \Delta z / H \quad (\text{B.18})$$

where H is the total water depth. In cases where Δz^* is very small and many layers would be required to maintain a uniform grid resolution for the entire depth of the basin, we maintain a uniformly refined grid only in the region of the underflow and increase the fractional depth by 10% per layer thereafter. We do this to minimize computational costs. For Δz^* greater than 0.02, the vertical grid resolution is constant throughout the depth of the basin. The tests presented here have a Δz^* range from 0.001 to 0.2.

The initial salinity in the basin is set to zero. The saline underflow has an input salinity of 15‰, a density anomaly on the same orders as the minimum density contrast between Corpus Christi Bay and Oso Bay. The inflow velocity of the gravity current is 7.5 cm/s in the bottom meter of boundary A. This inflow condition was selected based on rough observations in field data taken from Corpus Christi Bay in the summer of 2005. We run simulations for just over seven times the time scale for reaching the end of the basin (based on the inlet velocity). This corresponds to a simulation time of 120 hours. We analyze data from x-coordinates of 500 m to 3000 m, because the gravity current's initial adjustment to steady state and final drop off the sloping shelf are not processes with which we are concerned and from visual inspection are contained in the first and last 500 m of the shelf.

B.3 Test Cases

We present model results from two different test cases in this appendix. Within each test case, we run simulations at several vertical grid resolutions. The first case, the MY test case, is a series of tests with the Mellor-Yamada (1982) turbulence closure (as modified by Galperin et al, 1988). We also run simulations with the turbulence closure turned off (non-turbulent, or NT test cases). Because underflows are often turbulent phenomena, laminar representation of gravity currents in a model is non-physical, and alone is not useful for modeling gravity currents. The NT test case, when compared to the MY test case, tells us how the model behaves external to the turbulence closure. Because the diffusivity of the salt in the underflow is set to molecular levels in the NT test case ($10^{-9} \text{ m}^2/\text{s}$), negligible mixing should occur in these tests. Any mixing that we detect is therefore a result of numerical error. The Δz^* values for the various grid resolutions used in our simulations are displayed in Table B.1.

Table B.1: Summary of vertical grid resolution for simulations run.

$\Delta z/H$	NT	MY	Cells in Underflow
0.001	X	X	180
0.002	X	X	85
0.005	X	X	30
0.008	X	X	15-20
0.02	X	X	5-10
0.04	X	X	2-3
0.1	X	X	<1
0.2		X	<1

B.4 Results and Discussion

In comparing the simulations results for different grid resolutions, we want to discern the effects of the turbulence model from the model's behavior without the turbulence closure; this helps us determine the origin of numerical effects. It is for this reason that we examine both results from MY and NT simulations. We analyze data from x-coordinates of 500 m to 3000 m, because the gravity current's initial adjustment to steady state and final drop off the sloping shelf are not processes with which we are concerned and from visual inspection seem to be contained in the first and last 500 m of the shelf.

B.4.a Flow Observations

Before we begin assessing the effects of resolution on mixing in the basin, we examine the impact of grid resolution on our model results via the velocity and salinity profiles. In Figure B.2, we see the profiles for three representative MY tests. Our first observation is that the velocity maximum is in the same location as the maximum density gradient for the most resolved test. This observation is consistent with the literature (Ellison and Turner, 1959). However, the maximum velocity is located progressively further away from δ as resolution worsens. Another feature that declines as resolution becomes coarse is the salinity profile's shape. In Figure B.2(a), the salinity has a sharp interface at δ that clearly defines the gravity current. However, this interface becomes less well-defined as resolution goes down in Figures B.2(b) and B.2(c).

In comparison with the MY tests, the salinity profiles in the NT tests shown in Figure B.3 do not have a sharp interface between underflow and ambient fluid. While there is a region near the bed with higher salinity, the profile in these tests is smooth. In addition, we also note that the velocity maximum is in approximately the same vertical location as δ for the two more resolved NT cases.

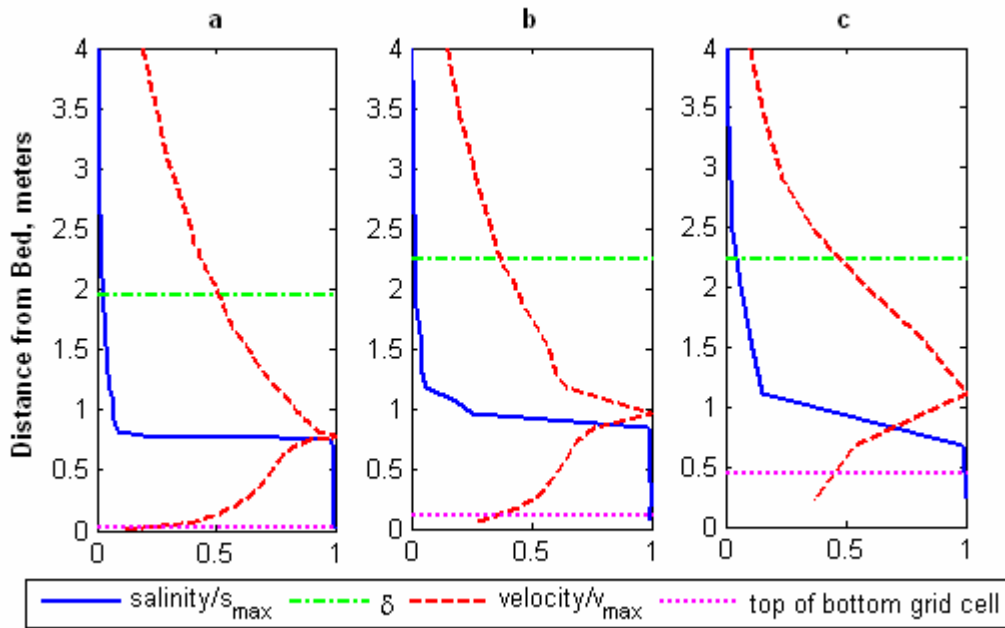


Figure B.2. Profiles of salinity and velocity (at 2475 meters from the source) for select MY tests. Velocity and salinity values are non-dimensionalized by v_{max} and s_{max} , where v_{max} and s_{max} are the maximum velocity and salinity in the water column, respectively. The symbol δ refers to z at the maximum density gradient. The values of Δz^* in these tests are (a) 0.001, (b) 0.005, and (c) 0.02.

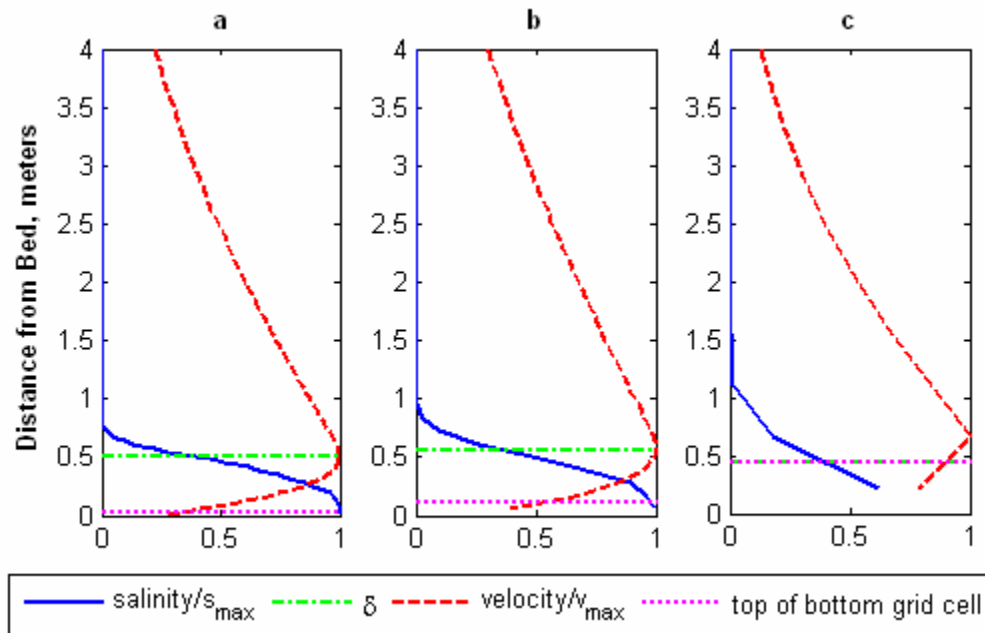


Figure B.3. Profiles of salinity and velocity (at 2475 meters from the source) for select NT tests. Velocity and salinity values are non-dimensionalized by v_{max} and s_{max} , where v_{max} and s_{max} are the maximum velocity and salinity in the water column, respectively. The symbol δ refers to z at the maximum density gradient. The values of Δz^* in these tests are (a) 0.001, (b) 0.005, and (c) 0.02.

B.4.b Froude Number and Entrainment Rate

As is expected, the Froude number is constant with distance down-slope (Figure B.4) in the MY test cases. The correlation coefficient between Fr^2 from the most resolved case and x is 0.195. In addition, the Froude number varies with resolution. The four most resolved cases have approximately the same Froude number. The four cases with the more coarse resolution, however, have Froude numbers that vary much more. This trend is more apparent from Figure B.5. It appears that there is a threshold of resolution after which Fr^2 does not change with resolution. We could think of this resolution as the minimum resolution for accurate gravity current modeling, because a resolution below it impacts the properties of the flow. We see the same trend for bulk characteristic variables, as well.

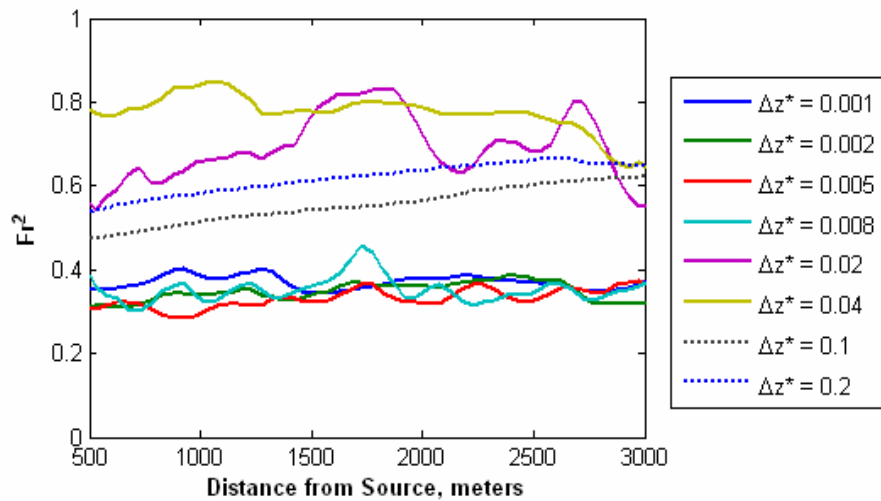


Figure B.4: Square of the Densimetric Froude Number, varying in resolution and in distance along slope.

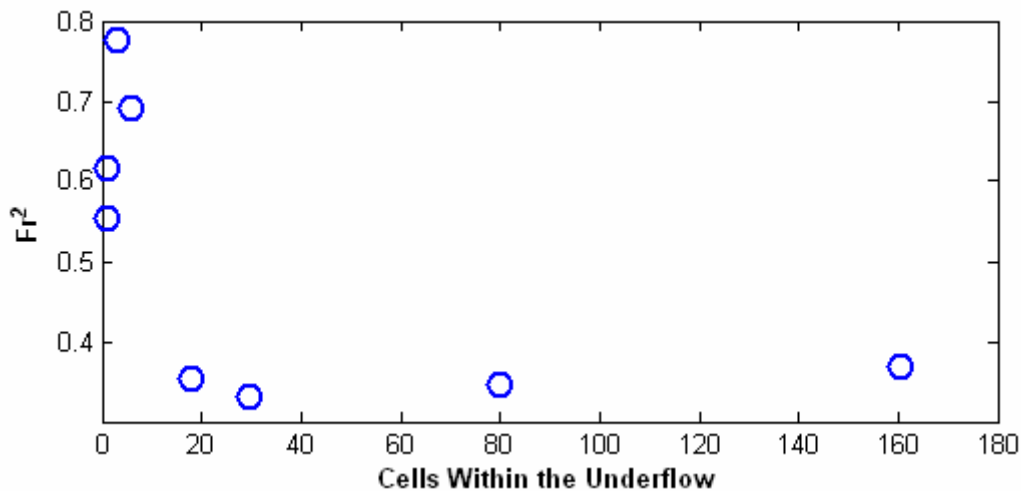


Figure B.5: Mean Froude Number (squared) plotted against grid resolution.

Entrainment rates were also calculated from equation B.17, for both the MY and the NT test cases. It may seem meaningless to calculate entrainment for the NT cases, but we do this because it gives us a quantitative measure of the numerical effects of EFDC on mixing. Because the turbulence model is turned off, all mixing should be due to molecular Brownian motion, and E should be essentially zero. Therefore, any entrainment calculated from the NT runs can be considered “background” numerical effects. Non-turbulent entrainment rates should be at least an order of magnitude below MY entrainment rates for the numerical error to be considered negligible.

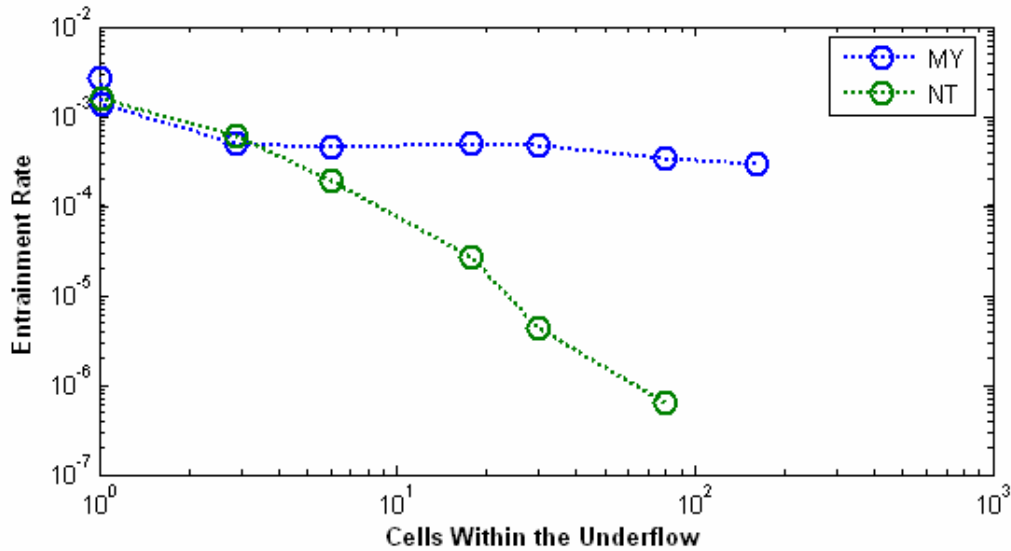


Figure B.6: Log-log plot of mean Entrainment Rate plotted against grid resolution.

The NT entrainment rate in Figure B.6 is several orders of magnitude smaller than the entrainment rate in the MY tests for the high resolution simulations. This implies that numerical entrainment external to the turbulence model is negligible for these cases. However, the entrainment rate in the NT cases increases in a nearly logarithmically as resolution decreases. At the threshold of between ten and twenty grid cells within the underflow, the background entrainment rate reaches the same order of magnitude as the MY entrainment rate. This implies that this threshold is the resolution at which background numerical effects become significant.

In order to be confident in a model’s calculated entrainment rate, two characteristics are desirable. First, the background entrainment rate must be low compared with the modeled turbulent entrainment rate, as discussed above. Second, the modeled turbulent entrainment rate must not be a function of grid resolution in the range of resolution being used. Figure B.6 shows that entrainment is not a function of resolution for most of the simulations, but becomes variable at very low resolutions.

B.5 Conclusion

We have run several simulations of a gravity current flowing down a slight incline in a 2D basin. We varied only the vertical grid resolution and the turbulence settings; the flow conditions

remained the same in all simulations. All differences between simulation results were therefore a result of numerical effects, not changes in the physical phenomenon being studied.

We also found that for the tests with the turbulence models turned on, all tests with a grid resolution of twenty or more grid cells within the gravity current had very similar results in terms of Froude Number and entrainment rate, implying that at these finer grid resolutions gravity current flow is not a function of resolution. However, tests with resolutions less than twenty grid cells had Froude Numbers and entrainment rates that vary with grid resolution. In addition, background numerical effects become significant at this same threshold.

This threshold of resolution has implications for gravity current modeling. Practical models of a system such as Corpus Christi Bay might include no more than ten or twenty grid cells in the entire water column. For a system such as Corpus Christi Bay, this would be equivalent to the coarsest tests presented in our results. The importance of vertical grid resolution for capturing gravity currents has been discussed in the literature with respect to z-coordinate models, but not for σ -coordinate models such as EFDC. These results imply that care must be taken when modeling thin stratification, regardless of the coordinate system used.

APPENDIX C 3D modeling of the Oso Bay outflow

C.1 Introduction

Using our information regarding 2D gravity current behavior in EFDC to model a 3D current in Corpus Christi Bay gives us insight into realistic situations where EFDC would be used. The tests presented in this section include a comparison of the stratification captured by a model of the Oso Bay – Corpus Christi exchange flows with different vertical grid structures. This comparison demonstrates the results that we found in our 2D modeling tests, and documents the limitations of EFDC in capturing stratification due to a thin underflow.

C.2 Basin Characteristics and Computational Space

The computational domain consists of a nine square kilometer region surrounding the outlet of Oso Bay, as shown in Figure C.1. In the horizontal plane, grid cells are Cartesian. They have the dimensions 20 meters by 20 meters at the mouth of Oso Bay, and the grid spacing in the x- and y- directions increases at a 7.5% expansion rate thereafter until the boundaries are reached. The cells in our computational space that correspond to the physical locations of profiles taken in field tests in 2005 are shown with black vertical lines in the figure, and this is where model output is taken. This provides a direct comparison between the model results and field data.

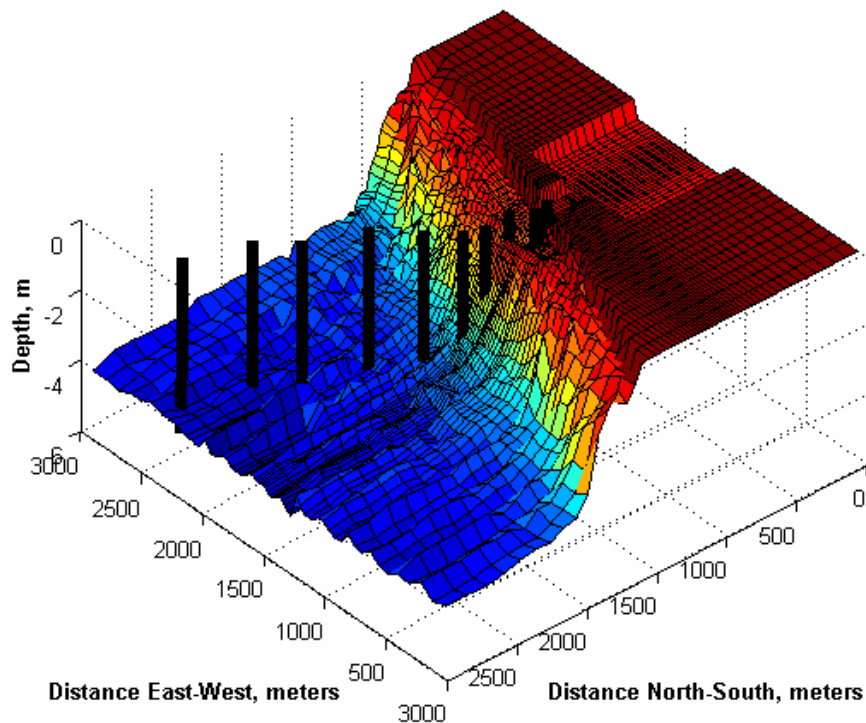


Figure C.1 Bathymetry of Computational Domain. The vertical black lines represent the physical location of model results.

Oso Bay is represented by a square box with a uniform depth of 0.5 meters in EFDC. A lack of information regarding the bathymetry of Oso Bay necessitates this approximation, but should have little impact on the hydrodynamics of Corpus Christi Bay. All open boundaries have Dirichelet boundary conditions with salinity and temperature values equal to the initial conditions at abutting water cells. Initial salinity in Oso Bay is 50 practical salinity units (psu), while the initial salinity in Corpus Christi Bay is 35 psu.

This initial horizontal density gradient is the only force present to act on the domain in the model; wind, tidal, inflow and other forces are neglected. While the interaction of wind, tides and baroclinic pressure gradients is very complex and requires further field observations of Corpus Christi Bay to be fully understood, we can speculate as to the impacts their omission may have on our model results when compared to field data. Because wind transfers kinetic energy into a water body, we would expect any mixing between the underflow and the ambient fluid to be under-estimated in our model due to a lack of the wind's mixing effects. In addition, it is possible that at times of strong tides the barotropic pressure gradient could prevent the underflow from exiting Oso Bay. During the period of time when field data presented in this report was collected, the tidal signature was minimal (the amplitude of the tides was 5 cm), and we would therefore expect that field data taken from this period of time is less likely to be impacted from tides than data from other times of the year.

The initial temperature in Oso Bay is 35° C, and the initial temperature in Corpus Christi Bay is 32.5 ° C. We force the temperature in Oso Bay to vary with time on a sinusoid to approximate the temperature variations seen in the field data. As seen in Figure C.2, this approximation is not an exact replication of the field data, but the period and amplitude are on the same order of magnitude. The contribution of temperature to density variation is minimal compared to that of the salinity in this system, and therefore temperature serves as a tracer in our model and field data. In this capacity, the known temporal variation in temperature in Oso Bay allows us to infer the approximate velocity of water in the underflow in a way that is comparable to the field data.

Temperature in Oso Bay in our model is forced on a sinusoidal pattern with a period of 24 hours and an amplitude of 2.5 ° C. The simulation begins at “noon”, or the maximum temperature. Output is collected every hour from hour 13 until hour 36, providing a 24 hour period of model results. Results from the first 12 hours of the simulation is not collected, because the field data shows that it takes the gravity current almost twelve hours to reach the end of our transect.

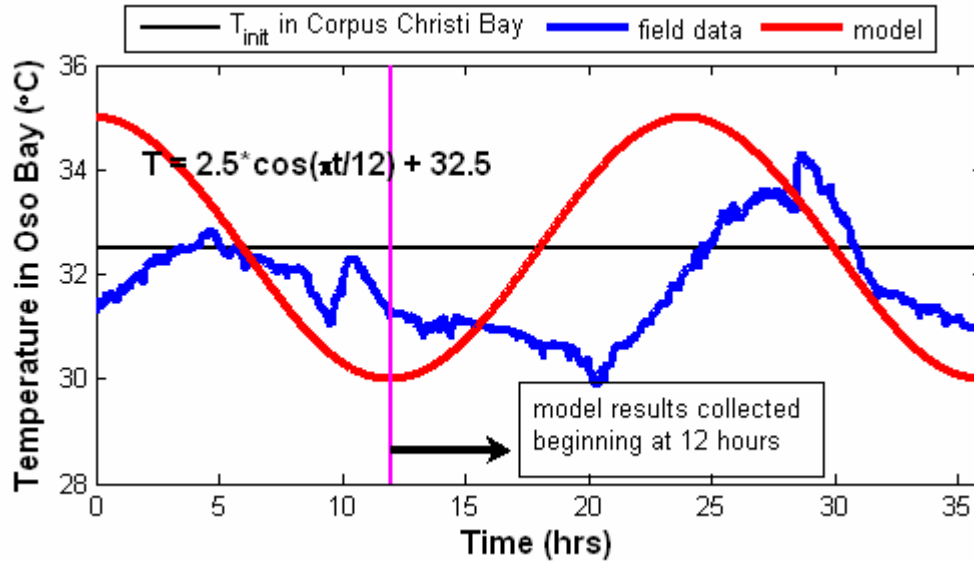


Figure C.2 Temperature forcing in Oso Bay, plotted with real temperature data taken from a pressure transducer placed in Oso Bay by the Texas Water Development Board. Data is shown for 8/21/05 at 12:35 p.m. through 8/23/05 at 12:34 a.m.

Three different test cases of this simulation are considered. The first test case, the “stretched” case, contains a total of forty eight vertical layers. These layers are spaced to allow for approximately ten layers in the underflow, and the grid cells expand at a rate of 7.5% thereafter. This stretching is done for computational efficiency. Maintaining the high resolution of the underflow region throughout the water column would require approximately 150 layers. The second test case we consider is referred to as the “uniform” case. There are 20 uniformly spaced vertical layers in this test case, which leads to approximately two grid cells in the underflow. The third test case is referred to as the “sparse” case, because it contains only three vertical layers in the water column. A schematic depicting these test cases is shown in Figure C.3.

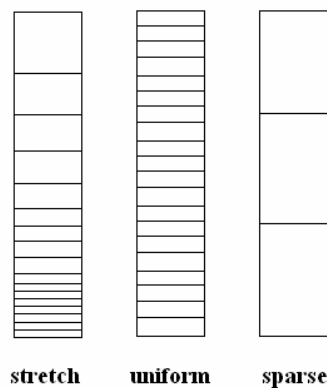


Figure C.3: A sample column of cells in each of the three test cases.

C.3 Results and Discussion

C.3.a Qualitative Analysis

An examination of the temperature signature in the stretched test case demonstrates that EFDC produces results similar to the field data, even without the presence of wind and other forcings. This comparison between field and modeling results shows that with enough grid cells in the underflow, EFDC can capture the bulk velocity of the underflow, at least on an order of magnitude. A more quantitative comparison of the temperature signatures is not practical, because the temperature fluctuations in Oso Bay are not truly sinusoidal as in the model. In addition, the transects collected in the field were collected over a period of two to three hours, compared with the instantaneous “snap shot” produced by the model results. Temperature transects of the field data shown in Figure 3 are repeated here in Figure C.4 for ease of comparison with the model results in Figure C.5.

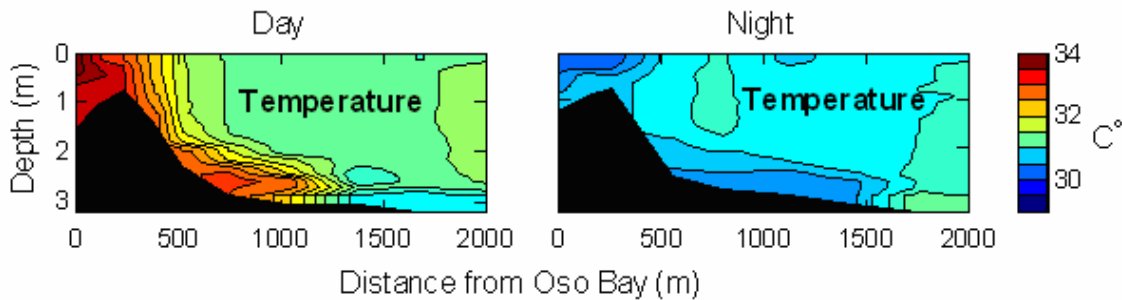


Figure C.4. Evolution of temperature from the Oso Bay nexus with Corpus Christi Bay.

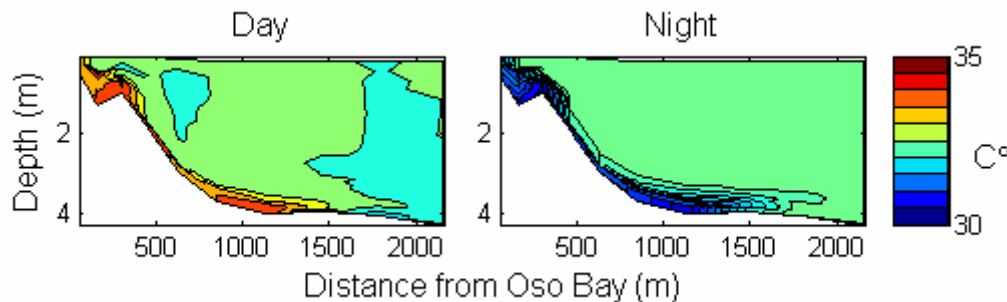


Figure C.5. Contours of the temperature signature from the stretched test case in EFDC. The “Day” plot is a transect taken from what is effectively 4 p.m. on the temperature sinusoid in Oso Bay, and the “Night” plot is a transect taken from 4 a.m.

Salinity contours of the transects created by the three model test cases are presented in Figure C.6 (and also Figure 4 in the body of this report). The difference in salinity signature between the sparse and stretched test cases is particularly apparent, but we also observe a difference between the uniform and stretched case. This difference is marked by both a difference in the magnitude of the salinity stratification, and also by the horizontal extent of it. The sparse case transect only shows a stratification extending to the one kilometer mark, while the entire domain of the transect in the stretched case is stratified.

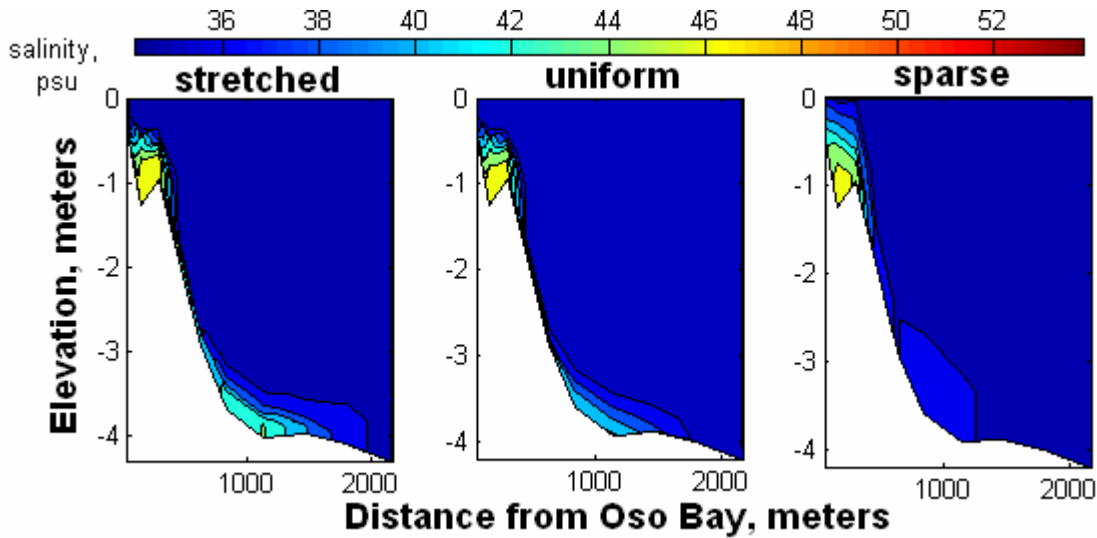


Figure C.6 EFDC model results for a) stretched grid of 48 layers with thinnest at bottom; b) uniform grid of 20 layers, and c) sparse grid of 3 layers. Obtaining model results with 44 psu salinity requires the stretched grid, which has 2 cm grid spacing near the bottom boundary.

C.3.b Sigma-t Analysis

There are several ways to quantify the stratification produced by each model test case. The simplest may be the sigma-t method, which quantifies the difference in magnitude of the water density at the surface and bottom waters:

$$\Delta\sigma_t = \rho_b - \rho_s \quad (\text{C.1})$$

where ρ_b and ρ_s are density in kg/m^3 at the bottom and surface of the water column, respectively. Focusing on a single profile location located near the one kilometer mark on the transects in Figure C.6 provides a location for assessing the water column that is far from boundaries in the model (and is thus less likely to be impacted by boundary effects of the model), but is also far enough from the source that the gravity current should be at a steady Froude number and entrainment rate.

The EPA classifies a water body as “stratified” if it has a $\Delta\sigma_t$ value greater than one. By this definition, the bay would barely be classified as stratified according to the results from the sparse test case shown in Figure C.7. In contrast, the uniform and stretched test cases, as well as the field data, show high values of $\Delta\sigma_t$. While the field results actually have a slightly lower $\Delta\sigma_t$ than the more resolved model test cases, this is not necessarily indicative of model error. We must remember that in the field forces such as wind and tides are acting on the gravity current, and those effects may be weakening the stratification in the field. These forces are absent from the model, and therefore we would expect the model to predict a higher stratification than observed in the field. The sigma-t analysis method is simple in the respect that only takes the magnitude of density differences into account, not the shape of the density profile or the vertical scales over which the stratification occurs. However, it is a useful metric for comparison among water bodies because it is so widely used.

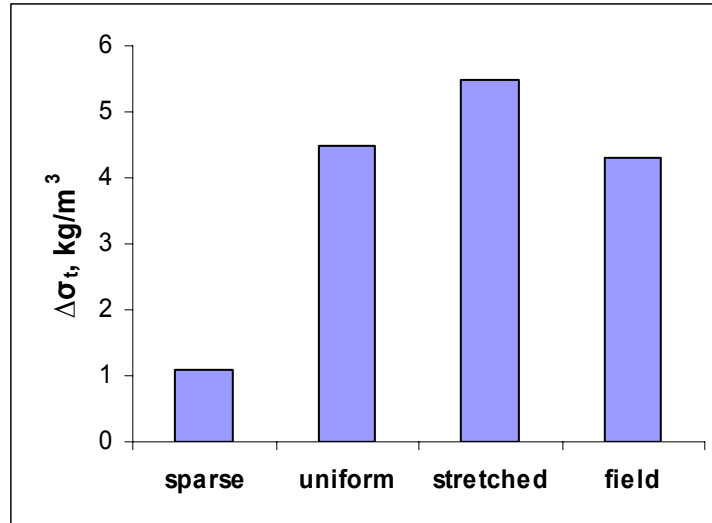


Figure C.7. Change in Sigma-t value between bottom and surface waters at a given sample location in Oso Bay based on field and model results.

C.3.c Potential Energy Analysis

Potential Energy (PE) is another metric that can be used to compare stratifications. While more complicated than the sigma-t calculation, it is more informative because it both measures the magnitude of the salinity, and also weighs the salinity values in the profile based on their vertical locations in the water column. Thinking of stratification in terms of energy helps us relate stratification to events that will contribute to or alleviate it, such as strong wind events. Similar approaches have been used in the literature to quantify stratification (eg Gale et al, 2006) and there is much literature relating stratification to the energetics of mixing via potential energy (Hodges et al 2000, Spigel et al. 1986, Kraus and Turner, 1967, e.g.)

If we want to know how much external energy is needed to mix the water column, we must examine the PE increase due to “lifting” the dense fluid at the bottom of the water column and mixing it with the ambient fluid. Because this lifting process converts turbulent kinetic energy (tke) to PE, the PE of the water column is greater after a mixing event than before. While losses are present in the transfer of energy from tke to PE, calculating the difference in PE before and after mixing gives us a metric for how much energy a source such as the wind would need to give the water column to mix it. This relationship between tke and PE is illustrated in Fig. C.8.

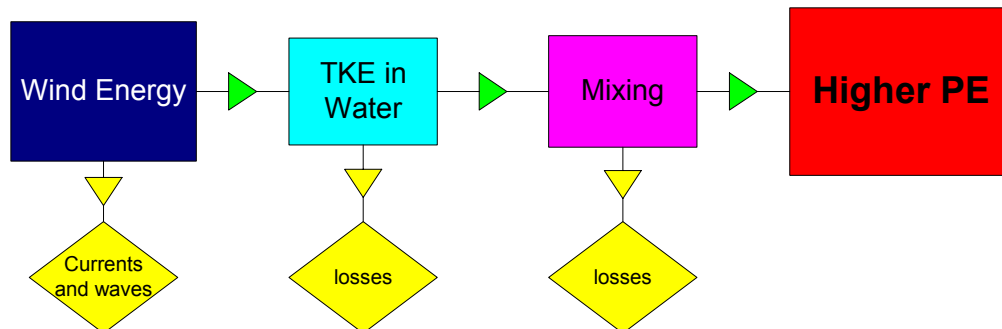


Figure C.8. Energy flow showing the relationship between the wind and the potential energy of the water column.

The difference in PE before and after complete mixing is:

$$\Delta PE = \frac{1}{2} g \rho_m H^2 - \int_0^\eta \frac{1}{2} g \rho z dz \quad (C.2)$$

where ρ_i is the density in kg/m^3 at a given water depth, z_t and z_b are the elevations at the top and bottom of each cell layer, respectively, N is the total number of layers, ρ_m is the depth-averaged density (the density after an ideal mixing event), H is the total water depth and η is the surface elevation. The difference between the potential energy before and after a theoretical mixing event is the Potential Energy Deficit (ΔPE).

As mentioned in the discussion of the $\Delta\sigma_t$ method, the model does not take external energy sources into account. If the sources of the present in the field, such as wind and tidal forces, had been included in the model, we would expect ΔPE to be the same between the model and field results. A ΔPE value below the field results would reflect that the model was not capturing the stratification present in the field. However, the present model results are obtained from a system absent of external tke sources. Therefore, if our model is accurately representing the underflow, it will have a higher ΔPE than the field data. Because the model has no tke sources, it should represent a “worst case scenario” of the stratification we would expect in the field. Therefore, model results with a ΔPE equal to or below the field data reflect that the model is not capturing the stratification.

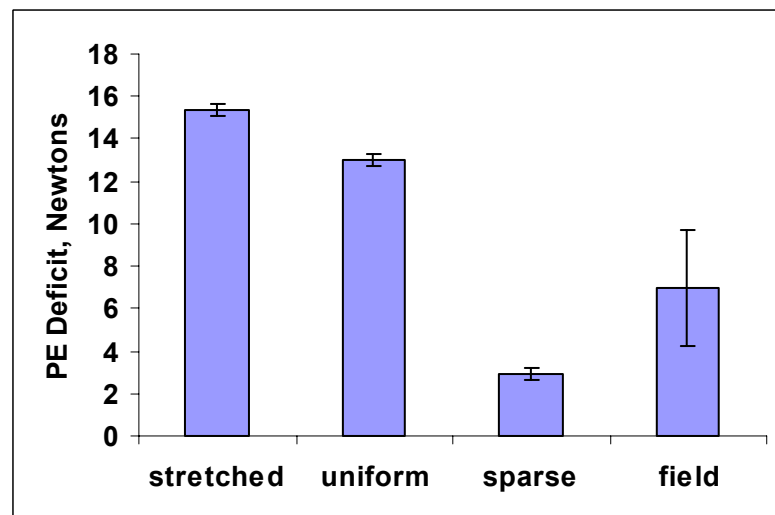


Figure C.9 Potential Energy Deficit in the test cases in EFDC and the field data from the summer of 2005, all calculated from profiles at the same location in the bay.

The values of for the field sample site mentioned above are plotted in Figure C.9. The same water column is used for the PE analysis as was used in the $\Delta\sigma_t$ analysis. In the figure, the error bars for the field data are large, and the ΔPE from the field is also not as large as it is for the two more resolved model test cases. Both findings are to be expected. It is necessary to recall that wind is not present in the model simulations, and therefore its variability is also not present. In addition, the presence of wind in the field gives the value of the potential energy deficit a

slightly different meaning. This is the potential energy deficit after the wind has already transferred energy to the water column. It is therefore logical that the PE Deficit of the field data would be lower than that of the simulations. It is also important to note that even in the absence of wind forcings, the sparse test case cannot predict the potential energy deficit attained from the field. These results are consistent with the $\Delta\sigma_t$ analysis.

C.4 Computational Expense

While this study indicates the need for high grid resolution when modeling thin underflows, the computational expense involved in doing so quickly becomes unmanageable. Table C.1 Shows the computation time required to run the simulations for our test cases. In order to run a 36-hour simulation of the entire bay, using the stretched case grid resolution would require 130 days of CPU time. These extrapolations are calculated by linear extrapolation, and are therefore a “best case” scenario. The actual CPU times to simulate the entire bay are likely to be higher than those in the table. The machine used for our simulations in the present computational domain shown in Figure C.1 is a Xeon CPU, 3.6 GHz, with 3.5 GB of RAM.

Table C.1 CPU time required to run a 36 hour simulation. Values for All of Corpus Christi Bay are determined by linear extrapolation.

Test Case	Present Domain	All of Corpus Christi Bay
Sparse	0.2 days	8 days
Uniform	1.1 days	54 days
Stretched	2.7 days	130 days

C.5 Conclusion

The tests presented in this appendix demonstrate the limitations of EFDC in capturing the stratification posed by thin underflows in three dimensions, both qualitatively and quantitatively. Because stratification impacts the isolation of bottom waters, miscalculating the stratification of the water column could lead to incorrect predictions regarding parameters such as hypoxia. Both qualitative and quantitative analysis of the EFDC model results show that low vertical grid resolution drowns out small scale phenomena. Further analysis of the impact of forces such as tide, wind, inflows, and other forces specific to Corpus Christi Bay would improve our understanding of the bay itself and our abilities to model these phenomena.

The test cases also demonstrate that the requirements for resolving the gravity current are computationally expensive. A linear extrapolation of the computational time required to run the test cases presented here on all of Corpus Christi Bay suggests that the stretched case would require 130 days to run, and the uniform case would require fifty four days to run. The sparse case would require only eight days. These are “back of the envelope”, linear extrapolations, and are therefore conservative estimates of computational expense. The computational time required to model the entire bay with adequate resolution to capture the stratification is not practical in engineering practice, and a better method of modeling thin underflows is desirable.

C.6 Matlab Functions

Following are the Matlab functions and scripts that were used in order to process the data. The first lines of each program describe its use.

PEDEF.M

```
function [pe_mix,pe_column,pe_def]=pedef(H,s_ccb,dz,zz_ccb,t_ccb,limit)
% function for calculating the Potential Energy Deficit of a water column
% cells (data points) need not be evenly spaced
%
% H must be (+), = total depth
% limit is the z-level up to which integration takes place
% the following variables are column arrays for the water column:
% zz_ccb is the z-location of t and s values with 0 at the bed
% s_ccb is salinity in psu
% t_ccb is temperature in degrees C
% dz is delta z, the thickness of each cell, divided by the total water
% depth H.

%% this function only integrates up to a depth that is less than or equal to
%% the free surface (limit). In other words, only a portion of the water
%% column is integrated. As long as all stratification is included in the
%% portion of the water column that is stratified, this should not
%% adversely impact results. It also allows us to compare water columns
%% that do not have exactly the same total depth H.

n = length(dz); % number of layers
[rho] = ies80(s_ccb,t_ccb,zz_ccb);
% ies80.m is adapted from "Calculate_sigmaT.m", written by Jordan Furnans,
% and calculates water density
h_min = zz_ccb - dz.*H./2;
% the bottom of each grid cell
h_max = zz_ccb + dz.*H./2;
% the top of each grid cell

% crop column to only include information below limit

a = 1;
for i = 1:n
    if h_min(i)<limit
        if h_max(i)<limit
            shortz(a) = zz_ccb(i);
            shorthrho(a) = rho(i);
            shorthmax(a) = h_max(i);
```

```

        shorthmin(a) = h_min(i);
    end
    % for cells that are partially in the integration range
    if h_max(i)>limit
        shortrho(a) = rho(i);
        shortz(a) = mean([h_min(i) limit]);
        shorthmax(a) = limit;
        shorthmin(a) = h_min(i);
    end
    a = a+1;
end
end
shortz = shortz';
shortrho = shortrho';
shorthmax = shorthmax';
shorthmin = shorthmin';
n = length(shortrho); % number of layers in shortened

% calculate the PE of the stratified water column
% PE = sum [0.5*g*rho*(h1^2-h2^2)]
pe = shortrho.*(shorthmax.^2-shorthmin.^2)*9.81*0.5;
pe_column = sum(pe);

% calculate the PE of the mixed water column
rho_weighted = shortrho.*(shorthmax-shorthmin);
rho_mix = sum(rho_weighted)./(shorthmax(1,:)-shorthmin(n,:));
pe_mix = 0.5 * ( (shorthmax(1,:).^2 - (shorthmin(n,:)).^2 ) * 9.81 .* rho_mix;

pe_def = pe_mix-pe_column;

return

```

IES80.M

```

function [rho] = ies80(S,T,Depth)
% adapted from from Jordan Furnans' "Calculate_sigmaT.m"
% rho is in kg/m^3
% input may be vectors
% depth is in meters
% T is in degrees C
% S is in psu

% Calculate_sigmaT.m
% This script computes water density according to the

```

% International Equation of State of Sea Water (1980)
 % As described in "Introductory Dynamical Oceanography -2nd Edition by Pond
 % & Pickard (1983)

%Values are for point z308 from 8/23/05
 %rho(s,t,p) = rho(s,t,0)/[1-p/K(s,t,p)];
 %rho(s,t,0) =
 %999.842594+6.793952*10^-2*T-9.095290*10^-3*T^2+1.001685*10^-4*T^3-1,120083
 %*10^-6*T^4+6.536332*10^-9*T^5+8.24493*10^-1*S-4.0899*10^-3*T*S+7.6438*10^-
 %5*T^2*S-8.2467*10^-7*T^3*S+5.3875*10^-4*T*S^(3/2)-1.6546*10^-6*T^2*S^(1.5)
 %+4.8314*10^-4*S^2

%Note - pressure is derived from the depth and density integral. We'll
 %assume rho = 1000 kg/m3 in calculating pressure from depth

P = 1000*9.81*Depth*10^-5; %in Bars

rho_atmospheric = 0;
 rho_atmospheric = rho_atmospheric + 999.842594;
 rho_atmospheric = rho_atmospheric + 6.793952*10^-2*T;
 rho_atmospheric = rho_atmospheric - 9.095290*10^-3*T.^2;
 rho_atmospheric = rho_atmospheric + 1.001685*10^-4*T.^3;
 rho_atmospheric = rho_atmospheric - 1.120083*10^-6*T.^4;
 rho_atmospheric = rho_atmospheric + 6.536332*10^-9*T.^5;
 rho_atmospheric = rho_atmospheric + 8.24493*10^-1*S-4.0899*10^-3.*T.*S;
 rho_atmospheric = rho_atmospheric + 7.6438*10^-5*T.^2.*S-8.2467*10^-7.*T.^3.*S;
 rho_atmospheric = rho_atmospheric + 5.3875*10^-9*T.^4.*S;
 rho_atmospheric = rho_atmospheric - 5.72466*10^-3*S.^(3/2);
 rho_atmospheric = rho_atmospheric + 1.0227*10^-4*T.*S.^(3/2);
 rho_atmospheric = rho_atmospheric - 1.6546*10^-6*T.^2.*S.^(1.5);
 rho_atmospheric = rho_atmospheric + 4.8314*10^-4*S.^2;
 Kdepth = 0;
 Kdepth = Kdepth + 19652.21;
 Kdepth = Kdepth + 148.4206*T;
 Kdepth = Kdepth - 2.327105*T.^2;
 Kdepth = Kdepth + 1.360477*10^-2*T.^3;
 Kdepth = Kdepth - 5.155288*10^-5*T.^4;
 Kdepth = Kdepth + 3.239908 * P;
 Kdepth = Kdepth + 1.43713*10^-3*T.*P;
 Kdepth = Kdepth + 1.16092*10^-4*T.^2.*P;
 Kdepth = Kdepth - 5.77905*10^-7*T.^3.*P;
 Kdepth = Kdepth + 8.50935*10^-5*P.^2;
 Kdepth = Kdepth - 6.12293*10^-6*T.*P.^2;
 Kdepth = Kdepth + 5.2787*10^-8*T.^2.*P.^2;
 Kdepth = Kdepth + 54.6746*S;

```
Kdepth = Kdepth - 0.603459*T.*S;  
Kdepth = Kdepth + 1.09987*10^-2*T.^2.*S;  
Kdepth = Kdepth -6.1670*10^-5*T.^3.*S;  
Kdepth = Kdepth + 7.944*10^-2*S.^1.5;  
Kdepth = Kdepth + 1.6483*10^-2*T.*S.^1.5;  
Kdepth = Kdepth - 5.3009*10^-4*T.^2.*S.^1.5;  
Kdepth = Kdepth + 2.2838*10^-3*P.*S;  
Kdepth = Kdepth - 1.0981*10^-5*T.*P.*S;  
Kdepth = Kdepth - 1.6078*10^-6*T.^2.*P.*S;  
Kdepth = Kdepth + 1.91075*10^-4*P.*S.^1.5;  
Kdepth = Kdepth - 9.9348*10^-7*P.^2.*S;  
Kdepth = Kdepth + 2.0816*10^-8*T.*P.^2.*S;  
Kdepth = Kdepth + 9.1697*10^-10*T.^2.*P.^2.*S;  
rho = rho_atmospheric./(1-P./Kdepth);
```

```
% NOTE: pressure-depth solution iterations not performed because for the  
% purposes of the present analysis, other inaccuracies from field data  
% collection, etc. render outweigh the inaccuracies encountered by not  
% performing iterations.  
return
```


APPENDIX D Theory for a new vertical mixing model

D.1 Introduction

The approach used by Hodges et al. (2000) for vertical mixing follows the general approach known as “mixed-layer modeling,” wherein the mixing between model grid layers is quantified by turbulent kinetic energy and turbulent scalar fluxes rather than a partial differential equation for diffusion. The mixed-layer method decouples vertical mixing from advection, horizontal diffusion and reaction equations. In the following, we develop the theory for a new approach to mixed-layer modeling that addresses previous deficiencies associated with modeling thin-layer stratification. The innovative ideas in this new mixing model are: 1) “representative” scalar concentrations to complement the mean concentrations, and 2) the use of mixing layer thicknesses to constrain the gradient regions across grid-cell boundaries.

Any mixed layer model for a stratified water column is based upon quantifying the rates at which different mixing energies are supplied and examining how the rate of energy supply is related to its dissipation and the work required for mixing. These rates are of the form $\partial E / \partial t$ where E is an energy per unit area (w/m^2), or $(kg\ m^2/s^2) / (m^2\ s)$, which reduces to (kg / s^3) . The sources of mixing energy are: 1) wind stirring, 2) convective overturns, and 3) shear mixing by Kelvin-Helmholtz (K-H) billows, and 4) boundary shear. The general modeling approach is to compute a mixing region starting from the turbulent kinetic energy (TKE) source (i.e. either a boundary or the K-H billow density interface) and proceeding outward from the source. Thus, bottom boundary shear mixing is computed in a bottom-up sweep, whereas surface mixing (including wind stirring and convective overturns) is computed in a top-down sweep². Internal shear mixing by K-H billows will be a separate computation either prior to, or after bottom and surface boundary mixing are conducted (advantages/disadvantages of timing is not clear at this time).

In contrast to the ELCOM approach (Hodges et al, 2000), we will integrate the surface thermodynamics directly in the mixing routine rather than conducting separate algorithms. In ELCOM, surface thermodynamics algorithms are used to create a new density profile (due to heating/cooling/evaporation), and the mixing routine is subsequently used to remove convective instabilities that may result. In the new approach, the surface thermodynamics provide the rate of energy supplied to the water column during the mixing routine, which may be either stabilizing (increasing temperature so as to provide a larger negative density gradient), or destabilizing (through cooling that leads to overturns). Note that this approach allows us to calculate the rate at which destabilizing energy is supplied (which should affect dissipation). That is, we might imagine a case where the heating and cooling are exactly in balance so that the net rate of stabilizing energy exactly equals the net rate of destabilizing energy. In the ELCOM approach, this would be considered a system with zero “available energy” for mixing. Since the ELCOM dissipation rate was based solely on the net available energy for mixing, the

² Note: the algorithm for meeting of two mixing layer has not been fully developed.

parameterization has no ability to distinguish between zero heating/cooling (i.e. quiescence), or an active interplay between heating/cooling that leads to no available energy for mixing, but still engenders turbulence and dissipation.

A key issue for this new model is the treatment of dissipation. In Hodges et al (2000), dissipation is simply a function of available mixing energy. Herein, we apply three new concepts: 1) dissipation is treated as a function of the overall thickness of the mixing layer; 2) time-dependency of the dissipation is required so that we have higher dissipation rates when the wind is just getting started (low mixing efficiency) and lower dissipation rates when it is winding down (higher mixing efficiency in decaying turbulence); and 3) dissipation a function of the overall level of turbulence, rather than just the available mixing energy (as discussed above for convection). Note that this dissipation formulation is principally for the surface and bottom boundary mixing layers. For shear regions, the dissipation is already considered in the empirical mixing efficiency of K-H billows.

A method of partial mixing is required for all parts of the mixing scheme to obtain the maximum practical time and grid-spacing independence of the model. A partial mixing scheme allows a fraction of one grid cell to be mixed with a fraction of a vertically-adjacent grid cell and the resulting transfer will affect the density gradient within the mixing layer, and the thickness of the mixing layer. The approach to partial mixing is closely linked to the use of mixing-layer thicknesses at the interface between grid cells. As an example, if the mixing layer thickness at the upper face of a grid cell is less than half the grid-cell thickness, then it cannot communicate any fluid through the lower face of the grid cell.

The mixing layer thickness is treated as a variable that will influence the dissipation rate and the rate of deepening. Ideally, this approach should allow the mixing scheme to be used with a homogenous fluid.

Unstable density gradient are expected to only physically be developed in the surface mixing layer, where they will be removed in the mixing process. Where unstable density gradients are developed in other parts of the flow through transport (e.g. where a gravity current flows over a step), the unstable gradient will be resolved by flipping the fluid volumes.

The new mixing model ensures that all mixed scalar concentrations are exactly conserved during the mixing process; i.e. the algebraic sum of the mixing mass fluxes through the faces of a grid cell will be exactly equal to the change in the scalar mass in the grid cell.

D.2 Outline for model implementation

Much as in ELCOM, the mixing model will be implemented at the start of a time step. The following are the basic mechanisms:

1. Compute K-H billow shear mixing of surface and bottom boundary layers.
2. Store two sets of the system state (set A and set B).

3. Using set A, compute the bottom boundary layer mixing.
4. Using set B, compute the surface mixing, integrated with surface thermodynamics.
5. Resolve any overlap in set A and set B results. Determine if mixing is top to bottom in water column.
6. Conduct hydrodynamic solution and transport.
7. Look for instability provided by transport and flip to stability.

D.3 Notes on notation

In general, we will put grid indexes such as (k) in parenthesis so that it is easier to distinguish from a necessary plethora of subscripts. To avoid double subscripts, the 'k' index of the bottom will be represented as a subscript '(D)'. The 'k' index of the free surface will be given as subscript (S). The 'k' index of the partially-mixed cell at the bottom of the surface mixed layer will be subscript (P), while the 'k' index of the partially-mixed cell at the top of the lower layer will be (C). Note that subscripts 'T' 'B' and 'R' without parenthesis are not 'k' indexes.

The free surface will be denoted by η and the bottom will be denoted by 'b'.

D.4 Goal of time step and grid size independence

The model is characterized by a model time step Δt_M , grid layers of $\Delta z_{(k)}$ for $k = k_D, k_{D+1} \dots k_S$ being the integers from the bottom layer (k_D) to the surface layer (k_S) in any water column. There is no *a priori* requirement for a strictly z-layer grid as long as the $\partial(\Delta z)/\partial x$ can be considered small. To make the scheme relatively independent of both Δz and Δt_M we need to invoke some extra terms for the cells as discussed below.

D.5 Defining sub-time steps

The process of mixing will occur in sub-time steps across a grid face, so we will keep track of the time remaining (or the time left) for mixing on the $k+1/2$ face of a grid cell as $\Delta t_{L(k+1/2)}$. The subtime steps will be applied separately in each part of the mixing routine.

D.6 Representative and mean concentrations

A conserved scalar volume concentration in a cell will generally denoted by ϕ . Thus, ϕ may represent temperature, salinity or any other conserved scalar. It is often useful to neglect the nonlinearity of the equation of state and also treat density (ρ) as a locally-conserved scalar that can be mixed. For example, if we need to fully-mix two grid cells of differing temperatures and salinities, the physically-correct approach requires: 1) mixing the temperature, 2) mixing the salinity, and 3) using a nonlinear equation of state to compute the resulting mixed density. However, for many of the interim steps of the model, the nonlinear effects should be significantly smaller than the uncertainty of the empirical mixing model coefficients. It follows that simple linear mixing of the density should suffice. This approach is generally justified by the small density gradients for incompressible stratified flows, and the even smaller effect of nonlinearity for such gradients.

For the new model, we will characterize the volume concentration in a single grid cell by both the mean value $\bar{\phi}$ and a representative value, ϕ_R as shown in Figure D.1 for a simple mixing layer. The representative value provides a better approximation of gradients between cells and reduces the grid-cell size dependence caused by using mean values. For each grid cell, there may be top and bottom mixing layers of thickness $h_{T(k)}$ and $h_{B(k)}$, respectively. The mixing layer thicknesses must meet the requirement that

$$h_{T(k)} + h_{B(k)} \leq \Delta z_{(k)} \quad (D.1)$$

so that there exists a region of fluid with ϕ_R in the center of the cell. When the inequality of eq. (D.1) is violated during the mixing process, the entire cell is considered well-mixed and we set the mixing layer thicknesses to zero:

$$h_{T(k)} = h_{B(k)} = 0 \quad (D.2)$$

and the representative concentration will be identical to the mean concentration:

$$\phi_{R(k)} = \bar{\phi}_{(k)} \quad (D.3)$$

In effect, this resetting the cell as well-mixed implies that the processes are being adequately resolved on the model grid scale. Where mixing allows eq. (D.1) to be satisfied, an approach referred to as “thin-layer” mixing will be used (i.e. the mixing layer is considered thin compared to the grid cell and is poorly resolved by the model). Where conditions of eq. (D.1) are not satisfied, the model effectively resolves the mixing layers and a “thick-layer” mixing approach is used.

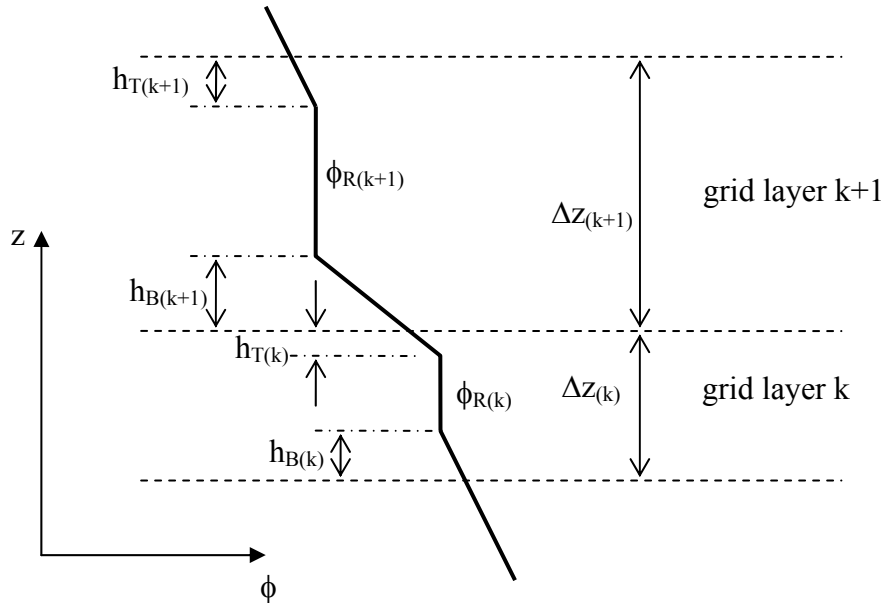


Figure D.1 Scalar concentration profile over two grid cells with the representative scalar concentration (ϕ_R) and mixing layer heights (h) identified

It is convenient to represent the difference between the scalar concentrations on the 'k' and 'k+1' grid layers by

$$\Delta\phi_{(k+1/2)} = \phi_{(k+1)} - \phi_{(k)} \quad (\text{D.4})$$

Thus, when ϕ is used to represent the density (ρ), a stable density gradient always requires $\Delta\rho_{(k+1/2)} \leq 0$.

The mixing layer from the 'k' to the 'k+1' cell is characterized by a linear gradient of the representative concentration; i.e. from $\phi_{R(k)}$ to $\phi_{R(k+1)}$ over the mixing layer thickness $h_{T(k)} + h_{B(k+1)}$. This gradient can be explicitly evaluated, so the relationship between the representative value and the mean value in a grid cell can be computed by integrating the profiles over the grid cell. The result can be presented as

$$\bar{\phi}_{(k)} = \phi_{R(k)} \left[1 - \left(\frac{h_{T(k)}}{\Delta z_{(k)}} + \psi_{T(k)} \right) - \left(\frac{h_{B(k)}}{\Delta z_{(k)}} - \psi_{B(k)} \right) \right] + \phi_{R(k+1)} \psi_{T(k)} - \phi_{R(k-1)} \psi_{B(k)} \quad (\text{D.5})$$

where

$$\psi_{T(k)} \equiv \frac{h_{T(k)}}{\Delta z_{(k)}} \left\{ \frac{1}{h_{T(k)} + h_{B(k+1)}} \right\} \quad (\text{D.6})$$

$$\psi_{B(k)} \equiv \frac{h_{B(k)}}{\Delta z_{(k)}} \left\{ \frac{1}{h_{B(k)} + h_{T(k-1)}} \right\}$$

Note the above implies a tridiagonal matrix relationship that can be written as

$$\begin{bmatrix} B_{(S)} & C_{(S)} & 0 & 0 & 0 & 0 & 0 \\ A_{(S-1)} & B_{(S-1)} & C_{(S-1)} & 0 & 0 & 0 & 0 \\ 0 & A_{(S-2)} & B_{(S-2)} & C_{(S-2)} & 0 & 0 & 0 \\ \vdots & \vdots & \vdots & \vdots & \vdots & \vdots & \vdots \\ 0 & 0 & 0 & A_{(D+2)} & B_{(D+2)} & C_{(D+2)} & 0 \\ 0 & 0 & 0 & 0 & A_{(D+1)} & B_{(D+1)} & C_{(D+1)} \\ 0 & 0 & 0 & 0 & 0 & A_{(D)} & B_{(D)} \end{bmatrix} \begin{bmatrix} \phi_{R(S)} \\ \phi_{R(S-1)} \\ \phi_{R(S-2)} \\ \vdots \\ \phi_{R(D+2)} \\ \phi_{R(D+1)} \\ \phi_{R(D)} \end{bmatrix} = \begin{bmatrix} \bar{\phi}_{(S)} \\ \bar{\phi}_{(S-1)} \\ \bar{\phi}_{(S-2)} \\ \vdots \\ \bar{\phi}_{(D+2)} \\ \bar{\phi}_{(D+1)} \\ \bar{\phi}_{(D)} \end{bmatrix} \quad (\text{D.7})$$

where (S) indicates the k index at the surface and (D) indicates the k index at the bottom and

$$A_{(k)} \equiv +\psi_{T(k)}$$

$$B_{(k)} \equiv 1 - \left(\frac{h_{T(k)}}{\Delta z_{(k)}} + \psi_{T(k)} \right) - \left(\frac{h_{B(k)}}{\Delta z_{(k)}} - \psi_{B(k)} \right) \quad (\text{D.8})$$

$$C_{(k)} \equiv -\psi_{B(k)}$$

Thus, we can directly solve eq. (D.5) to obtain the mean values $\bar{\phi}$ for given values of ϕ_R , h_T , h_B and Δz . Furthermore, we can invert the tridiagonal of eq. (D.7) to obtain the values of ϕ_R for any set of $\bar{\phi}$, h_T , h_B and Δz . This reversible relationship between the representative values

and the mean values is key to the new method. Within the mixing routine, we are principally interested in using the representative values (especially when the grid scale is large compared to the physics) to characterize gradients between grid cells, but the hydrodynamic transport routines need to use mean values to retain exact conservation of scalars. Thus, within the mixing routine we use ϕ_R to compute changes in h_T and h_B that affect $\bar{\phi}$ through eq. (D.5). The transport routine subsequently solves for the transport of $\bar{\phi}$, h_T and h_B , which are then used to find the new ϕ_R for the mixing routine at the start of the next time step.

D.7 Mixing energy from wind

Hodges et al. (2000) followed Spigel et al. (1986) in modeling the production due to wind stirring as

$$\frac{1}{2}C_N^3 u_*^3 \quad (D.9)$$

where C_N is an empirical coefficient and u_* is the wind shear velocity scale. We note that this term has the units m^3/s^3 . If we multiply by density, we obtain $(kg/m^3)(m^3/s^3)$, which is simply (kg/s^3) , and so is a value of $\partial E/\partial t$. Let us continue with this form and write

$$\frac{\partial E_N}{\partial t} = \frac{C_N^3}{2} \rho_0 u_*^3 \quad (D.10)$$

D.8 Integrating thermodynamics, convective mixing and the surface mixed layer

The surface thermodynamics can either stabilize or destabilize the surface mixing layer. The first task of the mixing algorithm is to determine whether the near-surface layers are stabilized or destabilized by thermodynamics. Starting at the water surface (defined as $z = \eta$), we assume there exists a thin layer δ_e , such that $\eta - \delta_e \leq z \leq \eta$, where evaporative mass fluxes and sensible/evaporative heat transfer uniformly affect the water column (i.e. a thin layer that is uniformly-mixed). A second thin layer, δ_r , where $\eta - \delta_r \leq z \leq \eta$, is assumed to exist where penetrative solar radiation is preferentially absorbed in the near surface region (i.e. where Beer's law of exponential decay does not apply). We assume that $\delta_e < \delta_r$. It can be shown that the rate that TKE is made available for mixing if the thermodynamics is convectively unstable in the near-surface region $\eta - \delta_r \leq z \leq \eta$ is:

$$\frac{\partial E_{p\delta a}}{\partial t} = \frac{1}{2}(\delta_r - \delta_e) \left\{ g\beta\rho V_e S_\eta - g \frac{\alpha}{c_p} Q_h \right\} \quad (D.11)$$

where α, β are the thermal and salinity expansion coefficients, V_e is the evaporative flux rate, S_η is the salinity at the free surface and Q_h is the net heating/cooling due to sensible/evaporative sources (i.e. without solar radiation). Note that solar radiation does not appear in the above as it is assumed to be linearly absorbed across the entire region $\eta - \delta_r \leq z \leq \eta$ and therefore does not affect stability in the region $\eta - \delta_e \leq z \leq \eta$ as $\delta_e < \delta_r$.

D.9 Surface and bottom mixing layers

D.9.a Layer definitions

The surface and bottom mixing layers are somewhat more complex than the simple internal grid cell interface mixing layer shown in Figure D.1. In general, these boundary mixing layers will extend over multiple grid cells of homogeneous properties, but will end in a gradient region where entrainment and K-H billowing may occur. We will denote the surface and bottom mixing layers height by H_S and H_B respectively. It is also useful to keep track of the number of complete cells in the mixing layers as N and M . We will first look at only the surface mixing layer. For simplicity in notation (and avoiding double superscripting), we define the ‘k’ index of the partially mixed cell at the base of the surface layer as

$$P = S - N \quad (D.12)$$

That is, the grid cell layer $k = P$ is the partially-mixed grid cell layer at the base of the surface-mixed layer where $k = S$ is the grid cell layer containing the free surface and N is the number of grid cells that are entirely in the surface mixing layer.

From the above definitions, it follows that

$$H_S = \delta_{H(P)} + \sum_{q=P+1}^S \Delta z_{(q)} \quad (D.13)$$

where $\delta_{H(P)}$ is the well-mixed upper portion of cell $k = P$, i.e. the portion of cell $k = P$ that is mixed with the surface mixed layer. Thus, it is required that for $k = P$ to be the partially-mixed cell, the thickness $\delta_{H(P)}$ must be bounded as

$$0 < \delta_{H(P)} \leq \Delta z_{(P)} \quad (D.14)$$

We may then consider the existence of a gradient region *below* the surface-mixing layer that has a length scale of G_S . This gradient region is the connection between the surface-mixing layer and the fluid below the layer that may be entrained. There are three possible conditions for this gradient region:

$$\begin{aligned} G_S + \delta_{H(P)} &\leq \Delta z_{(P)} && : \text{gradient in 1 cell} \\ \Delta z_{(P)} &< G_S + \delta_{H(P)} \leq \Delta z_{(P)} + \Delta z_{(P-1)} && : \text{gradient in 2 cells} \\ \Delta z_{(P)} + \Delta z_{(P-1)} &< G_S + \delta_{H(P)} && : \text{gradient in more than 2 cells} \end{aligned} \quad (D.15)$$

In the first case provided in eq. (D.15), the gradient region and any entrainment/billowing is entirely within the partial mixed-layer grid cell. In the second case, the gradient region extends into the next grid layer, and so may be characterized by a mixing height regions of $h_{B(P)}$ and

$h_{T(P-1)}$ as is used for KH billows. In the third case, the gradient region is considered “resolved” by the grid, resulting in the simplest treatment. Layer definitions for the bottom mixing layer are similar to the surface layer definitions.

D.9.b Surface/bottom mixing layer equations

The surface and bottom mixing layer algorithms provide the means of predicting the increase/decrease in the thicknesses of H (the layer thickness) and G (the thickness of the adjacent of the gradient region). H remains constant when turbulent production is exactly balanced by dissipation. H increases when production is greater than dissipation, and decreases when production is less than dissipation. The thickness of G will depend on whether H is actively entraining, holding steady, or decreasing. In the case of an entraining mixed layer, G will decrease as H increases until the shear is sufficient at the base of the mixed layer to develop K-H billows (which increases G). When H is holding steady, K-H billows may occasionally form and increase G. When H is decreasing, G will increase and eventually become well-resolved by the model grid.

The modeling approach will be to track the “background” TKE, designated (per unit volume) as e_B , which is the TKE that is sustained in the mixing layer at some instant of time. Using scaling arguments, we derive an equilibrium TKE, (e_E) that represents the expected background TKE if production and dissipation were in balance. The extent to which they are out of balance and the time scale of overturns in the mixing layer leads to a rate at which the background TKE increases or decreases. Using this rate of increase/decrease along with the dissipation rate and the rate of mixing energy supplied, we develop an energy balance that predicts the rate of increase/decrease of the mixing layer thickness.

We define the time used for mixing as

$$\Delta t_U = \min \{ \Delta t, C_T T_H \} \quad (D.16)$$

where T_H is the eddy turnover time scale, given by

$$T_H = H \sqrt{\frac{\rho}{2e_B}} \quad (D.17)$$

and C_T is the proportional constant for the number of eddy turnover time scales required to mix the background TKE to equilibrium TKE. The change in background TKE and depth of the mixing layer are given by

$$e_B^{nM} = e_B^n + \Delta t_U \frac{\partial e_B}{\partial t} \quad (D.18)$$

$$H^{nM} = H^n + \Delta t_U \frac{\partial H}{\partial t} \quad (D.19)$$

where the ‘nM’ superscript indicates the time ‘n’ value after mixing for time Δt_U , whereas the ‘n’ superscript indicates the time ‘n’ value before mixing. The rate of change of the background TKE is found as

$$\frac{\partial e_B}{\partial t} = \frac{e_E - e_B}{C_T H} \sqrt{\frac{2e_B}{\rho}} \quad (D.20)$$

The equilibrium TKE is computed from

$$e_E = \frac{1}{2} \left\{ \rho^{1/2} \frac{(1 - C_{\varepsilon 2})}{C_{\varepsilon 1}} \frac{\partial E_s}{\partial t} \right\}^{2/3} \quad (D.21)$$

where $\partial E_s / \partial t$ is the rate of production for stirring TKE from all sources. The $C_{\varepsilon 1}$ and $C_{\varepsilon 2}$ are empirical coefficients relating the dissipation rate due to the existing turbulence level and the dissipation rate due to the supply of mixing energy (respectively).

The rate of change of the mixed layer depth is found as

$$\frac{\partial H}{\partial t} = \frac{\sqrt{\frac{2}{\rho}} \left\{ 2C_{\varepsilon 1} \left[(e_E)^{3/2} - (e_B)^{3/2} \right] - \frac{\sqrt{e_B}}{C_T} (e_E - e_B) \right\}}{e_B (1 + 2\hbar C_{\varepsilon 3}) + \hbar \frac{\rho}{2} \Delta U^2 - \hbar g \Delta \rho \frac{H}{2}} \quad (D.22)$$

The coefficient $C_{\varepsilon 3}$ is introduced for dissipation that occurs in the entrainment process. In eq. (D.22), \hbar is a Heaviside step function, evaluated as

$$\hbar \equiv \begin{cases} 1 & : 2C_{\varepsilon 1} \left[(e_E)^{3/2} - (e_B)^{3/2} \right] > \frac{\sqrt{e_B}}{C_T} (e_E - e_B) \\ 0 & : 2C_{\varepsilon 1} \left[(e_E)^{3/2} - (e_B)^{3/2} \right] \leq \frac{\sqrt{e_B}}{C_T} (e_E - e_B) \end{cases} \quad (D.23)$$

so that $\hbar = 1$ only occurs with a positive value of $\partial H / \partial t$ (i.e. deepening of mixed layer). Thus, eq. (D.20) and (D.22) provide the prediction of the change in the background TKE and the change in the mixed layer thickness.

The following behaviors may be noted for the coefficients in eqs. (D.20) through (D.22) that will control their values:

- $C_{\varepsilon 1}$ principally affects the equilibrium TKE level. Increasing $C_{\varepsilon 1}$ will increase the dissipation rate of the background TKE and so reduces the equilibrium level of TKE. The value of this coefficient may be set from prior work and arguments, but unity should be a good starting place.
- $C_{\varepsilon 2}$ affects the dissipation rate associated with the production rate. Note that if $C_{\varepsilon 2} = 1$, then all energy production is dissipated before it can cause any stirring, so it will cause $e_E = 0$. In contrast, when $C_{\varepsilon 2} = 0$, none of the stirring energy is dissipated, so the dissipation rate is only dependent on the background TKE and not the production rate, which leads to the minimum dissipation and the maximum value for e_E . It is not clear how to best set this coefficient, but 0.5 would probably be a good initial point for experimentation.
- $C_{\varepsilon 3}$ may be fairly important in entrainment under neutral stability by reducing the rate of deepening. Increasing $C_{\varepsilon 3}$ will reduce the rate of deepening by increasing the dissipation

rate in the entrainment process. It is not clear how to best set this coefficient, but we probably should start from unity..

- C_T will increase the time it takes to mix to equilibrium, so will make more energy available for deepening. Arguably this should be set to unity.

D.9.c Surface/bottom mixing layer algorithm

The solution of the surface mixing layer proceeds after solution of the convective mixing algorithm so that the convective mixing energy can be included with wind stirring or bottom shear energy in obtaining the value for production, $\partial E_s / \partial t$.

D.10 Mixing by Kelvin-Helmholtz billows

D.10.a Overview

Kelvin-Helmholtz billows are caused by shear across a region of density and momentum gradients. As a model process, K-H billows are a means of changing the mixing layer thicknesses $h_{T(k)}$ and $h_{B(k+1)}$ across the grid cell interface $k+1/2$. We can postulate two basic relationships between the model grid and the K-H mixing layer: 1) the mixing layer is thin compared to the grid cell thickness, or 2) the mixing layer is thick compared to the grid cell thickness. Our basic approach will be to solve a sub-time step of thin-layer mixing followed by a sub-time step of thick-layer mixing and then continue to iterate the two mixing algorithms until the model time step is reached.

At the start of the K-H mixing routine, we set the time left for mixing to the model time step, i.e.

$$\Delta t_{L(k+1/2)}^0 = \Delta t_M \quad : \quad k = k_b, \dots, k_\eta \quad (D.24)$$

where Δt_L is the time left for mixing, the '0' superscript indicates the time left with zero mixing steps conducted and Δt_M is the model time step. The Δt_L value is individually decremented for each grid cell boundary throughout the mixing process. The general approach will be to compute the KH mixing for successive sub-time steps Δt_U^m , where 'm' is a subtime-step counter. The time used for the 'm' mixing subtime-step is defined as the minimum of the time left or the time-scale of a KH billow, T_{KH} as

$$\Delta t_{U(k+1/2)}^m = \min \left\{ \Delta t_{L(k+1/2)}^{m-1}, T_{KH(k+1/2)}^{m-1} \right\} \quad (D.25)$$

where the time scale for the billow is defined from Thorpe as

$$T_{KH(k+1/2)} = -\frac{20\rho_0}{g\Delta\rho_{R(k+1/2)}} \sqrt{\left(\Delta U_{R(k+1/2)}\right)^2 + \left(\Delta V_{R(k+1/2)}\right)^2} \quad (D.26)$$

where $\Delta U_{R(k+1/2)}$ is the difference between the representative 'x' velocity components on the $k+1$ and k layers, and $\Delta V_{R(k+1/2)}$ is the similar quantity for the 'y' velocity components.

Thus, if the time step is sufficiently small such that $\Delta t_M \leq T_{KH}$, it follows that there will only be a single KH mixing step. Generally, if the grid cells are large compared to the thickness of the KH billows, we will also find that there will be only a single mixing time step as the mixing routine will increase the mixing layer thickness to the point where another billow cannot occur without further large-scale transport. Multiple sub-time mixing steps should only occur in limited cases when $T_{KH} < \Delta t_M$ and there is thick-layer mixing such that mixing across the $k-1/2$ boundary during some sub-time step affects the shear and density gradient across the $k+1/2$ boundary. This combination of factors may allow a second KH billow to form.

D.10.b Thin layer K-H mixing

It can be shown that the change in $h_{T(k)}$ for some time used in mixing (Δt_U) out of the time step left for mixing $\Delta t_L \leq \Delta t_M$, can be found for the ‘m’ mixing sub-time step as

$$\Delta h_{k+1/2}^m = \frac{\Delta t_U^m}{2T_{KH(k+1/2)}^m} \left\{ \delta_{KH(k+1/2)}^m - (h_{Tk}^{m-1} + h_{Bk+1}^{m-1}) \right\} \quad \text{where} \quad \Delta t_U^m = \min \left\{ \Delta t_L^{m-1}, T_{KH(k+1/2)}^m \right\} \quad (D.27)$$

The Kelvin-Helmholtz interface thickness is defined following Sherman et al. (1978) for the ‘m’ mixing time step as

$$\delta_{KH(k+1/2)}^m \equiv -\frac{0.3\rho_0}{g \Delta \rho_{R(k+1/2)}^{m-1}} \left\{ \left(\Delta U_{R(k+1/2)}^{m-1} \right)^2 + \left(\Delta V_{R(k+1/2)}^{m-1} \right)^2 \right\} \quad (D.28)$$

Note that we assume top and bottom symmetry in the KH mixing layer, which allows only one value of $\Delta h_{(k+1/2)}$, so it follows that the mixing layers are thickened as

$$h_{T(k)}^m = h_{T(k)}^{m-1} + \Delta h_{(k+1/2)}^m \quad : \quad \Delta h_{(k+1/2)}^m > 0 \quad (D.29)$$

$$h_{B(k+1)}^m = h_{B(k+1)}^{m-1} + \Delta h_{(k+1/2)}^m \quad : \quad \Delta h_{(k+1/2)}^m > 0 \quad (D.30)$$

Note that if $\Delta h_{(k+1/2)} < 0$ then there is no mixing as the existing mixing thickness is too large and/or shear is too small to produce billows.

To implement the model, we compute δ_{KH} , T_{KH} , and the resulting Δh at each grid cell interface. We then check each grid cell to see that eq. (D.1) will be satisfied if the Δh values are enforced in eqs. (D.29) and (D.30). This check provides a bifurcation in the method. Where eq. (D.1) is satisfied in cell ‘k’ and ‘k+1’, then both the $h_{T(k)}$ and $h_{B(k+1)}$ mixing layer heights are incremented. Similarly, where eq. (D.1) is satisfied in both cell ‘k’ and ‘k-1’, then both the $h_{B(k)}$ and $h_{T(k-1)}$ mixing layer heights are incremented. Conversely, where eq. (D.1) is *not* satisfied for one or both cells on either side of a boundary, the grid cell is considered small relative to the scale of the K-H billow, so we cannot use eq. (D.27) to compute the K-H mixing across the boundary and eq. (D.29) and (D.30) cannot be used (i.e. we must switch to “thick-layer” mixing). For example, if grid cell ‘k’ fails to satisfy eq. (D.1), both the $k-1/2$ and the $k+1/2$ boundaries are affected. It follows that we set both $\Delta h_{(k-1/2)} = 0$ and $\Delta h_{(k+1/2)} = 0$ before storing new values for ‘h’ using eq. (D.29) and (D.30). Computing the mixing across the boundaries of cells that do not satisfy eq. (D.1) is conducted in a “thick-layer” mixing algorithm, described in section D.10.d.

Once the initial increase in the layer thicknesses have been computed (as described above), the time left is decremented as

$$\Delta t_{L(k+1/2)}^1 = \Delta t_{L(k+1/2)}^0 - \Delta t_{U(k+1/2)}^1 \quad : \quad k = k_b, \dots, k_\eta \quad (\text{D.31})$$

where Δt_U^1 is the time used in the first K-H mixing sweep. The general form is

$$\Delta t_{L(k+1/2)}^m = \Delta t_{L(k+1/2)}^{m-1} - \Delta t_{U(k+1/2)}^m \quad : \quad k = k_b, \dots, k_\eta \quad (\text{D.32})$$

where Δt_U^m is defined from eq. (D.25).

Note that thin-layer mixing, i.e. with eq. (D.1) satisfied, the representative scalar values ϕ_R are not changed. That is, the K-H billows slowly increase the mixing layer thickness and erode the region with representative concentrations of ϕ_R , but do not change the value of ϕ_R . Thus, a K-H billow at the top of a grid cell cannot affect the concentration used in computations at the bottom of the grid cell until the grid cell is fully mixed; i.e. until eq. (D.1) is not satisfied. Furthermore, it follows that even if there is time left after the first KH billow mixing, i.e. if $\Delta t_L^1 > 0$ (which implies $T_{KH}^1 < \Delta t_M$ and $T_{KH}^1 = \Delta t_U^1$), then a successive computation of eq. (D.28) would return $\delta_{KH}^2 = \delta_{KH}^1$. It is an identity that

$$\delta_{KH(k+1/2)}^m = h_{Tk}^m + h_{Bk+1}^m \quad (\text{D.33})$$

so it follows that in eq. (D.27) the term

$$\delta_{KH(k+1/2)}^m - (h_{Tk}^{m-1} + h_{Bk+1}^{m-1}) \quad (\text{D.34})$$

must evaluate to exactly zero for $m=2$. Thus, if the thin layer mixing is not followed by any thick-layer mixing, there will be only a single KH billow resolvable in the time step.

D.10.c Advancing the mean concentrations after thin-layer KH mixing

In grid cells where only thin-layer KH mixing has been conducted, the updated mean volume concentrations of scalars after mixing is given by

$$\begin{aligned} \bar{\phi}_{(k)}^{nM} = \bar{\phi}_{(k)}^n + \frac{1}{2\Delta z_{(k)}} & \left(\Delta\phi_{R(k+1/2)}^n \left\{ \frac{[h_{T(k)}^{nM}]^2}{h_{T(k)}^{nM} + h_{B(k+1)}^{nM}} - \frac{[h_{T(k)}^n]^2}{h_{T(k)}^n + h_{B(k+1)}^n} \right\} \right. \\ & \left. - \Delta\phi_{R(k-1/2)}^n \left\{ \frac{[h_{T(k-1)}^{nM}]^2}{h_{T(k-1)}^{nM} + h_{B(k)}^{nM}} - \frac{[h_{T(k-1)}^n]^2}{h_{T(k-1)}^n + h_{B(k)}^n} \right\} \right) \end{aligned} \quad (\text{D.35})$$

where the ‘nM’ superscript indicates the time ‘n’ value after mixing, whereas the ‘n’ superscript indicates the time ‘n’ value before mixing.

D.10.d Thick layer K-H mixing

The justification for a thick-layer mixing algorithm is to account for cases where violation of eq. (D.1) leads to the mixing in the region containing the representative scalar values, as shown in Figure D.2. The approach to thick-layer mixing is to mix the mean concentrations of the grid cell

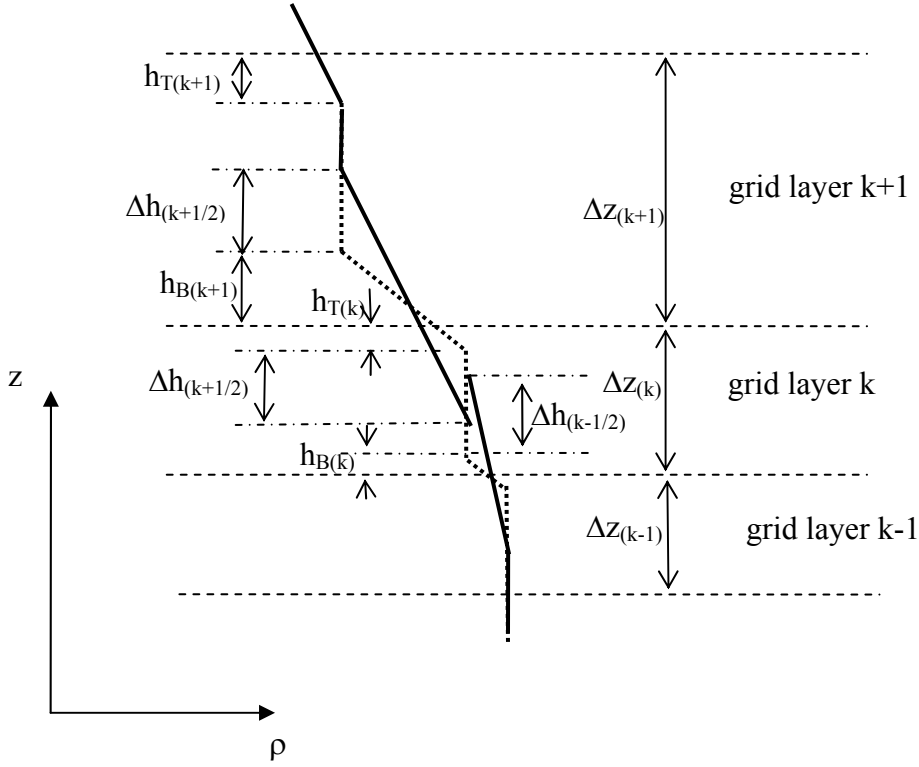


Figure D.2. Case where thin layer KH mixing from the $k-1/2$ and $k+1/2$ boundaries causes mixing of representative scalar values. The dashed line represents the scalar profile prior to thin layer mixing, the solid line represents the unacceptable profile that would result from thin-layer mixing in violation of eq. (D.1).

(rather than the representative values) in mixing subtime steps where no more than $1/4$ of the volume of a grid cell is exchanged across a boundary.

The time required to exchange $1/4$ of the volume of the 'k' cell across the top boundary (into cell $k+1$) for the 'm' sub-time step is found by

$$\Delta t_{RT(k)}^m = \frac{-g [\Delta z_{(k)}]^2 \Delta \bar{\rho}_{(k+1/2)}^{m-1}}{4C_c \rho_0} \left\{ (\Delta \bar{U}_{(k+1/2)}^{m-1})^2 + (\Delta \bar{V}_{(k+1/2)}^{m-1})^2 \right\}^{-3/2} \quad (D.36)$$

Similarly, the time required to exchange $1/4$ of the volume of the 'k+1' cell across its lower boundary (into cell k) at the 'm' subtime step is found by

$$\Delta t_{RB(k+1)}^m = \frac{-g [\Delta z_{(k+1)}]^2 \Delta \bar{\rho}_{(k+1/2)}^{m-1}}{4C_c \rho_0} \left\{ (\Delta \bar{U}_{(k+1/2)}^{m-1})^2 + (\Delta \bar{V}_{(k+1/2)}^{m-1})^2 \right\}^{-3/2} \quad (D.37)$$

The mixing time used in the 'm' subtime step is defined by

$$\Delta t_{U(k+1/2)}^m = \min \left[\Delta t_{L(k+1/2)}^{m-1}, \Delta t_{RT(k)}^m, \Delta t_{RB(k+1)}^m, T_{KH(k+1/2)}^0 - \sum_{q=1, m-1} \Delta t_{U(k+1/2)}^q \right] \quad (D.38)$$

That is, the time for the next mixing subtime step is the minimum of the time left, the time required for mixing $\frac{1}{4}$ of the volume, or the time remaining for a K-H billow event based on the stratification before any mixing started.

It is possible that a cell may have thick-layer mixing over one or both boundaries. Both boundaries are thick-layer mixing boundaries when

$$h_{T(k)} + h_{B(k)} > \Delta z_{(k)} \quad (D.39)$$

The top boundary alone will be a thick-layer mixing boundary when

$$h_{T(k+1)} + h_{B(k+1)} > \Delta z_{(k+1)} \quad \text{and} \quad h_{T(k)} + h_{B(k)} \leq \Delta z_{(k)} \quad (D.40)$$

Similarly, the lower boundary alone will be a thick-layer mixing boundary when

$$h_{T(k-1)} + h_{B(k-1)} > \Delta z_{(k-1)} \quad \text{and} \quad h_{T(k)} + h_{B(k)} \leq \Delta z_{(k)} \quad (D.41)$$

For the case with both boundaries as thick layer mixing, the mean value of conservative scalar concentrations are updated over the ‘m’ subtime step as

$$\begin{aligned} \bar{\phi}_{(k)}^m = \bar{\phi}_{(k)}^{m-1} + \frac{1}{2\Delta z_{(k)}} \left(\frac{C_C \rho_0}{g} \right)^{1/2} & \left(\Delta \bar{\phi}_{(k+1/2)}^{m-1} \left\{ \frac{\Delta t_{U(k+1/2)}^m}{-\Delta \bar{\rho}_{(k+1/2)}^{m-1}} \right\}^{1/2} \left\{ [\Delta \bar{U}_{(k+1/2)}^{m-1}]^2 + [\Delta \bar{V}_{(k+1/2)}^{m-1}]^2 \right\}^{3/4} \right. \\ & \left. - \Delta \bar{\phi}_{(k-1/2)}^{m-1} \left\{ \frac{\Delta t_{U(k-1/2)}^m}{-\Delta \bar{\rho}_{(k-1/2)}^{m-1}} \right\}^{1/2} \left\{ [\Delta \bar{U}_{(k-1/2)}^{m-1}]^2 + [\Delta \bar{V}_{(k-1/2)}^{m-1}]^2 \right\}^{3/4} \right) \end{aligned} \quad (D.42)$$

However, where only the upper boundary is involved in thick-layer mixing, updating the mean value of the scalar is simply

$$\bar{\phi}_{(k)}^m = \bar{\phi}_{(k)}^{m-1} + \frac{1}{2\Delta z_{(k)}} \left(\frac{C_C \rho_0}{g} \right)^{1/2} \Delta \bar{\phi}_{(k+1/2)}^{m-1} \left\{ \frac{\Delta t_{U(k+1/2)}^m}{-\Delta \bar{\rho}_{(k+1/2)}^{m-1}} \right\}^{1/2} \left\{ [\Delta \bar{U}_{(k+1/2)}^{m-1}]^2 + [\Delta \bar{V}_{(k+1/2)}^{m-1}]^2 \right\}^{3/4} \quad (D.43)$$

Likewise, when only the lower boundary is involved in thick-layer mixing, updating the mean value of the scalar is simply

$$\bar{\phi}_{(k)}^m = \bar{\phi}_{(k)}^{m-1} - \frac{1}{2\Delta z_{(k)}} \left(\frac{C_C \rho_0}{g} \right)^{1/2} \Delta \bar{\phi}_{(k-1/2)}^{m-1} \left\{ \frac{\Delta t_{U(k-1/2)}^m}{-\Delta \bar{\rho}_{(k-1/2)}^{m-1}} \right\}^{1/2} \left\{ [\Delta \bar{U}_{(k-1/2)}^{m-1}]^2 + [\Delta \bar{V}_{(k-1/2)}^{m-1}]^2 \right\}^{3/4} \quad (D.44)$$

As long as $\Delta t_U^m > 0$, the thick-mixing boundaries need to be recursively computed, with new values of $\Delta \bar{U}$, $\Delta \bar{\rho}$, $\Delta \bar{\phi}$ being computed in each cycle.

D.10.e Representative scalar values after thick-layer mixing

Any cell with both boundaries involved in thick-layer mixing will have the representative scalar values set to the mean values after the end of thick-layer mixing, i.e.

$$\phi_{R(k)}^{nM} = \bar{\phi}_{(k)}^{nM} \quad \text{where} \quad h_{T(k)} + h_{B(k)} > \Delta z_{(k)} \quad (D.45)$$

However, where only one boundary is involved in thick-layer mixing, we require

$$\bar{\phi}_{(k)} = \phi_{R(k)} \left[1 - \left(\frac{h_{T(k)}}{\Delta z_{(k)}} + \psi_{T(k)} \right) - \left(\frac{h_{B(k)}}{\Delta z_{(k)}} - \psi_{B(k)} \right) \right] + \phi_{R(k+1)} \psi_{T(k)} - \phi_{R(k-1)} \psi_{Bk} \quad (D.46)$$

where ψ 's are given by eq. (D.6). If the top boundary is involved in thick-layer mixing, then $h_{T(k)} = 0$ and $\psi_{T(k)} = 0$. Similarly, if only the bottom boundary is involved in thick-layer mixing, then $h_{B(k)} = 0$ and $\psi_{B(k)} = 0$. For bottom thick-layer mixing, the value of $\phi_{R(k+1)}$ is as previously determined from thin-layer mixing. Similarly, for top thick layer mixing, the value of $\phi_{R(k-1)}$ is as found in thin-layer mixing. Thus, we solve for the representative scalar where the top boundary is thick-layer mixed as

$$\phi_{R(k)} = \frac{\bar{\phi}_{(k)} + \phi_{R(k-1)} \psi_{Bk}}{1 - \left(\frac{h_{B(k)}}{\Delta z_{(k)}} - \psi_{B(k)} \right)} \quad (D.47)$$

Whereas the representative scalar where the bottom boundary is thick-layer mixed is

$$\phi_{R(k)} = \frac{\bar{\phi}_{(k)} - \phi_{R(k+1)} \psi_{T(k)}}{1 - \left(\frac{h_{T(k)}}{\Delta z_{(k)}} + \psi_{T(k)} \right)} = \quad (D.48)$$

Once new representative values have been computed, a second thin-layer mixing cycle can be carried out.

D.10.f Linking thin-layer and thick-layer KH mixing

For cells that have one boundary with thin-layer mixing and one boundary with thick-layer mixing, there is a possibility of the thick-layer mixing leading to a second (or multiple) KH billows at the thin-layer boundary. Arguably, we could devise a very sophisticated algorithm that check for the relationship between the local thick-layer Δt_L and the thin-layer Δt_L after each mixing step and try to match the timing. It is unlikely that the extra effort would be worthwhile. Instead, we take the following fairly simple approach. Thin-layer mixing is conducted for a single mixing sub-time step following the procedures in sections D.10.b and D.10.c. If necessary, thick-layer mixing is conducted, with multiple sub-time step cycles to account for the entire time step. We then find any thin-layer mixing boundaries where $\Delta t_L > 0$, i.e. the initial $T_{KH} < \Delta t_M$, and an adjacent boundary was involved in thick-layer mixing. On these boundaries we can then conduct another thin-layer mixing step for a second billow. Since we have already performed thick-layer mixing over the complete time step, there is no need for further cycling.

This page intentionally left blank

APPENDIX E Field report on a hypoxic event in SE Corpus Christi Bay

E.1 Summary

A field trip was conducted from July 10 - 17, 2006 (including travel time) with the original intent to gain a better understanding of the characteristics in Corpus Christi Bay along Mustang Island where hypoxia has previously been documented. This field trip was conducted by Ben R. Hodges (author of this appendix). As the field trip serendipitously coincided with an extensive hypoxia episode, the data collection was focused on identifying the geographic area (in a SSW to NNE line about 2 km offshore) that was impacted by hypoxia. Two boat deployments were made to survey bathymetry in the shallows along the Mustang Island coast. Six boat deployments were made to measure profiles of salinity, temperature and dissolved oxygen (DO) in the bay. A total of 67 profiles with a Manta water quality profiles were collected over a 72 hours period. Preliminary review of the data showed an extensive region of hypoxia that was in place in the evening of July 13, 2006 with 44 psu salinity at the benthos and 39 psu salinity at the surface. Over the next two days, the stratification and associated hypoxia moved north in the bay, and slowly began to mix out. By July 16, 2006, the salinity at the bottom was only 42 psu, and the hypoxic region had significantly shrunk.

This report is intended as a historical reference, providing an outline of the project Goals and Scope (§E.2), Instruments and Methods (§E.3), Lessons Learned (§E.4), Data Types Collected (§E.5), and a listing of data from all Manta profiles. This report does not provide analysis of the data.

E.2 Goals and Scope

The original scope of this field trip was a reconnaissance of the area of south-eastern Corpus Christi Bay where Montagna and collaborators at the University of Texas Marine Science Institute have previously documented episodic hypoxia. The goals of this trip were 1) obtaining a better understanding of the general stratification and mixing characteristics in the south-eastern part of the bay using a Eureka Manta and PME SCAMP, and 2) determining if a Lowrance LMS 339CDF IGPS sonar/GPS could be used for basic bathymetric charting. However, the original goals were modified when initial profiling showed an episode of hypoxia was already in progress. As it is difficult to predict the onset of hypoxia and plan a field trip around such an episode, the principal goal of the trip was altered to try to determine the extent an origination of stratification that accompanied the hypoxia. Some data was collected for evaluating the Lowrance sonar unit for bathymetric plotting. A Manta was extensively used for profiling through the southeastern bay (to the east of the Gulf Intra-Coastal WaterWay and south of Shamrock Island). The SCAMP was not deployed due to the extra time it required to document large sections of the bay.

E.3 Instruments and Methods

E.3.a Boat and personnel

All data was collected from a Tracker Marine 14 foot jon boat with a 15 hp Mercury motor. All data was collected by the author as the sole boat occupant.

E.3.b Instruments

A Eureka Manta was used to collect profiles for this field trip. A Eureka Amphibian (with HP iPAQ handheld) was connected to the Manta for data collection. Originally a Dell M50 laptop was planned for use, but water splashing on the keyboard during the first deployment rendered the computer inoperable. Data from that first profile has not been recovered. The Manta used is capable of recording depth, conductivity, salinity, temperature, pH, ORP, DO, DO% saturation, GPS latitude/longitude/time. However, see §E.4.b of Lessons Learned.

A Lowrance LMS 339CDF IGFS depth sonar/GPS was used for positioning the boat at desired profiling locations and for recording bathymetric data.

A Kestrel 4000 (Nielsen-Kellerman instruments) hand-held weather station was used for weather sampling during some of the deployments. This instrument can store 250 data points of wind speed, relative humidity, air temperature, etc. Note that it cannot store wind direction as it depends upon the user to point the instrument directly at the wind.

E.3.c Methods for profiling with the Manta

Profiling started just below surface and was conducted as manual interval logging (vice continuous sampling at predefined time intervals). Each sample depth was logged after the temperature, DO and salinity were given time to stabilize. Stabilization time was, in all cases, determined by DO. When the boat motion was considerable, the DO never completely stabilized, but would slowly oscillate both up and down by several hundredths of a mg/l. However, the DO sensor did not respond as fast as the boat motion, so the reading should be representative of the sampled volume. Under such conditions, logging was attempted when the boat was between the trough and crest of its excursions.

For first sampling point, the Manta was held such that the upper metal bracket was even with the boat gunwale at the aft thwart. The second sampling point was with the 2 foot marker on the umbilical even with the gunwale. Subsequent sampling points were at one foot intervals at the gunwale (based on the umbilical markers) as long as there were no significant gradients in DO or salinity. As gradients occurred, sampling was at 6 inch and then 3 inch intervals (visually interpolated between the 1 foot markers). Note that the boat vertical motion is a posteriori estimated at 6 inches to 1 foot during much of the surveying. When the wind was stronger, the seas were steep and choppy with wavelengths much smaller than the boat. Under these conditions the boat movement was actually smaller (a posteriori estimated as 3 inches to 6 inches) than under weaker wind conditions that were dominated by long-wavelength swell. It may be possible to use the sonar data to obtain a better estimate of the boat excursion.

E.3.d Manta calibration

The Eureka Manta was calibrated for conductivity on May 21, 2006, and again on July 6, 2006. On both occasions it was found to have had no significant drift. Additional conductivity calibrations were not conducted for this field trip.

Calibration for DO was accomplished using the DO% saturation option. The calibration cup was filled to slightly below the DO sensor. The sensor membrane was dabbed with a dry handkerchief to remove any water on the membrane. The calibration cup was capped and allowed to reach equilibrium. The night-time calibrations can be considered to be reasonable, but there is some question as to the accuracy of the day-time calibration on 7/14/06. During this calibration, the bimini top was not up on the boat (due to wind) and the Manta was in the direct sunlight. I noted on a later trip (afternoon of 7/16/06) that direct sunlight caused the Manta DO reading to continually creep up slowly with direct sunlight. The calibration settings during the experiment are provided in Table E.1.

E.3.e Deploying the Kestrel weather station

The Kestrel was deployed intermittently during the profiling. It was not consistently used at each profiling station. When it was deployed, a number of readings (typically 4 to 6) were taken. The Kestrel was deployed standing on the boat seat with my arm outstretched, so was approximately 7 to 8 feet off the water surface.

E.3.f Boat deployments and profiling locations

Profiles were mostly centered on the sampling sites M24, M23, M22, M19, M20 that were previously used by Montagna and collaborators from UT-MSI. These sites are on a northeast trending line (from M24 to M20) and are (with the exception of M24) over 11 feet deep. Sites M23, M19 and M20 have some of the highest probabilities of finding hypoxia in the southeastern Corpus Christi Bay based on preliminary analysis of Montagna (pers. comm. 2006). Note that M19 is the site of a continuous profiling instrument deployed by Bonner and the SERF program at Texas A&M. Table E.2 through Table E.4 provide the target waypoint locations and actual boat locations during profiling.

There were eight boat deployments during the field trip. The first and second boat deployments (July 11 and 12) were only for bathymetry surveying close to Mustang Island (due to choppy seas and strong winds).

The third boat deployment (night of July 13-14) initially collected profiles on a transect from the shoreline of Mustang Island out to M19 to look for density underflows that might be developed by differential evaporation in the shallows of Mustang Island (W60a, W61a, W62a, W64a, W63a, M19a). Upon finding 44 psu salinity and hypoxia at M19, the remainder of the third boat deployment was used in a transect of the main sites south of M19 (M19a, M22a, M23a, M24a, M09a). Unfortunately, the northern site M20 was not profiled on this night, so the northern extent of the hypoxia was not determined in this boat deployment. To examine possible sources of high salinity water from Laguna Madre, transects in shallower water (5 to 7 feet) at the southern end of CC Bay were examined. W74a, W75a, M24b provide a perpendicular

offshore transect close to the eastern edge of the Laguna Madre connection to the eastern part of CC Bay. Similarly, W72a, W71a, M09a provide a perpendicular offshore transect somewhat west of the center of the Laguna Madre connection. W80a (renamed from W73a) is a single point in the center between these two transects. M24 was selected as a point for making two samples on every night boat deployment (starting and ending) so that a better temporal resolution of one point could be obtained. When time allowed, two samples of M23 were also made on each boat deployment.

The fourth boat deployment (afternoon of July 14) started with a profile moving northeast along the main transect (M24c, M23c, M22c, M19c, W70c, M20c). The new site W70 was sampled after M20; no stratification or hypoxia was found at the latter. W70 appeared to be near the front of the stratified zone.

The fifth boat deployment (night of July 14 - 15) started with the main northeast transect (M24d, M23d, M22d, M19d, W70d, M20d, W73d, M17d), which was extended from the afternoon sampling in the fourth deployment. No hypoxia was found at M17, so point W73 about midway between M20 and M17 was subsequently sampled and showed strong stratification. The transect was completed about 0430 hours, then southern sites M23e, M24e were resampled to allow better temporal resolution of these sites. Initial review of the transects perpendicular to M09 and M24 that were conducted the previous night (third boat deployment) did not show any interesting features in the shallows, so a large scale transect along the southern-western edge of Mustang Island at about 9 to 10 feet depth was made (M09e, M24e, W77e, W76e, M26e, M10e).

The sixth boat deployment (afternoon of July 15) was shortened by a failure of the Manta. The battery was not sufficiently charged during the morning and I failed to bring the inverter and Manta adapter. During this deployment, full profiles were collected at M24f and M23f only. A partial profile was collected at M22f.

The seventh boat deployment (night of July 15 - 16) again began with a transect to the northeast (M24g, M23g, M22g, M19g, M20g, W73g, M17g, M18g, W79g, W78g, M16g) that was extended from the previous night's deployment as the hypoxia had spread further north. No hypoxia was found at M16, so the sites W78 then W79 were investigated to better identify the northern limit. Site M23h was resampled. A more limited version of the prior night's transect was conducted (M09h, M24h, M77h, M76h); the upper sites M26 and M10 were left out as they did not seem interesting on the initial review of data and I was getting tired.

The eighth boat deployment (afternoon of July 16) consisted entirely of the northeast transect of the main points (M24i, M23i, M22i, M19i, M20i, M17i, M18i, W78i, M16i). Stratification was much weaker throughout, and hypoxia only evident at M22, M19, and M20. Returned to sample M24j for temporal resolution.

E.4 Lessons Learned

E.4.a Amphibian date setting

The Eureka Amphibian with HP iPAQ does not retain the date when the battery runs out, which was not noted during its initial use during this project. Thus, the local date/times in the raw data files do not match the local date/times of the chronology. Once the problem was noted, it was decided *not* to correct the iPAQ so that the data would all have a consistent offset. The conversion between the Amphibian time and U.S Central Daylight Time (CDT) for all data are provide in Table E.5 through Table E.11. The date/times in the chronology associated with profiling are the date/times the profiles were recorded on the Amphibian, which is the time of the last data point in a profile. All times below are local time (US central daylight time)

E.4.b Amphibian “view” setting and data logging

Note that sampling data principally consists of temperature, DO, DO%Sat, salinity and depth. Unfortunately, I did not realize that the Amphibian setting for “view” also limits the data recorded to the log file. I had set the view to the few parameters that I was interested in monitoring on the boat so that I would get larger fonts on the screen. Thus, the data recorded mostly do not include pH, ORP, GPS, conductivity.

E.4.c Getting the boat to plane

With a single person in the Tracker jon boat and the 15 hp motor, the boat can get up on a plane and reach 19 or 20 mph if all the extra weight (gasoline, anchors, instruments, etc) are stored very far forward. If there is any significant headwind, the boat cannot plane. However, it is possible to get the boat onto a plane going downwind, and then turn it back upwind and maintain the planing operation. There is a need for more tie-downs forward in the boat to keep gear from shifting.

E.4.d Boat motion at anchor

Under long swells, the jon boat will have less motion if the anchor is led through the boat tie-down closer to the water (i.e, not simply through the chock on the bow). This can be accomplished with a harness run through the tie-down, but is somewhat cumbersome. An improved means of running the anchor line through the tie-down should be made before the next trip.

E.4.e Downloading Kestrel weather data

In the future, we need to have a computer with a serial port for downloading the Kestrel 4000 weather data. Also, we should make sure that the Kestrel software is brought on a disk so that it can be loaded on a back-up computer in case of computer failure. Alternatively, note that the Kestrel can store 250 data points, so divide the sampling time to only use this amount of sampling during the field experiment.

E.4.f Sonar trail default

The Lowrance sonar default for “trail” length is 2000 points, so on a long bathymetry survey, it will not be able to display the historic trail (i.e. once it reaches 2000 points, it overwrites old points). Menu options for trails can be used to set the length to 9999 points. Periodically

starting a new trail file is a good idea. Note there does not seem to be a good way to export the trails from the GDM 6 software. Note that this does not mean the position/depth data is lost, only the display trail that is useful for seeing where the boat has gone in real-time. As a result of losing the trail, there is a section of the 7/12/2006 bathymetry survey between M10 and M11 that appears to have fewer trails through it.

E.5 Data Types Collected

E.5.a Bathymetry data

The bathymetric data collected are of varying quality and cover principally the shallow regions along Mustang Island from M24 to M12. Data collected on July 11 - 12 are the best data for bathymetric surveying as the boat deployments were at slow speed (~ 5 mph) and were focused on bathymetric data collection. On other occasions, the sonar was recording position/depth, but the boat speed may have been too high (transiting between profiling sites) for accurate survey purposes. Of principal interest in the survey of July 12 is the evidence of a series of channel/bar configurations moving outward from the coast along Mustang Island. In several places, there were two or three channels parallel to the Mustang Island shoreline that were 3 to 4 feet deep, and were separate by shallow bars at about 1-1/2 feet deep (also running parallel to the shoreline).

E.5.b Manta profiles

A total of 67 Manta profiles were collected. Due to the problems noted in §E.4.b of Amphibian “view” setting and data logging under the Lessons Learned section above, the only data consistently recorded were depth, DO, DO% saturation, temperature, salinity. Examples of data from profile M19a are shown in Figure E.1. Preliminary review of this data with the strong salinity and DO profiles caused the focus of the field trip to change focus as discussed in §E.2.

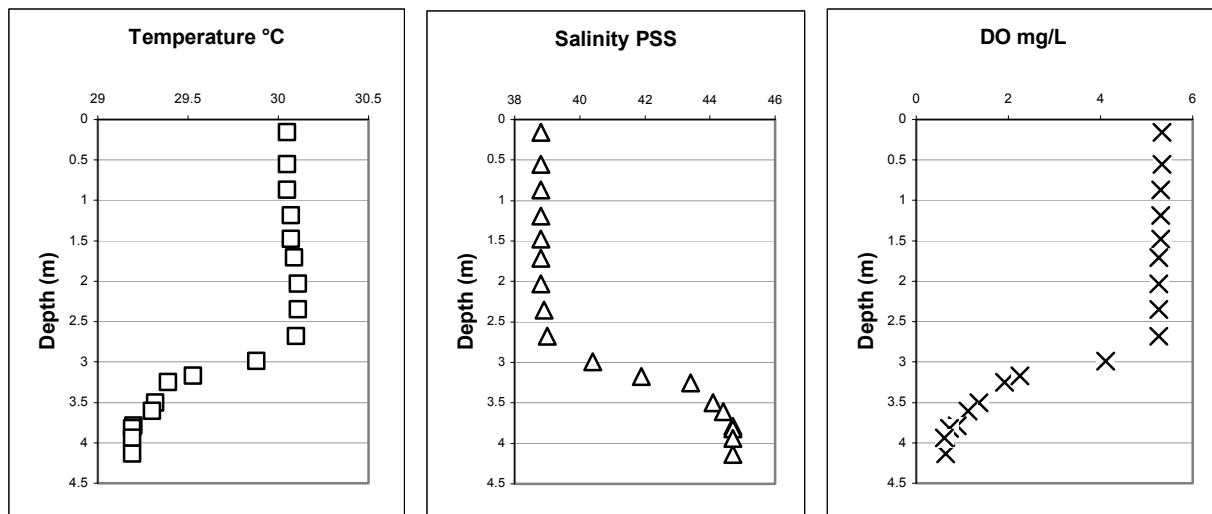


Figure E.1. Data from profile M19a

E.5.c Kestrel weather data

The Kestrel was deployed from 7/13/2006 through 1413 hours on 7/16/2006, when it ran out of memory. Due to the failure of the Dell laptop, I was unable to download data during the field trip and clear the memory. Data recorded are date and time (DT), wind speed (WS) in m/s, temperature (TP) in C, wind chill (WC) in C, relative humidity (RH) in %, heat index (HI) in C, dew point (DP) in C, wet bulb temperature (WB) in C, barometric pressure (BP) in millibars (hectoPascals), altitude (AL) in m, density altitude (DA) in m.

E.5.d Weather data from TCOON network

On-line weather data from the TCOON network was retrieved to provide insight into the large-scale wind conditions around Corpus Christi Bay, as shown in Figure E.2. Note that winds were on a declining trend with a day/night oscillation throughout the field experiment.

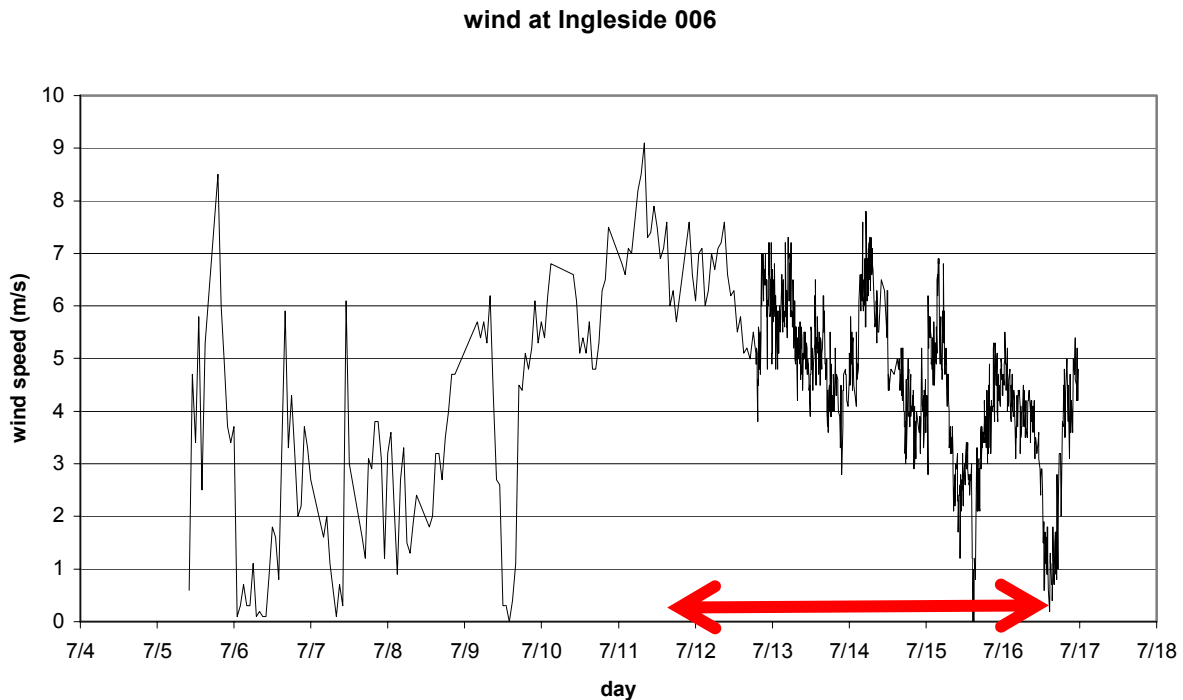


Figure E.2. TCOON data for wind at Ingleside station 006 during mid-July 2006. The field experiment was conducted during the times indicated by the arrow. Data were available hourly through 7/12/06 and at 6 minute intervals thereafter.

E.6 Data Files on CD-ROM

E.6.a Overall organization

Files for Manta profiles and sonar data are organized in top level folders using the date of collection (e.g. “2006_07_14” for data gathered July 14, 2006). Second level folders within these top-level folders are “Sonar” and “Manta” respectively. Weather data is stored in a top-level folder “2006_07_weather.” Software used for processing the data is found in the top-level folder “software.”

E.6.b Sonar data

The sonar creates a *.slg file that can be read by the SonarViewer application to display the sonar log. The data from the sonar is exported from SonarViewer into a *.csv file with the data types shown in

Table E.10. Note that the *.csv file has a time column that counts the milliseconds since the beginning of the log. The actual start time can be obtained by viewing the *.slg file and pointing the mouse at the start of the run. The actual start times for each sonar log are given in Table E.. Note that the sonar appears to record the local time as two hours earlier than actual local time. The sonar time is automatically obtained from the GPS satellite, so it is not clear what setting is wrong in the unit.

E.6.c Manta data

The Manta data is provided in the *.loc files used by the Amphibian when logging data and the converted *.csv files created with the Eureka software. As a convention, the files are named using the waypoint name and a suffix in the set {a, b, c, d, e, f, g, h, i, j} to indicate the time sequencing of the profile. Thus all profiles 'a' were accomplished sequentially in time in some logical fashion without any repetition of points. For example, the 'a' profiles provide a transect from W60 to M19, a second transect from M19 to M09 and two short transects with points W71 through W75. During the same boat deployment, a second profile was taken at M24, so the new profile was given an M24b filename. Upon beginning the next boat deployment, the first set of transects were given the 'c' suffix. Note that all the time stamps in the Manta data files are wrong as discussed in § E.4.a of the Lessons Learned section above. The time conversion for all files is provided in Table E.5.

E.7 Tables

Table E.1. Manta calibration

Day	Time	Barometric pressure used (mmHg)	Calibration adjustment (% DO sat)	Start/end of deployment	Comments
7/13/2006	2010	not noted	not noted	start	Using laptop
7/13/2006	2015	764.59	not noted		Using laptop - performed additional check because of 110% DO saturation. Recall as having no significant change.
7/13/2006	2045	not noted	not noted	start	Using Amphibian. Recall as having no significant change.
7/14/2006	1500	764	-5.01 %	start	Wrong atmospheric pressure.
7/14/2006	1515	760.2	-1.19 %	start	Recalibration. This appears to be affected by direct sunlight on the instrument and was likely not actually stabilized. Based on the subsequent night calibration (below), it is estimated that this daytime calibration is ~ 5% DO saturation too low; i.e. the actual DO levels should be increased by about 5% DO saturation for data taken after this calibration.
7/15/2006	0015	760.087	+4.54 %	start	Seems large. Suspect this is an adjustment for poor calibration during the day.
7/15/2006	0730	764.715	-2.66 %	end	Not shaded. May be affected by morning sunlight.
7/15/2006	1345	766.146	+1.24 %	start	Bimini top up on boat (instrument shaded). Again appears to somewhat compensate for minus calibration without shading
7/15/2006	2230	766.095	-0.12 %	start	Night calibration. Note that it is not significantly changed from the afternoon calibration taken in the shade.
7/16/2006	0810	766.937	-0.88 %	end	Morning calibration. Not shaded.
7/16/2006	1315	765.3	-0.44 %	start	Bimini top up (instrument shaded)
7/16/2006	1805	762.89	+0.62 %	end	Bimini top down (instrument in sun), noted a slow continual climb in DO during calibration. Shaded with towel and DO stabilized close to 100%.

Table E.2. Waypoint and profile coordinates (part 1)

Way point	Profile	Latitude (W)		Longitude (N)		Date Time (CST)	Depth feet
		deg	min	deg	min		
m09		27	41.5832	97	12.6674		
	m09a	27	41.5920	97	12.6730	7/14/06 12:41 AM	8.9
	m09e	27	41.5860	97	12.6640	7/15/06 5:48 AM	8.7
	m09h	27	41.5850	97	12.5750	7/16/06 8:00 AM	8.9
m10		27	42.7951	97	10.8070		
	m10e	27	42.7970	97	10.8040	7/15/06 6:49 AM	10.8
m16		27	45.7230	97	10.8422		
	m16g	27	45.7060	97	10.8270	7/16/06 5:08 AM	10.2
	m16i	27	45.7260	97	10.8560	7/16/06 5:19 PM	10.2
m17		27	44.5711	97	11.0893		
	m17d	27	44.5660	97	11.0880	7/15/06 3:54 AM	12.0
	m17g	27	44.5620	97	11.0860	7/16/06 4:00 AM	12.4
	m17i	27	44.5830	97	11.0840	7/16/06 4:07 PM	12.5
m18		27	44.8501	97	10.8692		
	m18g	27	44.8380	97	10.8570	7/16/06 4:27 AM	11.6
	m18i	27	44.8580	97	10.8690	7/16/06 4:31 PM	11.7
m19		27	43.3600	97	11.3868		
	m19a	27	43.3920	97	11.3280	7/13/06 10:38 PM	12.9
	m19c	27	43.3620	97	11.3630	7/14/06 4:27 PM	13.0
	m19d	27	43.4000	97	11.3640	7/15/06 2:09 AM	12.7
	m19g	27	43.3810	97	11.3260	7/16/06 1:21 AM	12.8
	m19i	27	43.4080	97	11.3830	7/16/06 3:15 PM	12.7
m20		27	44.0838	97	11.1872		
	m20c	27	44.0940	97	11.1960	7/14/06 4:52 PM	12.7
	m20d	27	44.0830	97	11.1900	7/15/06 3:19 AM	12.0
	m20g	27	44.0850	97	11.1830	7/16/06 2:43 AM	12.5
	m20i	27	44.0890	97	11.1860	7/16/06 3:42 PM	12.4
m22		27	42.9430	97	11.5469		
	m22a	27	42.9480	97	11.5550	7/13/06 11:04 PM	12.7
	m22c	27	42.9380	97	11.5470	7/14/06 4:04 PM	13.0
	m22d	27	42.9070	97	11.5710	7/15/06 1:27 AM	12.7
	m22f					7/15/06 3:32 PM	12.9
	m22g	27	42.9440	97	11.5410	7/16/06 12:39 AM	12.8
	m22i	27	42.9370	97	11.5560	7/16/06 2:56 PM	12.7
m23		27	42.2852	97	11.9141		
	m23a	27	42.2820	97	11.9150	7/13/06 11:31 PM	11.3
	m23c	27	42.2900	97	11.9130	7/14/06 3:41 PM	11.5
	m23d	27	42.2890	97	11.9100	7/15/06 1:06 AM	11.3
	m23e	27	42.2800	97	11.9240	7/15/06 4:43 AM	11.1
	m23f					7/15/06 3:11 PM	11.6
	m23g	27	42.2930	97	11.9390	7/16/06 12:05 AM	11.5
	m23h	27	42.2910	97	11.9220	7/16/06 6:52 AM	11.3
	m23i	27	42.2850	97	11.9080	7/16/06 2:40 PM	11.3

Table E.3. Waypoint and profile coordinates (Part 2)

Way point	Profile	Latitude (W)		Longitude (N)		Date Time (CST)	Depth feet
		deg	min	deg	min		
m24		27	41.7312	97	12.1790		
	m24a	27	41.7350	97	12.1780	7/13/06 11:57 PM	9.1
	m24b	27	41.7500	97	12.1700	7/14/06 2:24 AM	8.9
	m24c	27	41.7480	97	12.1780	7/14/06 3:16 PM	9.4
	m24d	27	41.7410	97	12.1710	7/15/06 12:44 AM	9.3
	m24e	27	41.7430	97	12.1630	7/15/06 5:21 AM	9.1
	m24f					7/15/06 2:43 PM	9.2
	m24g	27	41.7470	97	12.1720	7/15/06 11:34 PM	9.4
	m24h	27	41.7310	97	12.1690	7/16/06 7:44 AM	9.1
	m24i	27	41.7260	97	12.1600	7/16/06 2:25 PM	9.2
	m24j	27	41.7290	97	12.1800	7/16/06 5:57 PM	9.1
m26		27	42.2220	97	11.1380		
	m26e	27	42.2190	97	11.1380	7/15/06 6:30 AM	9.8
w60		27	42.8820	97	10.4330		
	w60a	27	42.8830	97	10.4290	7/13/06 9:28 PM	2.0
w61		27	42.9170	97	10.4740		
	w61a	27	42.9170	97	10.4740	7/13/06 9:08 PM	2.6
w62		27	42.9320	97	10.5450		
	w62a	27	42.9320	97	10.5450	7/13/06 9:38 PM	5.6
w63		27	43.0240	97	10.6790		
	w63a	27	43.0240	97	10.6790	7/13/06 9:52 PM	11.1
w64		27	42.9810	97	10.6270		
	w64a	27	42.9810	97	10.6270	7/13/06 10:15 PM	6.3
w70		27	43.8400	97	11.2140		
	w70c	27	43.8400	97	11.2140	7/14/06 5:11 PM	12.9
	w70d	27	43.8270	97	11.2150	7/15/06 2:49 AM	12.3
	w70g	27	43.8410	97	11.2170	7/16/06 1:57 AM	12.6
w71		27	41.4240	97	12.7030		
	w71a	27	41.4240	97	12.7030	7/14/06 12:47 AM	7.3
w72		27	41.3430	97	12.7450		
	w72a	27	41.3430	97	12.7450	7/14/06 1:13 AM	4.8
w73		27	44.3750	97	11.1700		
	w73d	27	44.3750	97	11.1700	7/15/06 4:12 AM	12.1
	w73g	27	44.3700	97	11.1710	7/16/06 3:17 AM	12.2
w74		27	41.5160	97	12.0430		
	w74a	27	41.5160	97	12.0430	7/14/06 1:52 AM	5.3
w75		27	41.5760	97	12.0770		
	w75a	27	41.5760	97	12.0770	7/14/06 2:08 AM	6.9

Table E.4. Waypoint and profile coordinates (Part 3)

Way point	Profile	Latitude (W)		Longitude (N)		Date Time (CST)	Depth feet
		deg	min	deg	min		
w76		27	41.7940	97	11.5870		
	w76e	27	41.7940	97	11.5870	7/15/06 6:10 AM	9.1
	w76h	27	41.7960	97	11.5960	7/16/06 7:18 AM	9.2
w77		27	41.7400	97	11.9300		
	w77e	27	41.7400	97	11.9300	7/15/06 7:10 AM	9.1
	w77h	27	41.7450	97	11.9460	7/16/06 7:32 AM	9.2
w78		27	45.4140	97	10.8270		
	w78g	27	45.4140	97	10.8350	7/16/06 5:34 AM	10.1
	w78i	27	45.4200	97	10.8300	7/16/06 4:55 PM	10.1
w79		27	45.1470	97	10.8350		
	w79g	27	45.1470	97	10.8350	7/16/06 6:00 AM	11.5
w80		27	41.3650	97	12.5750		
	w73a	27	41.3650	97	12.5750	7/14/06 1:31 AM	5.3

Table E.5. Time correction from Amphibian time to Central Daylight Time

Time correction key	
Amphibian	7/4/05 4:12
CDT	7/19/06 13:57
difference	380.40625 days

Table E.6. Time correction for Manta files of third boat deployment

Third boat deployment		Amphibian date/time		Corrected date/time (CDT)	
waypoint file	logbook waypoint	profile start	profile end	actual start	actual end
w61a	w61a	6/28/05 11:23	6/28/05 11:24	7/13/06 21:08	7/13/06 21:09
w60a	w60a	6/28/05 11:43	6/28/05 11:45	7/13/06 21:28	7/13/06 21:30
w62a	w62a	6/28/05 11:53	6/28/05 11:56	7/13/06 21:38	7/13/06 21:41
w63a	w63a	6/28/05 12:07	6/28/05 12:20	7/13/06 21:52	7/13/06 22:05
w64a	w64a	6/28/05 12:30	6/28/05 12:39	7/13/06 22:15	7/13/06 22:24
m19a	w65a	6/28/05 12:53	6/28/05 13:02	7/13/06 22:38	7/13/06 22:47
m22a	m22/w66a	6/28/05 13:19	6/28/05 13:27	7/13/06 23:04	7/13/06 23:12
m23a	w68a	6/28/05 13:46	6/28/05 13:55	7/13/06 23:31	7/13/06 23:40
m24a	w69a	6/28/05 14:12	6/28/05 14:20	7/13/06 23:57	7/14/06 0:05
m09a	m09/w70a	6/28/05 14:36	6/28/05 14:45	7/14/06 0:21	7/14/06 0:30
w71a	w71a	6/28/05 15:02	6/28/05 15:10	7/14/06 0:47	7/14/06 0:55
w72a	w72a	6/28/05 15:28	6/28/05 15:31	7/14/06 1:13	7/14/06 1:16
w80a	w73a	6/28/05 15:46	6/28/05 15:50	7/14/06 1:31	7/14/06 1:35
w74a	w74a	6/28/05 16:07	6/28/05 16:10	7/14/06 1:52	7/14/06 1:55
w75a	w75a	6/28/05 16:23	6/28/05 16:28	7/14/06 2:08	7/14/06 2:13
m24a	m24/w69b	6/28/05 16:39	6/28/05 16:45	7/14/06 2:24	7/14/06 2:30

Table E.7. Time correction for Manta files of fourth boat deployment

Fourth boat deployment		Amphibian date/time		Corrected date/time (CDT)	
waypoint file	logbook waypoint	profile start	profile end	actual start	actual end
m24c	m24/w69c	6/29/05 5:31	6/29/05 5:39	7/14/06 15:16	7/14/06 15:24
m23c	m23/w68c	6/29/05 5:56	6/29/05 6:05	7/14/06 15:41	7/14/06 15:50
m22c	m22/w66c	6/29/05 6:19	6/29/05 6:32	7/14/06 16:04	7/14/06 16:17
m19c	m19/w65c	6/29/05 6:42	6/29/05 6:53	7/14/06 16:27	7/14/06 16:38
m20c	m20c	6/29/05 7:07	6/29/05 7:13	7/14/06 16:52	7/14/06 16:58
w70c	w70c	6/29/05 7:26	6/29/05 7:33	7/14/06 17:11	7/14/06 17:18

Table E.8. Time correction for Manta files of fifth boat deployment

Fifth boat deployment		Amphibian date/time		Corrected date/time (CDT)	
waypoint file	logbook waypoint	profile start	profile end	actual start	actual end
m24d	m24d	6/29/2005 14:59	6/29/05 15:08	7/15/06 0:44	7/15/06 0:53
m23d	m23d	6/29/2005 15:21	6/29/05 15:30	7/15/06 1:06	7/15/06 1:15
m22d	m22d	6/29/2005 15:42	6/29/05 15:55	7/15/06 1:27	7/15/06 1:40
m19d	m19d	6/29/2005 16:24	6/29/05 16:37	7/15/06 2:09	7/15/06 2:22
w70d	w70d	6/29/2005 17:04	6/29/05 17:17	7/15/06 2:49	7/15/06 3:02
m20d	m20d	6/29/2005 17:34	6/29/05 17:46	7/15/06 3:19	7/15/06 3:31
m17d	m17d	6/29/05 18:09	6/29/05 18:15	7/15/06 3:54	7/15/06 4:00
w73d	w73d	6/29/05 18:27	6/29/05 18:35	7/15/06 4:12	7/15/06 4:20
m23e	m23e	6/29/05 18:58	6/29/05 19:17	7/15/06 4:43	7/15/06 5:02
m24e	m24e	6/29/05 19:36	6/29/05 19:53	7/15/06 5:21	7/15/06 5:38
m09e	m09e	6/29/05 20:03	6/29/05 20:12	7/15/06 5:48	7/15/06 5:57
w76e	w76e	6/29/05 20:25	6/29/05 20:35	7/15/06 6:10	7/15/06 6:20
m26e	m26e	6/29/05 20:45	6/29/05 20:53	7/15/06 6:30	7/15/06 6:38
m10e	m10e	6/29/05 21:04	6/29/05 21:11	7/15/06 6:49	7/15/06 6:56
w77e	w77e	6/29/05 21:25	6/29/05 21:33	7/15/06 7:10	7/15/06 7:18

Table E.9. Time correction for Manta files of sixth boat deployment

Sixth boat deployment		Amphibian date/time		Corrected date/time (CDT)	
waypoint file	logbook waypoint	profile start	profile end	actual start	actual end
m24f	m24f	6/30/05 4:58	6/29/05 5:08	7/15/06 14:43	7/14/06 14:53
m23f	m23f	6/30/05 5:26	6/29/05 5:36	7/15/06 15:11	7/14/06 15:21
m22f	m22f	6/30/05 5:47	6/30/05 5:49	7/15/06 15:32	7/15/06 15:34

Table E.10. Time correction for Manta files of seventh boat deployment

Seventh boat deployment					
waypoint file	logbook waypoint	Amphibian date/time		Corrected date/time (CDT)	
		profile start	profile end	actual start	actual end
m24g	m24g	6/30/05 13:49	6/30/05 14:05	7/15/06 23:34	7/15/06 23:50
m23g	m23g	6/30/05 14:20	6/30/05 14:37	7/16/06 0:05	7/16/06 0:22
m22g	m22g	6/30/05 14:54	6/30/05 15:15	7/16/06 0:39	7/16/06 1:00
m19g	m19g	6/30/05 15:36	6/30/05 15:57	7/16/06 1:21	7/16/06 1:42
w70g	w70g	6/30/05 16:12	6/30/05 16:33	7/16/06 1:57	7/16/06 2:18
m20g	m20g	6/30/05 16:58	6/30/05 17:14	7/16/06 2:43	7/16/06 2:59
w73g	w73g	6/30/05 17:32	6/30/05 17:48	7/16/06 3:17	7/16/06 3:33
m17g	m17g	6/30/05 18:15	6/30/05 18:29	7/16/06 4:00	7/16/06 4:14
m18g	m18g	6/30/05 18:42	6/30/05 18:57	7/16/06 4:27	7/16/06 4:42
m16g	m16g	6/30/05 19:23	6/30/05 19:33	7/16/06 5:08	7/16/06 5:18
w78g	w78g	6/30/05 19:49	6/30/05 20:01	7/16/06 5:34	7/16/06 5:46
w79g	w79g	6/30/05 20:15	6/30/05 20:26	7/16/06 6:00	7/16/06 6:11
m23h	m23h	6/30/05 21:07	6/30/05 21:20	7/16/06 6:52	7/16/06 7:05
w76h	w76h	6/30/05 21:33	6/30/05 21:39	7/16/06 7:18	7/16/06 7:24
w77h	w77h	6/30/05 21:47	6/30/05 21:53	7/16/06 7:32	7/16/06 7:38
m24h	m24h	6/30/05 21:59	6/30/05 22:07	7/16/06 7:44	7/16/06 7:52
m09h	m09h	6/30/05 22:15	6/30/05 22:23	7/16/06 8:00	7/16/06 8:08

Table E.11. Time correction for Manta files of eighth boat deployment

Eighth boat deployment					
waypoint file	original waypoint file	Amphibian date/time		Corrected date/time (CDT)	
		profile start	profile end	actual start	actual end
m24i	m24i	7/1/05 4:40	7/1/05 4:46	7/16/06 14:25	7/16/06 14:31
m23i	m23i	7/1/05 4:55	7/1/05 5:02	7/16/06 14:40	7/16/06 14:47
m22i	m22i	7/1/05 5:11	7/1/05 5:23	7/16/06 14:56	7/16/06 15:08
m19i	m19i	7/1/05 5:30	7/1/05 5:47	7/16/06 15:15	7/16/06 15:32
m20i	m20i	7/1/05 5:57	7/1/05 6:15	7/16/06 15:42	7/16/06 16:00
m17i	m17i	7/1/05 6:22	7/1/05 6:40	7/16/06 16:07	7/16/06 16:25
m18i	m18i	7/1/05 6:46	7/1/05 7:03	7/16/06 16:31	7/16/06 16:48
w78i	w78i	7/1/05 7:10	7/1/05 7:27	7/16/06 16:55	7/16/06 17:12
m16i	m16i	7/1/05 7:34	7/1/05 8:05	7/16/06 17:19	7/16/06 17:50
m24j	m24j	7/1/05 8:12	7/1/05 8:20	7/16/06 17:57	7/16/06 18:05

Table E.12. Headers and interpretation of sonar *.csv file

header	data
UpperLimit	Upper depth limit of the transducer in use
LowerLimit	Lower depth limit of the transducer in use
DepthValid	T/F as to whether the depth measurement in the succeeding column is considered valid by the instrument
Depth	Water depth in feet
WaterTempValid	T/F as to whether the water temperature measurement in the succeeding column is considered valid by the instrument
WaterTemp	Water temperature in C
Temp2Valid	n/a
Temp2	n/a
Temp3Valid	n/a
Temp3	n/a
WaterSpeedValid	T/F as to whether the speed measurement in the succeeding column is considered valid by the instrument
WaterSpeed	Speed through the water from the paddlewheel speed sensor.
PositionValid	T/F as to whether x,y position in the succeeding columns are considered valid by the instrument
PositionX	Mercator meter X position
PositionY	Mercator meter Y position
SurfaceDepth	T/F as to whether surface depth in the succeeding column is considered valid by the instrument. Note that this header should logically be switched with the header of the next column.
SurfaceValid	It isn't clear what this means in the Lowrance literature, but it appears to be the depth of the surface noise signature. This header should logically be switched with the header of the prior column.
TopOfBottomDepth	T/F as to whether "Top of Bottom" depth in the succeeding column is considered valid by the instrument. Note that this header should logically be switched with the header of the next column.
TopOfBottomValid	It isn't clear what this means in the Lowrance literature. This header should logically be switched with the header of the prior column.
ColumnIs50kHz	T/F whether the 50 kHz (deep sonar) is used instead of the 200 kHz
TimeValid	T/F whether the time offset in the succeeding column is considered valid by the instrument.
TimeOffset	Time (in milliseconds) from start of the log.
SpeedTrackValid	T/F as to whether the speed and track in the succeeding two columns are considered valid by the instrument.
Speed	Speed in mph based on GPS data
Track	It isn't clear what this means in the Lowrance literature.
AltitudeValid	T/F as to whether the altitude measurement in the succeeding column is considered valid by the instrument
Altitude	Altitude above sea level as determined by GPS

Table E.13. Sonar file start time

Sonar File	Recorded Date/Time	Adjusted CDT Date/Time
Chart 7_11_06 [0]	7/11/06 5:04	7/11/06 7:04
Chart [0]	no valid time	
Chart 7_12_06 [1]	7/12/06 3:51	7/12/06 5:51
Chart 7_12_06 [2]	7/12/06 3:58	7/12/06 5:58
Chart 7_12_06 [3]	7/12/06 12:02	7/12/06 14:02
Chart 7_13_06 [0]	7/13/06 16:47	7/13/06 18:47
Chart 7_13_06 [1]	7/13/06 17:39	7/13/06 19:39
Chart 7_14_06 [0]	7/14/06 12:28	7/14/06 14:28
Chart 7_14_06 [1]	7/14/06 21:40	7/14/06 23:40
Chart 7_15_06 [0]	7/15/06 0:36	7/15/06 2:36
Chart 7_15_06 [1]	7/15/06 12:09	7/15/06 14:09
Chart 7_15_06 [2]	7/15/06 21:53	7/15/06 23:53
Chart 7_16_06 [0]	7/16/06 13:35	7/16/06 15:35
Adjustment	2 hours	

E.8 Chronology from logbook

E.8.a Notes and conventions

All GPS positions given below are recorded in the field logbook from the Lowrance LMS 339CDF IGPS sonar/GPS unit at the start of profiling. All W## waypoints are new waypoints, all M## are prior UT-MSI waypoints. In some cases, waypoints were (unfortunately) double named with both W## and M## designations. In such cases, the cleaned files use the UTMSI waypoint designations only. The chronology below gives both.

E.8.b Errors and corrections

The m09/w70a profile on 07/13/06 was mislabeled. This was an m09 profile and does not correspond to the later w70 positions.

The w73a profile position on 07/13/06 does not correspond to the later w73 profiles, so this has been relabeled the w80 profile.

E.8.c Translation from logbook

7/10/2006 - Travel from Austin to Corpus Christi Bay.

7/11/2006: 0745 - 1100 hours CDT. First boat deployment (bathymetry survey).

Launched into ICW in CRWR 14 foot boat. Winds strong with choppy seas and white caps. Conditions were unsafe for anchoring to deploy Manta or SCAMP. Conducted bathymetry survey using Lowrance LMS 339CDF IGFS depth sonar/GPS from Shamrock Island along the Corpus Christi Bay side of Mustang Island. Operated in sheltered waters with 1.5 to 3 feet depth. Depth sounder typically blanked at 1.4 feet. Grounded in soft sediment on multiple occasions. Boat speed (by GPS) during sampling around 5 mph.

7/12/2006: 0530 - 1630 hours. Second boat deployment (bathymetry survey)

Launched as above. Winds medium strength, choppy conditions away from coast, but fairly calm close in. Conducted more detailed bathymetry survey along Mustang Island to get a better picture of the multiple channel/bar configuration. Lost satellite fix several times so the sonar log is split into pieces when the unit was rebooted. Using shallow draft engine setting and slow speed, able to get soundings in 1.3 feet and 1.2 feet of water. Typically ran at speeds of 4 to 6 mph. Tried to maintain data collection speed below 5 mph.

7/13/2006: 0900 - 1600 hours. Analyzed bathymetry data to better understand the channel/bar geomorphology along the Mustang Island coast. Determined that an outer bathymetry trail was necessary for better data. Developed a plan for transects perpendicular to the coast.

7/13/2006: 1845 hours - 7/14/2006: 0330 hours. Third boat deployment (night 1 Manta profiles)

7/13/2006: 1845 - 1930 hours. Winds and sea are manageable for boat. Conducted a bathymetry track (Trail 5 on GPS) as an outer perimeter from marker near M45. Survey speed approximately 9 mph.

7/13/2006: 1930 - 2030 hours. Setting up equipment for profiling transect out to M19. Calibrating DO on Manta using laptop computer at W60 (27d 42.882' N 97d 10.433' W, depth 2.0 feet). Barometric pressure 764.59 mmHg from Manta. DO levels at W60 were ~ 110%, so the instrument was recalibrated, which resulted in no significant change. The sun was still up at this time and the water appeared very green, so it may be presumed that there was significant photosynthesis at this time.

7/13/2006: 2030 - 2110 hours. Using Manta/laptop at waypoint W61 (27d 42.917' N; 97d 10.474' W; depth 2.6 feet). Laptop failed so switched to Amphibian for profile W61a, completed at 2109 hours. DO appeared low, so recalibrated.

7/13/2006: 2110 - 2130 hours. Due to laptop failure, returned to re-profile W60a (27d 42.883' N; 97d 10.429' W; depth 2.0 feet), completed at 2130 hours.

7/13/2006: 2130 - 2300 hours. Profiling at successive locations towards M19:

W62a (27d 42.932' N; 97d 10.454' W; depth 5.6 feet) completed 2141 hours.

W63a (27d 43.024' N; 97d 10.679' W; depth 11.1 feet) completed 2205 hours.

W64a (27d 42.981' N; 97d 10.627' W; depth 6.3 feet) completed 2224 hours.

M19a/W65a (27d 43.392' N; 97d 11.328' W; depth 12.9 feet) completed 2247 hours.

Note that W64a is a shallower depth (closer to shore) and was conducted after the planned point W63a to check whether the hypoxia seen in W63a would also be seen closer to shore.

7/13/2006: 2300 hours. Based on results of transect from W60a through M19a, it appeared that hypoxia was strong out away from shore. The sampling plan was changed to try to document the extent of the hypoxia. Subsequent profiles were based on the main UT MSI points M22, M23, M24.

7/13/2006: 2300 hours - 7/14/2006: 0005 hours. Profiling in SSW direction starting at M22

M22a/W66a/W67a (27d 42.948' N; 97d 11.555' W; depth 12.7 feet) completed 2312 hours. Observed on GPS that anchor appeared to drag from initial position (W66) to final position (W67).

M23a/W68a (27d 42.282' N; 97d 11.915' W; depth 11.3 feet) completed 2340 hours.

M24a/W69a (27d 41.735' N; 97d 12.173' W; depth 9.1 feet) completed 0005 hours of 7/14/2006.

M09a (27d 41.735 N; 97 12.178' W; depth 8.9 feet), completed 0030 hours (note correction, this is not a w70 waypoint).

7/14/2006: 0030 - 0215 Profiling shallower water (5 to 7 feet) near Laguna Madre to look for possible underflow of dense water.

W71a (27d 41.424' N; 97d 12.703' W; depth 7.3 feet) completed 0055 hours.
W72a (27d 41.353' N; 97d 12.745' W; depth 4.8 feet) completed 0116 hours.
W73a (27d 41.365' N; 97d 12.575' W; depth 5.3 feet) completed 0135 hours.
W74a (27d 41.516' N; 97d 12.043' W; depth 5.3 feet) completed 0155 hours.
W75a (27d 41.576' N; 97d 12.077' W; depth 6.9 feet) completed 0213 hours.

7/14/2006: 0215 - 0230. Profiling at M24 to provide a more detailed temporal data set at one location. M24b/W69b (27d 41.750' N; 97d 12.170' W; depth 8.9 feet) completed at 0230.

7/14/2006: 0230 - 0330. Return home. Did not recalibrate Manta DO (too tired).

7/14/2006: 1430 - 1845 hours. Fourth boat deployment (afternoon 1 Manta profiles)

7/14/2006: 1500 - 1525 hours. M24c/W69c (27d 41.748' N; 97d 12.178' W, depth 9.4 feet). Calibrating Manta DO and profiling. Barometric pressure initially set (incorrectly) at 764 mmHg, for which calibration was -5.01% DO. Pressed the menu button that I thought would not accept the calibration, but later realized that it did accept the calibration but simply did not log it in the file. Checked barometric pressure using Manta; correct value of 760.2 mmHg used to recalibrate DO. Result was -1.19% DO. Result is that the instrument was reset to a total of -6.21% DO from nighttime. However, based on later observations, it is not clear that this calibration is as precise as night-time calibration. At this point, I did not understand the importance of shading the instrument when calibrating on a sunny day (to ensure thermal equilibrium). Based on calibration in the evening that results in a +4.54% DO adjustment), the instrument is likely underestimating DO saturation by 5% to 6% during this set of deployments. Note that later calibrations did not show such great swings between day/night, so there is more confidence in the later data sets. Completed profiling M24c at 1524 hours.

7/14/2006: 1525 - 1640 hours. Profiling main transect up the bay to get same points done previous night.

M23c/W63c (27d 42.290' N; 97d 11.913' W; depth 11.5 feet) completed at 1550 hours. Noted in the log book that there was evidence of Langmuir circulations (photos were later taken) in windrows of foam and bubbles. All days thus far had seen evidence of such circulations.

M22c/W66c (27d 42.938' N; 97d 11.547' W; depth 13.0 feet) completed at 1617 hours.

M19c/W65c (27d 43.362' N; 97d 11.362' W; depth 13.0 feet) completed at 1638 hours.

7/14/2006: 1640 - 1720 hours. Additional profiling to find northward limit of stratification/hypoxia.

M20c (27d 44.094' N; 97d 11.196' W; depth 12.7 feet) completed 1658 hours. M20c showed no indication of stratification/hypoxia. Back-tracked to the south about half-way to M19c for next profile (M09c/W70c).

M09c/W70c (27d 43.840' N; 97d 11.214' W; depth 12.9 feet) completed 1718 hours. This profile appeared to be near the front of the stratified zone.

7/14/2006: 1720 - 1845. Returned home. Did not calibrate Manta DO (too tired).

7/15/2006: 0000 - 0845 hours. Fifth boat deployment (night 2 Manta profiles)

7/14/2006: 2330 hours. Launched boat as above.

7/15/2006: 0015 - 0055 hours. M24d (27d 41.741' N; 97d 12.171' W; depth 9.3 feet). Calibrating DO. Atmospheric pressure 760.087. Calibration +4.54%. This large swing is evidence that the prior daytime calibration was off due to solar heating. Seas are somewhat calmer than previous day/night. Still see evidence of Langmuir circulations. Developed a short in the boat running lights and improvised using a flashlight for required white all-around light. Finished profile at 0053 hours.

7/15/2006: 0055 - 0331 hours. Profiling northward along the main transect of previously sampled points.

M23d (27d 42.289' N; 97d 11.910' W; depth 11.3 feet) completed at 0115 hours.

M22d (27d 42.907' N; 97d 11.571' W; depth 12.7 feet) completed at 0140 hours.

M19d (27d 43.400' N; 97d 11.364' W; depth 12.7 feet) completed at 0222 hours.

M09d/W70d (27d 43.827' N; 97d 11.215' W; depth 12.3 feet) completed at 0302 hours.

Noted that wind speed and waves were significantly lower, but still signs of Langmuir circulations

M20d (27d 44.083' N; 97d 11.190' W; depth 12.0 feet) completed at 0331 hours.

7/15/2006: 0331 - 0420 hours. Profiling further northward to find limit of stratification/hypoxia.

M17d (27d 44.567' N; 97.11.088' W; depth 12.0 feet) completed 0400 hours. No significant stratification. Backtracking to south and chose a site (W73) that is about half way between M17 and M20.

W73d (27d 44.375' N; 97 11.170' W; depth 12.1 feet) completed 0420. Hypoxia strong at bottom.

7/15/2006: 0420 - 0720 hours. Returning to south to re-do points M23/M24 for improved temporal data set and to look for stratification along the south western coast of Mustang Island at approximately 9 feet of depth.

M23e (27d 42.280' N; 97d 11.924' W; depth 11.1 feet) completed at 0502 hours.

M24e (27d 41.743' N; 97d 12.163' W; depth 9.1 feet) completed at 0538 hours.

M09e (27d 41.586' N; 97d 12.664' W; depth 8.7 feet) completed 0557 hours.

W76e (27d 41.794' N; 97d 11.587' W; depth 9.1 feet) completed 0620 hours. New point inside of M23 at 9 foot depth.

M26e (27d 42.219' N; 97d 11.138' W; depth 9.8 feet) completed 0638 hours. No wind, calm seas.

M10e (27d 42.797' N; 97d 10.804' W; depth 10.8 feet) completed 0656 hours.

W77e (27d 41.740° N; 97d 11.930° W; depth 9.1 feet) completed 0718 hours. Note this point is between M24 and W76 such that M09/M24/W77/W76/M26/M10 form a transect along the southwestern coast of Mustang Island.

7/15/2006: 0720 - 0730 hours. Calibrating DO. Barometric pressure 764.715 mmHg. Calibration of -2.66% DO sat.

7/15/2006: 0845 hours. Returned home.

7/15/2006: 1345 - 1600 hours. Sixth boat deployment (day 2 Manta profiles)

7/15/2006: 1345 - 1440 hours. Launch as above and transit to M24. Calmer weather. Less choppy seas. Still signs of Langmuir circulations. Calibrating DO. Barometric pressure 766.146 mmHg. Calibration +1.24% DO sat. Put up bimini top on boat. Combination of extra sail area and longer wavelength swells cause greater horsing of boat. Doesn't keep station well on position (moves around anchor in an arc of about 20 degrees), making it useless to record a GPS position from the Lowrance sonar/GPS unit. Put out all the anchor line (~ 100 feet).

7/15/2006: 1440 - 1540 hours. Profiling

M24f (depth 9.2 feet), completed at 1453 hours.

M23f (depth 11.6 feet), completed at 1521 hours.

M22f (depth 12.9 feet), Amphibian failure (insufficient battery charge) at 1534. Profile not complete. Did not bring inverter and power supply along.

7/15/2006: 1600 hours. Returned home.

7/15/2006: 2230 hours - 7/16/2006: 0900 hours. Seventh boat deployment (night 3 Manta profiles)

7/15/2006: 2230 - 2330 hours. Launched as above and transit to M24. Calibrating DO. Atmospheric pressure 766.095 mmHg. Adjustment -0.12% DO sat. Noted that Amphibian date/time was June 30, 2005, 1343 hours for local day/time 7/15/2006 at 2329 hours. Winds light, calm seas. Still signs of Langmuir circulations.

7/15/2006: 2330 - 7/15/2006: 0615 hours. Profiling main transect from south to north.

M24g (27d 41.747° N; 97d 12.172° W; depth 9.4 feet), completed at 2350 hours on 7/15/2006. Some horsing at anchor with more significant vertical motions than on other days. It looked like this might show up some artificial salinity/DO inversions. Only about 1/3 anchor line is out (~30 feet) on small (10 lb.) anchor.

M23g (27d 42.293° N; 97d 11.939° W; depth 11.5 feet), completed at 0022 hours on 7/16/2006. Still horsing significantly. Put more anchor line out (~60 feet).

M22g (27d 42.944° N; 97d 11.541° W; depth 12.8 feet), completed at 0100 hours. All anchor line out (~100 feet) on small anchor. Boat still has significant horsing.

M19g (27d 43.381' N; 97d 11.326' W; depth 12.8 feet), completed at 0142 hours.

M09g/W70g (27d 43.841' N; 97d 11.217' W; depth 12.6 feet), completed at 0218 hours.

M20g (27d 44.085' N; 97d 11.183' W; depth 12.5 feet), completed at 0259 hours.

W73g (27d 44.370' N; 97d 11.171' W; depth 12.2 feet), completed at 0333 hours.

M17g (27d 44.562' N; 97d 11.086' W; depth 12.4 feet), completed at 0414 hours. Anchor dragging and had to reset from first deployment. Did not document in log book, but I believe (a posteriori) that this is when I created an anchor pennant to lead the anchor through the bow tie down. This approach seemed to reduce the horsing somewhat.

M18g (27d 44.838' N; 97d 10.857' W; depth 11.6 feet), completed at 0442 hours. Noted in log book that horsing of boat was worse than other nights as long swells move the boat more than short chop. On the Manta depth gage, excursions seemed about 3-5 cm with about 10 cm as the largest excursions.

M16g (27d 45.706' N; 97d 10.827' W; depth 10.2 feet), completed at 0518 hours. No hypoxia evident at this site, so backtracked to new site W78

W78g (27d 45.414' N; 97d 10.835' W; depth 10.1 feet), completed at 0546 hours. Note that this site was chosen based on doing quick (undocumented) profiling to look for hypoxia. This position appeared to be the furthest north intrusion of significant stratification.

W79g (27d 45.147' N; 97d 10.835' W; depth 11.5 feet), completed at 0611 hours. Slightly south of W78 and shows stronger salinity gradient.

7/16/2006: 0615 - 0810 hours. Returning to profile in south of bay

M23h (27d 42.291' N; 97d 11.922' W; depth 11.3 feet), completed at 0705 hours. Winds dropped. Very calm. No horsing of boat.

W76h (27d 41.796' N; 97d 11.596' W; depth 9.2 feet), completed at 0724 hours. Noted lots of sea grasses floating near surface.

W77h (27d 41.745' N; 97d 11.946' W; depth 9.2 feet), completed at 0738 hours.

M24h (27d 41.731' N; 97d 12.169' W; depth 9.1 feet), completed at 0752 hours.

M09h (27d 41.585' N; 97d 12.676' W; depth 8.9 feet), completed at 0808 hours.

7/16/2006: 0810 - 0900 hours. Calibrating DO. Barometric pressure 766.937 mmHg. Calibration -0.88% DO saturation. Returning home.

7/16/2006: 1315 - 1900 hours. Eighth boat deployment (day 3 Manta profiles)

7/16/2006: 1315 - 1420 hours. Launched as above and transit to M24. DO calibration. Barometric pressure 765.3 mmHg. DO calibration -0.44% DO saturation. Calibration conducted with bimini top (shade) up on boat.

7/16/2006: 1420 - 1805 hours. Profiling along main northward track

M24i (27d 41.726' N; 97d 12.160' W; depth 9.2 feet), completed at 1431 hours.

M23i (27d 42.285' N; 97d 11.908' W; depth 11.3 feet), completed at 1447 hours.

M22i (27d 42.937' N; 97d 11.556' W; depth 12.7 feet), completed at 1508 hours.

M19i (27d 43.408' N; 97d 11.383' W; depth 12.7 feet), completed at 1532 hours.
M20i (27d 44.089' N; 97d 11.186' W; depth 12.4 feet), completed at 1600 hours.
M17i (27d 44.583' N; 97d 11.084' W; depth 12.5 feet), completed at 1625 hours.
M18i (27d 44.858' N; 97d 10.869' W; depth 11.7 feet), completed at 1648 hours.
W78i (27d 45.420' N; 97d 10.830' W; depth 10.1 feet), completed at 1712 hours.
M16i (27d 45.726' N; 97d 10.858' W; depth 10.2 feet), completed at 1750 hours.
M24j (27d 41.729' N; 97d 12.180' W; depth 9.1 feet), completed at 1805 hours.

7/16/2006: 1805 - 1830 hours. Calibrating DO and equipment clean up while at site M24j. Barometric pressure 762.89 mmHg. Calibration DO +0.62% DO saturation. Calibration was attempted with bimini top (shade) down, but the direct sun on the instrument caused the temperature to keep slowly rising and the Manta DO saturation would not stabilize. Draped a towel loosely over the Manta to keep the direct sun rays out and the stabilization improved.

7/16/2006: 1830 - 1900 hours. Returned home.

7/17/2006: Morning - cleaned boat and equipment prior to travel.

7/17/2006: Afternoon - returned to Austin.

E.9 Data from all Manta profiles

The following data is from the file CCBay_profile_table.xls, which was formed by concatenating the Manta profile files (*.loc files) using the Eureka software. The raw data are found in the file CCBay_profiles_2006_07_1316_all.csv. The date/time stamp in the following tables has been adjusted to account for the time offset in the Amphibian software. Column headings are self-explanatory except for "Circulator," which is the binary (1 = on, 0 = off) identifier for the state of the Manta circulator that ensures adequate flow across the DO sensor membrane.

Profile	Depth m	Date Time	Temperature °C	Salinity PSS	DO Saturation %	Dissolved Oxygen mg/L	Circulator
m09a	0.03	7/14/06 12:21 AM	27.77	40.5	85.04	5.35	1
m09a	0.15	7/14/06 12:22 AM	29.68	39.9	85.14	5.22	1
m09a	0.57	7/14/06 12:22 AM	29.69	39.9	86.60	5.30	1
m09a	0.91	7/14/06 12:23 AM	29.69	40.0	86.65	5.31	1
m09a	1.17	7/14/06 12:23 AM	29.72	40.0	86.51	5.29	1
m09a	1.51	7/14/06 12:23 AM	29.66	40.8	84.35	5.14	1
m09a	1.82	7/14/06 12:24 AM	29.67	41.1	81.57	4.96	1
m09a	2.04	7/14/06 12:25 AM	29.72	41.4	77.61	4.71	1
m09a	2.08	7/14/06 12:25 AM	29.67	42.3	70.33	4.25	1
m09a	2.30	7/14/06 12:26 AM	29.63	42.9	61.30	3.69	1
m09a	2.30	7/14/06 12:26 AM	29.60	43.4	60.05	3.61	1
m09a	2.36	7/14/06 12:27 AM	29.55	43.8	50.51	3.03	1
m09a	2.62	7/14/06 12:28 AM	29.52	44.0	40.74	2.44	1
m09a	2.69	7/14/06 12:29 AM	29.53	44.0	38.72	2.32	1
m09a	2.80	7/14/06 12:29 AM	29.49	44.2	30.99	1.86	1
m09a	2.93	7/14/06 12:30 AM	29.48	44.1	29.24	1.75	1
m09a	2.85	7/14/06 12:30 AM	29.49	44.1	28.79	1.72	1
m09e	0.14	7/15/06 5:48 AM	29.37	39.5	77.17	4.73	1
m09e	0.11	7/15/06 5:48 AM	29.39	39.5	76.95	4.72	1
m09e	0.59	7/15/06 5:48 AM	29.39	39.5	76.46	4.68	1
m09e	0.88	7/15/06 5:48 AM	29.39	39.5	76.21	4.67	1
m09e	1.07	7/15/06 5:49 AM	29.46	40.0	72.82	4.45	1
m09e	1.19	7/15/06 5:50 AM	29.59	40.7	67.53	4.10	1
m09e	1.36	7/15/06 5:50 AM	29.67	41.2	59.79	3.61	1
m09e	1.50	7/15/06 5:51 AM	29.46	41.4	55.55	3.36	1
m09e	1.62	7/15/06 5:52 AM	29.26	41.6	51.68	3.14	1
m09e	1.79	7/15/06 5:52 AM	29.29	41.8	50.16	3.04	1
m09e	1.96	7/15/06 5:53 AM	29.27	42.0	49.47	2.99	1
m09e	2.11	7/15/06 5:53 AM	29.29	42.0	48.27	2.92	1
m09e	2.25	7/15/06 5:54 AM	29.32	42.1	46.97	2.84	1
m09e	2.40	7/15/06 5:54 AM	29.41	42.3	41.80	2.52	1
m09e	2.57	7/15/06 5:55 AM	29.46	42.4	38.81	2.34	1
m09e	2.74	7/15/06 5:56 AM	29.54	42.5	33.48	2.01	1
m09e	2.76	7/15/06 5:56 AM	29.56	42.6	31.14	1.87	1
m09e	2.89	7/15/06 5:57 AM	29.59	42.7	25.32	1.52	1
m09h	0.14	7/16/06 7:59 AM	29.51	39.8	76.85	4.73	1
m09h	0.12	7/16/06 7:59 AM	29.51	39.8	77.02	4.74	1
m09h	0.60	7/16/06 8:00 AM	29.53	39.8	76.13	4.69	1
m09h	0.93	7/16/06 8:00 AM	29.54	39.9	75.88	4.67	1
m09h	1.21	7/16/06 8:00 AM	29.59	39.9	74.83	4.60	1
m09h	1.37	7/16/06 8:01 AM	29.64	40.0	71.49	4.39	1
m09h	1.51	7/16/06 8:01 AM	29.67	40.1	69.69	4.27	1
m09h	1.68	7/16/06 8:02 AM	29.71	40.2	67.81	4.15	1
m09h	1.80	7/16/06 8:02 AM	29.79	40.4	65.76	4.02	1
m09h	2.00	7/16/06 8:03 AM	29.72	40.6	64.78	3.96	1
m09h	2.14	7/16/06 8:03 AM	29.68	40.6	64.66	3.95	1
m09h	2.28	7/16/06 8:04 AM	29.66	40.7	62.76	3.83	1
m09h	2.46	7/16/06 8:05 AM	29.71	41.2	49.79	3.03	1
m09h	2.56	7/16/06 8:05 AM	29.74	41.3	48.31	2.94	1
m09h	2.72	7/16/06 8:06 AM	29.76	41.4	43.07	2.62	1
m09h	2.89	7/16/06 8:07 AM	29.76	41.5	36.62	2.22	1

Profile	Depth m	Date Time	Temperature °C	Salinity PSS	DO Saturation %	Dissolved Oxygen mg/L	Circulator
m09h	2.98	7/16/06 8:07 AM	29.75	41.7	30.09	1.82	1
m10e	0.09	7/15/06 6:49 AM	29.50	38.5	75.81	4.66	1
m10e	0.15	7/15/06 6:49 AM	29.50	38.4	75.41	4.64	1
m10e	0.58	7/15/06 6:49 AM	29.52	38.5	74.53	4.58	1
m10e	0.86	7/15/06 6:49 AM	29.54	38.5	74.25	4.56	1
m10e	1.19	7/15/06 6:49 AM	29.54	38.5	74.23	4.56	1
m10e	1.47	7/15/06 6:50 AM	29.58	38.7	71.90	4.41	1
m10e	1.79	7/15/06 6:50 AM	29.57	39.0	70.85	4.34	1
m10e	2.08	7/15/06 6:50 AM	29.52	39.5	68.42	4.18	1
m10e	2.26	7/15/06 6:51 AM	29.42	39.9	61.84	3.78	1
m10e	2.46	7/15/06 6:52 AM	29.49	40.4	49.34	3.00	1
m10e	2.56	7/15/06 6:53 AM	29.53	41.9	22.98	1.38	1
m10e	2.72	7/15/06 6:53 AM	29.56	42.8	12.71	0.76	1
m10e	2.85	7/15/06 6:54 AM	29.56	43.1	12.21	0.73	1
m10e	3.01	7/15/06 6:54 AM	29.55	43.3	10.40	0.62	1
m10e	3.15	7/15/06 6:55 AM	29.52	43.3	7.48	0.44	1
m10e	3.32	7/15/06 6:55 AM	29.43	43.4	4.13	0.24	1
m10e	3.49	7/15/06 6:56 AM	29.40	43.4	2.94	0.17	1
m10e	3.58	7/15/06 6:56 AM	29.39	43.4	2.58	0.15	1
m16g	0.16	7/16/06 5:07 AM	30.11	38.1	75.74	4.66	1
m16g	0.12	7/16/06 5:07 AM	30.11	38.1	75.70	4.66	1
m16g	0.64	7/16/06 5:08 AM	30.12	38.1	75.53	4.65	1
m16g	0.58	7/16/06 5:08 AM	30.12	38.1	74.96	4.61	1
m16g	0.89	7/16/06 5:08 AM	30.12	38.1	73.97	4.55	1
m16g	1.19	7/16/06 5:08 AM	30.12	38.1	74.74	4.60	1
m16g	1.51	7/16/06 5:09 AM	30.12	38.1	73.97	4.55	1
m16g	1.46	7/16/06 5:09 AM	30.12	38.1	73.78	4.54	1
m16g	1.79	7/16/06 5:09 AM	30.13	38.1	74.54	4.59	1
m16g	2.14	7/16/06 5:10 AM	30.15	38.2	73.15	4.50	1
m16g	2.39	7/16/06 5:11 AM	30.17	38.2	71.63	4.40	1
m16g	2.70	7/16/06 5:11 AM	30.23	38.3	68.26	4.19	1
m16g	2.85	7/16/06 5:12 AM	30.25	38.3	65.37	4.01	1
m16g	2.84	7/16/06 5:12 AM	30.26	38.3	65.52	4.02	1
m16g	2.98	7/16/06 5:13 AM	30.29	38.4	62.23	3.81	1
m16g	3.15	7/16/06 5:14 AM	30.30	38.7	47.44	2.90	1
m16g	3.16	7/16/06 5:15 AM	30.29	38.9	34.51	2.11	1
m16g	3.25	7/16/06 5:16 AM	30.28	39.0	29.49	1.80	1
m16g	3.30	7/16/06 5:16 AM	30.26	39.1	20.43	1.24	1
m16g	3.40	7/16/06 5:17 AM	30.24	39.2	17.10	1.04	1
m16g	3.33	7/16/06 5:18 AM	30.25	39.2	20.09	1.22	1
m16i	0.19	7/16/06 5:19 PM	31.51	38.0	109.27	6.58	1
m16i	0.14	7/16/06 5:19 PM	31.52	38.0	109.38	6.58	1
m16i	0.57	7/16/06 5:19 PM	31.52	38.1	109.06	6.56	1
m16i	0.82	7/16/06 5:20 PM	31.53	38.1	109.13	6.56	1
m16i	1.15	7/16/06 5:20 PM	31.50	38.0	108.75	6.55	1
m16i	1.51	7/16/06 5:21 PM	31.47	38.1	106.44	6.41	1
m16i	1.79	7/16/06 5:22 PM	31.43	38.1	106.05	6.39	1
m16i	2.08	7/16/06 5:24 PM	31.09	38.2	99.63	6.03	1
m16i	2.11	7/16/06 5:25 PM	31.10	38.2	96.25	5.82	1

Profile	Depth m	Date Time	Temperature °C	Salinity PSS	DO Saturation %	Dissolved Oxygen mg/L	Circulator
m16i	2.19	7/16/06 5:25 PM	30.86	38.4	93.75	5.69	1
m16i	2.32	7/16/06 5:26 PM	30.85	38.4	83.18	5.05	1
m16i	2.34	7/16/06 5:26 PM	30.36	39.2	74.40	4.53	1
m16i	2.44	7/16/06 5:27 PM	30.34	39.4	72.85	4.43	1
m16i	2.53	7/16/06 5:27 PM	30.32	39.5	71.66	4.36	1
m16i	2.58	7/16/06 5:28 PM	30.30	39.5	69.84	4.25	1
m16i	2.65	7/16/06 5:28 PM	30.27	39.9	69.36	4.21	1
m16i	2.74	7/16/06 5:29 PM	30.16	40.5	56.38	3.42	1
m16i	2.78	7/16/06 5:30 PM	30.08	41.1	44.96	2.72	1
m16i	2.87	7/16/06 5:31 PM	30.01	41.3	35.49	2.14	1
m16i	3.00	7/16/06 5:31 PM	30.01	41.2	33.16	2.00	1
m16i	2.99	7/16/06 5:31 PM	30.04	41.2	36.56	2.21	1
m16i	3.08	7/16/06 5:32 PM	29.98	41.4	30.01	1.81	1
m16i	3.11	7/16/06 5:33 PM	29.97	41.4	29.02	1.75	1
m16i	3.17	7/16/06 5:33 PM	29.97	41.4	28.56	1.73	1
m16i	3.29	7/16/06 5:33 PM	29.96	41.4	27.77	1.68	1
m16i	3.32	7/16/06 5:34 PM	29.97	41.4	27.68	1.67	1
m16i	0.00	7/16/06 5:34 PM	30.31	0.0	83.51	6.31	1
m16i	0.01	7/16/06 5:49 PM	27.71	0.0	96.25	7.61	1
m17d	0.01	7/15/06 3:53 AM	27.64	40.4	82.13	5.15	1
m17d	0.13	7/15/06 3:54 AM	29.92	38.8	84.79	5.17	1
m17d	0.56	7/15/06 3:54 AM	29.94	38.8	85.39	5.21	1
m17d	0.90	7/15/06 3:54 AM	29.94	38.8	84.91	5.18	1
m17d	1.23	7/15/06 3:55 AM	29.94	38.8	85.14	5.19	1
m17d	1.48	7/15/06 3:55 AM	29.94	38.8	85.37	5.21	1
m17d	1.88	7/15/06 3:55 AM	29.94	38.8	85.99	5.24	1
m17d	2.03	7/15/06 3:56 AM	29.94	38.9	86.36	5.26	1
m17d	2.43	7/15/06 3:56 AM	29.95	39.0	87.20	5.31	1
m17d	2.67	7/15/06 3:56 AM	29.95	39.0	87.53	5.33	1
m17d	3.00	7/15/06 3:57 AM	29.94	39.0	87.88	5.35	1
m17d	3.25	7/15/06 3:57 AM	30.00	39.3	78.37	4.76	1
m17d	3.60	7/15/06 3:58 AM	30.01	39.3	75.25	4.57	1
m17d	3.92	7/15/06 3:58 AM	30.02	39.4	70.79	4.30	1
m17d	4.03	7/15/06 3:59 AM	29.97	40.7	46.36	2.79	1
m17d	3.86	7/15/06 4:00 AM	30.02	39.4	66.71	4.05	1
m17g	0.15	7/16/06 4:00 AM	30.25	38.5	76.77	4.70	1
m17g	0.11	7/16/06 4:00 AM	30.26	38.5	77.53	4.75	1
m17g	0.49	7/16/06 4:00 AM	30.25	38.6	77.10	4.72	1
m17g	0.84	7/16/06 4:01 AM	30.26	38.6	76.90	4.71	1
m17g	1.14	7/16/06 4:01 AM	30.26	38.6	77.10	4.72	1
m17g	1.49	7/16/06 4:01 AM	30.26	38.6	77.53	4.75	1
m17g	1.77	7/16/06 4:02 AM	30.26	38.6	77.25	4.73	1
m17g	2.06	7/16/06 4:02 AM	30.25	38.6	77.47	4.75	1
m17g	2.39	7/16/06 4:02 AM	30.24	38.6	77.79	4.77	1
m17g	2.58	7/16/06 4:03 AM	30.25	38.9	65.54	4.01	1
m17g	2.65	7/16/06 4:04 AM	30.24	39.0	60.77	3.71	1
m17g	2.80	7/16/06 4:04 AM	30.08	39.9	41.62	2.54	1
m17g	2.88	7/16/06 4:05 AM	30.06	40.0	38.16	2.32	1
m17g	2.88	7/16/06 4:06 AM	30.00	40.5	32.22	1.96	1

Profile	Depth m	Date Time	Temperature °C	Salinity PSS	DO Saturation %	Dissolved Oxygen mg/L	Circulator
m17g	3.03	7/16/06 4:06 AM	29.98	40.8	27.52	1.67	1
m17g	3.08	7/16/06 4:07 AM	29.95	41.3	25.13	1.52	1
m17g	3.18	7/16/06 4:07 AM	29.92	41.5	23.94	1.45	1
m17g	3.26	7/16/06 4:08 AM	29.86	42.0	22.15	1.34	1
m17g	3.29	7/16/06 4:08 AM	29.83	42.2	21.66	1.31	1
m17g	3.37	7/16/06 4:09 AM	29.78	42.5	19.98	1.20	1
m17g	3.50	7/16/06 4:09 AM	29.71	42.8	16.25	0.98	1
m17g	3.52	7/16/06 4:10 AM	29.66	43.0	12.69	0.76	1
m17g	3.61	7/16/06 4:10 AM	29.62	43.2	7.20	0.43	1
m17g	3.67	7/16/06 4:11 AM	29.57	43.3	2.55	0.15	1
m17g	3.78	7/16/06 4:12 AM	29.56	43.4	1.70	0.10	1
m17g	3.80	7/16/06 4:12 AM	29.55	43.4	1.26	0.07	1
m17g	3.90	7/16/06 4:12 AM	29.55	43.4	1.30	0.07	1
m17g	3.89	7/16/06 4:13 AM	29.55	43.4	1.10	0.06	1
m17g	3.98	7/16/06 4:13 AM	29.55	43.4	1.07	0.06	1
m17g	4.07	7/16/06 4:14 AM	29.55	43.3	0.96	0.05	1
m17g	3.98	7/16/06 4:14 AM	29.55	43.4	1.01	0.06	1
m17i	0.09	7/16/06 4:07 PM	31.53	38.3	97.40	5.85	1
m17i	0.11	7/16/06 4:07 PM	31.53	38.3	97.76	5.87	1
m17i	0.52	7/16/06 4:07 PM	31.52	38.3	98.76	5.93	1
m17i	0.84	7/16/06 4:08 PM	31.49	38.3	98.62	5.93	1
m17i	1.13	7/16/06 4:08 PM	31.46	38.3	99.22	5.96	1
m17i	1.49	7/16/06 4:08 PM	31.24	38.4	97.50	5.88	1
m17i	1.74	7/16/06 4:08 PM	31.01	38.5	94.16	5.69	1
m17i	1.90	7/16/06 4:09 PM	30.73	38.7	90.92	5.52	1
m17i	1.94	7/16/06 4:09 PM	30.61	38.8	88.31	5.37	1
m17i	2.01	7/16/06 4:10 PM	30.47	39.0	84.81	5.16	1
m17i	2.06	7/16/06 4:10 PM	30.39	39.1	82.78	5.04	1
m17i	2.17	7/16/06 4:11 PM	30.32	39.4	80.14	4.88	1
m17i	2.20	7/16/06 4:11 PM	30.31	39.5	80.17	4.88	1
m17i	2.36	7/16/06 4:11 PM	30.29	39.6	80.04	4.87	1
m17i	2.40	7/16/06 4:11 PM	30.26	39.8	80.21	4.87	1
m17i	2.42	7/16/06 4:12 PM	30.23	40.1	80.65	4.89	1
m17i	2.54	7/16/06 4:12 PM	30.20	40.4	80.53	4.88	1
m17i	2.57	7/16/06 4:12 PM	30.19	40.5	79.93	4.84	1
m17i	2.68	7/16/06 4:13 PM	30.16	40.6	78.80	4.77	1
m17i	2.73	7/16/06 4:13 PM	30.15	40.7	78.91	4.78	1
m17i	2.77	7/16/06 4:13 PM	30.15	40.7	78.32	4.74	1
m17i	2.86	7/16/06 4:13 PM	30.13	40.7	78.26	4.74	1
m17i	2.98	7/16/06 4:15 PM	29.99	41.6	58.21	3.52	1
m17i	3.07	7/16/06 4:15 PM	29.98	41.6	56.54	3.42	1
m17i	3.17	7/16/06 4:16 PM	29.95	41.7	53.19	3.21	1
m17i	3.22	7/16/06 4:17 PM	29.94	41.8	50.16	3.03	1
m17i	3.23	7/16/06 4:17 PM	29.93	41.9	49.39	2.98	1
m17i	3.37	7/16/06 4:18 PM	29.90	42.1	42.33	2.55	1
m17i	3.42	7/16/06 4:19 PM	29.89	42.1	36.09	2.18	1
m17i	3.54	7/16/06 4:19 PM	29.88	42.1	34.46	2.08	1
m17i	3.63	7/16/06 4:20 PM	29.83	42.5	26.09	1.57	1
m17i	3.66	7/16/06 4:21 PM	29.78	42.6	19.16	1.15	1

Profile	Depth m	Date Time	Temperature °C	Salinity PSS	DO Saturation %	Dissolved Oxygen mg/L	Circulator
m17i	3.68	7/16/06 4:22 PM	29.78	42.6	15.92	0.96	1
m17i	3.74	7/16/06 4:22 PM	29.78	42.6	15.85	0.95	1
m17i	3.76	7/16/06 4:22 PM	29.76	42.6	13.70	0.82	1
m17i	3.90	7/16/06 4:23 PM	29.73	42.7	10.54	0.63	1
m17i	3.96	7/16/06 4:24 PM	29.73	42.7	8.99	0.54	1
m17i	4.11	7/16/06 4:24 PM	29.72	42.4	5.58	0.33	1
m17i	4.10	7/16/06 4:25 PM	29.72	42.5	6.14	0.37	1
m18g	0.20	7/16/06 4:27 AM	30.19	38.5	71.92	4.41	1
m18g	0.16	7/16/06 4:27 AM	30.18	38.6	72.96	4.48	1
m18g	0.59	7/16/06 4:27 AM	30.20	38.5	73.63	4.52	1
m18g	0.94	7/16/06 4:27 AM	30.21	38.6	73.23	4.49	1
m18g	1.18	7/16/06 4:27 AM	30.22	38.5	72.84	4.46	1
m18g	1.50	7/16/06 4:28 AM	30.22	38.6	72.81	4.46	1
m18g	1.80	7/16/06 4:28 AM	30.24	38.6	72.80	4.46	1
m18g	2.10	7/16/06 4:28 AM	30.25	38.6	71.05	4.35	1
m18g	2.41	7/16/06 4:29 AM	30.26	38.6	70.42	4.31	1
m18g	2.51	7/16/06 4:30 AM	30.25	38.6	67.76	4.15	1
m18g	2.62	7/16/06 4:30 AM	30.25	38.7	67.88	4.16	1
m18g	2.76	7/16/06 4:31 AM	30.27	38.8	60.47	3.70	1
m18g	2.80	7/16/06 4:32 AM	30.26	39.1	52.52	3.21	1
m18g	2.83	7/16/06 4:32 AM	30.24	39.4	47.55	2.90	1
m18g	2.95	7/16/06 4:33 AM	30.16	40.0	35.62	2.17	1
m18g	3.09	7/16/06 4:34 AM	30.13	40.5	33.15	2.01	1
m18g	3.07	7/16/06 4:35 AM	30.12	40.6	33.03	2.00	1
m18g	3.14	7/16/06 4:35 AM	30.07	41.0	32.81	1.99	1
m18g	3.22	7/16/06 4:36 AM	30.01	41.4	28.79	1.74	1
m18g	3.30	7/16/06 4:37 AM	29.91	41.9	21.53	1.30	1
m18g	3.36	7/16/06 4:38 AM	29.83	42.2	16.58	1.00	1
m18g	3.45	7/16/06 4:38 AM	29.83	42.2	16.27	0.98	1
m18g	3.42	7/16/06 4:39 AM	29.79	42.4	13.21	0.79	1
m18g	3.52	7/16/06 4:39 AM	29.73	42.6	8.87	0.53	1
m18g	3.62	7/16/06 4:40 AM	29.67	42.8	5.50	0.33	1
m18g	3.70	7/16/06 4:41 AM	29.66	42.9	2.71	0.16	1
m18g	3.77	7/16/06 4:41 AM	29.66	42.9	2.51	0.15	1
m18g	3.85	7/16/06 4:42 AM	29.65	42.8	1.83	0.11	1
m18g	3.86	7/16/06 4:42 AM	29.65	42.9	1.81	0.10	1
m18g	3.77	7/16/06 4:42 AM	29.65	42.9	1.77	0.10	1
m18i	0.00	7/16/06 4:31 PM	28.22	0.0	93.65	7.34	1
m18i	0.11	7/16/06 4:32 PM	31.32	38.5	95.35	5.74	1
m18i	0.54	7/16/06 4:32 PM	31.39	38.5	97.47	5.86	1
m18i	0.84	7/16/06 4:32 PM	31.31	38.5	96.05	5.78	1
m18i	1.14	7/16/06 4:33 PM	31.10	38.6	96.73	5.84	1
m18i	1.41	7/16/06 4:33 PM	30.97	38.7	95.00	5.74	1
m18i	1.58	7/16/06 4:33 PM	30.63	39.0	87.48	5.31	1
m18i	1.77	7/16/06 4:34 PM	30.77	38.9	86.59	5.25	1
m18i	1.93	7/16/06 4:34 PM	30.53	39.1	87.01	5.29	1
m18i	1.96	7/16/06 4:35 PM	30.35	39.4	79.32	4.82	1
m18i	2.07	7/16/06 4:35 PM	30.30	39.7	75.82	4.61	1
m18i	2.13	7/16/06 4:36 PM	30.29	39.8	75.85	4.61	1

Profile	Depth m	Date Time	Temperature °C	Salinity PSS	DO Saturation %	Dissolved Oxygen mg/L	Circulator
m18i	2.22	7/16/06 4:36 PM	30.28	39.9	75.13	4.56	1
m18i	2.35	7/16/06 4:36 PM	30.27	40.1	75.21	4.56	1
m18i	2.35	7/16/06 4:36 PM	30.25	40.2	73.74	4.47	1
m18i	2.47	7/16/06 4:37 PM	30.19	40.7	70.44	4.26	1
m18i	2.55	7/16/06 4:37 PM	30.18	40.8	70.38	4.26	1
m18i	2.60	7/16/06 4:38 PM	30.15	41.0	65.17	3.94	1
m18i	2.71	7/16/06 4:39 PM	30.13	41.0	62.08	3.75	1
m18i	2.73	7/16/06 4:39 PM	30.13	41.1	61.88	3.74	1
m18i	2.84	7/16/06 4:39 PM	30.12	41.2	59.69	3.61	1
m18i	2.92	7/16/06 4:40 PM	30.09	41.4	56.47	3.41	1
m18i	2.99	7/16/06 4:41 PM	30.04	41.6	53.51	3.23	1
m18i	3.05	7/16/06 4:41 PM	30.04	41.6	50.63	3.05	1
m18i	3.17	7/16/06 4:42 PM	30.00	41.8	45.61	2.75	1
m18i	3.21	7/16/06 4:43 PM	29.97	41.9	41.23	2.49	1
m18i	3.31	7/16/06 4:44 PM	29.93	42.1	33.62	2.02	1
m18i	3.39	7/16/06 4:44 PM	29.87	42.3	23.19	1.39	1
m18i	3.44	7/16/06 4:45 PM	29.81	42.5	12.62	0.76	1
m18i	3.49	7/16/06 4:46 PM	29.76	42.6	6.72	0.40	1
m18i	3.61	7/16/06 4:46 PM	29.72	42.6	3.26	0.19	1
m18i	3.59	7/16/06 4:46 PM	29.73	42.6	2.96	0.17	1
m18i	3.63	7/16/06 4:47 PM	29.71	42.6	2.04	0.12	1
m18i	3.73	7/16/06 4:47 PM	29.72	42.6	1.64	0.09	1
m18i	3.87	7/16/06 4:48 PM	29.71	42.5	1.54	0.09	1
m19a	0.07	7/13/06 10:38 PM	28.33	40.4	90.08	5.62	1
m19a	0.16	7/13/06 10:38 PM	30.05	38.8	87.05	5.33	1
m19a	0.55	7/13/06 10:39 PM	30.05	38.8	87.08	5.34	1
m19a	0.87	7/13/06 10:39 PM	30.05	38.8	86.42	5.30	1
m19a	1.19	7/13/06 10:39 PM	30.07	38.8	86.46	5.30	1
m19a	1.48	7/13/06 10:40 PM	30.07	38.8	86.53	5.30	1
m19a	1.71	7/13/06 10:40 PM	30.09	38.8	86.13	5.27	1
m19a	2.03	7/13/06 10:40 PM	30.11	38.8	86.07	5.27	1
m19a	2.35	7/13/06 10:41 PM	30.11	38.9	86.02	5.26	1
m19a	2.68	7/13/06 10:41 PM	30.10	39.0	86.01	5.26	1
m19a	2.99	7/13/06 10:42 PM	29.88	40.4	67.50	4.11	1
m19a	3.25	7/13/06 10:43 PM	29.39	43.4	31.93	1.92	1
m19a	3.17	7/13/06 10:43 PM	29.53	41.9	37.05	2.25	1
m19a	3.50	7/13/06 10:44 PM	29.32	44.1	22.67	1.36	1
m19a	3.61	7/13/06 10:44 PM	29.30	44.4	18.81	1.13	1
m19a	3.79	7/13/06 10:45 PM	29.20	44.7	14.83	0.89	1
m19a	3.82	7/13/06 10:45 PM	29.19	44.7	12.13	0.72	1
m19a	4.14	7/13/06 10:45 PM	29.19	44.7	10.70	0.64	1
m19a	3.94	7/13/06 10:46 PM	29.19	44.7	10.23	0.61	1
m19c	0.02	7/14/06 4:27 PM	30.43	38.5	91.98	5.58	1
m19c	0.00	7/14/06 4:27 PM	30.43	38.5	92.13	5.58	1
m19c	0.46	7/14/06 4:28 PM	30.43	38.6	91.48	5.54	1
m19c	0.86	7/14/06 4:28 PM	30.44	38.5	91.93	5.57	1
m19c	1.15	7/14/06 4:28 PM	30.45	38.5	91.72	5.56	1
m19c	1.45	7/14/06 4:29 PM	30.42	38.5	91.61	5.55	1
m19c	1.74	7/14/06 4:29 PM	30.37	38.6	91.54	5.55	1

Profile	Depth m	Date Time	Temperature °C	Salinity PSS	DO Saturation %	Dissolved Oxygen mg/L	Circulator
m19c	2.08	7/14/06 4:29 PM	30.31	38.6	89.82	5.45	1
m19c	1.92	7/14/06 4:29 PM	30.31	38.6	90.12	5.47	1
m19c	2.33	7/14/06 4:30 PM	30.27	38.7	89.26	5.42	1
m19c	2.60	7/14/06 4:30 PM	30.20	38.8	88.48	5.38	1
m19c	2.90	7/14/06 4:31 PM	30.05	39.0	84.36	5.13	1
m19c	3.13	7/14/06 4:31 PM	29.62	40.3	65.00	3.95	1
m19c	3.18	7/14/06 4:32 PM	29.58	40.5	58.09	3.53	1
m19c	3.29	7/14/06 4:32 PM	29.54	41.2	47.49	2.87	1
m19c	3.38	7/14/06 4:33 PM	29.53	41.5	43.38	2.62	1
m19c	3.40	7/14/06 4:33 PM	29.52	42.1	36.37	2.19	1
m19c	3.53	7/14/06 4:33 PM	29.53	42.6	28.89	1.73	1
m19c	3.62	7/14/06 4:35 PM	29.54	43.3	17.51	1.04	1
m19c	3.76	7/14/06 4:35 PM	29.54	43.7	16.32	0.97	1
m19c	3.85	7/14/06 4:36 PM	29.53	44.0	12.20	0.72	1
m19c	3.99	7/14/06 4:36 PM	29.51	44.2	7.37	0.43	1
m19c	4.03	7/14/06 4:36 PM	29.50	44.2	5.68	0.33	1
m19c	4.06	7/14/06 4:37 PM	29.50	44.2	5.08	0.30	1
m19c	4.14	7/14/06 4:37 PM	29.50	44.1	4.92	0.29	1
m19c	4.22	7/14/06 4:38 PM	29.50	44.0	4.29	0.25	1
m19c	4.17	7/14/06 4:38 PM	29.50	44.1	4.24	0.25	1
m19d	0.11	7/15/06 2:08 AM	29.93	38.8	73.05	4.46	1
m19d	0.08	7/15/06 2:09 AM	29.93	38.8	78.85	4.81	1
m19d	0.59	7/15/06 2:09 AM	29.95	38.8	78.83	4.81	1
m19d	0.87	7/15/06 2:10 AM	29.96	38.8	79.46	4.84	1
m19d	1.17	7/15/06 2:10 AM	29.96	38.8	79.74	4.86	1
m19d	1.42	7/15/06 2:10 AM	29.96	38.8	80.53	4.91	1
m19d	1.76	7/15/06 2:10 AM	29.96	38.8	80.84	4.93	1
m19d	2.06	7/15/06 2:11 AM	29.97	38.8	80.60	4.91	1
m19d	2.42	7/15/06 2:11 AM	29.97	38.8	80.35	4.90	1
m19d	2.65	7/15/06 2:11 AM	29.97	38.8	80.39	4.90	1
m19d	2.80	7/15/06 2:12 AM	29.97	39.0	76.13	4.63	1
m19d	2.92	7/15/06 2:13 AM	29.85	40.2	55.69	3.37	1
m19d	3.08	7/15/06 2:14 AM	29.72	41.2	36.77	2.22	1
m19d	3.12	7/15/06 2:14 AM	29.67	42.3	30.31	1.82	1
m19d	3.17	7/15/06 2:15 AM	29.63	42.7	25.12	1.50	1
m19d	3.25	7/15/06 2:16 AM	29.63	42.8	23.16	1.39	1
m19d	3.36	7/15/06 2:16 AM	29.60	43.2	20.90	1.25	1
m19d	3.44	7/15/06 2:17 AM	29.59	43.3	18.65	1.11	1
m19d	3.49	7/15/06 2:18 AM	29.57	43.6	15.63	0.93	1
m19d	3.57	7/15/06 2:18 AM	29.55	43.8	11.89	0.71	1
m19d	3.67	7/15/06 2:19 AM	29.54	43.9	8.17	0.48	1
m19d	3.69	7/15/06 2:19 AM	29.53	43.9	7.27	0.43	1
m19d	3.80	7/15/06 2:20 AM	29.52	44.0	4.49	0.26	1
m19d	3.89	7/15/06 2:20 AM	29.50	44.1	2.68	0.16	1
m19d	3.98	7/15/06 2:21 AM	29.48	44.1	1.74	0.10	1
m19d	4.09	7/15/06 2:21 AM	29.46	44.2	1.21	0.07	1
m19d	3.96	7/15/06 2:21 AM	29.47	44.2	1.09	0.06	1
m19g	0.16	7/16/06 1:21 AM	30.18	39.3	82.56	5.04	1
m19g	0.14	7/16/06 1:22 AM	30.18	39.3	82.49	5.04	1

Profile	Depth m	Date Time	Temperature °C	Salinity PSS	DO Saturation %	Dissolved Oxygen mg/L	Circulator
m19g	0.59	7/16/06 1:22 AM	30.19	39.3	82.18	5.02	1
m19g	0.86	7/16/06 1:22 AM	30.20	39.3	81.55	4.98	1
m19g	1.16	7/16/06 1:23 AM	30.20	39.3	81.86	5.00	1
m19g	1.48	7/16/06 1:23 AM	30.19	39.3	81.99	5.01	1
m19g	1.76	7/16/06 1:23 AM	30.21	39.3	81.50	4.98	1
m19g	2.09	7/16/06 1:24 AM	30.21	39.3	82.44	5.03	1
m19g	2.38	7/16/06 1:24 AM	30.22	39.4	80.25	4.90	1
m19g	2.47	7/16/06 1:25 AM	30.19	39.7	71.47	4.35	1
m19g	2.56	7/16/06 1:25 AM	30.16	39.8	69.12	4.21	1
m19g	2.54	7/16/06 1:27 AM	30.14	39.9	66.59	4.06	1
m19g	2.61	7/16/06 1:28 AM	30.08	40.2	61.25	3.73	1
m19g	2.67	7/16/06 1:28 AM	29.99	40.7	49.17	2.99	1
m19g	2.79	7/16/06 1:29 AM	29.91	41.2	42.35	2.57	1
m19g	2.80	7/16/06 1:30 AM	29.88	41.4	38.45	2.33	1
m19g	2.90	7/16/06 1:30 AM	29.86	41.7	36.84	2.23	1
m19g	3.01	7/16/06 1:31 AM	29.86	41.8	36.08	2.18	1
m19g	3.07	7/16/06 1:31 AM	29.83	42.1	37.40	2.26	1
m19g	3.14	7/16/06 1:31 AM	29.81	42.2	39.18	2.37	1
m19g	3.16	7/16/06 1:32 AM	29.80	42.3	40.52	2.45	1
m19g	3.30	7/16/06 1:33 AM	29.79	42.4	42.07	2.54	1
m19g	3.40	7/16/06 1:33 AM	29.75	42.7	42.70	2.57	1
m19g	3.43	7/16/06 1:34 AM	29.72	42.9	41.03	2.47	1
m19g	3.51	7/16/06 1:35 AM	29.70	43.0	37.31	2.25	1
m19g	3.56	7/16/06 1:36 AM	29.68	43.1	32.88	1.98	1
m19g	3.68	7/16/06 1:36 AM	29.65	43.2	28.93	1.74	1
m19g	3.68	7/16/06 1:36 AM	29.65	43.2	28.93	1.74	1
m19g	3.75	7/16/06 1:37 AM	29.62	43.3	24.01	1.44	1
m19g	3.85	7/16/06 1:38 AM	29.60	43.4	17.94	1.08	1
m19g	3.90	7/16/06 1:39 AM	29.55	43.6	10.14	0.61	1
m19g	3.96	7/16/06 1:40 AM	29.52	43.7	3.58	0.21	1
m19g	4.07	7/16/06 1:40 AM	29.52	43.7	2.73	0.16	1
m19g	4.10	7/16/06 1:41 AM	29.45	43.8	1.21	0.07	1
m19g	4.19	7/16/06 1:41 AM	29.44	43.9	1.25	0.07	1
m19g	4.15	7/16/06 1:42 AM	29.45	43.8	1.02	0.06	1
m19i	-0.03	7/16/06 3:15 PM	27.89	0.0	100.98	7.96	0
m19i	0.09	7/16/06 3:16 PM	31.62	38.4	91.83	5.50	1
m19i	0.53	7/16/06 3:16 PM	31.64	38.4	92.21	5.52	1
m19i	0.84	7/16/06 3:16 PM	31.57	38.4	92.25	5.53	1
m19i	1.15	7/16/06 3:16 PM	31.46	38.5	92.08	5.53	1
m19i	1.49	7/16/06 3:17 PM	31.15	38.5	91.81	5.54	1
m19i	1.77	7/16/06 3:17 PM	30.46	38.8	91.14	5.55	1
m19i	1.77	7/16/06 3:17 PM	30.43	38.8	91.75	5.59	1
m19i	1.91	7/16/06 3:18 PM	30.38	38.9	89.58	5.46	1
m19i	2.08	7/16/06 3:18 PM	30.23	39.0	89.92	5.49	1
m19i	2.20	7/16/06 3:18 PM	30.25	39.1	88.48	5.40	1
m19i	2.38	7/16/06 3:19 PM	30.20	39.2	87.31	5.33	1
m19i	2.51	7/16/06 3:19 PM	30.11	39.3	85.75	5.24	1
m19i	2.68	7/16/06 3:19 PM	29.99	39.6	85.07	5.20	1
m19i	2.79	7/16/06 3:20 PM	29.98	39.7	82.93	5.07	1

Profile	Depth m	Date Time	Temperature °C	Salinity PSS	DO Saturation %	Dissolved Oxygen mg/L	Circulator
m19i	2.97	7/16/06 3:20 PM	29.93	39.8	82.88	5.06	1
m19i	3.08	7/16/06 3:22 PM	29.86	40.1	80.57	4.92	1
m19i	3.19	7/16/06 3:22 PM	29.83	40.2	79.73	4.87	1
m19i	3.21	7/16/06 3:22 PM	29.81	40.3	77.42	4.72	1
m19i	3.25	7/16/06 3:23 PM	29.76	40.5	72.02	4.39	1
m19i	3.33	7/16/06 3:24 PM	29.77	40.5	65.00	3.96	1
m19i	3.42	7/16/06 3:25 PM	29.74	41.0	57.60	3.50	1
m19i	3.50	7/16/06 3:26 PM	29.73	41.3	48.53	2.95	1
m19i	3.52	7/16/06 3:26 PM	29.73	41.4	48.57	2.95	1
m19i	3.50	7/16/06 3:27 PM	29.72	41.5	43.48	2.64	1
m19i	3.64	7/16/06 3:27 PM	29.69	41.9	31.68	1.92	1
m19i	3.76	7/16/06 3:28 PM	29.68	42.1	27.13	1.64	1
m19i	3.83	7/16/06 3:29 PM	29.66	42.3	21.51	1.30	1
m19i	3.87	7/16/06 3:29 PM	29.64	42.4	17.19	1.04	1
m19i	3.99	7/16/06 3:30 PM	29.62	42.6	12.96	0.78	1
m19i	3.99	7/16/06 3:30 PM	29.62	42.6	12.96	0.78	1
m19i	4.05	7/16/06 3:31 PM	29.60	42.7	8.97	0.54	1
m19i	4.12	7/16/06 3:31 PM	29.59	42.7	8.13	0.49	1
m19i	4.14	7/16/06 3:31 PM	29.59	42.7	7.14	0.43	1
m20c	0.04	7/14/06 4:51 PM	30.63	38.5	89.60	5.41	1
m20c	0.05	7/14/06 4:51 PM	30.64	38.5	90.46	5.47	1
m20c	0.53	7/14/06 4:52 PM	30.64	38.5	89.99	5.44	1
m20c	0.76	7/14/06 4:52 PM	30.65	38.5	89.80	5.42	1
m20c	1.09	7/14/06 4:52 PM	30.64	38.5	90.60	5.47	1
m20c	1.43	7/14/06 4:53 PM	30.63	38.6	90.15	5.45	1
m20c	1.72	7/14/06 4:53 PM	30.63	38.6	90.48	5.47	1
m20c	1.96	7/14/06 4:53 PM	30.63	38.5	90.08	5.44	1
m20c	2.29	7/14/06 4:54 PM	30.59	38.6	90.10	5.45	1
m20c	2.61	7/14/06 4:54 PM	30.54	38.6	89.47	5.41	1
m20c	2.93	7/14/06 4:55 PM	30.50	38.6	88.68	5.37	1
m20c	3.19	7/14/06 4:55 PM	30.37	38.7	86.70	5.26	1
m20c	3.23	7/14/06 4:56 PM	30.43	38.6	87.44	5.30	1
m20c	3.52	7/14/06 4:56 PM	29.87	38.9	82.18	5.01	1
m20c	3.48	7/14/06 4:56 PM	29.84	38.9	78.49	4.79	1
m20c	3.84	7/14/06 4:57 PM	29.82	38.9	76.59	4.68	1
m20c	4.07	7/14/06 4:57 PM	29.83	38.9	73.43	4.48	1
m20c	4.00	7/14/06 4:57 PM	29.83	38.9	74.00	4.52	1
m20d	0.01	7/15/06 3:19 AM	27.62	40.5	83.63	5.25	1
m20d	0.14	7/15/06 3:20 AM	29.90	39.0	83.92	5.12	1
m20d	0.57	7/15/06 3:20 AM	29.91	39.0	82.58	5.03	1
m20d	0.90	7/15/06 3:20 AM	29.91	39.0	82.43	5.03	1
m20d	1.21	7/15/06 3:21 AM	29.92	39.0	82.22	5.01	1
m20d	1.45	7/15/06 3:21 AM	29.92	39.0	82.40	5.02	1
m20d	1.79	7/15/06 3:21 AM	29.93	39.0	82.73	5.04	1
m20d	2.05	7/15/06 3:21 AM	29.94	39.0	82.52	5.03	1
m20d	2.39	7/15/06 3:22 AM	29.94	39.0	82.37	5.02	1
m20d	2.64	7/15/06 3:22 AM	29.93	39.0	83.15	5.07	1
m20d	2.98	7/15/06 3:22 AM	29.97	39.1	81.54	4.96	1
m20d	3.29	7/15/06 3:23 AM	30.00	39.6	70.62	4.28	1

Profile	Depth m	Date Time	Temperature °C	Salinity PSS	DO Saturation %	Dissolved Oxygen mg/L	Circulator
m20d	3.37	7/15/06 3:25 AM	29.95	40.1	56.53	3.42	1
m20d	3.47	7/15/06 3:26 AM	29.80	41.1	33.68	2.03	1
m20d	3.51	7/15/06 3:27 AM	29.63	42.3	13.57	0.81	1
m20d	3.58	7/15/06 3:28 AM	29.49	43.4	4.86	0.29	1
m20d	3.75	7/15/06 3:29 AM	29.41	43.9	1.82	0.10	1
m20d	3.79	7/15/06 3:29 AM	29.36	44.0	1.64	0.09	1
m20d	3.89	7/15/06 3:30 AM	29.35	44.0	1.45	0.08	1
m20d	3.93	7/15/06 3:30 AM	29.34	44.0	1.46	0.08	1
m20d	4.01	7/15/06 3:30 AM	29.35	44.0	1.27	0.07	1
m20d	3.95	7/15/06 3:31 AM	29.35	44.0	1.29	0.07	1
m20g	0.12	7/16/06 2:43 AM	30.23	39.0	82.65	5.05	1
m20g	0.16	7/16/06 2:43 AM	30.23	39.0	82.82	5.06	1
m20g	0.59	7/16/06 2:43 AM	30.25	39.0	83.33	5.09	1
m20g	0.80	7/16/06 2:43 AM	30.25	39.0	83.14	5.08	1
m20g	1.14	7/16/06 2:44 AM	30.26	39.0	82.98	5.07	1
m20g	1.47	7/16/06 2:44 AM	30.26	39.0	82.80	5.06	1
m20g	1.45	7/16/06 2:44 AM	30.26	39.0	82.95	5.07	1
m20g	1.78	7/16/06 2:45 AM	30.26	39.0	82.98	5.07	1
m20g	2.06	7/16/06 2:45 AM	30.27	39.0	83.81	5.12	1
m20g	2.41	7/16/06 2:45 AM	30.26	39.0	82.40	5.03	1
m20g	2.57	7/16/06 2:46 AM	30.24	39.1	80.90	4.94	1
m20g	2.63	7/16/06 2:47 AM	30.24	39.2	78.93	4.82	1
m20g	2.72	7/16/06 2:47 AM	30.15	39.7	71.40	4.35	1
m20g	2.82	7/16/06 2:48 AM	30.11	39.9	61.39	3.74	1
m20g	2.90	7/16/06 2:49 AM	30.01	40.4	49.64	3.02	1
m20g	2.88	7/16/06 2:50 AM	29.92	41.1	38.45	2.33	1
m20g	3.00	7/16/06 2:51 AM	29.88	41.5	32.85	1.99	1
m20g	3.12	7/16/06 2:51 AM	29.84	42.0	29.57	1.79	1
m20g	3.17	7/16/06 2:52 AM	29.82	42.2	28.84	1.74	1
m20g	3.23	7/16/06 2:52 AM	29.80	42.4	28.98	1.75	1
m20g	3.23	7/16/06 2:52 AM	29.80	42.3	29.57	1.78	1
m20g	3.26	7/16/06 2:53 AM	29.78	42.5	29.24	1.76	1
m20g	3.41	7/16/06 2:53 AM	29.75	42.7	29.75	1.79	1
m20g	3.44	7/16/06 2:54 AM	29.72	42.9	28.19	1.70	1
m20g	3.57	7/16/06 2:55 AM	29.69	43.1	27.47	1.65	1
m20g	3.58	7/16/06 2:56 AM	29.65	43.5	21.60	1.30	1
m20g	3.66	7/16/06 2:56 AM	29.64	43.5	20.34	1.22	1
m20g	3.74	7/16/06 2:57 AM	29.57	43.7	9.56	0.57	1
m20g	3.81	7/16/06 2:57 AM	29.55	43.8	5.45	0.32	1
m20g	3.85	7/16/06 2:58 AM	29.54	43.8	5.85	0.35	1
m20g	3.83	7/16/06 2:58 AM	29.50	43.8	2.69	0.16	1
m20g	3.94	7/16/06 2:59 AM	29.49	43.8	1.62	0.09	1
m20g	4.08	7/16/06 2:59 AM	29.48	43.7	1.22	0.07	1
m20g	3.93	7/16/06 2:59 AM	29.48	43.8	1.08	0.06	1
m20i	0.10	7/16/06 3:42 PM	31.59	38.3	92.47	5.55	1
m20i	0.15	7/16/06 3:42 PM	31.58	38.3	92.66	5.56	1
m20i	0.55	7/16/06 3:42 PM	31.56	38.3	92.59	5.56	1
m20i	0.89	7/16/06 3:42 PM	31.49	38.3	93.66	5.63	1
m20i	1.17	7/16/06 3:43 PM	31.27	38.4	92.67	5.59	1

Profile	Depth m	Date Time	Temperature °C	Salinity PSS	DO Saturation %	Dissolved Oxygen mg/L	Circulator
m20i	1.44	7/16/06 3:43 PM	31.13	38.4	91.16	5.51	1
m20i	1.73	7/16/06 3:43 PM	30.83	38.6	89.66	5.44	1
m20i	2.10	7/16/06 3:44 PM	30.56	38.7	87.16	5.30	1
m20i	2.25	7/16/06 3:44 PM	30.43	38.9	86.02	5.24	1
m20i	2.32	7/16/06 3:45 PM	30.22	39.4	83.11	5.06	1
m20i	2.50	7/16/06 3:46 PM	30.22	39.4	82.54	5.03	1
m20i	2.67	7/16/06 3:46 PM	30.19	39.7	83.09	5.06	1
m20i	2.72	7/16/06 3:47 PM	30.13	40.2	81.21	4.93	1
m20i	2.81	7/16/06 3:47 PM	30.10	40.3	80.71	4.90	1
m20i	2.91	7/16/06 3:47 PM	30.08	40.4	80.48	4.89	1
m20i	3.00	7/16/06 3:48 PM	29.99	40.7	74.47	4.52	1
m20i	3.05	7/16/06 3:49 PM	29.97	40.9	69.10	4.19	1
m20i	3.10	7/16/06 3:50 PM	29.95	41.1	66.45	4.03	1
m20i	3.21	7/16/06 3:51 PM	29.91	41.4	57.18	3.46	1
m20i	3.30	7/16/06 3:51 PM	29.89	41.6	53.10	3.21	1
m20i	3.36	7/16/06 3:52 PM	29.88	41.7	50.04	3.03	1
m20i	0.00	7/16/06 3:53 PM	0.00	0.0	0.00	0.00	0
m20i	3.48	7/16/06 3:54 PM	29.83	42.0	41.74	2.52	1
m20i	3.48	7/16/06 3:55 PM	29.84	41.9	42.32	2.56	1
m20i	3.59	7/16/06 3:56 PM	29.78	42.3	32.76	1.98	1
m20i	3.67	7/16/06 3:56 PM	29.78	42.3	32.32	1.95	1
m20i	3.66	7/16/06 3:57 PM	29.79	42.3	32.63	1.97	1
m20i	3.73	7/16/06 3:57 PM	29.77	42.4	28.26	1.70	1
m20i	3.80	7/16/06 3:58 PM	29.75	42.5	23.92	1.44	1
m20i	3.93	7/16/06 3:58 PM	29.73	42.7	19.50	1.17	1
m20i	3.92	7/16/06 3:59 PM	29.72	42.6	17.40	1.05	1
m20i	4.04	7/16/06 3:59 PM	29.70	42.7	14.05	0.84	1
m22a	0.11	7/13/06 11:04 PM	29.95	38.8	85.96	5.27	1
m22a	0.58	7/13/06 11:05 PM	29.96	38.8	86.13	5.28	1
m22a	0.63	7/13/06 11:05 PM	29.96	38.9	86.95	5.33	1
m22a	0.83	7/13/06 11:05 PM	29.96	38.9	86.61	5.31	1
m22a	1.21	7/13/06 11:06 PM	29.97	38.9	87.14	5.34	1
m22a	1.46	7/13/06 11:06 PM	29.97	38.9	86.75	5.32	1
m22a	1.91	7/13/06 11:06 PM	29.96	38.9	86.23	5.29	1
m22a	2.12	7/13/06 11:06 PM	29.97	38.9	86.56	5.31	1
m22a	2.42	7/13/06 11:07 PM	29.98	39.1	84.89	5.20	1
m22a	2.68	7/13/06 11:08 PM	29.92	39.8	78.42	4.79	1
m22a	3.03	7/13/06 11:08 PM	29.72	42.9	52.60	3.17	1
m22a	3.28	7/13/06 11:09 PM	29.71	44.4	44.79	2.67	1
m22a	3.65	7/13/06 11:09 PM	29.66	45.0	43.02	2.56	1
m22a	3.85	7/13/06 11:10 PM	29.64	45.0	39.03	2.32	1
m22a	4.17	7/13/06 11:10 PM	29.64	44.8	36.74	2.19	1
m22c	0.08	7/14/06 4:04 PM	31.52	41.3	84.95	4.99	1
m22c	0.06	7/14/06 4:05 PM	30.41	38.7	93.03	5.63	1
m22c	0.53	7/14/06 4:05 PM	30.39	38.8	92.91	5.63	1
m22c	0.83	7/14/06 4:06 PM	30.39	38.8	92.72	5.62	1
m22c	1.09	7/14/06 4:06 PM	30.37	38.8	92.67	5.61	1
m22c	1.47	7/14/06 4:06 PM	30.34	38.8	92.46	5.60	1
m22c	1.71	7/14/06 4:07 PM	30.33	38.8	92.84	5.63	1

Profile	Depth m	Date Time	Temperature °C	Salinity PSS	DO Saturation %	Dissolved Oxygen mg/L	Circulator
m22c	2.04	7/14/06 4:07 PM	30.20	39.0	91.42	5.55	1
m22c	2.30	7/14/06 4:07 PM	30.12	39.2	90.79	5.51	1
m22c	2.58	7/14/06 4:08 PM	30.02	39.6	89.11	5.41	1
m22c	2.89	7/14/06 4:09 PM	29.85	40.8	78.54	4.74	1
m22c	2.98	7/14/06 4:09 PM	29.73	42.2	58.16	3.49	1
m22c	2.97	7/14/06 4:09 PM	29.71	42.3	57.16	3.43	1
m22c	3.05	7/14/06 4:10 PM	29.73	42.3	58.91	3.54	1
m22c	3.16	7/14/06 4:10 PM	29.67	43.0	48.52	2.90	1
m22c	3.25	7/14/06 4:11 PM	29.65	43.2	43.42	2.60	1
m22c	3.26	7/14/06 4:12 PM	29.60	43.9	34.12	2.03	1
m22c	3.50	7/14/06 4:12 PM	29.58	44.1	30.82	1.83	1
m22c	3.42	7/14/06 4:13 PM	29.57	44.2	28.19	1.68	1
m22c	3.53	7/14/06 4:14 PM	29.55	44.4	24.45	1.45	1
m22c	3.57	7/14/06 4:14 PM	29.54	44.3	23.45	1.39	1
m22c	3.65	7/14/06 4:14 PM	29.54	44.3	23.11	1.37	1
m22c	3.76	7/14/06 4:15 PM	29.51	44.5	20.27	1.20	1
m22c	3.82	7/14/06 4:15 PM	29.50	44.6	17.42	1.03	1
m22c	3.94	7/14/06 4:15 PM	29.49	44.6	13.54	0.80	1
m22c	4.00	7/14/06 4:16 PM	29.48	44.6	12.57	0.74	1
m22c	4.09	7/14/06 4:16 PM	29.48	44.6	11.84	0.70	1
m22c	4.23	7/14/06 4:16 PM	29.48	44.6	11.47	0.68	1
m22c	4.16	7/14/06 4:17 PM	29.48	44.6	10.99	0.65	1
m22d	0.19	7/15/06 1:26 AM	29.79	38.8	80.48	4.92	1
m22d	0.13	7/15/06 1:26 AM	29.78	38.8	80.73	4.94	1
m22d	0.54	7/15/06 1:27 AM	29.81	38.8	80.60	4.93	1
m22d	0.87	7/15/06 1:27 AM	29.81	38.8	80.68	4.93	1
m22d	1.19	7/15/06 1:27 AM	29.83	38.9	80.15	4.89	1
m22d	1.53	7/15/06 1:28 AM	29.82	38.8	80.68	4.93	1
m22d	1.76	7/15/06 1:28 AM	29.83	38.8	80.40	4.91	1
m22d	2.06	7/15/06 1:28 AM	29.84	38.9	79.88	4.88	1
m22d	2.34	7/15/06 1:29 AM	29.86	39.0	78.52	4.79	1
m22d	2.52	7/15/06 1:29 AM	29.87	39.4	70.64	4.30	1
m22d	2.72	7/15/06 1:30 AM	29.83	40.3	57.50	3.48	1
m22d	2.82	7/15/06 1:31 AM	29.79	41.0	44.78	2.70	1
m22d	2.85	7/15/06 1:32 AM	29.78	41.8	33.80	2.03	1
m22d	2.99	7/15/06 1:32 AM	29.75	42.3	30.32	1.82	1
m22d	3.09	7/15/06 1:33 AM	29.73	42.7	26.79	1.60	1
m22d	3.16	7/15/06 1:33 AM	29.69	43.1	24.48	1.46	1
m22d	3.20	7/15/06 1:34 AM	29.68	43.3	23.78	1.42	1
m22d	3.29	7/15/06 1:35 AM	29.63	43.6	25.50	1.52	1
m22d	3.32	7/15/06 1:35 AM	29.61	43.8	26.44	1.57	1
m22d	3.41	7/15/06 1:36 AM	29.58	43.9	27.10	1.61	1
m22d	3.52	7/15/06 1:36 AM	29.57	43.9	27.32	1.63	1
m22d	3.62	7/15/06 1:37 AM	29.53	44.0	23.43	1.39	1
m22d	3.67	7/15/06 1:37 AM	29.52	44.1	21.77	1.29	1
m22d	3.76	7/15/06 1:37 AM	29.51	44.1	20.65	1.23	1
m22d	3.84	7/15/06 1:38 AM	29.51	44.1	20.01	1.19	1
m22d	3.91	7/15/06 1:38 AM	29.51	44.1	18.70	1.11	1
m22d	4.01	7/15/06 1:39 AM	29.50	44.1	17.56	1.04	1

Profile	Depth m	Date Time	Temperature °C	Salinity PSS	DO Saturation %	Dissolved Oxygen mg/L	Circulator
m22d	4.05	7/15/06 1:39 AM	29.50	44.1	16.77	1.00	1
m22d	4.14	7/15/06 1:39 AM	29.50	44.0	15.44	0.92	1
m22d	4.02	7/15/06 1:40 AM	29.50	44.1	15.13	0.90	1
m22f	0.25	7/15/06 3:32 PM	30.93	38.6	95.30	5.78	1
m22f	0.19	7/15/06 3:32 PM	30.94	38.6	95.49	5.79	1
m22f	0.68	7/15/06 3:32 PM	30.93	38.7	94.49	5.73	1
m22f	0.87	7/15/06 3:32 PM	30.92	38.7	94.20	5.71	1
m22f	1.17	7/15/06 3:33 PM	30.89	38.7	95.29	5.78	1
m22f	1.52	7/15/06 3:33 PM	30.81	38.7	94.53	5.74	1
m22f	1.84	7/15/06 3:34 PM	30.50	39.0	93.58	5.70	1
m22g	0.14	7/16/06 12:39 AM	30.16	39.5	79.24	4.84	1
m22g	0.18	7/16/06 12:39 AM	30.16	39.6	79.53	4.85	1
m22g	0.59	7/16/06 12:39 AM	30.18	39.5	80.50	4.91	1
m22g	0.83	7/16/06 12:40 AM	30.18	39.5	80.01	4.88	1
m22g	1.16	7/16/06 12:40 AM	30.19	39.6	79.94	4.88	1
m22g	1.48	7/16/06 12:41 AM	30.19	39.6	80.13	4.89	1
m22g	1.76	7/16/06 12:41 AM	30.20	39.6	80.67	4.92	1
m22g	2.07	7/16/06 12:42 AM	30.24	39.8	75.31	4.58	1
m22g	2.24	7/16/06 12:43 AM	30.24	39.9	70.72	4.30	1
m22g	2.41	7/16/06 12:44 AM	30.10	40.4	59.25	3.60	1
m22g	2.49	7/16/06 12:45 AM	30.02	40.9	49.13	2.98	1
m22g	2.52	7/16/06 12:45 AM	30.01	40.9	47.16	2.86	1
m22g	2.62	7/16/06 12:46 AM	29.93	41.3	41.92	2.54	1
m22g	2.71	7/16/06 12:47 AM	29.90	41.6	38.96	2.36	1
m22g	2.77	7/16/06 12:47 AM	29.89	41.6	38.27	2.32	1
m22g	2.85	7/16/06 12:48 AM	29.88	41.7	37.27	2.26	1
m22g	2.95	7/16/06 12:48 AM	29.87	41.8	37.06	2.24	1
m22g	3.03	7/16/06 12:48 AM	29.87	41.9	37.07	2.24	1
m22g	3.06	7/16/06 12:49 AM	29.88	41.9	37.12	2.24	1
m22g	3.13	7/16/06 12:49 AM	29.86	42.1	38.36	2.32	1
m22g	3.21	7/16/06 12:50 AM	29.84	42.2	39.85	2.41	1
m22g	3.30	7/16/06 12:51 AM	29.80	42.3	41.40	2.50	1
m22g	3.37	7/16/06 12:52 AM	29.74	42.6	40.14	2.42	1
m22g	3.46	7/16/06 12:52 AM	29.71	42.8	38.60	2.33	1
m22g	3.52	7/16/06 12:53 AM	29.68	42.9	36.16	2.18	1
m22g	3.57	7/16/06 12:54 AM	29.67	42.9	33.86	2.04	1
m22g	3.59	7/16/06 12:54 AM	29.67	42.9	34.09	2.06	1
m22g	3.66	7/16/06 12:55 AM	29.64	43.0	30.07	1.81	1
m22g	3.76	7/16/06 12:56 AM	29.62	43.2	27.00	1.63	1
m22g	3.83	7/16/06 12:56 AM	29.59	43.3	21.74	1.31	1
m22g	3.91	7/16/06 12:57 AM	29.57	43.4	17.76	1.07	1
m22g	3.99	7/16/06 12:58 AM	29.53	43.5	10.19	0.61	1
m22g	4.06	7/16/06 12:59 AM	29.50	43.6	5.67	0.34	1
m22g	4.20	7/16/06 1:00 AM	29.45	43.8	2.27	0.13	1
m22g	4.20	7/16/06 1:00 AM	29.45	43.8	2.38	0.14	1
m22g	4.22	7/16/06 1:00 AM	29.43	43.7	2.85	0.17	1
m22i	0.10	7/16/06 2:55 PM	31.69	38.6	91.53	5.48	1
m22i	0.11	7/16/06 2:55 PM	31.69	38.6	91.80	5.49	1
m22i	0.52	7/16/06 2:56 PM	31.70	38.6	93.12	5.57	1

Profile	Depth m	Date Time	Temperature °C	Salinity PSS	DO Saturation %	Dissolved Oxygen mg/L	Circulator
m22i	0.86	7/16/06 2:56 PM	31.67	38.6	93.38	5.59	1
m22i	1.16	7/16/06 2:56 PM	31.56	38.6	93.51	5.61	1
m22i	1.45	7/16/06 2:56 PM	31.39	38.7	93.27	5.60	1
m22i	1.76	7/16/06 2:57 PM	31.06	38.8	93.44	5.64	1
m22i	2.07	7/16/06 2:57 PM	30.50	39.0	92.11	5.60	1
m22i	2.36	7/16/06 2:58 PM	30.10	39.2	89.55	5.47	1
m22i	2.66	7/16/06 2:58 PM	30.01	39.4	87.37	5.34	1
m22i	2.81	7/16/06 2:59 PM	29.99	39.4	88.32	5.40	1
m22i	3.00	7/16/06 2:59 PM	29.95	39.6	87.93	5.37	1
m22i	3.07	7/16/06 2:59 PM	29.90	39.9	86.71	5.30	1
m22i	3.28	7/16/06 3:01 PM	29.79	40.3	80.55	4.92	1
m22i	3.34	7/16/06 3:02 PM	29.74	40.4	71.73	4.38	1
m22i	3.44	7/16/06 3:02 PM	29.70	40.5	66.73	4.07	1
m22i	3.51	7/16/06 3:02 PM	29.66	40.8	60.35	3.68	1
m22i	3.64	7/16/06 3:03 PM	29.65	41.0	50.79	3.09	1
m22i	3.63	7/16/06 3:04 PM	29.65	41.0	45.87	2.79	1
m22i	3.76	7/16/06 3:04 PM	29.65	41.2	39.57	2.41	1
m22i	3.78	7/16/06 3:05 PM	29.63	41.5	32.79	1.99	1
m22i	3.91	7/16/06 3:06 PM	29.62	41.7	24.76	1.50	1
m22i	3.95	7/16/06 3:06 PM	29.60	41.8	18.86	1.14	1
m22i	4.04	7/16/06 3:07 PM	29.58	42.0	14.66	0.89	1
m22i	4.20	7/16/06 3:08 PM	29.56	42.0	12.96	0.78	1
m23a	0.02	7/13/06 11:31 PM	27.94	40.5	85.75	5.39	1
m23a	0.10	7/13/06 11:31 PM	29.80	39.5	85.48	5.24	1
m23a	0.60	7/13/06 11:32 PM	29.81	39.5	85.97	5.27	1
m23a	0.89	7/13/06 11:32 PM	29.82	39.6	85.56	5.24	1
m23a	1.12	7/13/06 11:32 PM	29.83	39.6	85.64	5.24	1
m23a	1.51	7/13/06 11:33 PM	29.81	39.7	85.30	5.22	1
m23a	1.73	7/13/06 11:33 PM	29.79	39.6	85.05	5.21	1
m23a	2.05	7/13/06 11:33 PM	29.79	39.7	84.31	5.16	1
m23a	2.33	7/13/06 11:34 PM	29.90	40.1	81.52	4.97	1
m23a	2.51	7/13/06 11:35 PM	29.84	42.3	67.28	4.06	1
m23a	2.70	7/13/06 11:35 PM	29.73	42.9	58.72	3.53	1
m23a	2.79	7/13/06 11:36 PM	29.57	44.3	47.72	2.86	1
m23a	2.92	7/13/06 11:37 PM	29.50	44.7	39.08	2.34	1
m23a	3.13	7/13/06 11:37 PM	29.48	44.8	35.72	2.13	1
m23a	3.23	7/13/06 11:38 PM	29.48	44.8	34.79	2.08	1
m23a	3.47	7/13/06 11:38 PM	29.47	44.9	33.78	2.02	1
m23a	3.59	7/13/06 11:39 PM	29.46	44.9	32.97	1.97	1
m23a	3.74	7/13/06 11:39 PM	29.45	44.9	31.78	1.90	1
m23a	3.66	7/13/06 11:39 PM	29.45	44.9	30.35	1.81	1
m23c	0.11	7/14/06 3:40 PM	31.54	41.2	79.84	4.69	1
m23c	0.05	7/14/06 3:41 PM	30.41	39.5	88.98	5.36	1
m23c	0.54	7/14/06 3:41 PM	30.40	39.6	89.07	5.37	1
m23c	0.53	7/14/06 3:42 PM	30.41	39.6	88.94	5.36	1
m23c	0.81	7/14/06 3:42 PM	30.39	39.6	88.69	5.35	1
m23c	1.10	7/14/06 3:42 PM	30.39	39.6	88.35	5.33	1
m23c	1.42	7/14/06 3:43 PM	30.32	39.6	88.34	5.33	1
m23c	1.78	7/14/06 3:43 PM	30.29	39.6	88.57	5.35	1

Profile	Depth m	Date Time	Temperature °C	Salinity PSS	DO Saturation %	Dissolved Oxygen mg/L	Circulator
m23c	2.07	7/14/06 3:44 PM	30.26	39.6	88.41	5.34	1
m23c	2.35	7/14/06 3:44 PM	30.15	39.8	87.28	5.28	1
m23c	2.47	7/14/06 3:45 PM	29.84	41.0	70.49	4.25	1
m23c	2.68	7/14/06 3:45 PM	29.82	41.5	69.85	4.20	1
m23c	2.79	7/14/06 3:46 PM	29.58	43.2	47.99	2.87	1
m23c	2.98	7/14/06 3:46 PM	29.54	43.5	41.96	2.51	1
m23c	3.08	7/14/06 3:47 PM	29.51	43.7	35.57	2.12	1
m23c	3.26	7/14/06 3:47 PM	29.50	43.8	30.76	1.83	1
m23c	3.36	7/14/06 3:48 PM	29.49	43.9	27.51	1.64	1
m23c	3.58	7/14/06 3:48 PM	29.50	44.1	21.20	1.26	1
m23c	3.71	7/14/06 3:49 PM	29.48	44.1	15.61	0.93	1
m23c	3.78	7/14/06 3:50 PM	29.48	44.1	14.99	0.89	1
m23c	3.72	7/14/06 3:50 PM	29.48	44.1	14.90	0.89	1
m23d	0.10	7/15/06 1:06 AM	29.84	39.2	80.93	4.93	1
m23d	0.14	7/15/06 1:07 AM	29.85	39.1	81.50	4.97	1
m23d	0.58	7/15/06 1:07 AM	29.84	39.2	81.94	5.00	1
m23d	0.90	7/15/06 1:07 AM	29.84	39.2	81.88	4.99	1
m23d	1.16	7/15/06 1:07 AM	29.85	39.2	82.21	5.01	1
m23d	1.48	7/15/06 1:08 AM	29.85	39.2	82.71	5.04	1
m23d	1.75	7/15/06 1:08 AM	29.86	39.2	82.15	5.01	1
m23d	2.02	7/15/06 1:08 AM	29.88	39.2	82.44	5.02	1
m23d	2.25	7/15/06 1:09 AM	29.93	39.6	77.46	4.70	1
m23d	2.34	7/15/06 1:09 AM	29.91	41.4	63.92	3.85	1
m23d	2.57	7/15/06 1:10 AM	29.78	42.9	54.97	3.28	1
m23d	2.68	7/15/06 1:10 AM	29.67	43.5	51.80	3.09	1
m23d	2.88	7/15/06 1:11 AM	29.58	43.8	50.64	3.02	1
m23d	2.95	7/15/06 1:11 AM	29.53	43.9	48.75	2.91	1
m23d	3.07	7/15/06 1:12 AM	29.49	43.9	47.29	2.82	1
m23d	3.26	7/15/06 1:12 AM	29.47	43.9	46.38	2.77	1
m23d	3.42	7/15/06 1:13 AM	29.43	44.0	44.25	2.64	1
m23d	3.59	7/15/06 1:13 AM	29.37	44.1	34.04	2.03	1
m23d	3.72	7/15/06 1:14 AM	29.35	44.1	31.39	1.87	1
m23d	3.72	7/15/06 1:14 AM	29.36	44.1	31.76	1.90	1
m23d	3.63	7/15/06 1:14 AM	29.37	44.1	30.11	1.80	1
m23e	-0.02	7/15/06 4:43 AM	27.58	40.4	85.42	5.36	1
m23e	0.14	7/15/06 4:43 AM	29.58	39.0	77.02	4.72	1
m23e	0.57	7/15/06 4:44 AM	29.59	39.0	76.77	4.70	1
m23e	0.88	7/15/06 4:44 AM	29.59	39.0	76.58	4.69	1
m23e	1.19	7/15/06 4:45 AM	29.60	39.0	75.99	4.65	1
m23e	1.50	7/15/06 4:45 AM	29.61	39.1	75.36	4.61	1
m23e	1.79	7/15/06 4:46 AM	29.69	39.1	73.70	4.50	1
m23e	1.91	7/15/06 4:47 AM	29.77	39.4	66.52	4.05	1
m23e	1.96	7/15/06 4:47 AM	29.78	39.5	64.10	3.90	1
m23e	2.01	7/15/06 4:49 AM	29.79	39.8	62.44	3.80	1
m23e	2.09	7/15/06 4:51 AM	29.83	40.3	49.60	3.00	1
m23e	2.18	7/15/06 4:52 AM	29.85	40.7	44.73	2.70	1
m23e	2.26	7/15/06 4:53 AM	29.86	41.2	38.64	2.33	1
m23e	2.30	7/15/06 4:53 AM	29.85	41.6	36.56	2.20	1
m23e	2.43	7/15/06 4:54 AM	29.84	41.8	35.00	2.10	1

Profile	Depth m	Date Time	Temperature °C	Salinity PSS	DO Saturation %	Dissolved Oxygen mg/L	Circulator
m23e	2.50	7/15/06 4:54 AM	29.84	41.9	34.65	2.08	1
m23e	2.57	7/15/06 4:54 AM	29.83	42.2	35.15	2.11	1
m23e	2.63	7/15/06 4:55 AM	29.82	42.3	36.22	2.17	1
m23e	2.73	7/15/06 4:55 AM	29.80	42.5	38.44	2.30	1
m23e	2.78	7/15/06 4:56 AM	29.78	42.5	39.14	2.34	1
m23e	2.85	7/15/06 4:56 AM	29.77	42.5	39.11	2.34	1
m23e	2.91	7/15/06 4:57 AM	29.73	42.7	39.15	2.34	1
m23e	3.02	7/15/06 4:57 AM	29.68	43.0	41.14	2.46	1
m23e	3.10	7/15/06 4:58 AM	29.65	43.1	40.99	2.45	1
m23e	3.08	7/15/06 4:58 AM	29.64	43.1	41.07	2.46	1
m23e	3.14	7/15/06 4:58 AM	29.59	43.3	41.03	2.45	1
m23e	3.19	7/15/06 4:58 AM	29.54	43.5	40.39	2.41	1
m23e	3.29	7/15/06 4:59 AM	29.54	43.5	37.06	2.21	1
m23e	3.39	7/15/06 5:00 AM	29.49	43.6	33.50	2.00	1
m23e	3.44	7/15/06 5:00 AM	29.46	43.7	29.87	1.78	1
m23e	3.53	7/15/06 5:01 AM	29.43	43.8	26.79	1.60	1
m23e	3.61	7/15/06 5:01 AM	29.41	43.8	24.94	1.49	1
m23e	3.66	7/15/06 5:02 AM	29.41	43.8	22.90	1.37	1
m23e	3.59	7/15/06 5:02 AM	29.41	43.8	23.18	1.38	1
m23f	0.18	7/15/06 3:10 PM	30.99	39.2	90.99	5.49	1
m23f	0.16	7/15/06 3:11 PM	31.01	39.2	90.92	5.49	1
m23f	0.21	7/15/06 3:11 PM	31.02	39.2	90.82	5.48	1
m23f	0.57	7/15/06 3:11 PM	31.01	39.2	89.84	5.42	1
m23f	0.87	7/15/06 3:11 PM	30.99	39.3	90.29	5.45	1
m23f	1.20	7/15/06 3:12 PM	30.92	39.3	89.74	5.42	1
m23f	1.51	7/15/06 3:12 PM	30.82	39.4	88.72	5.36	1
m23f	1.84	7/15/06 3:12 PM	30.56	39.6	86.58	5.25	1
m23f	2.16	7/15/06 3:13 PM	30.32	39.8	85.54	5.20	1
m23f	2.42	7/15/06 3:13 PM	30.01	40.1	86.34	5.27	1
m23f	2.66	7/15/06 3:14 PM	29.91	40.6	83.42	5.08	1
m23f	2.89	7/15/06 3:14 PM	29.87	40.9	78.07	4.75	1
m23f	3.03	7/15/06 3:15 PM	29.84	41.2	73.67	4.48	1
m23f	3.19	7/15/06 3:15 PM	29.82	41.4	70.59	4.29	1
m23f	3.27	7/15/06 3:15 PM	29.69	42.2	54.00	3.27	1
m23f	3.41	7/15/06 3:17 PM	29.64	42.4	35.47	2.15	1
m23f	3.45	7/15/06 3:17 PM	29.60	42.6	28.59	1.73	1
m23f	3.53	7/15/06 3:18 PM	29.57	42.7	22.70	1.37	1
m23f	3.60	7/15/06 3:19 PM	29.56	42.8	16.94	1.02	1
m23f	3.71	7/15/06 3:20 PM	29.53	42.9	14.57	0.88	1
m23f	3.78	7/15/06 3:20 PM	29.53	43.0	13.54	0.81	1
m23f	3.84	7/15/06 3:20 PM	29.53	42.9	13.08	0.79	1
m23f	3.76	7/15/06 3:21 PM	29.53	42.9	13.35	0.80	1
m23g	0.11	7/16/06 12:05 AM	30.16	40.6	82.84	5.03	1
m23g	0.15	7/16/06 12:05 AM	30.16	40.6	82.93	5.03	1
m23g	0.56	7/16/06 12:05 AM	30.15	40.6	82.44	5.00	1
m23g	0.86	7/16/06 12:06 AM	30.16	40.6	82.96	5.04	1
m23g	1.19	7/16/06 12:06 AM	30.17	40.6	83.72	5.08	1
m23g	1.45	7/16/06 12:07 AM	30.16	40.6	81.85	4.97	1
m23g	1.76	7/16/06 12:07 AM	30.17	40.6	82.35	5.00	1

Profile	Depth m	Date Time	Temperature °C	Salinity PSS	DO Saturation %	Dissolved Oxygen mg/L	Circulator
m23g	2.06	7/16/06 12:08 AM	30.20	40.6	82.37	4.99	1
m23g	2.37	7/16/06 12:08 AM	30.17	40.6	81.74	4.96	1
m23g	2.49	7/16/06 12:09 AM	30.19	40.7	76.24	4.62	1
m23g	2.53	7/16/06 12:10 AM	30.18	40.8	74.89	4.54	1
m23g	2.59	7/16/06 12:10 AM	30.15	41.0	66.43	4.02	1
m23g	2.69	7/16/06 12:11 AM	30.10	41.2	60.70	3.67	1
m23g	2.83	7/16/06 12:12 AM	29.97	41.7	53.05	3.21	1
m23g	2.90	7/16/06 12:13 AM	29.95	41.8	48.68	2.94	1
m23g	2.99	7/16/06 12:14 AM	29.79	42.4	44.24	2.67	1
m23g	3.06	7/16/06 12:15 AM	29.76	42.6	41.99	2.53	1
m23g	3.13	7/16/06 12:15 AM	29.75	42.6	40.52	2.44	1
m23g	3.22	7/16/06 12:16 AM	29.71	42.8	35.34	2.13	1
m23g	3.28	7/16/06 12:16 AM	29.70	42.8	34.71	2.09	1
m23g	3.38	7/16/06 12:17 AM	29.67	42.9	32.49	1.96	1
m23g	3.38	7/16/06 12:17 AM	29.67	43.0	32.67	1.97	1
m23g	3.45	7/16/06 12:18 AM	29.62	43.1	26.10	1.57	1
m23g	3.50	7/16/06 12:18 AM	29.62	43.1	25.28	1.52	1
m23g	3.56	7/16/06 12:19 AM	29.62	43.1	24.11	1.45	1
m23g	3.68	7/16/06 12:20 AM	29.58	43.2	17.24	1.04	1
m23g	3.67	7/16/06 12:20 AM	29.60	43.2	20.32	1.22	1
m23g	3.83	7/16/06 12:21 AM	29.56	43.2	14.81	0.89	1
m23g	3.79	7/16/06 12:21 AM	29.54	43.2	13.18	0.79	1
m23h	0.13	7/16/06 6:51 AM	29.76	39.7	69.43	4.26	1
m23h	0.15	7/16/06 6:51 AM	29.75	39.7	69.48	4.26	1
m23h	0.55	7/16/06 6:52 AM	29.78	39.7	68.14	4.18	1
m23h	0.85	7/16/06 6:53 AM	29.78	39.7	66.95	4.11	1
m23h	1.18	7/16/06 6:53 AM	29.79	39.8	67.64	4.15	1
m23h	1.47	7/16/06 6:53 AM	29.77	39.9	69.44	4.26	1
m23h	1.79	7/16/06 6:54 AM	29.75	39.9	71.28	4.37	1
m23h	2.09	7/16/06 6:54 AM	29.86	40.1	68.86	4.21	1
m23h	2.21	7/16/06 6:55 AM	30.01	40.4	63.74	3.88	1
m23h	2.26	7/16/06 6:55 AM	30.05	40.4	63.51	3.86	1
m23h	2.29	7/16/06 6:55 AM	30.05	40.5	63.24	3.85	1
m23h	2.39	7/16/06 6:56 AM	30.03	40.6	63.86	3.88	1
m23h	2.46	7/16/06 6:56 AM	30.02	40.7	64.33	3.91	1
m23h	2.57	7/16/06 6:56 AM	30.00	40.8	64.06	3.89	1
m23h	2.61	7/16/06 6:57 AM	29.99	40.8	64.85	3.94	1
m23h	2.70	7/16/06 6:57 AM	29.96	40.9	65.10	3.96	1
m23h	2.77	7/16/06 6:57 AM	29.90	40.9	65.36	3.97	1
m23h	2.82	7/16/06 6:58 AM	29.88	41.0	64.94	3.95	1
m23h	2.91	7/16/06 6:58 AM	29.86	41.0	64.37	3.91	1
m23h	3.00	7/16/06 6:58 AM	29.83	41.1	63.58	3.87	1
m23h	3.08	7/16/06 6:59 AM	29.82	41.1	62.74	3.82	1
m23h	3.12	7/16/06 6:59 AM	29.80	41.2	62.19	3.78	1
m23h	3.22	7/16/06 7:00 AM	29.77	41.3	56.02	3.41	1
m23h	3.32	7/16/06 7:01 AM	29.71	41.6	37.15	2.25	1
m23h	3.36	7/16/06 7:01 AM	29.67	41.9	25.69	1.56	1
m23h	3.44	7/16/06 7:02 AM	29.65	42.1	18.72	1.13	1
m23h	3.50	7/16/06 7:03 AM	29.60	42.3	9.12	0.55	1

Profile	Depth m	Date Time	Temperature °C	Salinity PSS	DO Saturation %	Dissolved Oxygen mg/L	Circulator
m23h	3.62	7/16/06 7:04 AM	29.58	42.5	5.11	0.31	1
m23h	3.71	7/16/06 7:04 AM	29.57	42.4	4.63	0.28	1
m23h	3.72	7/16/06 7:04 AM	29.57	42.4	4.30	0.26	1
m23i	-0.01	7/16/06 2:39 PM	30.52	1.4	92.21	6.89	1
m23i	0.10	7/16/06 2:40 PM	31.69	38.9	94.46	5.64	1
m23i	0.54	7/16/06 2:40 PM	31.64	38.9	95.62	5.71	1
m23i	0.84	7/16/06 2:40 PM	31.63	39.0	95.95	5.73	1
m23i	1.14	7/16/06 2:41 PM	31.39	39.1	95.99	5.75	1
m23i	1.43	7/16/06 2:41 PM	31.22	39.1	96.20	5.78	1
m23i	1.76	7/16/06 2:41 PM	31.21	39.2	96.39	5.79	1
m23i	2.05	7/16/06 2:41 PM	31.13	39.2	96.24	5.79	1
m23i	2.04	7/16/06 2:42 PM	31.06	39.2	96.42	5.81	1
m23i	2.34	7/16/06 2:42 PM	30.93	39.3	97.74	5.89	1
m23i	2.63	7/16/06 2:42 PM	30.85	39.3	97.02	5.86	1
m23i	2.91	7/16/06 2:42 PM	30.75	39.3	96.66	5.85	1
m23i	3.24	7/16/06 2:43 PM	30.17	39.6	89.94	5.48	1
m23i	3.13	7/16/06 2:44 PM	30.44	39.3	94.91	5.77	1
m23i	3.19	7/16/06 2:44 PM	30.13	39.7	87.35	5.32	1
m23i	3.31	7/16/06 2:45 PM	29.85	40.1	79.01	4.82	1
m23i	3.55	7/16/06 2:45 PM	29.63	40.4	67.63	4.14	1
m23i	3.73	7/16/06 2:47 PM	29.62	40.4	59.98	3.67	1
m23i	3.77	7/16/06 2:47 PM	29.62	40.4	59.53	3.64	1
m24a	0.20	7/13/06 11:57 PM	29.82	39.9	84.56	5.17	1
m24a	0.18	7/13/06 11:57 PM	29.81	39.9	84.68	5.18	1
m24a	0.58	7/13/06 11:57 PM	29.82	39.9	85.24	5.21	1
m24a	0.90	7/13/06 11:57 PM	29.84	40.0	85.40	5.22	1
m24a	1.18	7/13/06 11:58 PM	29.85	40.0	85.79	5.24	1
m24a	1.45	7/13/06 11:58 PM	29.83	40.3	84.84	5.17	1
m24a	1.78	7/13/06 11:58 PM	29.82	41.8	79.40	4.80	1
m24a	1.65	7/13/06 11:59 PM	29.82	41.4	76.69	4.65	1
m24a	1.77	7/13/06 11:59 PM	29.81	41.8	72.71	4.40	1
m24a	1.93	7/14/06 12:00 AM	29.78	42.6	68.30	4.12	1
m24a	2.05	7/14/06 12:00 AM	29.73	42.9	63.97	3.85	1
m24a	2.25	7/14/06 12:01 AM	29.67	43.3	59.59	3.58	1
m24a	2.34	7/14/06 12:01 AM	29.59	43.6	52.90	3.18	1
m24a	2.51	7/14/06 12:02 AM	29.50	43.9	40.27	2.42	1
m24a	2.74	7/14/06 12:03 AM	29.39	44.2	29.92	1.79	1
m24a	2.87	7/14/06 12:04 AM	29.38	44.3	27.05	1.62	1
m24a	3.01	7/14/06 12:04 AM	29.37	44.4	26.99	1.62	1
m24a	2.94	7/14/06 12:04 AM	29.37	44.4	25.24	1.51	1
m24b	0.00	7/14/06 2:24 AM	27.55	40.7	87.19	5.50	1
m24b	0.07	7/14/06 2:24 AM	29.33	41.1	78.16	4.78	1
m24b	0.55	7/14/06 2:25 AM	29.35	41.1	76.31	4.67	1
m24b	0.82	7/14/06 2:25 AM	29.35	41.1	75.14	4.60	1
m24b	1.09	7/14/06 2:25 AM	29.36	41.2	74.76	4.57	1
m24b	1.52	7/14/06 2:26 AM	29.38	41.2	73.81	4.51	1
m24b	1.73	7/14/06 2:26 AM	29.61	42.2	69.19	4.19	1
m24b	1.90	7/14/06 2:26 AM	29.74	42.9	59.65	3.59	1
m24b	2.04	7/14/06 2:27 AM	29.68	43.3	55.74	3.35	1

Profile	Depth m	Date Time	Temperature °C	Salinity PSS	DO Saturation %	Dissolved Oxygen mg/L	Circulator
m24b	2.25	7/14/06 2:27 AM	29.64	43.4	50.22	3.02	1
m24b	2.37	7/14/06 2:27 AM	29.51	43.9	41.78	2.51	1
m24b	2.52	7/14/06 2:28 AM	29.44	44.3	33.57	2.01	1
m24b	2.64	7/14/06 2:29 AM	29.40	44.4	28.36	1.70	1
m24b	2.83	7/14/06 2:29 AM	29.37	44.5	24.26	1.45	1
m24b	2.94	7/14/06 2:29 AM	29.37	44.5	23.52	1.41	1
m24b	2.85	7/14/06 2:30 AM	29.37	44.5	22.52	1.35	1
m24c	0.29	7/14/06 3:15 PM	31.81	37.0	99.90	5.97	0
m24c	0.03	7/14/06 3:17 PM	30.37	41.0	79.95	4.78	1
m24c	0.50	7/14/06 3:17 PM	30.36	41.0	78.32	4.69	1
m24c	0.79	7/14/06 3:18 PM	30.37	41.0	78.31	4.69	1
m24c	1.12	7/14/06 3:18 PM	30.36	41.0	77.67	4.65	1
m24c	1.41	7/14/06 3:18 PM	30.37	41.0	77.54	4.64	1
m24c	1.70	7/14/06 3:19 PM	30.29	41.1	76.62	4.59	1
m24c	2.02	7/14/06 3:19 PM	30.17	41.2	73.61	4.42	1
m24c	2.33	7/14/06 3:20 PM	29.94	41.6	66.69	4.01	1
m24c	2.47	7/14/06 3:21 PM	29.79	41.9	61.66	3.70	1
m24c	2.64	7/14/06 3:21 PM	29.51	42.6	56.69	3.41	1
m24c	2.76	7/14/06 3:22 PM	29.36	43.4	40.81	2.45	1
m24c	2.94	7/14/06 3:23 PM	29.34	43.5	33.20	1.99	1
m24c	3.13	7/14/06 3:23 PM	29.32	43.5	28.76	1.72	1
m24c	3.10	7/14/06 3:24 PM	29.32	43.5	28.12	1.68	1
m24d	0.09	7/15/06 12:43 AM	28.67	0.0	100.02	7.72	1
m24d	0.08	7/15/06 12:45 AM	29.72	40.2	83.35	5.06	1
m24d	0.54	7/15/06 12:45 AM	29.74	40.2	82.22	4.99	1
m24d	0.85	7/15/06 12:45 AM	29.75	40.2	81.62	4.95	1
m24d	1.15	7/15/06 12:46 AM	29.78	40.3	80.34	4.87	1
m24d	1.42	7/15/06 12:46 AM	29.88	40.9	77.03	4.65	1
m24d	1.66	7/15/06 12:47 AM	29.88	41.5	68.88	4.14	1
m24d	1.76	7/15/06 12:48 AM	29.87	41.9	63.92	3.84	1
m24d	1.94	7/15/06 12:48 AM	29.80	42.2	57.15	3.43	1
m24d	2.09	7/15/06 12:49 AM	29.72	42.4	54.45	3.27	1
m24d	2.23	7/15/06 12:49 AM	29.66	42.5	50.91	3.05	1
m24d	2.41	7/15/06 12:50 AM	29.62	42.7	45.36	2.72	1
m24d	2.56	7/15/06 12:51 AM	29.60	42.8	40.31	2.42	1
m24d	2.72	7/15/06 12:51 AM	29.58	43.1	36.82	2.20	1
m24d	2.79	7/15/06 12:52 AM	29.50	43.5	30.12	1.80	1
m24d	2.96	7/15/06 12:53 AM	29.46	43.6	22.18	1.32	1
m24d	3.02	7/15/06 12:53 AM	29.45	43.6	22.60	1.35	1
m24d	2.94	7/15/06 12:53 AM	29.46	43.6	22.52	1.34	1
m24e	0.02	7/15/06 5:21 AM	27.52	40.4	86.17	5.42	1
m24e	0.14	7/15/06 5:21 AM	29.43	39.3	75.70	4.64	1
m24e	0.55	7/15/06 5:21 AM	29.42	39.3	75.01	4.60	1
m24e	0.87	7/15/06 5:22 AM	29.44	39.3	74.57	4.57	1
m24e	1.09	7/15/06 5:22 AM	29.59	39.5	71.56	4.37	1
m24e	1.18	7/15/06 5:23 AM	29.65	39.9	66.27	4.04	1
m24e	1.34	7/15/06 5:24 AM	29.73	40.3	59.84	3.63	1
m24e	1.32	7/15/06 5:24 AM	29.74	40.5	59.50	3.60	1
m24e	1.41	7/15/06 5:25 AM	29.75	40.6	57.05	3.46	1

Profile	Depth m	Date Time	Temperature °C	Salinity PSS	DO Saturation %	Dissolved Oxygen mg/L	Circulator
m24e	1.53	7/15/06 5:26 AM	29.79	40.8	54.09	3.27	1
m24e	1.60	7/15/06 5:26 AM	29.81	40.9	52.50	3.17	1
m24e	1.69	7/15/06 5:27 AM	29.81	40.9	51.11	3.09	1
m24e	1.71	7/15/06 5:28 AM	29.83	41.3	47.78	2.88	1
m24e	1.82	7/15/06 5:28 AM	29.83	41.6	44.65	2.68	1
m24e	1.90	7/15/06 5:29 AM	29.83	41.8	42.32	2.54	1
m24e	1.94	7/15/06 5:29 AM	29.82	41.9	41.30	2.48	1
m24e	2.01	7/15/06 5:30 AM	29.82	41.9	40.71	2.44	1
m24e	2.12	7/15/06 5:30 AM	29.80	42.0	40.02	2.40	1
m24e	2.15	7/15/06 5:31 AM	29.77	42.1	39.21	2.35	1
m24e	2.24	7/15/06 5:31 AM	29.73	42.2	39.30	2.36	1
m24e	2.34	7/15/06 5:32 AM	29.65	42.2	39.37	2.36	1
m24e	2.42	7/15/06 5:32 AM	29.61	42.2	39.51	2.37	1
m24e	2.43	7/15/06 5:32 AM	29.59	42.2	39.60	2.38	1
m24e	2.50	7/15/06 5:33 AM	29.55	42.3	39.68	2.39	1
m24e	2.54	7/15/06 5:33 AM	29.54	42.3	39.17	2.36	1
m24e	2.61	7/15/06 5:34 AM	29.51	42.4	36.97	2.22	1
m24e	2.73	7/15/06 5:34 AM	29.49	42.6	32.06	1.93	1
m24e	2.77	7/15/06 5:35 AM	29.49	42.7	28.24	1.70	1
m24e	2.83	7/15/06 5:35 AM	29.48	42.8	24.78	1.49	1
m24e	2.94	7/15/06 5:36 AM	29.45	43.0	19.55	1.17	1
m24e	3.00	7/15/06 5:36 AM	29.42	43.1	12.06	0.72	1
m24e	2.87	7/15/06 5:38 AM	29.46	42.9	20.07	1.20	1
m24f	0.14	7/15/06 2:43 PM	30.35	37.3	94.45	5.82	1
m24f	0.11	7/15/06 2:45 PM	30.31	37.2	99.13	6.11	1
m24f	0.05	7/15/06 2:46 PM	30.51	39.7	93.13	5.65	1
m24f	0.53	7/15/06 2:47 PM	30.50	39.7	92.77	5.63	1
m24f	0.86	7/15/06 2:47 PM	30.51	39.7	91.46	5.55	1
m24f	1.11	7/15/06 2:47 PM	30.51	39.7	91.89	5.57	1
m24f	1.53	7/15/06 2:48 PM	30.50	39.7	91.19	5.53	1
m24f	1.70	7/15/06 2:48 PM	30.50	39.8	91.18	5.53	1
m24f	2.09	7/15/06 2:49 PM	30.38	40.0	87.60	5.32	1
m24f	2.33	7/15/06 2:49 PM	30.18	40.3	86.50	5.26	1
m24f	2.52	7/15/06 2:50 PM	30.05	40.7	83.17	5.05	1
m24f	2.69	7/15/06 2:51 PM	29.88	41.1	66.87	4.06	1
m24f	2.83	7/15/06 2:51 PM	29.84	41.2	57.50	3.49	1
m24f	2.94	7/15/06 2:52 PM	29.52	41.6	40.65	2.48	1
m24f	3.09	7/15/06 2:52 PM	29.47	41.6	36.83	2.24	1
m24f	2.99	7/15/06 2:53 PM	29.49	41.6	42.39	2.58	1
m24g	0.16	7/15/06 11:34 PM	29.82	40.2	80.95	4.95	1
m24g	0.12	7/15/06 11:34 PM	29.86	40.3	82.31	5.03	1
m24g	0.53	7/15/06 11:35 PM	29.83	40.3	82.68	5.05	1
m24g	0.83	7/15/06 11:35 PM	29.85	40.3	82.36	5.03	1
m24g	1.14	7/15/06 11:36 PM	29.89	40.3	81.19	4.95	1
m24g	1.44	7/15/06 11:36 PM	30.00	40.5	79.92	4.86	1
m24g	1.61	7/15/06 11:37 PM	30.04	40.5	78.22	4.76	1
m24g	1.76	7/15/06 11:38 PM	30.12	40.8	75.82	4.60	1
m24g	1.86	7/15/06 11:39 PM	30.14	41.3	66.94	4.05	1
m24g	1.93	7/15/06 11:39 PM	30.13	41.4	63.97	3.87	1

Profile	Depth m	Date Time	Temperature °C	Salinity PSS	DO Saturation %	Dissolved Oxygen mg/L	Circulator
m24g	2.00	7/15/06 11:40 PM	30.03	41.8	54.14	3.27	1
m24g	2.07	7/15/06 11:41 PM	30.06	41.7	58.29	3.52	1
m24g	2.15	7/15/06 11:42 PM	30.01	41.8	51.27	3.10	1
m24g	2.20	7/15/06 11:43 PM	29.86	42.2	38.68	2.33	1
m24g	2.28	7/15/06 11:43 PM	29.85	42.2	37.95	2.29	1
m24g	2.38	7/15/06 11:44 PM	29.84	42.2	33.67	2.03	1
m24g	2.45	7/15/06 11:45 PM	29.77	42.3	29.88	1.80	1
m24g	2.54	7/15/06 11:45 PM	29.73	42.3	25.61	1.55	1
m24g	2.60	7/15/06 11:46 PM	29.72	42.4	23.90	1.44	1
m24g	2.68	7/15/06 11:47 PM	29.67	42.4	20.63	1.25	1
m24g	2.75	7/15/06 11:47 PM	29.67	42.4	18.55	1.12	1
m24g	2.78	7/15/06 11:48 PM	29.65	42.4	16.97	1.02	1
m24g	2.89	7/15/06 11:49 PM	29.64	42.4	16.42	0.99	1
m24g	2.99	7/15/06 11:49 PM	29.64	42.4	15.79	0.95	1
m24g	2.98	7/15/06 11:50 PM	29.64	42.3	15.88	0.96	1
m24g	3.09	7/15/06 11:50 PM	29.63	42.3	15.54	0.94	1
m24g	3.07	7/15/06 11:50 PM	29.63	42.4	15.01	0.91	1
m24h	0.15	7/16/06 7:43 AM	29.32	40.1	76.19	4.70	1
m24h	0.13	7/16/06 7:43 AM	29.36	40.2	73.61	4.53	1
m24h	0.61	7/16/06 7:44 AM	29.37	40.2	72.33	4.45	1
m24h	0.89	7/16/06 7:44 AM	29.39	40.3	70.05	4.31	1
m24h	1.20	7/16/06 7:45 AM	29.40	40.4	68.57	4.22	1
m24h	1.40	7/16/06 7:45 AM	29.42	40.5	65.15	4.00	1
m24h	1.53	7/16/06 7:45 AM	29.44	40.6	63.74	3.91	1
m24h	1.65	7/16/06 7:46 AM	29.45	40.7	61.56	3.77	1
m24h	1.69	7/16/06 7:46 AM	29.45	40.7	61.29	3.76	1
m24h	1.80	7/16/06 7:46 AM	29.46	40.7	60.91	3.73	1
m24h	1.98	7/16/06 7:47 AM	29.46	40.7	60.14	3.69	1
m24h	2.13	7/16/06 7:47 AM	29.49	40.9	56.00	3.43	1
m24h	2.30	7/16/06 7:48 AM	29.49	40.9	54.53	3.34	1
m24h	2.43	7/16/06 7:48 AM	29.50	41.0	52.16	3.19	1
m24h	2.62	7/16/06 7:49 AM	29.54	41.2	36.47	2.22	1
m24h	2.75	7/16/06 7:50 AM	29.55	41.3	31.96	1.95	1
m24h	2.84	7/16/06 7:50 AM	29.56	41.3	30.59	1.86	1
m24h	3.02	7/16/06 7:51 AM	29.56	41.4	28.50	1.73	1
m24h	3.03	7/16/06 7:51 AM	29.56	41.4	28.64	1.74	1
m24i	0.19	7/16/06 2:24 PM	31.47	38.6	92.44	5.55	1
m24i	0.12	7/16/06 2:24 PM	31.47	38.6	94.17	5.65	1
m24i	0.57	7/16/06 2:25 PM	31.47	38.6	97.06	5.82	1
m24i	0.85	7/16/06 2:25 PM	31.45	38.6	97.12	5.83	1
m24i	1.16	7/16/06 2:25 PM	31.42	38.6	97.45	5.85	1
m24i	1.43	7/16/06 2:25 PM	31.41	38.6	97.06	5.83	1
m24i	1.76	7/16/06 2:25 PM	31.38	38.6	97.44	5.86	1
m24i	2.07	7/16/06 2:26 PM	31.40	38.6	96.90	5.82	1
m24i	2.36	7/16/06 2:26 PM	31.23	38.6	97.80	5.89	1
m24i	2.52	7/16/06 2:26 PM	31.13	38.6	95.10	5.74	1
m24i	2.59	7/16/06 2:27 PM	30.97	38.7	94.53	5.71	1
m24i	2.70	7/16/06 2:27 PM	30.68	39.5	87.47	5.29	1
m24i	2.82	7/16/06 2:28 PM	30.36	39.9	80.59	4.89	1

Profile	Depth m	Date Time	Temperature °C	Salinity PSS	DO Saturation %	Dissolved Oxygen mg/L	Circulator
m24i	2.95	7/16/06 2:29 PM	30.23	40.0	74.70	4.54	1
m24i	3.04	7/16/06 2:30 PM	30.16	40.1	68.37	4.15	1
m24j	0.09	7/16/06 5:57 PM	31.90	37.7	96.98	5.81	1
m24j	0.07	7/16/06 5:57 PM	31.91	37.7	98.06	5.87	1
m24j	0.53	7/16/06 5:57 PM	31.92	37.7	99.98	5.99	1
m24j	0.53	7/16/06 5:58 PM	31.92	37.7	100.79	6.04	1
m24j	0.83	7/16/06 5:58 PM	31.92	37.8	101.00	6.05	1
m24j	1.13	7/16/06 5:59 PM	31.91	37.8	102.23	6.12	1
m24j	1.45	7/16/06 5:59 PM	31.89	37.8	102.34	6.13	1
m24j	1.76	7/16/06 5:59 PM	31.94	38.3	103.50	6.18	1
m24j	2.07	7/16/06 6:00 PM	31.65	38.6	102.32	6.12	1
m24j	2.20	7/16/06 6:00 PM	31.18	38.8	97.11	5.85	1
m24j	2.35	7/16/06 6:01 PM	31.00	39.0	93.42	5.64	1
m24j	2.50	7/16/06 6:02 PM	30.88	39.3	89.54	5.40	1
m24j	2.65	7/16/06 6:02 PM	30.85	39.4	86.91	5.24	1
m24j	2.80	7/16/06 6:03 PM	30.81	39.5	80.01	4.83	1
m24j	2.87	7/16/06 6:04 PM	30.73	39.6	76.07	4.59	1
m24j	3.01	7/16/06 6:05 PM	30.57	39.8	61.05	3.69	1
m26e	0.11	7/15/06 6:29 AM	29.47	38.6	76.46	4.70	1
m26e	0.11	7/15/06 6:29 AM	29.47	38.6	75.76	4.66	1
m26e	0.58	7/15/06 6:30 AM	29.50	38.7	75.04	4.61	1
m26e	0.89	7/15/06 6:30 AM	29.49	38.7	74.14	4.56	1
m26e	1.18	7/15/06 6:30 AM	29.55	38.8	73.01	4.48	1
m26e	1.52	7/15/06 6:31 AM	29.53	39.0	70.23	4.31	1
m26e	1.75	7/15/06 6:31 AM	29.41	39.3	67.06	4.11	1
m26e	2.09	7/15/06 6:32 AM	29.25	39.8	61.05	3.74	1
m26e	2.25	7/15/06 6:33 AM	29.28	40.7	47.85	2.92	1
m26e	2.43	7/15/06 6:34 AM	29.38	41.7	33.86	2.05	1
m26e	2.55	7/15/06 6:35 AM	29.44	41.9	28.78	1.74	1
m26e	2.69	7/15/06 6:35 AM	29.52	42.5	22.13	1.33	1
m26e	2.85	7/15/06 6:36 AM	29.52	42.8	14.61	0.87	1
m26e	3.00	7/15/06 6:37 AM	29.48	43.2	6.21	0.37	1
m26e	3.18	7/15/06 6:38 AM	29.42	43.3	2.59	0.15	1
m26e	3.25	7/15/06 6:38 AM	29.42	43.3	2.19	0.13	1
m70c	-0.01	7/14/06 5:11 PM	30.75	41.4	84.57	5.02	1
m70c	0.11	7/14/06 5:11 PM	30.53	38.4	90.64	5.49	1
m70c	0.54	7/14/06 5:11 PM	30.53	38.5	91.00	5.51	1
m70c	0.92	7/14/06 5:12 PM	30.53	38.5	81.97	4.96	1
m70c	1.07	7/14/06 5:12 PM	30.53	38.5	87.06	5.27	1
m70c	1.41	7/14/06 5:13 PM	30.52	38.5	88.94	5.38	1
m70c	1.78	7/14/06 5:13 PM	30.52	38.5	89.50	5.42	1
m70c	2.03	7/14/06 5:13 PM	30.50	38.5	89.72	5.43	1
m70c	1.99	7/14/06 5:13 PM	30.49	38.5	89.09	5.40	1
m70c	2.28	7/14/06 5:13 PM	30.47	38.5	89.82	5.44	1
m70c	2.66	7/14/06 5:14 PM	30.42	38.6	88.94	5.39	1
m70c	2.89	7/14/06 5:14 PM	29.99	39.0	84.89	5.17	1
m70c	3.12	7/14/06 5:14 PM	29.78	39.1	74.37	4.54	1
m70c	3.19	7/14/06 5:14 PM	29.77	39.1	72.10	4.40	1
m70c	3.42	7/14/06 5:15 PM	29.77	39.2	70.69	4.31	1

Profile	Depth m	Date Time	Temperature °C	Salinity PSS	DO Saturation %	Dissolved Oxygen mg/L	Circulator
m70c	3.57	7/14/06 5:15 PM	29.75	39.4	68.10	4.15	1
m70c	3.67	7/14/06 5:16 PM	29.67	40.0	54.03	3.29	1
m70c	3.76	7/14/06 5:16 PM	29.63	40.5	45.59	2.77	1
m70c	3.80	7/14/06 5:17 PM	29.50	41.9	27.84	1.68	1
m70c	3.82	7/14/06 5:17 PM	29.36	43.3	16.70	1.00	1
m70c	4.00	7/14/06 5:17 PM	29.32	43.8	10.21	0.61	1
m70c	4.00	7/14/06 5:17 PM	29.31	43.8	5.46	0.32	1
m70c	4.13	7/14/06 5:18 PM	29.31	43.7	4.30	0.25	1
m70c	3.94	7/14/06 5:18 PM	29.31	43.8	3.73	0.22	1
w60a	0.00	7/13/06 9:28 PM	29.13	40.3	95.88	5.91	1
w60a	0.10	7/13/06 9:29 PM	31.17	40.2	98.53	5.89	1
w60a	0.57	7/13/06 9:29 PM	31.19	40.2	99.99	5.97	1
w60a	0.76	7/13/06 9:30 PM	31.15	40.2	96.74	5.78	1
w61a	0.02	7/13/06 9:08 PM	30.09	39.4	85.13	5.20	1
w61a	0.56	7/13/06 9:08 PM	30.14	39.4	80.74	4.92	1
w61a	0.84	7/13/06 9:09 PM	30.16	39.4	80.62	4.91	1
w61a	0.09	7/13/06 9:09 PM	30.13	39.4	80.56	4.91	1
w62a	0.03	7/13/06 9:38 PM	28.99	40.3	95.44	5.90	1
w62a	0.12	7/13/06 9:39 PM	30.33	39.6	93.16	5.66	1
w62a	0.54	7/13/06 9:39 PM	30.39	39.7	92.19	5.59	1
w62a	0.86	7/13/06 9:40 PM	30.40	39.7	91.50	5.55	1
w62a	1.18	7/13/06 9:40 PM	30.47	39.8	91.94	5.57	1
w62a	1.51	7/13/06 9:40 PM	30.60	39.9	93.55	5.65	1
w62a	1.79	7/13/06 9:41 PM	30.72	40.1	94.81	5.71	1
w63a	0.10	7/13/06 9:52 PM	29.98	38.8	85.40	5.24	1
w63a	0.11	7/13/06 9:52 PM	29.98	38.8	85.02	5.21	1
w63a	0.56	7/13/06 9:52 PM	29.99	38.8	84.05	5.15	1
w63a	1.12	7/13/06 9:53 PM	30.00	38.8	83.46	5.12	1
w63a	1.77	7/13/06 9:53 PM	29.92	40.0	72.76	4.44	1
w63a	2.06	7/13/06 9:54 PM	29.76	40.8	49.84	3.03	1
w63a	2.31	7/13/06 9:54 PM	29.66	41.0	43.70	2.66	1
w63a	2.66	7/13/06 9:56 PM	29.59	41.8	28.25	1.71	1
w63a	2.90	7/13/06 9:56 PM	29.49	43.2	18.47	1.11	1
w63a	3.25	7/13/06 9:57 PM	29.35	43.7	4.17	0.25	1
w63a	3.53	7/13/06 9:58 PM	29.34	43.8	2.53	0.15	1
w63a	3.25	7/13/06 9:58 PM	29.35	43.7	2.13	0.12	1
w63a	3.00	7/13/06 9:59 PM	29.47	43.3	9.64	0.58	1
w63a	2.69	7/13/06 10:00 PM	29.55	42.3	21.43	1.29	1
w63a	2.40	7/13/06 10:01 PM	29.66	41.0	32.61	1.98	1
w63a	2.14	7/13/06 10:02 PM	29.76	40.7	45.66	2.78	1
w63a	1.81	7/13/06 10:02 PM	29.89	39.9	58.36	3.56	1
w63a	1.52	7/13/06 10:03 PM	29.96	39.2	72.64	4.45	1
w63a	1.23	7/13/06 10:04 PM	29.96	38.9	79.63	4.88	1
w63a	0.91	7/13/06 10:04 PM	29.96	38.9	81.07	4.97	1
w63a	0.63	7/13/06 10:05 PM	29.96	38.9	81.59	5.00	1
w63a	0.27	7/13/06 10:05 PM	29.95	38.9	82.53	5.06	1
w64a	0.03	7/13/06 10:15 PM	28.52	40.4	94.05	5.85	1
w64a	0.13	7/13/06 10:15 PM	29.85	39.3	82.47	5.06	1
w64a	0.60	7/13/06 10:16 PM	29.86	39.3	80.66	4.94	1

Profile	Depth m	Date Time	Temperature °C	Salinity PSS	DO Saturation %	Dissolved Oxygen mg/L	Circulator
w64a	0.85	7/13/06 10:16 PM	29.87	39.3	80.35	4.92	1
w64a	1.16	7/13/06 10:17 PM	30.05	39.6	80.09	4.89	1
w64a	1.42	7/13/06 10:17 PM	30.22	39.8	81.56	4.96	1
w64a	1.72	7/13/06 10:17 PM	30.09	39.9	77.69	4.73	1
w64a	1.96	7/13/06 10:19 PM	29.88	40.1	57.69	3.52	1
w64a	2.05	7/13/06 10:19 PM	29.76	40.2	49.03	2.99	1
w64a	2.15	7/13/06 10:20 PM	29.78	40.1	49.35	3.01	1
w64a	2.02	7/13/06 10:20 PM	29.78	40.1	48.70	2.97	1
w64a	2.02	7/13/06 10:21 PM	29.76	40.2	47.56	2.90	1
w64a	1.78	7/13/06 10:22 PM	30.01	40.0	64.15	3.91	1
w64a	1.44	7/13/06 10:22 PM	30.21	39.9	74.98	4.55	1
w64a	1.20	7/13/06 10:23 PM	30.33	40.0	82.77	5.02	1
w64a	0.84	7/13/06 10:23 PM	30.24	39.9	82.74	5.02	1
w64a	0.56	7/13/06 10:24 PM	29.93	39.4	81.62	4.99	1
w64a	0.28	7/13/06 10:24 PM	29.84	39.3	80.28	4.92	1
w70d	0.12	7/15/06 2:49 AM	29.96	38.8	83.93	5.12	1
w70d	0.10	7/15/06 2:49 AM	29.95	38.8	83.95	5.12	1
w70d	0.57	7/15/06 2:49 AM	29.96	38.8	82.94	5.06	1
w70d	0.87	7/15/06 2:49 AM	29.95	38.8	82.81	5.05	1
w70d	1.19	7/15/06 2:50 AM	29.97	38.8	82.89	5.05	1
w70d	1.48	7/15/06 2:50 AM	29.97	38.8	83.31	5.08	1
w70d	1.79	7/15/06 2:51 AM	29.96	38.8	83.39	5.08	1
w70d	2.07	7/15/06 2:51 AM	29.98	38.8	83.28	5.08	1
w70d	2.39	7/15/06 2:51 AM	29.99	38.8	82.54	5.03	1
w70d	2.66	7/15/06 2:52 AM	29.99	38.9	82.51	5.03	1
w70d	2.96	7/15/06 2:52 AM	30.00	39.0	81.07	4.93	1
w70d	3.17	7/15/06 2:53 AM	29.98	39.4	69.87	4.25	1
w70d	3.14	7/15/06 2:53 AM	29.97	39.5	67.67	4.11	1
w70d	3.20	7/15/06 2:54 AM	29.91	39.9	56.55	3.43	1
w70d	3.28	7/15/06 2:55 AM	29.85	40.5	46.60	2.82	1
w70d	3.37	7/15/06 2:56 AM	29.71	41.8	26.26	1.58	1
w70d	3.44	7/15/06 2:58 AM	29.61	43.1	14.80	0.88	1
w70d	3.51	7/15/06 2:58 AM	29.57	43.6	10.89	0.65	1
w70d	3.63	7/15/06 2:59 AM	29.55	43.8	7.63	0.45	1
w70d	3.69	7/15/06 3:00 AM	29.52	44.0	3.90	0.23	1
w70d	3.74	7/15/06 3:00 AM	29.51	44.0	3.26	0.19	1
w70d	3.78	7/15/06 3:01 AM	29.49	44.1	1.85	0.11	1
w70d	3.91	7/15/06 3:01 AM	29.48	44.1	1.46	0.08	1
w70d	4.02	7/15/06 3:02 AM	29.48	44.0	1.17	0.07	1
w70d	3.89	7/15/06 3:02 AM	29.48	44.1	1.11	0.06	1
w70g	0.15	7/16/06 1:57 AM	30.21	39.1	81.46	4.98	1
w70g	0.07	7/16/06 1:57 AM	30.23	39.1	82.77	5.06	1
w70g	0.24	7/16/06 1:58 AM	30.25	39.1	83.34	5.09	1
w70g	0.56	7/16/06 1:58 AM	30.25	39.1	82.93	5.07	1
w70g	0.85	7/16/06 1:59 AM	30.25	39.1	83.44	5.10	1
w70g	1.16	7/16/06 1:59 AM	30.25	39.1	82.76	5.06	1
w70g	1.47	7/16/06 1:59 AM	30.25	39.1	83.45	5.10	1
w70g	1.76	7/16/06 2:00 AM	30.25	39.1	83.64	5.11	1
w70g	2.05	7/16/06 2:00 AM	30.25	39.1	82.97	5.07	1

Profile	Depth m	Date Time	Temperature °C	Salinity PSS	DO Saturation %	Dissolved Oxygen mg/L	Circulator
w70g	2.43	7/16/06 2:01 AM	30.26	39.2	82.62	5.04	1
w70g	2.51	7/16/06 2:02 AM	30.24	39.4	78.01	4.76	1
w70g	2.59	7/16/06 2:02 AM	30.21	39.5	71.23	4.34	1
w70g	2.70	7/16/06 2:04 AM	30.11	40.0	60.73	3.70	1
w70g	2.76	7/16/06 2:05 AM	30.05	40.3	54.42	3.31	1
w70g	2.82	7/16/06 2:06 AM	30.01	40.4	48.93	2.98	1
w70g	2.91	7/16/06 2:07 AM	29.92	41.0	42.38	2.57	1
w70g	3.02	7/16/06 2:08 AM	29.87	41.4	35.51	2.15	1
w70g	3.05	7/16/06 2:09 AM	29.86	41.7	33.24	2.01	1
w70g	3.14	7/16/06 2:09 AM	29.84	42.0	32.45	1.96	1
w70g	3.23	7/16/06 2:10 AM	29.82	42.2	32.70	1.97	1
w70g	3.29	7/16/06 2:10 AM	29.80	42.3	34.08	2.06	1
w70g	3.40	7/16/06 2:11 AM	29.79	42.5	35.34	2.13	1
w70g	3.43	7/16/06 2:12 AM	29.76	42.7	33.88	2.04	1
w70g	3.43	7/16/06 2:12 AM	29.76	42.7	33.81	2.04	1
w70g	3.48	7/16/06 2:13 AM	29.71	43.0	30.50	1.84	1
w70g	3.55	7/16/06 2:13 AM	29.67	43.4	28.94	1.74	1
w70g	3.63	7/16/06 2:14 AM	29.63	43.5	26.33	1.58	1
w70g	3.73	7/16/06 2:14 AM	29.60	43.6	19.11	1.15	1
w70g	3.80	7/16/06 2:16 AM	29.55	43.8	6.46	0.38	1
w70g	3.86	7/16/06 2:17 AM	29.53	43.8	4.67	0.28	1
w70g	3.97	7/16/06 2:17 AM	29.49	43.9	1.89	0.11	1
w70g	4.06	7/16/06 2:18 AM	29.48	43.9	1.37	0.08	1
w70g	3.92	7/16/06 2:18 AM	29.50	43.8	1.25	0.07	1
w71a	0.11	7/14/06 12:47 AM	29.71	41.5	75.89	4.60	1
w71a	0.18	7/14/06 12:48 AM	29.72	41.5	76.28	4.63	1
w71a	0.58	7/14/06 12:48 AM	29.72	41.6	76.51	4.64	1
w71a	0.88	7/14/06 12:48 AM	29.74	41.6	76.58	4.64	1
w71a	1.17	7/14/06 12:49 AM	29.74	41.6	75.95	4.60	1
w71a	1.43	7/14/06 12:49 AM	29.74	41.6	75.78	4.59	1
w71a	1.63	7/14/06 12:50 AM	29.78	42.7	64.07	3.86	1
w71a	1.85	7/14/06 12:51 AM	29.77	42.8	61.83	3.72	1
w71a	1.93	7/14/06 12:51 AM	29.76	43.1	56.16	3.38	1
w71a	2.05	7/14/06 12:53 AM	29.76	43.2	45.22	2.72	1
w71a	2.26	7/14/06 12:54 AM	29.75	43.5	31.12	1.86	1
w71a	2.42	7/14/06 12:54 AM	29.75	43.5	28.53	1.71	1
w71a	2.32	7/14/06 12:54 AM	29.75	43.5	27.47	1.64	1
w72a	0.04	7/14/06 1:13 AM	27.73	40.6	84.28	5.31	1
w72a	0.12	7/14/06 1:13 AM	29.61	42.0	76.81	4.66	1
w72a	0.62	7/14/06 1:14 AM	29.65	42.1	70.59	4.27	1
w72a	0.87	7/14/06 1:14 AM	29.66	42.1	69.67	4.22	1
w72a	1.19	7/14/06 1:14 AM	29.68	42.1	69.48	4.20	1
w72a	1.45	7/14/06 1:15 AM	29.67	42.2	68.54	4.15	1
w72a	1.68	7/14/06 1:15 AM	29.66	42.2	67.88	4.11	1
w73d	0.11	7/15/06 4:12 AM	29.89	39.1	83.08	5.06	1
w73d	0.11	7/15/06 4:12 AM	29.88	39.2	83.68	5.10	1
w73d	0.56	7/15/06 4:12 AM	29.90	39.2	84.62	5.15	1
w73d	0.91	7/15/06 4:13 AM	29.91	39.2	84.48	5.14	1
w73d	1.21	7/15/06 4:13 AM	29.91	39.2	84.59	5.15	1

Profile	Depth m	Date Time	Temperature °C	Salinity PSS	DO Saturation %	Dissolved Oxygen mg/L	Circulator
w73d	1.50	7/15/06 4:13 AM	29.92	39.2	84.39	5.14	1
w73d	1.77	7/15/06 4:13 AM	29.93	39.2	84.52	5.14	1
w73d	2.08	7/15/06 4:14 AM	29.93	39.2	85.17	5.18	1
w73d	2.34	7/15/06 4:14 AM	29.94	39.2	85.72	5.22	1
w73d	2.69	7/15/06 4:14 AM	29.96	39.3	85.29	5.19	1
w73d	3.03	7/15/06 4:14 AM	29.97	39.3	85.57	5.20	1
w73d	3.29	7/15/06 4:15 AM	29.98	39.3	86.42	5.25	1
w73d	3.57	7/15/06 4:15 AM	30.01	39.4	83.93	5.10	1
w73d	3.71	7/15/06 4:16 AM	30.00	39.7	66.18	4.01	1
w73d	3.76	7/15/06 4:17 AM	29.81	40.7	40.43	2.44	1
w73d	3.84	7/15/06 4:18 AM	29.66	42.4	23.66	1.42	1
w73d	3.92	7/15/06 4:18 AM	29.44	43.7	5.40	0.32	1
w73d	3.96	7/15/06 4:19 AM	29.44	43.7	3.98	0.23	1
w73d	3.76	7/15/06 4:19 AM	29.49	43.5	3.90	0.23	1
w73g	0.16	7/16/06 3:17 AM	30.24	38.9	80.52	4.93	1
w73g	0.17	7/16/06 3:17 AM	30.25	38.9	80.45	4.92	1
w73g	0.60	7/16/06 3:18 AM	30.25	38.9	80.27	4.91	1
w73g	0.87	7/16/06 3:18 AM	30.26	38.9	80.82	4.94	1
w73g	1.13	7/16/06 3:19 AM	30.26	38.9	81.06	4.96	1
w73g	1.45	7/16/06 3:19 AM	30.26	38.9	81.40	4.98	1
w73g	1.76	7/16/06 3:19 AM	30.27	38.9	81.25	4.97	1
w73g	2.05	7/16/06 3:19 AM	30.27	38.9	80.96	4.95	1
w73g	2.33	7/16/06 3:20 AM	30.27	38.9	80.16	4.90	1
w73g	2.56	7/16/06 3:21 AM	30.28	39.0	74.82	4.57	1
w73g	2.70	7/16/06 3:21 AM	30.25	39.3	65.30	3.98	1
w73g	2.76	7/16/06 3:22 AM	30.21	39.5	53.63	3.27	1
w73g	2.85	7/16/06 3:23 AM	30.11	40.1	45.80	2.79	1
w73g	2.92	7/16/06 3:24 AM	30.00	40.4	42.36	2.58	1
w73g	2.99	7/16/06 3:24 AM	29.92	40.9	34.80	2.11	1
w73g	3.09	7/16/06 3:25 AM	29.92	41.1	31.53	1.91	1
w73g	3.16	7/16/06 3:26 AM	29.86	41.8	27.01	1.63	1
w73g	3.15	7/16/06 3:26 AM	29.85	41.9	25.03	1.51	1
w73g	3.22	7/16/06 3:27 AM	29.84	42.1	24.29	1.47	1
w73g	3.29	7/16/06 3:27 AM	29.79	42.5	24.66	1.49	1
w73g	3.37	7/16/06 3:28 AM	29.77	42.7	25.06	1.51	1
w73g	3.44	7/16/06 3:28 AM	29.73	42.9	25.31	1.52	1
w73g	3.52	7/16/06 3:29 AM	29.66	43.3	19.81	1.19	1
w73g	3.58	7/16/06 3:30 AM	29.57	43.6	9.08	0.54	1
w73g	3.68	7/16/06 3:31 AM	29.56	43.6	6.95	0.41	1
w73g	3.74	7/16/06 3:31 AM	29.55	43.7	4.20	0.25	1
w73g	3.82	7/16/06 3:32 AM	29.53	43.7	2.46	0.14	1
w73g	3.88	7/16/06 3:32 AM	29.53	43.7	1.63	0.09	1
w73g	4.03	7/16/06 3:32 AM	29.53	43.6	1.42	0.08	1
w73g	4.01	7/16/06 3:32 AM	29.53	43.5	1.48	0.08	1
w73g	3.83	7/16/06 3:33 AM	29.53	43.7	1.28	0.07	1
w74a	0.17	7/14/06 1:52 AM	29.15	42.5	72.68	4.42	1
w74a	0.11	7/14/06 1:52 AM	29.15	42.5	70.76	4.31	1
w74a	0.57	7/14/06 1:53 AM	29.17	42.6	68.76	4.18	1
w74a	0.55	7/14/06 1:53 AM	29.17	42.6	68.64	4.18	1

Profile	Depth m	Date Time	Temperature °C	Salinity PSS	DO Saturation %	Dissolved Oxygen mg/L	Circulator
w74a	0.82	7/14/06 1:53 AM	29.16	42.6	68.15	4.15	1
w74a	1.14	7/14/06 1:53 AM	29.16	42.6	66.69	4.06	1
w74a	1.46	7/14/06 1:54 AM	29.16	42.6	65.69	4.00	1
w74a	1.70	7/14/06 1:55 AM	29.30	42.8	55.68	3.38	1
w74a	1.81	7/14/06 1:55 AM	29.39	43.2	49.72	3.00	1
w74a	1.74	7/14/06 1:55 AM	29.37	43.1	47.66	2.88	1
w75a	0.08	7/14/06 2:08 AM	29.39	42.0	73.38	4.46	1
w75a	0.13	7/14/06 2:08 AM	29.40	42.1	69.52	4.23	1
w75a	0.56	7/14/06 2:09 AM	29.40	42.1	66.52	4.04	1
w75a	0.86	7/14/06 2:09 AM	29.41	42.1	65.75	3.99	1
w75a	0.90	7/14/06 2:09 AM	29.41	42.1	65.05	3.95	1
w75a	1.16	7/14/06 2:10 AM	29.43	42.2	63.92	3.88	1
w75a	1.41	7/14/06 2:10 AM	29.41	42.2	62.99	3.83	1
w75a	1.70	7/14/06 2:11 AM	29.49	42.9	54.69	3.30	1
w75a	1.94	7/14/06 2:11 AM	29.49	43.6	40.60	2.44	1
w75a	2.04	7/14/06 2:12 AM	29.48	43.8	32.80	1.97	1
w75a	2.21	7/14/06 2:12 AM	29.48	43.8	30.27	1.82	1
w75a	2.27	7/14/06 2:12 AM	29.48	43.8	28.90	1.74	1
w75a	2.21	7/14/06 2:13 AM	29.48	43.8	28.68	1.72	1
w75a	2.19	7/14/06 2:13 AM	29.48	43.8	27.98	1.68	1
w76e	0.12	7/15/06 6:10 AM	29.30	39.2	73.10	4.49	1
w76e	0.13	7/15/06 6:10 AM	29.31	39.2	73.01	4.49	1
w76e	0.57	7/15/06 6:11 AM	29.34	39.2	71.81	4.41	1
w76e	0.86	7/15/06 6:11 AM	29.35	39.2	70.82	4.35	1
w76e	1.20	7/15/06 6:11 AM	29.43	39.4	68.61	4.20	1
w76e	1.48	7/15/06 6:12 AM	29.34	39.5	68.62	4.21	1
w76e	1.65	7/15/06 6:12 AM	29.34	39.7	64.93	3.98	1
w76e	1.80	7/15/06 6:13 AM	29.36	39.9	61.14	3.74	1
w76e	1.93	7/15/06 6:13 AM	29.28	40.0	59.51	3.64	1
w76e	2.10	7/15/06 6:14 AM	29.22	40.3	56.77	3.47	1
w76e	2.25	7/15/06 6:14 AM	29.16	40.7	55.99	3.42	1
w76e	2.43	7/15/06 6:15 AM	29.20	41.1	49.07	2.99	1
w76e	2.53	7/15/06 6:16 AM	29.34	41.6	42.56	2.58	1
w76e	2.70	7/15/06 6:17 AM	29.50	42.3	29.62	1.78	1
w76e	2.85	7/15/06 6:18 AM	29.50	42.8	18.77	1.12	1
w76e	2.94	7/15/06 6:19 AM	29.47	43.0	9.27	0.55	1
w76e	3.01	7/15/06 6:20 AM	29.47	43.0	9.13	0.54	1
w76h	0.13	7/16/06 7:18 AM	29.42	40.7	74.11	4.55	1
w76h	0.13	7/16/06 7:18 AM	29.41	40.7	74.05	4.54	1
w76h	0.62	7/16/06 7:18 AM	29.43	40.7	73.92	4.53	1
w76h	0.95	7/16/06 7:18 AM	29.44	40.7	73.94	4.54	1
w76h	1.20	7/16/06 7:19 AM	29.45	40.7	73.68	4.52	1
w76h	1.51	7/16/06 7:19 AM	29.48	40.8	72.88	4.46	1
w76h	1.82	7/16/06 7:19 AM	29.50	40.9	72.67	4.45	1
w76h	2.10	7/16/06 7:20 AM	29.52	41.0	70.26	4.30	1
w76h	2.27	7/16/06 7:20 AM	29.49	41.0	65.34	4.00	1
w76h	2.41	7/16/06 7:21 AM	29.46	41.1	62.51	3.82	1
w76h	2.60	7/16/06 7:22 AM	29.37	41.2	52.15	3.19	1
w76h	2.71	7/16/06 7:22 AM	29.37	41.3	46.09	2.82	1

Profile	Depth m	Date Time	Temperature °C	Salinity PSS	DO Saturation %	Dissolved Oxygen mg/L	Circulator
w76h	2.86	7/16/06 7:23 AM	29.38	41.3	45.12	2.76	1
w76h	3.04	7/16/06 7:23 AM	29.37	41.3	43.93	2.69	1
w76h	3.09	7/16/06 7:23 AM	29.37	41.3	43.69	2.67	1
w77e	0.02	7/15/06 7:09 AM	27.46	40.5	82.53	5.19	1
w77e	0.13	7/15/06 7:10 AM	29.31	39.1	72.21	4.44	1
w77e	0.60	7/15/06 7:10 AM	29.32	39.1	71.72	4.41	1
w77e	0.89	7/15/06 7:11 AM	29.32	39.2	71.48	4.39	1
w77e	1.19	7/15/06 7:11 AM	29.30	39.3	70.81	4.35	1
w77e	1.49	7/15/06 7:11 AM	29.21	39.4	70.17	4.31	1
w77e	1.65	7/15/06 7:12 AM	29.25	39.7	66.31	4.07	1
w77e	1.79	7/15/06 7:13 AM	29.33	40.0	57.08	3.49	1
w77e	1.97	7/15/06 7:13 AM	29.43	40.5	50.17	3.05	1
w77e	2.10	7/15/06 7:14 AM	29.43	40.7	48.04	2.92	1
w77e	2.27	7/15/06 7:14 AM	29.31	41.1	48.09	2.92	1
w77e	2.42	7/15/06 7:15 AM	29.35	41.4	45.40	2.75	1
w77e	2.58	7/15/06 7:15 AM	29.47	41.9	39.86	2.41	1
w77e	2.75	7/15/06 7:16 AM	29.51	42.1	35.66	2.15	1
w77e	2.86	7/15/06 7:17 AM	29.49	42.3	28.93	1.74	1
w77e	3.01	7/15/06 7:17 AM	29.45	42.6	17.30	1.04	1
w77e	3.00	7/15/06 7:18 AM	29.45	42.6	16.55	0.99	1
w77h	0.16	7/16/06 7:31 AM	29.52	40.8	71.79	4.39	1
w77h	0.15	7/16/06 7:31 AM	29.53	40.8	70.74	4.33	1
w77h	0.59	7/16/06 7:31 AM	29.54	40.8	69.64	4.26	1
w77h	0.93	7/16/06 7:32 AM	29.55	40.8	68.09	4.17	1
w77h	1.23	7/16/06 7:32 AM	29.55	40.8	67.63	4.14	1
w77h	1.55	7/16/06 7:33 AM	29.55	40.8	67.04	4.10	1
w77h	1.82	7/16/06 7:33 AM	29.55	40.8	66.19	4.05	1
w77h	2.14	7/16/06 7:34 AM	29.49	40.9	59.94	3.67	1
w77h	2.44	7/16/06 7:34 AM	29.46	41.0	56.30	3.45	1
w77h	2.57	7/16/06 7:35 AM	29.46	41.2	47.87	2.92	1
w77h	2.76	7/16/06 7:36 AM	29.48	41.3	36.24	2.21	1
w77h	2.88	7/16/06 7:37 AM	29.49	41.5	30.21	1.84	1
w77h	3.03	7/16/06 7:37 AM	29.50	41.5	27.56	1.68	1
w77h	3.09	7/16/06 7:38 AM	29.50	41.5	26.90	1.64	1
w78g	0.06	7/16/06 5:34 AM	27.78	40.5	72.95	4.60	1
w78g	0.05	7/16/06 5:35 AM	27.76	40.4	82.44	5.20	1
w78g	0.17	7/16/06 5:36 AM	30.10	38.4	73.83	4.54	1
w78g	0.61	7/16/06 5:36 AM	30.09	38.4	72.34	4.45	1
w78g	0.82	7/16/06 5:37 AM	30.10	38.4	72.12	4.43	1
w78g	1.16	7/16/06 5:37 AM	30.09	38.4	72.00	4.43	1
w78g	1.51	7/16/06 5:37 AM	30.09	38.4	72.22	4.44	1
w78g	1.48	7/16/06 5:37 AM	30.09	38.4	71.76	4.41	1
w78g	1.78	7/16/06 5:38 AM	30.10	38.4	71.71	4.41	1
w78g	1.81	7/16/06 5:38 AM	30.10	38.4	71.76	4.41	1
w78g	2.08	7/16/06 5:38 AM	30.10	38.4	72.41	4.45	1
w78g	2.37	7/16/06 5:38 AM	30.11	38.4	71.77	4.41	1
w78g	2.70	7/16/06 5:39 AM	30.11	38.4	71.00	4.36	1
w78g	2.85	7/16/06 5:39 AM	30.11	38.5	69.32	4.26	1
w78g	2.90	7/16/06 5:40 AM	30.11	38.5	68.53	4.21	1

Profile	Depth m	Date Time	Temperature °C	Salinity PSS	DO Saturation %	Dissolved Oxygen mg/L	Circulator
w78g	2.98	7/16/06 5:40 AM	30.10	38.6	66.97	4.11	1
w78g	3.02	7/16/06 5:41 AM	30.08	38.8	63.26	3.88	1
w78g	3.12	7/16/06 5:42 AM	30.08	39.2	49.90	3.05	1
w78g	3.25	7/16/06 5:43 AM	30.08	39.9	37.47	2.28	1
w78g	3.27	7/16/06 5:44 AM	30.03	40.3	19.90	1.21	1
w78g	3.32	7/16/06 5:44 AM	30.02	40.7	13.46	0.81	1
w78g	3.36	7/16/06 5:45 AM	30.01	40.8	10.99	0.66	1
w78g	3.32	7/16/06 5:45 AM	30.02	40.5	16.56	1.00	1
w78i	-0.02	7/16/06 4:55 PM	29.90	0.0	88.82	6.76	1
w78i	0.13	7/16/06 4:56 PM	31.67	38.5	104.95	6.28	1
w78i	0.54	7/16/06 4:57 PM	31.64	38.5	105.74	6.33	1
w78i	0.82	7/16/06 4:58 PM	31.60	38.6	104.99	6.29	1
w78i	1.15	7/16/06 4:58 PM	31.62	38.5	105.44	6.32	1
w78i	1.43	7/16/06 4:58 PM	31.41	38.5	103.70	6.23	1
w78i	1.67	7/16/06 4:59 PM	31.06	38.6	98.85	5.97	1
w78i	1.52	7/16/06 5:00 PM	31.31	38.6	99.22	5.97	1
w78i	1.65	7/16/06 5:00 PM	31.16	38.6	98.72	5.95	1
w78i	1.74	7/16/06 5:00 PM	31.05	38.8	96.53	5.83	1
w78i	1.88	7/16/06 5:01 PM	30.46	39.0	89.86	5.47	1
w78i	2.03	7/16/06 5:01 PM	30.27	39.2	82.94	5.06	1
w78i	2.21	7/16/06 5:02 PM	30.22	39.7	74.35	4.52	1
w78i	2.32	7/16/06 5:03 PM	30.23	40.1	70.28	4.27	1
w78i	2.39	7/16/06 5:03 PM	30.23	40.1	68.23	4.14	1
w78i	2.43	7/16/06 5:04 PM	30.23	40.2	67.06	4.07	1
w78i	2.54	7/16/06 5:04 PM	30.19	40.5	63.12	3.82	1
w78i	2.59	7/16/06 5:05 PM	30.19	40.6	59.82	3.62	1
w78i	2.68	7/16/06 5:05 PM	30.05	41.4	54.14	3.27	1
w78i	2.77	7/16/06 5:06 PM	30.07	41.3	50.96	3.08	1
w78i	2.86	7/16/06 5:06 PM	30.01	41.6	44.65	2.69	1
w78i	2.92	7/16/06 5:07 PM	29.95	41.8	30.40	1.83	1
w78i	2.97	7/16/06 5:09 PM	29.95	41.7	25.74	1.55	1
w78i	2.99	7/16/06 5:09 PM	29.91	41.9	23.45	1.41	1
w78i	3.12	7/16/06 5:10 PM	29.88	41.8	18.45	1.11	1
w78i	3.15	7/16/06 5:10 PM	29.87	41.9	18.39	1.11	1
w78i	3.24	7/16/06 5:10 PM	29.87	41.9	17.65	1.06	1
w78i	3.25	7/16/06 5:11 PM	29.88	41.9	17.25	1.04	1
w78i	3.33	7/16/06 5:11 PM	29.87	41.9	16.38	0.99	1
w79g	0.05	7/16/06 5:59 AM	27.64	40.4	72.48	4.58	1
w79g	0.12	7/16/06 6:00 AM	30.13	38.4	73.84	4.54	1
w79g	0.61	7/16/06 6:00 AM	30.17	38.4	72.67	4.46	1
w79g	0.90	7/16/06 6:01 AM	30.17	38.4	72.56	4.45	1
w79g	1.21	7/16/06 6:01 AM	30.18	38.4	72.42	4.45	1
w79g	1.49	7/16/06 6:01 AM	30.18	38.4	72.53	4.45	1
w79g	1.81	7/16/06 6:01 AM	30.19	38.4	72.20	4.43	1
w79g	2.10	7/16/06 6:02 AM	30.18	38.4	72.57	4.45	1
w79g	2.40	7/16/06 6:02 AM	30.18	38.5	71.38	4.38	1
w79g	2.73	7/16/06 6:02 AM	30.18	38.5	70.50	4.33	1
w79g	3.04	7/16/06 6:03 AM	30.16	38.5	69.48	4.26	1
w79g	3.04	7/16/06 6:03 AM	30.16	38.6	69.37	4.26	1

Profile	Depth m	Date Time	Temperature °C	Salinity PSS	DO Saturation %	Dissolved Oxygen mg/L	Circulator
w79g	3.13	7/16/06 6:04 AM	30.11	38.8	62.63	3.84	1
w79g	3.20	7/16/06 6:05 AM	30.08	38.8	57.17	3.51	1
w79g	3.24	7/16/06 6:05 AM	30.00	40.0	39.28	2.39	1
w79g	3.30	7/16/06 6:06 AM	29.93	41.0	20.75	1.26	1
w79g	3.37	7/16/06 6:07 AM	29.89	41.4	8.38	0.50	1
w79g	3.45	7/16/06 6:08 AM	29.85	41.7	5.38	0.32	1
w79g	3.52	7/16/06 6:09 AM	29.83	41.9	3.24	0.19	1
w79g	3.60	7/16/06 6:09 AM	29.75	42.4	1.75	0.10	1
w79g	3.77	7/16/06 6:10 AM	29.70	42.6	1.54	0.09	1
w79g	3.70	7/16/06 6:10 AM	29.69	42.7	1.22	0.07	1
w79g	3.80	7/16/06 6:11 AM	29.69	42.7	1.17	0.07	1
w80a	0.03	7/14/06 1:31 AM	27.71	40.6	73.51	4.63	1
w80a	0.11	7/14/06 1:31 AM	29.35	42.8	64.46	3.91	1
w80a	0.54	7/14/06 1:32 AM	29.34	42.8	62.41	3.78	1
w80a	0.82	7/14/06 1:32 AM	29.40	42.9	60.44	3.66	1
w80a	1.16	7/14/06 1:33 AM	29.43	42.9	59.15	3.58	1
w80a	1.44	7/14/06 1:33 AM	29.46	43.0	55.62	3.36	1
w80a	1.61	7/14/06 1:34 AM	29.49	43.1	52.84	3.19	1
w80a	1.73	7/14/06 1:34 AM	29.42	42.9	54.62	3.30	1
w80a	1.82	7/14/06 1:35 AM	29.47	43.1	53.25	3.21	1

APPENDIX F Review comments from TWDB on draft report

Comments were provided by Texas Water Development Board personnel on the draft version of this document, dated 6/30/2006. The comments are provided below in accordance with the Interagency Cooperation Contract. The TWDB comments are provided in standard font; our response is provide in italic.

F.1 Comments by Jordan Furnans, Ph.D., P.E., 7/10/06

Page 12 – You say “Based on preliminary work of the Shoreline Environmental Research Facility....” - Is this sentence in reference specifically to Corpus Christi Bay? Please clarify.

Report revised. Full notation on SERF provided.

Page 13 – The 3rd principal issue you list is unclear

Report revised.. The sentence is rewritten.

Page 13-14 – The “excuses paragraph” is valid however poorly written. Clarification is needed, although I believe the arguments based on what I know of the project and results.

Report revised. This paragraph (page 15-16) has been entirely rewritten and expanded into two paragraphs to clarify the connection between the completed work, the SOW, ongoing NSF work, and the new knowledge gained during this project.

Page 14 – The future work sounds like you will eventually accomplish the tasks of the SOW. In this paragraph, you should note how each SOW task will be addressed from now on.

Report revised. Several new sentences added to “Future Work” 7.

Provide the link to the CRWR online report of Cedric David’s thesis – it is needed to provide full documentation for this report.

Report revised. See footnote at start of Appendix A.

In Appendix A – there are many references to “Section 0” which is confusing.

Report revised. Cross-references all checked.

Conclusions on Appendix B need to be re-written and clarified. State whether NT or MY is better for underflow modeling. Last sentence (page 111) is confusing.

Report revised. Appendix B was completely re-written, and the suggestions for better modeling based on the tests run in the appendix were clarified

At times in Appendix B, MY is incorrectly typed. Please review and revise for clarity.

Report revised. Appendix B was completely re-written.

Pg 114 (Appendix C) – you state that winds, tidal forcing and other forces are not included in the oso bay –CC Bay simulation. I understand and accept the approach, however we would like to see a few sentence description of how adding winds and tides might affect the results and the representation of the underflow. I would surmise that the tides would causes the underflow to move faster, whereas the winds would be problematic based on the vertical mixing model employed within EFDC. Please add a bit of discussion/conjecture – this would be a good lead in toward future projects.

Report revised. The effects of forces not included in the model simulations are now discussed.

Pg 114 - Figure C 2 shows the artificial temperature forcing, but the text is written to suggest it shows the field observed temperatures. Can you add the field observed temperatures to the figure (TWDB can provide temperature data from the pressure transducer we installed within Oso Bay from 8/21-8/24).

Report revised. Figure C.2 is being replaced to a) Include field temperature data, and b) Reflect the suggested formatting changes.

Page 114 – change the statement “Data from the first 12 hours of the simulation is not collected, because the gravity current may not yet be developed” to state whether or not it was developed. There should not be ambiguity here. You could just say the model was spun-up for 12 hours before data collection commenced.

Report revised. The ambiguity has been removed.

On Figure C.2. – I’d replace the green arrow with a filled-in rectangle overwhich the sinusoid is plotted. You could then plot an arrow if you wish, but I think a rectangle better conveys the concept you are trying to get across. Use the following matlab commands:

```
XX = [12 36 36 12 12];
YY = [28 28 40 40 28];
HH = fill(XX,YY,[0.9 0.9 0.9]);
set(hh,'LineStyle','none');
hold on
set(gca,'TickDir','out')
plot([0 36 36 0 0],[29 29 36 36 0],'k-')
... ADD CODE FOR Sinusoid and other features
```

*** In general, I’d try to get away from using powerpoint to edit/create figures. Matlab lets you reproduce the figures easily and therefore edit figures more simply to meet new needs. Often I create individual matlab scripts for each figure I create – ie for this one I would name the script “FigureC2.m” that way I would always know where the figure came from and how to modify it.

Report revised. See new Figure C.2

Page 114 – I would like to see a figure of the three cases you present – ie show rectangles (representing the water column) partitioned as you would in the model. It is best to put a graphic

here as this is key to the point of your analysis. The text is clear, but a figure would not hurt and I believe would help.

Report revised. A figure showing the differences among the test cases was included (Figure C.3).

Page 115 – In the text describing the result san analysis, you say it matches well with the field data – while this is true, you need to present the field data next to Figure C.3 so the reader can make this comparison without having to go back through the report.

Report revised. Field data was included with the model results for clarity. (Figure C.4)

Page 115 – I am unclear how by looking at the temperature results we can determine the model is able to capture the bulk velocity of the underflow at at least an order-of-magnitude scale with reference to field data. Also, I would think that the principle driver of the underflow is the tidal forcing, which you are not including in the model. I suggest re-analyzing this data and reporting only on a comparison between results from the 3 vertical grid resolutions. You can say that the stretched case shows evidence of and underflow similar to that seen in the field, but you don't need to go any further with field/model comparisons. Hammer the point home that the grid resolution is critical to representing the underflow.

Report revised. The use of temperature in approximating order-of-magnitude velocities of the underflow was clarified. However, this section was not removed from the results section as suggested, because it is significant to note that the model could replicate observed bulk properties such as velocity, even if the comparison can only be qualitative. The use of temperature as a tracer also supports the conjecture that the underflow is, in fact, originating from Oso Bay.

Page 116 – Let's adjust the quantification of stratification to consider density stratification (which is common in oceanography literature and was used in a recent study of brine discharges into a florida coastal system). I have attached my review of this florida work, including a description of how I calculated the sigmat stratification values using the equation of state relating temperature and salinity to density. I think the potential energy approach is valid, but we are likely going to use this report to back-up our argument regarding the florida work, and therefore it would be illustrative to demonstrate your point using their analysis methodology. See accompanying documents "Calculate_sigmaT.m", "Florida_Review_JF.pdf", and "Extract_Florida_Report.pdf". Feel free to circulate the matlab file, but the other two files are to be held confidential until otherwise noted by TWDB.

Report revised. A sigma-t analysis is now included in the stratification analysis.

Page 16 – please provide an equation for the potential energy calculation. This approach toward quantification of stratification is new to me, and I want to be able to reproduce it in future work. Also, if you could provide the data used in calculating the PE values discussed in Figure C5, that would be great. Perhaps you already have put it on the accompanying CD – but if not, we need it.

Report revised. An equation for the potential energy calculation was included in the report (equation C.2). In addition, the discussion of this calculation was extended for clarity, and a figure explaining the relationship between potential energy and wind mixing was included (Figure C.8)

Page 116-117 – The entire PE deficit discussion is not clear to me – I can't get my head around this approach. Please provide a more in-depth discussion of the method of analysis (including any references of where else it has been used), the method of calculation, and what the PE deficit actually means. For example, I am not sure by looking at Figure C.5 which model is better – is it better to have a lower PE deficit, or are we trying to recreate the PE deficit shown in the field data? Is this analysis truly valid given that the model does not consider wind. What is the theoretical mixing event in the model that is used to calculate the PE deficit. I am baffled. You could look at figure C.5 and argue that the case closes to the field data is the sparse grid case, and therefore it is better. A better description of this analysis method is needed to avoid misconstruing conclusions based on Figure C.5.

Report revised. See comment above.

Page 117 – strictly speaking, you have not mathematically established a link between stratification and hypoxia, so you can not really say “these limitations [] could lead to erroneous under-predictions of hypoxia”. You need to stick to stratification and maybe reference how incorrectly modeled stratification may lead to incorrect estimates of the presence and extent of hypoxia.

Report revised. The statement of establishing a link between hypoxia and stratification was amended to a link between stratification and grid resolution that could impact hypoxia predictions.

You have not demonstrated computational expense (page 117). Please provide a table outlining the run times & simulation times for each of the 3 grid structures discussed. This is how you can show computational expense. Include in table linear extrapolations for running the entire CC Bay system, and a brief discussion of how doing so would be impractical. Note that linear extrapolation is a “best case” scenario and is not likely to be the real case. Your conclusion is good, but needs to be made stronger with greater documented support.

Report revised. A table was provided giving computational time for the test cases (Table C.1).

Appendix D grammar needs to be revised for clarity

Report revised. Grammar has been improved throughout.

Page 122 – Equation 14 – I am not sure how density fits in here. Please explain or correct.

Report revised. Now eq. (D.5) on page 122. Density was a typographical error

Page 123 – Equation 18 – C_N and u^* are not explicitly defined. Also need to specify that η refers to the water surface. Eq. 20 has a value a which is undefined.

Report revised. Now eq. (D.9). Definitions provided on page 123.

Page 128 – Section 0 is referenced. This needs to be revised.

Report revised. Cross-references are now correct.

Appendix D discussion is too obtuse to handle – provides headaches to readers. I am confident the presented material satisfies the requirements for Task 1 of the scope of work, and I understand how Task 2 was not possible given the complexity of the results of Task 1 and the difficulty of implementing the new mixing model. I require that Appendix D be revised for grammar, readability, and completeness, with the intention of using this section as the starting point for a new project for the coming year.

Report revised. Extensive new discussion provided on pages 118, 119, and 120, with other clarifying sentences throughout. New summary discussions on pages 14 and 15 should also help clarify the approach.

F.2 Comments by Dharhas Pothina

Pg 99 - Definition of dz : Include figure to demonstrate definition of dz and show the grid with the uniform grid in the underflow and the increase in fractional depth above that. Need not be to scale.

Report revised. Appendix B was completely rewritten.

Pg 100 – Last line : “This is not something we would have predicted...” If possible add a suggested explanation, ie, along the lines of ‘We think this is caused by numerical diffusion inherent in the model etc’

Report revised. Appendix B was completely rewritten.

Pg 101 – “We note that vel. Profiles do not resemble field or other simulations...” : any suggestions as to cause? Looks like it may have been discussed on page107. In which case add a sentence indicating that this will be discussed in the following pages.

Report revised. Appendix B was completely rewritten.

Pg 114 – “wind,tidal, and other forces are neglected.” I assume there is no river inflow. Change to say “wind, tidal, river inflow, and other forces ..” for clarity since river inflow is another major forcing that is being neglected

Report revised. Inflow was included in the list of neglected forces in our simulations.

Pg 114 – How long was the simulation for? Ie ‘real time’.

Report revised. Simulation vs real time was clarified.

Pg 117 – “Corpus Christi .. take 130 days to run...” . How long a simulation is that? Ie 130 days to run a 30 day simulation etc.

Report revised. Simulation vs real time was clarified.

F.3 Comments by Ruben S. Solis, Ph.D. 7/20/2006

The report provides a good explanation for observed occurrences of hypoxia in Corpus Christi Bay. It shows the significance of thin-layer underflows of dense, highly saline water from Oso Bay and the upper Laguna Madre, and identifies this as the likely culprit. Field measurements collected for this study using new innovative instruments support this conclusion. Improved methods for modeling vertical mixing of conservative tracers are presented. Overall, this work is well-done and breaks new ground in our understanding and modeling of processes in Texas bays, and it meets the project contract requirements.

In general, the report itself needs cleaning up and the presentation of the material could be improved. Remaining questions and suggestions follow below.

Report revised. Extensive cleaning up of grammar, cross-references and graphic have been completed.

Can non-conservative tracers also be modeled with this approach? Would dissolved oxygen be modeled non-conservatively?

Report revised. Added a short discussion to the report (bottom of page 15). In general, a conservative mixing/transport approach is applicable to non-conservative tracers by decoupling advection and diffusion from the reaction solution.

Do the mixing algorithms described simply replace the "diffusion" component of the advection-diffusion equation? This was not clear.

Report revised. Discussion in third paragraph on page 15 should make clear that vertical diffusion is replaced by the vertical mixing model.

P. 11, Figure 2. A location map showing the location of the cross-section depicted in this figure would be helpful. The reader has no reference with respect to location at this point in the report. Supporting information on this figure such as date, nature of measurements (instantaneous, averaged, ...) would also help. Were the night-time measurements for temperature and salinity collected from a different transect than that for dissolved oxygen? The blacked-out portion of the figure representing the bottom looks different for dissolved oxygen than for the other two. (Is this an artifact of the graphics?)

Report revised. A new Figure 2 now provides a location map. The old Figure 2 is now Figure 3. Information on data collection date/times are provided. The discrepancy in the blacked out portion for the DO was a from a bug in the data processing script - the correct bathymetry was previously used for the nighttime Temperature and Salinity graphs, but the daytime bathymetry was being used for the nighttime DO graph,

p. 16, bottom paragraph. "Hypoxia occurs ... predominantly in the southeast region of Corpus Christi Bay ..." - A location map would be useful for the reader.

Report revised. A new figure A.3 has been added.

p. 18, Figure A.2. Reason for use of the county labels that were used is not clear.

Report revised. Labels have only been left on the counties that are adjacent to Corpus Christi Bay.

p. 19, second sentence. Figure number is missing (A.3??)

Report revised. Cross-references have been corrected.

p. 19. The connection to Aransas Bay via the Aransas Channel is through the Lydia Ann Channel.

Report revised.

p. 20. Change "Figure A>4" to "Figure A.4"

Report revised.

p. 22, second sentence. Change "physical behaviors" to "physical behavior".

Report revised. Retained the plural sense but removed the preceding article "the" implying singular.

p. 22, bottom paragraph. Would be useful if UTMSI sampling sites were identified in Figure A.6.

Report revised to include Figure A.3 with the UTMSI sampling sites. Old figure A.6 (now A.5) would be too cluttered if the UTMSI designators were included. Also, this information is readily available in the public reports of UTMSI to Coastal Bend and Bays Estuaries Program.

p. 22, bottom paragraph. What was the amount of time elapsed between the first and last samples collected during a given data collection run?

Report revised. Page 25.

p. 23, Figure A.6. Suggest eliminating Figures A.4 and A.5 and just using Figure A.6.

Report revised. A.4 and A.5 removed. New A.3 added.

p. 24. What is the difference between a "fast" and an "accurate" sensor?

Report revised. This is now explained.

p. 26, second paragraph. Change "The SCAMP is the support to multiple sensors." to "The SCAMP supports multiple sensors."

Report revised.

p. 26, second paragraph. Not sure what "Section 0" refers to.

Report revised. All cross-references are now correct.

p. 26, second paragraph, last sentence. Change "to compute gradients" to "compute small-scale gradients".

Report revised.

p. 30, second paragraph. Provide location for measurement in second sentence. Again, a reference map for sites indicated in this paragraph and in Figure A.13 would be useful.

Report revised. Cross-references are given to the new Figure 2 and Figure A.5 for locations

p. 35, first paragraph. Correct reference to Section 0.

Report revised. All cross-references are now correct.

p. 36, Figure A.21. Would be useful to indicate on this figure that these are 10-second average measurements, and that the sampling interval changed from 30 seconds to 10 minutes on July 6, leading to the change in appearance of the data.

Report revised. Changes made to caption. This is now Figure A.20

p. 49, paragraph 3. "...its movable charges flow, ...". Needs clarification.

Report revised. The sentence now reads "...an electric current is induced."

p. 51, second paragraph. "Both tidal elevation and wind are part of meteorological forcing, ..." Not clear what this means.

Report revised. These are now discussed as "physical forcing mechanisms."

p. 53. Would recommend making correction for salt water density if this is relatively easy to correct since this is a known error.

Report not revised. We agree that this correction eventually must be addressed in the processed data. However, we noted that failure to adjust the SCAMP default calibration is not an unusual occurrence; the calibration setting is on a screen that includes setting a user should not be changing. Because this is likely to be an ongoing issue with the instrument, we plan to develop a comprehensive approach to adjusting the data after collection. Because developing, testing and debugging new post-processing code is not a trivial effort, we did not attempt it for the present data set.

p. 60, top paragraph and Figures A.41, A.42. "...binned average of the absolute value of temperature gradient profile, and its standard deviation for each location ...". Not obvious on the figures which is the mean, which the standard deviation. Also, why is absolute value of temperature gradient used? (Useful for determining local diffusion?)

*Report revised. Additional text added to captions of Figures A.40 and A.41.
Explanation of absolute valued provided.*

p. 119, first paragraph. Diagram of Kelvin-Helmholtz (K-H) billows relative to the model grid would be useful.

Report not revised. The scale of a K-H billow depends upon the scale of the stratification and the forcing, so that it is theoretically possible to have a K-H billow that is either very small or very large. Thus, it is possible to have a K-H billow that is "resolvable" on the model grid (however, such a model would require a non-hydrostatic solution), while simultaneously having billows that are unresolvable. A good animation of billowing can be found at http://fluid.stanford.edu/~fringer/movies/shear_convect/kh.html

p. 123, bottom paragraph. "TKE" - total kinetic energy?

Report revised. Yes.

p. 126, last sentence. "The ..." ?

Report revised. Extraneous word deleted.

p. 127, equation 35. Define U, V (velocities I assume).

Report revised. Now eq. (D.26). Yes, these are velocities.

This page intentionally left blank

REFERENCES

- Applebaum, S., Montagna, P. A., and Ritter, C. (2005). "Status and trends of dissolved oxygen in Corpus Christi Bay, Texas, USA." *Environmental Monitoring and Assessment*, **107**, 297-311.
- Buckee, C., Kneller, B., and Peakall, J. (2001). *Turbulence Structure in Steady, Solute-Driven Gravity Currents*. In: McCaffery, W. D., Kneller, B. C., and Peakall, J. (eds) "Particulate Gravity Currents". IAS Special Publication, 31, pp. 173-187.
- Dallimore, C. J., Imberger, J., and Ishikawa, T. (2001). *Entrainment and Turbulence in Saline Underflow in Lake Ogawara*. *Journal of Hydraulic Engineering*. 127(11): 937-948.
- Dallimore, C.J., J. Imberger and B.R. Hodges (2004), "Modeling a plunging underflow," *Journal of Hydraulic Engineering*, **130**(11):1068-1076.
- Dallimore, C., B.R. Hodges, J. Imberger (2003), "Coupling an underflow model to a 3D hydrodynamic model," *Journal of Hydraulic Engineering*, **129**(10):748-757.
- Dauer, D. M., Rodi, A. J., and Ranasinghe, J. A. (1992). "Effects of low dissolved oxygen events on the macrobenthos of the lower Chesapeake Bay." *Estuaries*, **15**(3), 384-391.
- Ellison, T. H., and Turner, J. S. (1959). *Turbulent entrainment in stratified flows*. J. Fluid Mech., Cambridge, U.K., 6(3), 423-448.
- Felix, M. (2004). *The significance of single value variables in turbidity currents*. *Journal of Hydraulic Research*. 42 (3): 323-330.
- Gale, Emma, Pattiaratchi, Charitha, and Ranasinghem Roshanka. 2006. *Vertical mixing processes in Intermittently Closed and Open Lakes, and Lagoons, and the dissolved oxygen response*. *Estuarine, Coastal and Shelf Science*. 69: 205-216.
- Galperin, B., Kantha, L. H., Hassid, S., and Rosati, A. (1988). *A Quasi-Equilibrium Turbulent Kinetic Energy Model for Geophysical Flows*. *Journal of Atmospheric Sciences*. 45(1): 55-62.
- Garcia, M. H. (1993). *Hydraulic Jumps in Sediment-Driven Bottom Currents*. *Journal of Hydraulic Engineering*. 119(10): 1094-1117.
- Garcia, M. H. (1994). *Depositional Turbidity Currents Laden With Poorly Sorted Sediment*. *Journal of Hydraulic Engineering*. 120(11): 1240-1263.
- Gunter, G. (1942). "Offatts Bayou, a Locality with Recurrent Mortality of Marine Organisms." *American Midland Naturalist*, **28**(3), 631-633.
- Hamrick, J. (1992). *A Three-dimensional Environmental Fluid Dynamics Computer Code: Theoretical and Computational Aspects*, The College of William and Mary, Virginia Institute of Marine Science, Special Report 317.
- Hebbert, B., Patterson, J., Loh, I., and Imberger, J. (1979). *Collie River overflow into the Wellington reservoir*. *J. Hydr. Div., ASCE*, 105(5), 533-545.
- Hodges, B.R., J. Imberger, A. Saggio and K. Winters (2000), "Modeling basin-scale internal waves in a stratified lake," *Limnology and Oceanography*, **45**(7):1603-1620.
- Kraus, E. B. and Turner, J. S. (1967). A one-dimensional model of the seasonal thermocline II. The general theory and its consequences. *Tellus*. XIX, 1: 98-105.

- Kulis, P. (2005), *Modeling Approaches Reflecting the Interfacial Physics of Gravity Currents*, M.S. Departmental Report, Department of Civil, Architectural and Environmental Engineering, University of Texas at Austin, 58 pages.
- Kulis, P. and B.R. Hodges (2005), "Improved techniques for gravity current modeling," Mechanics and Materials Conference (McMat 2005), June 1-3, 2005, Louisiana State University, Baton Rouge, Electronic Proceedings (CD-ROM), 4 pgs.
- Laval, B., B.R. Hodges and J. Imberger (2003), "Reducing numerical diffusion effects with pycnocline filter" *Journal of Hydraulic Engineering*, **129**(3):215-224.
- Mellor, G. L., and Yamada, T. (1982). *Development of a Turbulence Closure Model for Geophysical Fluid Problems*. Rev. Geophys. Space. Phys. 20(4): 851-875.
- Montagna, P. A., and Kalke, R. D. (1992). "The effect of freshwater inflow on meiofaunal and macrofaunal populations in the Guadalupe and Nueces estuaries, Texas." *Estuaries*, **15**, 307-326.
- Morehead, S., and Montagna, P. A. (2003). *Monitoring Hypoxia (Low Oxygen) Conditions in Corpus Christi Bay*. Technical Report TR/03-01, University of Texas at Austin, Marine Science Institute.
- Morehead, S., and Montagna, P. A. (2004). *Monitoring Hypoxia (Low Oxygen) Conditions in Corpus Christi Bay - 2003*. Technical Report TR/03-04, University of Texas at Austin, Marine Science Institute.
- Morehead, S., Simanek, C., and Montagna, P. A. (2002). *GIS Database of Hypoxia (Low Oxygen) Conditions in Corpus Christi Bay*. Technical Report TR/02/001, University of Texas at Austin, Marine Science Institute.
- Orlando, S. P., Rozas, L. P., Ward, G. H., and Klein, C. J. (1991). "Analysis of salinity structure and stability for Texas estuaries." Strategic Assessment Branch, NOS/NOAA, Rockville, Maryland.
- Pond, G. and Pickard, G. (1983). "Introductory Dynamical Oceanography, 2nd Edition". Pergamon Press, New York. pp. 310-311.
- Ritter, C., and Montagna, P. A. (1999). "Seasonal hypoxia and models of benthic response in a Texas estuary." *Estuaries*, **22**(3), 7-20.
- Ritter, C., and Montagna, P. A. (2001). *Cause and effect of hypoxia (low oxygen) in Corpus Christi Bay, Texas*. Technical Report 2001-001, University of Texas at Austin, Marine Science Institute.
- Spigel, R. H., Imberger, J. and Rayner, K.N. (1986). *Modeling the diurnal mixed layer*. Limnology and Oceanography. 31(3): 533-556.
- Stanley, D. W., and Nixon, S. W. (1992). "Stratification and Bottom-Water Hypoxia in the Pamlico River Estuary." *Estuaries*, **15**(3), 270-281.
- Tanny, J., Chai, A., and Kit, E. (1995). *On the law of turbulent entrainment across a density interface*. Fluid Dynamics Research. 15: 69-74.
- Turner, J. S. (1973). *Buoyancy effects in fluids*. Cambridge Monographs on Mechanics and Applied Mathematics, C. U. Press, ed.
- Turner, R. E., Schroeder, W. W., and Wiseman, W., J. Jr. (1987). "The Role of Stratification in the Deoxygenation of Mobile Bay and Adjacent Shelf Bottom Waters." *Estuaries*, **10**(1), 13-19.
- UNESCO. (1981). "Tenth Report of the Joint Panel on Oceanographic Tables and Standards." UNESCO Technical Papers in Marine Science, 24.
- USEPA. (1999). *The Ecological Condition of Estuaries in the Gulf of Mexico*. EPA 620-R-98-004, United States Environmental Protection Agency.

- Ward, G. H. (1980). "Hydrography and circulation processes of gulf estuaries." *Estuarine and Wetland Processes*, 183-215.
- Ward, G. H. (1997). "Processes and Trends of Circulation Within the Corpus Christi Bay National Estuary Program Study Area." CCBNEP-21, Corpus Christi Bay National Estuary Program.
- Zhang, Y.-L., Baptista, A.M. and Myers, E.P. (2004). "A cross-scale model for 3D baroclinic circulation in estuary-plume-shelf systems: I. Formulation and skill assessment." *Cont. Shelf Res.*, **24**: 2187-2214

Cited Internet links

- <http://pme.com/scamp.htm> SCAMP home page
- <http://www.eurekaenvironmental.com/manta/overview.htm> Manta home page
- <http://www.trimble.com/pathfinderproxrs.shtml> Differential GPS receiver
- <http://www.magellangps.com/en/products/product.asp?PRODID=91> Handheld GPS receiver
- <http://lighthouse.tamucc.edu/TCOON/HomePage> TCOON home page
- <http://www.coastalenvironmental.com> CES weather station
- <http://www.nkhome.com/ww/wwindex.html> Kestrel handheld weather station
- <http://www.epa.gov/owow/estuaries/>
- <http://www.MathWorks.com> Matlab home page
- http://www.boat-ed.com/tx/handbook/pdf_index.htm The Handbook of Texas Boating Laws and